Chair of Geology and Economic Geology

Master's Thesis

# Geochemical investigations in the Mur River catchment (Styria)

Tanja Verena Oksakowski, BSc

May 2022

**MONTANUNIVERSITÄT LEOBEN**
www.unileoben.ac.at

## EIDESSTATTLICHE ERKLÄRUNG

Ich erkläre an Eides statt, dass ich diese Arbeit selbständig verfasst, andere als die angegebenen Quellen und Hilfsmittel nicht benutzt, und mich auch sonst keiner unerlaubten Hilfsmittel bedient habe.

Ich erkläre, dass ich die Richtlinien des Senats der Montanuniversität Leoben zu "Gute wissenschaftliche Praxis" gelesen, verstanden und befolgt habe.

Weiters erkläre ich, dass die elektronische und gedruckte Version der eingereichten wissenschaftlichen Abschlussarbeit formal und inhaltlich identisch sind.

Datum 22.05.2022

Unterschrift Verfasser/in
Tanja Verena Oksakowski

## Abstract

The Mur River has a length of 453 km and a total catchment area of 13,824 km². 290 km of the river flow through Styria. In this province, the Mur has a watershed of about 9400 km². Along the 290 km, which lie in the MUR planning area within the jurisdiction of Styria, a total of 424 monitoring points publicly available via the H2O database of the Federal Ministry of Agriculture, Regions and Tourism were evaluated. 33 of these monitoring sites collect heavy metal data measured in the flowing wave (F-parameters) or in the sediment (S-parameters). Furthermore, data sets of the Austrian stream sediment survey were examined and used for evaluation. In addition, data from ten sediment samples around Leoben were evaluated.

The stream sediment survey database reflects the geogenic background. It was also found that high values in the stream sediment layer are not always reflected in the data of the H2O database and vice versa. At the sites with elevated values in the H2O database without elevated values in the stream sediment layer, anthropogenic influence is expected. An example of this is monitoring site FW61400187 (Vordernbergerbach). It shows high heavy metal values in both the water and sediment samples not mapped in the Austrian stream sediment survey. This suggests a connection with nearby industry. In a corresponding sample point in Leoben, the above-average measurement results of measuring point FW61400187 is only detected for a few elements. It was observed that elevated readings in a sediment sample at one monitoring site are not related to elevated readings in the water sample. Furthermore, flow and heavy metal concentration in the water sample are uncorrelated.

# Zusammenfassung

Die Mur hat eine Länge von 453 km und ein Gesamteinzugsgebiet von 13.824 km². 290 km des Flusses fließen durch die Steiermark. In diesem Bundesland hat die Mur ein Einzugsgebiet von etwa 9400 km². Entlang der 290 km, die im Planungsraum MUR im Zuständigkeitsbereich der Steiermark liegen, sind insgesamt 424 Messpunkte zu finden. Die Daten dieser Messstellen sind über die $H_2O$-Datenbank des Bundesministeriums für Landwirtschaft, Regionen und Tourismus öffentlich abrufbar. 33 dieser Messstellen besitzen Schwermetallmessungen, also im Gewässer gemessene Parameter in der fließenden Welle (F-Parameter) oder im Sediment (S-Parameter). Weiters wurden Datensätze des Geochemischen Atlas von Österreich, insbesondere der Bachsedimentelayer, begutachtet und zur Auswertung herangezogen. Zusätzlich wurden die Daten von 10 Sedimentproben um Leoben ausgewertet.

Mit Hilfe aller Daten wurden Schwermetallanomalien im gesamten Einzugsgebiet der Mur einschließlich der Mürz, in Wasser und Sediment ermittelt sowie der Zusammenhang von Schwermetallen in Wasser- und Sedimentproben untersucht.

Die Datenbank des Geochemischen Atlas von Österreich bietet gute Rückschlüsse auf die geogene Hintergrundbelastung. Erhöhte Messwerte im Bachsedimente Layer des Geochemischen Atlas bildet nicht immer die Daten der H2O-Datenbank ab und umgekehrt. An den Standorten mit erhöhten Werten der H2O-Datenbank ohne erhöhte Werte im Bachsedimente Layer ist mit anthropogenem Einfluss zu rechnen. Beispiel dafür ist die Messstelle FW61400187 (Vordernbergerbach). Sie weist oft erhöhte Werte sowohl in der Wasser- als auch in der Sedimentprobe auf, diese werden aber nicht im Geochemischen Atlas abgebildet. Dies lässt auf einen Zusammenhang mit der nahegelegenen Industrie schließen. In der zur Messstelle FW61400187 korrespondierenden Probenahmestelle in Leoben konnten die überdurchschnittlichen Messergebnisse der Messstelle FW61400187 nur für wenige Elemente reproduziert werden. Zusätzlich dazu wurde beobachtet, dass erhöhte Messwerte in einer Sedimentprobe an einer Messstelle nicht zuverlässig im Zusammenhang mit erhöhten Messwerten der Wasserprobe stehen. Es ergibt sich kein Zusammenhang zwischen einem erhöhten Durchfluss und einer erhöhten oder niedrigeren Schwermetallkonzentration in der Wasserprobe.

# Acknowledgments

Special thanks to Prof. Gerd Rantitsch, who supported me throughout my Master's thesis and answered many questions patiently. I would also like to thank him for his extremely quick corrections and flexibility in scheduling, which helped me significantly in the realisation of my master's thesis.
I am especially grateful to my parents, Birgit and Udo, who made this degree possible for me, as well as to my sister Nina for her wonderful moral and active support during this entire phase of my life, especially towards the end.
I would also like to thank Romana Bojar for all her encouragement and help throughout my whole time at university.

# Table Of Content

# Annex

# Introduction

Stream sediments are controlled by the lithological composition of the catchment area. To study river systems, the geochemical analysis of these sediments offer a widely applied approach. Especially the mineral occurrences can be investigated well (Levinson, 1980), but also with regard to environmental questions the evaluation of the geochemical results finds application (Förstner, 1983).
The chemistry of the sediments is mainly influenced by the lithological as well as morphological conditions of the hinterland (Rantitsch, 2001). Small high mountain streams that flow into the valley rivers are significant sediment suppliers (Kammerlander et al., 2017). Another important influencing factor is climate and the associated erosion rate of rocks and soils. Furthermore, the prevailing flora and fauna are characterized by it (e.g. Salomons & Förstner (1984)). Blöschl et al. (2020) shows that the recent decades are among the most flooded periods in Europe, in the last 500 years. Not only changing climatic conditions, but also anthropogenic activities have an impact on sediments, for example land use and population density (Berner & Berner, 2012).

For this thesis, heavy metal anomalies in water and sediment were identified with the help of public data (H2O database and Geochemical Atlas of Austria). The entire catchment area of the Mur River including the Mürz is investigated. After the analysis of the governmental data, the area with the highest heavy metal concentration was investigated in more detail with sediment samples. The aim of this work is to identify heavy metal anomalies in the water and sediment of the entire catchment area of the Mur (incl. Mürz). Furthermore, the relation between the heavy metal concentrations in the water and sediment is investigated.

# Study area

## 1.1 The Mur River

The Mur River rises at about 1950 m above sea level as a source of debris in the Niedere Tauern mountains at the Flachkar in Lungau (Salzburg). The river is 453 km long and has a total catchment area of 13,824 km². In Slovenia, Legrad (130 m a.s.l.), it flows into the Drau River. The Mur reclines the first 60 km in Salzburg (up to Predlitz) and has a catchment area of ca. 1000 km². The remaining 290 km of the river, which are on Austrian territory (Figure 1), flow through the province of Styria with a catchment area of 9400 km² (Getzner et al., 2011). This part of the river constitutes the study area (Figure 1).

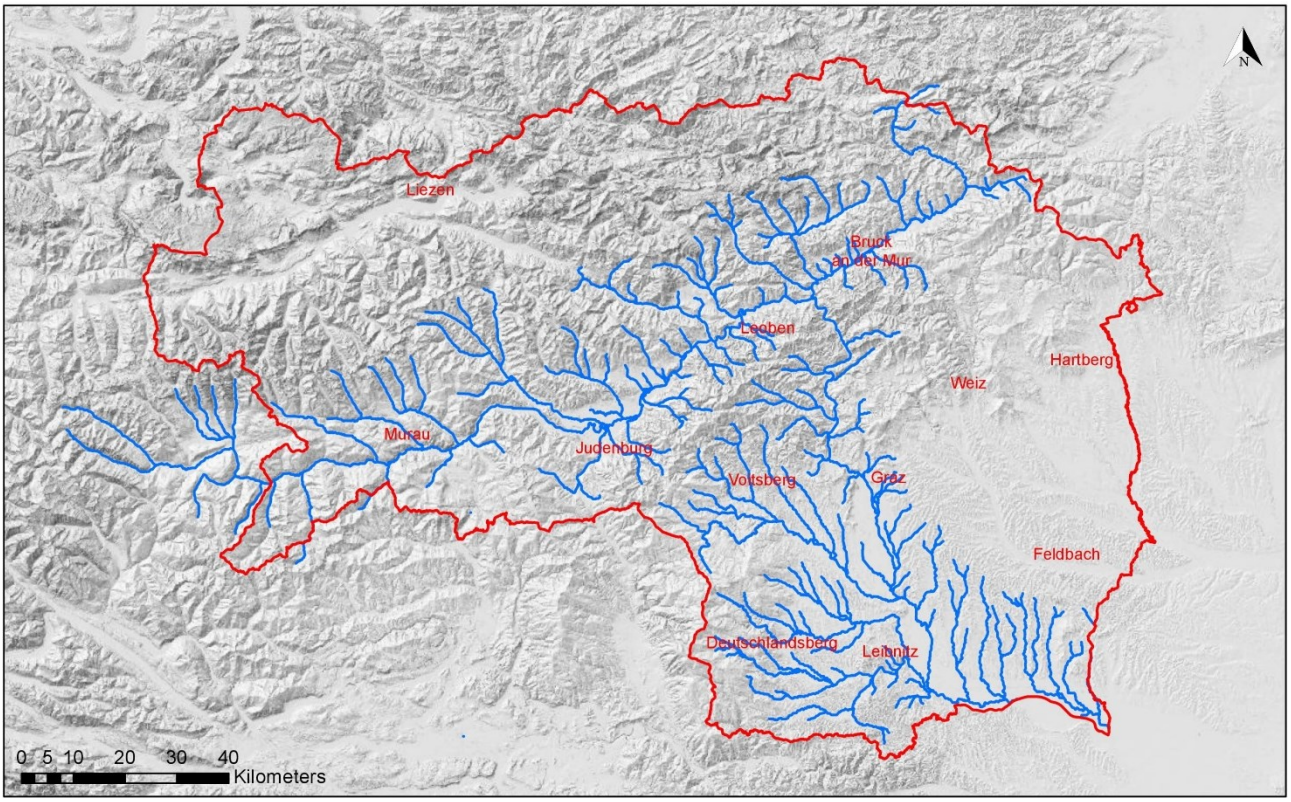


*Figure 1: Styrian territory of the Mur River; all terrain maps © basemap.at*

The course of the river is divided into three areas. The inner alpine Mur region, which has an approximately west-east course, the breakthrough section between Bruck and Graz with a north-south course and the lower, outer alpine Mur region. This division is also given by the geological setting. In the inner alpine area, the central Alps are drained. The Murtal valley is striped downstream by the Greywacke zone from the Enns and Liesing valleys into the Mürz valley. From Bruck an der Mur on, the Mur flows through the Grazer Bergland. The extra-alpine Mur area includes the Styrian Basin.

From Graz, the Mur flows through the broad bed-valley soils of the Graz, Leibnitz, Mureck and Radkersburg fields. In the bed and bed-notch valleys, the meandering and the oscillating river types are predominant. Characteristic for the notch valleys of this unit is mainly the elongated river type, whereas in the transition to the Styrian Basin the meandering type becomes more prominent again (Getzner et al., 2011).

The discharge at mean water is about 8 m³/s when entering Styria. It increases at Bruck an der Mur from 80 m³/s to 105 m³/s due to the inflow of the Mürz. At the end of the Styrian Mur the discharge is about 150 m³/s. The ratio between low and high water is about 1:125 at the beginning of the Styrian Mur, and about 1:29 at the end (Getzner et al., 2011).

| **Location** | **LQ** | **MLQ** | **MQ** | **HQ** | **LQ:HQ** |
|---|---|---|---|---|---|
| | [m³/s] | [m³/s] | [m³/s] | [m³/s] | [m³/s] |
| **Muhr** | 0.10 | 0.51 | 2.66 | 53.00 | 1:530 |
| **St. Michael (Lungau)** | 0.88 | 1.70 | 7.64 | 110.00 | 1:125 |
| **Mörtelsdorf** | 1.12 | 2.02 | 9.24 | 106.00 | 1:95 |
| **Gestüthof** | 2.60 | 8.55 | 36.10 | 490.00 | 1:188 |
| **St.Georgen** | 5.20 | 12.10 | 45.80 | 550.00 | 1:106 |
| **Zeltweg** | 8.16 | 14.70 | 568.00 | 610.00 | 1:75 |
| **Leoben** | 13.30 | 22.40 | 79.90 | 840.00 | 1:63 |
| **Bruck/Mur (incl. Mürz)** | 22.00 | 34.70 | 105.00 | 782.00 | 1:36 |
| **Friesach** | 25.40 | 38.70 | 114.00 | 748.00 | 1:29 |
| **Graz** | 24.00 | 355.60 | 116.00 | 1180.00 | 1:49 |
| **Mureck** | 38.10 | 56.20 | 146.00 | 1087.00 | 1:29 |

*Table 1: Annual discharge values of various locations, after (Muhar et al., 1998), from (Getzner et al., 2011)*
*LQ describes the low water discharge, i.e. the lowest discharge value in a certain period of time, in m³/s. MLQ represents the arithmetic mean of the annual low flows of a continuous series of years. MQ shows the mean discharge in m³/s during a certain period of time and HQ represents the flood discharge, i.e. the highest discharge value of a certain period of time, in m³/s (Getzner et al., 2011)*

## 1.2 Lithology of the Mur catchment area in Styria

Due to the large extent of the Mur catchment area, the geological setting varies greatly (Figure 2). Thus, a general subdivision into areas with predominantly mica schists and gneisses, with predominantly quartzite schists and finally with carbonates can be made. The Austroalpine nappe system summarises the geologically exposed alpine part of Styria. Austroalpine units consist of multiphase deformed as well as partly metamorphosed crystalline and sedimentary rocks. In contrast, the Styrian Basin overlying these units is formed of significantly less deformed (Gasser et al., 2009).

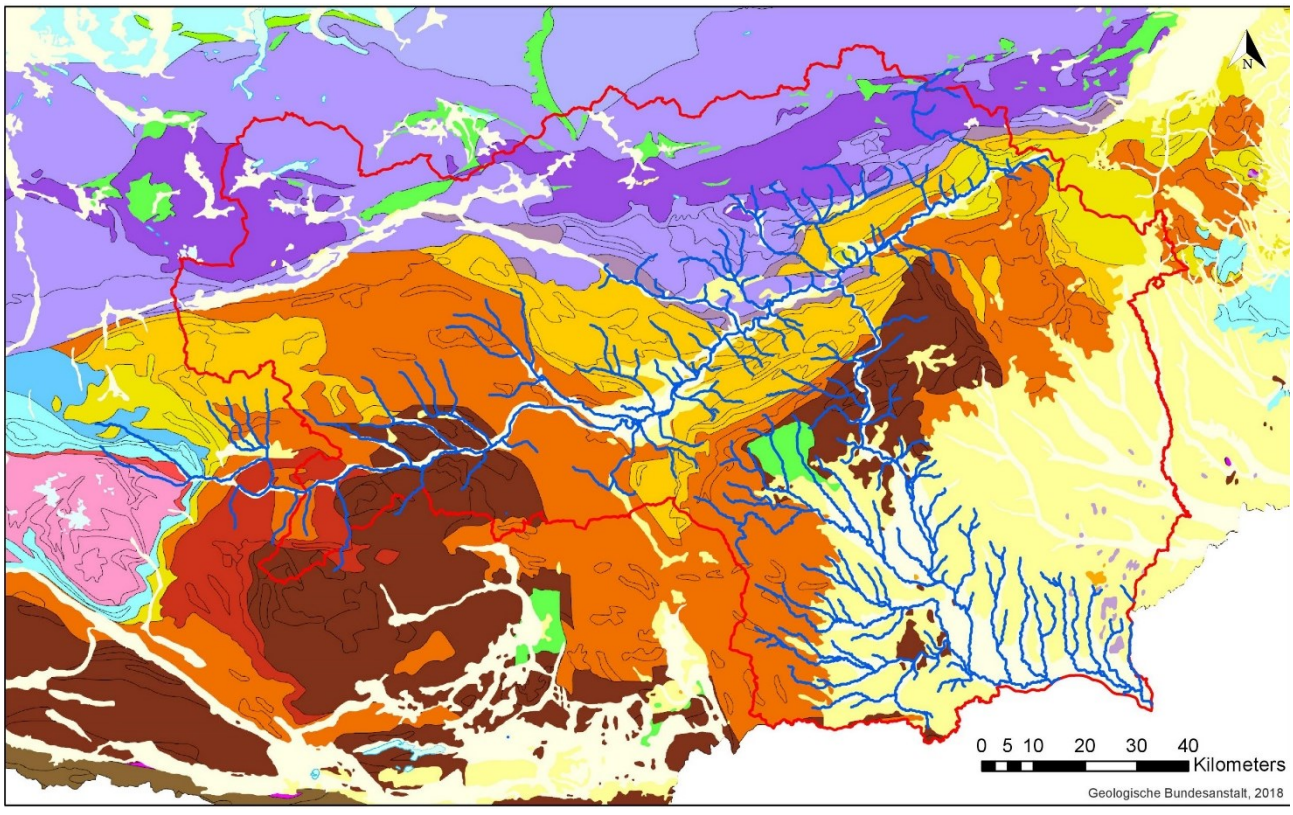


*Figure 2: Geological nappe systems of Styria, (Geologische Bundesanstalt, 2018)*

### 1.2.1 Austroalpine nappe units

According to Schmid et al. (2004), the Austroalpine nappe system in Styria is divided into nappe systems:

- Semmering-Wechsel Nappe System
- Silvretta-Seckau Nappe System
- Koralpe-Wölz Nappe System
- Ötztal-Bundschuh Nappe System
- Drauzug-Gurktal Nappe System

These are described in more detail below.

#### 1.2.1.1 Semmering-Wechsel Nappe System

Paragneisses and phyllitic mica schists, but also orthogneisses, green schists, amphibolites and quartzites form the Semmering-Wechsel nappe system. These rocks are overlain by Permomesozoic metasediments, which are composed of carbonaceous, siliciclastic and volcanoclastic metasediments. The Semmering-Wechsel nappe system belongs to the lower Austroalpine units (Schmid et al., 2004).

#### 1.2.1.2 Silvretta-Seckau Nappe System

The Silvretta-Seckau nappe system is the tectonically deepest part of the Upper Austroalpine nappe stack. Crystalline rocks consist of biotite-plagioclase gneisses, (two-)mica gneisses, quartz-rich gneisses, hornblende gneisses and biotite-rich mica schists. Numerous amphibolite ranges, augen gneisses and pegmatite occurrences are characteristic. Metasediments appear as Semmering quartzite and lower Triassic carbonates. Migmatites, ultramafic complexes and remnants of Permo-Mesozoic overburden are found locally (Schuster et al., 2001; Gasser et al., 2009).

#### 1.2.1.3 Koralpe-Wölz Nappe System

Large parts of Styria are assigned to this nappe system, including wide areas of the western Niedere Tauern, the Seetaler Alps, the Koralpe and the Fischbacher Alps. It is a high-pressure nappe system and has an often pressure-dominated, eoalpine metamorphic overprint. Rocks occurring in it are mainly mica schists, paragneisses, pegmatites and orthogneisses. Permo-Mesozoic metasediments are completely absent in this unit (Schmid et al., 2004; Schuster, 2004; Gasser et al., 2009).

#### 1.2.1.4 Ötztal-Bundschuh Nappe System

As the Mur enters Styria, it flows through the Ötztal-Bundschuh nappe system. It is mainly composed of biotite-plagioclase gneisses, mica schists, amphibolites and orthogneisses and thus has a similar lithological composition as the Silvretta-Seckau nappe system. (Schmid et al., 2004; Schuster, 2004; Gasser et al., 2009).

#### 1.2.1.5 Drauzug-Gurktal Nappe System

This nappe system exists in two separate areas in Styria and describes the uppermost unit of the Austroalpine nappe stack. The Gurktal nappes are mainly described by the Murau, Stolzalpe and Ackerl nappes. Within the Murau Group, the clastic stratigraphic sequence of the Murau nappe is represented. Stratigraphically, the phyllites, which are garnet and biotite-bearing, form the footwall layers. Black shales and conglomerate horizons are intercalated towards the hanging part. The conglomerates contain calcareous marble, phyllite and quartz nodules. Among other, the Stolzalpe nappe is composed of different metabasite. Predominantly metadiabase with pyroxene relicts, keratophyres, a cataclastic reshelled augen gneiss, and widespread metatuffs and -tuffites are found (Flügel & Neubauer, 1984; Neubauer & Pistotnik, 1984; Gasser et al., 2009).

With a size of about 1,500 km², the Graz Palaeozoic is a detached complex of the Austroalpine units. It is composed of Silurian to Carboniferous rocks (e.g. Gasser et al., 2010). Gasser et al. (2010) compiled 13 different rock associations belonging to the Laufnitzdorf, Kalkschiefer, Schöckl, Rannach and Hochlantsch facies. Lithologically, the northern part around Breitenau consists of calcareous schists (Devonian - Carboniferous) and pelitic sediments of the Kalkschiefer as well as Laufnitzdorf facies. Basal volcanites of the Silurian characterise the central and southern part. These volcanites are overlain by siliceous and carbonate rocks (Flügel & Hubmann, 2000; Gasser et al., 2009, 2010).

### 1.2.2 Eastern Greywacke zone

The Greywacke zone forms a band of maximum 23 km width of Palaeozoic rocks (phyllites, schists, metamorphic volcanics, weakly metamorphic limestones (marbles), quartzites and Greywacke). It is the base of the Northern Calcareous Alps and shows a predominantly gentle landscape with a medium altitude (Schönlaub, 1980).

In the Styrian area, the Greywacke zone is divided into four major tectonic units (Neubauer et al., 1994):

- Noric Nappe

- Kaintaleck Nappe
- Silbersberg Nappe
- Veitscher Nappe

#### 1.2.2.1 Veitsch-Silbersberg Nappe

At the southern edge of the Greywacke zone from Bruck an der Mur via Leoben, St. Michael and the northern edge of the Palten-Liesing valley the Veitsch Nappe is composed of carbonatic metasediments, with intercalations of metamorphic coal and magnesite. Clastic sediments are also found in places. South of Trieben, the sequence is divided into three formations. The lowest, the Steilbachgraben Formation, consists of clastics and a few carbonates, the overlying Triebenstein Formation is characterised by carbonates and some green shales. The hanging formation (Sunk Formation) is composed of black schists and marble. It also contains anthracite/graphite deposits (Ratschbacher, 1987; Neubauer & Vozarova, 1990; Neubauer et al., 1994).

Silbersberg Nappe is characterised by the Silbersberg conglomerate and the Alpine Verrucano formation (light green, quartzitic phyllites). Carbonate-chlorite schists, quartz phyllites and gneisses are found at the base. The Silbersberg nappe is exposed at the eastern edge of the Greywacke zone (Hermann, 1992).

The Kaintaleck slice consists of allochthonous deposits (mica schists, amphibolites and paragneisses and Kalwang conglomerate) and is found northwest of Leoben (Neubauer et al., 1994).

#### 1.2.2.2 Tirolic-Noric Nappe

The main part of the Greywacke zone in Styria is formed by this nappe. In it, Mesozoic sediments overlie greenschist facies metasediments. The Noric Nappe forms a sedimentary-volcanogenic stack of layers, grey-sandy, phyllitic and micaceous slates, sandstones, quartzites and banded limestones. Hanging is ingnimbritic rocks of the Blasseneck Porphyiod. Siderite mineralisation is found in the Devonian limestones (e.g. Erzberg). The top unit of the Noric nappe is the Eisenerz Formation (e.g. Schuster, 2015).

### 1.2.3 Northern Calcareous Alps

The main part of the Northern Calcareous Alps is formed by Permo-Triassic sediments of a passive continental margin (Mandl, 2000). Three tectonic units have been distinguished. The Bajuvaric, the Tirolic and the Juvavic units (Tollmann, 1985). The Bajuvaric is only exposed at the northern edge of Styria (Krystyn et al., 2008) and thus not part of the Mur catchment area. In general, the sedimentary sequence of the Tyrolian shows siliciclastic, evaporites (anhydrite, salt, gypsum; commonly known as the Haselgebirge) and carbonates. The southern unit of the Calcareous Alps in Styria is built up by the Reifling dolomite, the Wetterstein dolomite, the Leckkogel layers and the Waxeneck dolomite, as well as the Dachstein limestone and the Aflenz Formation Quartzites, sands, silts, clays and carbonates of the Werfen formation as well as clays, salts and gypsums build up this unit (Frisch & Gawlick, 2003).

### 1.2.4 Styrian Basin

The Styrian Basin forms a marginal basin of the Pannonian Basin System, as it is separated by high zones and was connected via corridors to the adjacent Mura-Zala Basin and Radgona-Vas Basin during certain periods. The basin overlies the Eastern Alpine units (Berka, 2015).

In the Ottnangium, the basin filling began with limnic-fluviatile sediments (Kollmann, 1964). In the western Gnas Basin, stratigraphic sequences of shallow marine environment up to 1000 m thick are assumed (Sachsenhofer et al., 1996). The "Steirischer Schlier" are several hundred m thick clay-siltstones, formation depths of more than 100 m. In the transition to the West Styrian Basin, marginal marine sediments develop, which are interpreted as subaqueous mass movements, and in the Eibiswald sub-basin limnic-fluviatile cycles form, leading to coal seams (Gross, 2000). Acidic to intermediate volcanism developed in the Gnas Basin. Towards the end of the Carpathian, the increase in tectonic activity causes block rotations and uplift at the margin of the West Styrian Basin. An extensive regression initiated fan formation and erosion at the basin margins (Gross, 2000). In the Badenian, basement uplift progressed and volcanism shifted northwards; in the East Styrian Basin, deep-water development continues with turbidites. Around the high zones, the shallow-marine siliciclastics (Weissenegg Formation) formed, which are interlocked with coarse-clastic, deltaic deposits. Lagoonal fossil-rich sediments are found in the West Styrian Basin (Friebe, 1990; Gross, 2000). In the lower Sarmatian the transgressive tendency continued again, but the salinity decreased due to the strong freshwater supply and the restricted marine connections. In the East Styrian Basin, the Sarmatian sediments are

relatively homogeneous, but are subject to considerable variations in thickness (Gross, 2000). After a regression phase, the highly sweetened Central Paratethys flooded large parts of the East Styrian Basin. Clay/silt, marl and fine sands (partly with fossils) form in the brackish lake area. With decreasing subsidence, most of the East Styrian Basin was included in a fluviatile sedimentation area in the higher Lower Pannonian and the alluvial fans change towards the open basin into interlaced meandering rivers and subsequently into deltaic environment, deltaic/meander displacements and tectonic processes cause complex and rapid facies interlocking in this shallow depositional area. Middle and Upper Pannonian sediments underwent a similar lithological and fascial evolution (Gross, 1998, 2000). In the Pliocene, the uplift of the basin began. As a result, thick sediment packages are eroded. In addition, a second volcanic phase began with basaltic lava ex- and intrusions, covered by reservoir loams and fluviatile fine gravels (Pöschl, 1991; Fritz, 1996; Gross, 2000).

## 1.3 Previous studies on stream sediments in Styria

Manser et al. (1989) investigated the river section from Judenburg to Spielfeld. The question was addressed as to whether strongly fluctuating heavy metal concentrations are caused by antropogenic or geogenic factors. The heavy metals *Pb, Ni, Cu, Cr, Zn, Co* and *Hg* were investigated. It was found that the antropogenic input of heavy metals in the sediments is significantly higher than that due to mineralisation. It was also found that the influence of mineralogy and grain size distribution on comparability can be minimised by choosing a favourable fraction (< 40 um) (Manser et al., 1989).

In recent years, magnetic measurements have increasingly been used as an indicator of the heavy metal content of soils and sediments, especially those resulting from industrial emissions. Since it is difficult to determine how far back the contamination goes, Hanesch et al. (2003) obtain information on the current distribution of magnetic dust by means of magnetic measurements of tree leaves. For this purpose, 102 sites around Leoben were sampled. It was found that the soil map (magnetic susceptibility of the soil) and that of the leaves correspond. The main anomaly at the steel plant is identical in both maps. This suggests that both long-term and short-term input occurs at this site. The situation is different for the landfill areas (north-east of the steelworks). This anomaly is only evident in the soil map. This means that either the soils are more affected by landfilling than the foliage or that there has been no deposition activity during the growth period of the foliage. Disregarding these differences, both maps show the same general distribution of magnetic dust around the source (Hanesch et al., 2003).

Another study was conducted by Hanesch et al. (2007) to distinguish between signals of anthropogenic and geogenic pollution. The statistical evaluation of the analysis of susceptibility values, heavy metal concentrations and soil parameters in a large soil data set from the eastern part of Austria shows an influence of lithology and soil type on the magnetic susceptibility signal. All the approaches investigated managed to identify the main anomalies of the study area and could bypass the erroneous anomalies due to soil formation processes. However, knowledge of the lithological background is still essential for a meaningful interpretation of the results. This can only be replaced by a large amount of data. It was also found that the specific heavy metal signature represented by the susceptibility values must be determined separately for each area. Such a correlation was carried out in the Linz area. Both the magnetic susceptibility and the heavy metals were normally distributed. From this it was concluded that the anthropogenic input must be the only source in this area. In Carinthia, the measurement methods were used to successfully identify the large geogenic anomalies (Hanesch et al., 2007).

# Data Base

## 1.4 H2O database

The Federal Ministry of Agriculture, Regions and Tourism operates the H2O database of the Water Information System Austria (WISA). Since 1991, a large number of data have been collected on a regular basis within the framework of the national water monitoring programme. Every year, about 6.500 water samples are taken in Austria as part of the Gewässerzustandsüberwachungsverordnung, GZÜV and to survey water quality. These are chemically analysed for up to 140 individual parameters. This results in about 400.000 data sets annually throughout Austria, which are standardised for storage in the H2O technical database of the Federal Environment Agency. The data are made available as well validated raw data (https://wasser.umweltbundesamt.at/h2odb/fivestep/abfrageQdPublic.xhtml;
date of access: April 2021 – August 2021). the H2O database provides data on flowing waters, lakes and groundwater, as well as data from the isotope monitoring network. The results of the individual measuring points can be accessed via the database. collected data are then evaluated to draw conclusions about the natural condition and also to determine changes caused by polluting nutrient inputs or chemical pollutants. Such information is recorded in annual reports on Austria's water quality (BMLRT, 2021, 2022).

The retrieval of the monitoring sites for this work was done with the following workflow:

- Type of monitoring site: by type (flowing water) and allocation (responsibility).
- Monitoring sites: By jurisdiction (Styria) and planning area (MUR).
- Parameters: by parameter type (F and S)
- Period: by year (1991 - 2021)
- Output: as Excel file

Both F and S parameters were used. F-parameters represent the data measured in the water, S-parameters contain the measured values of the sediments. For water, the data are given in mg/l, for sediment, they are available in mg/kg dry sediment < 40 μm. In particular, the data of the elements aluminium, iron, manganese, arsenic, cadmium, chromium, copper, mercury, nickel, lead and zinc were selected. Furthermore, extraction of the flow rate data was used for this study.

## 1.5 Geochemical Atlas of Austria

For the compilation of the Geochemical Atlas of Austria (Pirkl et al., 2015), stream sediments were investigated nationwide over a long period of time. The raw material information system "IRIS Online" is a most comprehensive information system on deposits and occurrences of mineral raw materials in Austria. In addition to the location and detailed information on more than 5700 raw material deposits, various geological, aerogeophysical and geochemical information can be found. The totality of all raw material deposits, in the same tectonic unit, secondary rock bond, form, valuable material content and genesis, was subdivided into metallogenetic districts (Pirkl et al., 2015; Geologische Bundesanstalt, 2018; Lipiarski et al., 2019).

There are a total of 18 IRIS-Online data levels that can be accessed in the online application. For this study, special attention was paid to the layer of stream sediments (http://gisgba.geologie.ac.at/arcgis/rest/services/projekte_iris/IRIS_Bachsediment_Geochemie/MapServer; date of access: February 2021 – March 2021).
For this layer the federal territory has been systematically sampled geochemically since 1978. More than 34,500 samples were taken and analysed for a total of 35 elements (Geologische Bundesanstalt, 2018; Lipiarski et al., 2019). In Pirkl et al. (2015) the results were published in a summarising documentation. Via IRIS Online, these results of stream sediment geochemistry are displayed on an overview scale, either calculated by area (up to 1:200,000) or as point symbols.

# Methodics

## 1.6 H2O database

A total of 424 monitoring points are located in the study area. Data were selected according to the parameters relevant for this work. 33 monitoring sites (see Figure 3) have data sets relevant to this work, i.e. parameters measured in flowing water in the flowing wave (F-parameters) or in the sediment (S-parameters). Of these 33 measuring points, 28 points have both F- and S-parameters, the remaining measuring points only have F-parameters (Annex 1).

The parameters include the elements aluminium, arsenic, lead, cadmium, chromium, iron, copper, manganese, nickel, mercury and zinc, as well as flow rate. From the F parameters, the data representing the dissolved fraction in the flowing water are used. The sediment parameters contain the elements of arsenic, lead, cadmium, chromium, copper, nickel, mercury and zinc, given in mg/kg dry sediment < 40 µm.

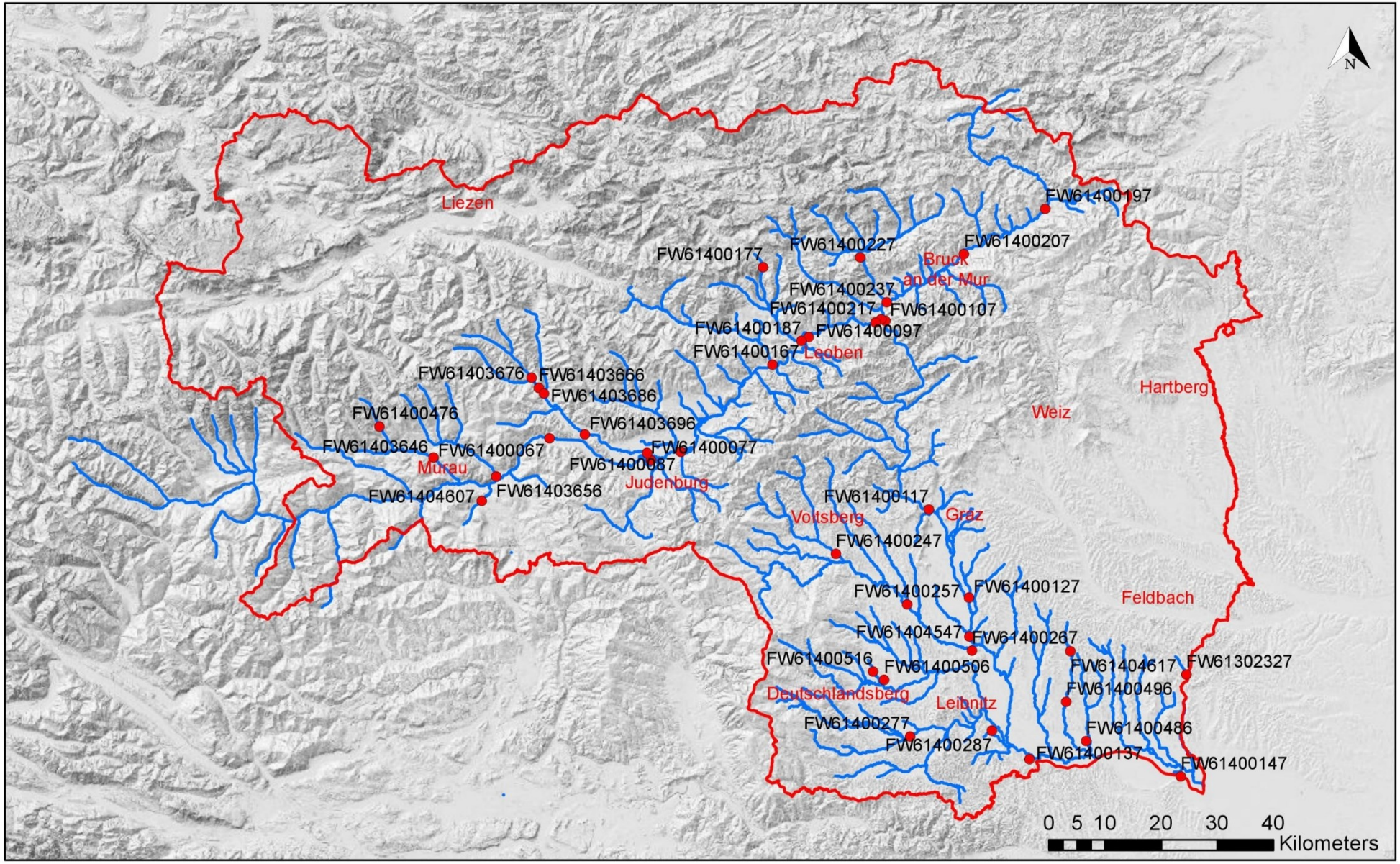


*Figure 3: Sampling points in Styria*

## 1.7 Sampling and analysis

### 1.7.1 Selection of sample points

Based on the data from the H2O technical database, a location was selected where, a more detailed analysis of the sediment was carried out. The area with the highest heavy metal concentration from the governmental data was selected. Since the measuring point of the Vordernberger Bach shows highest values of several heavy metals (see below), Leoben was chosen. Along the Mur, ten sampling points were defined, extending from Häuselberg to Proleb (see Figure 4).

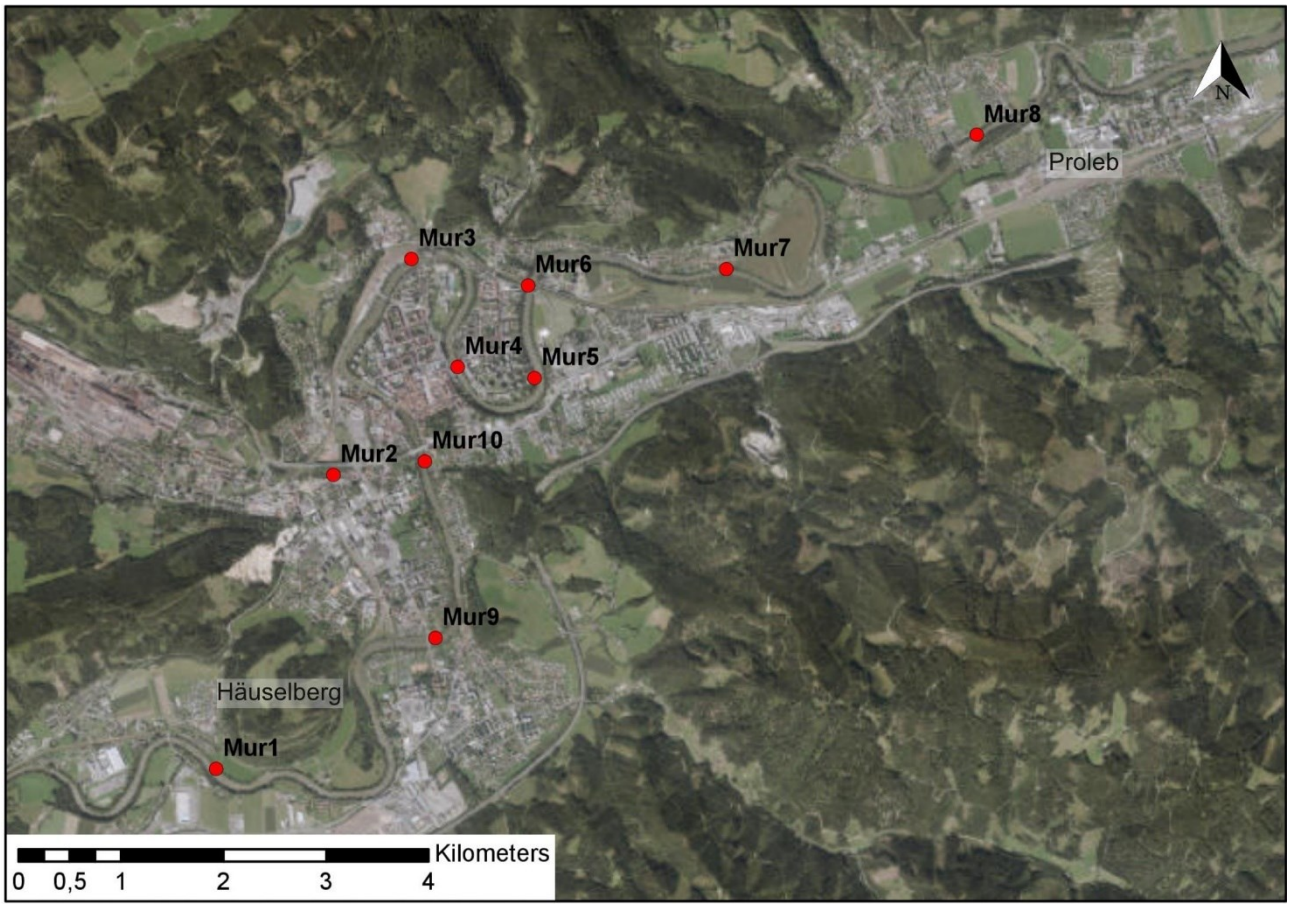


*Figure 4: Sampling points in Leoben; all orthophotos © basemap.at*

### 1.7.2 Sampling

About 1kg of the fine-grained fraction of the stream sediment was taken. Sampling was carried out on the river bank in the shallow water area (see Figure 5). The stream sediment was taken with a plastic cup and filled into paper bags (see Figure 5).

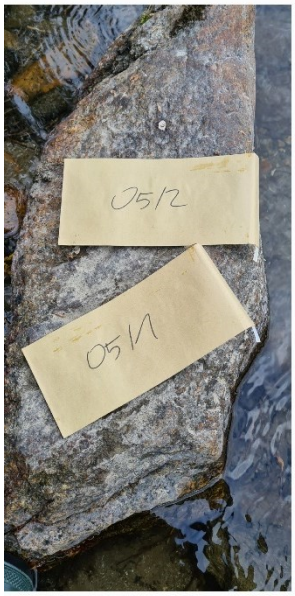


*Figure 5: Sampling Point and sampling tools*

### 1.7.3 Sample preparation and sample analysis

The samples were dried in an oven at 105 °C until mass constancy. Subsequently, the grain fractions smaller than 0.18 mm were separated using a sieve (see Figure 6) and further ground (see Figure 6). The samples were then dried again and cooled to room temperature in a desiccator.

In a second step, about 4g of the prepared samples were filled and weighed, then burned at 1050 °C (see Figure 7) and weighed again to determine the loss on ignition.

In the third step, the samples were prepared for XRF measurements. For this purpose, 1.0000 g (± 0.0005 g) of the annealed samples was filled into a platinum tigel (see Figure 7) and 8.0000 g (± 0.0005 g) of di-lithium tetraborate was added as flux. The samples were then melted at 1200 °C in an Eagon melting furnace (see Figure 7) and cast into platelets (see Figure 7).

The cooled samples were analysed with a PANalytical Axios X-ray fluorescence spectrometer with XRF (using a calibration created with GeoPT rock standards) (see Figure 7).


*Figure 6: 0.18 mm sieve and ball mill*

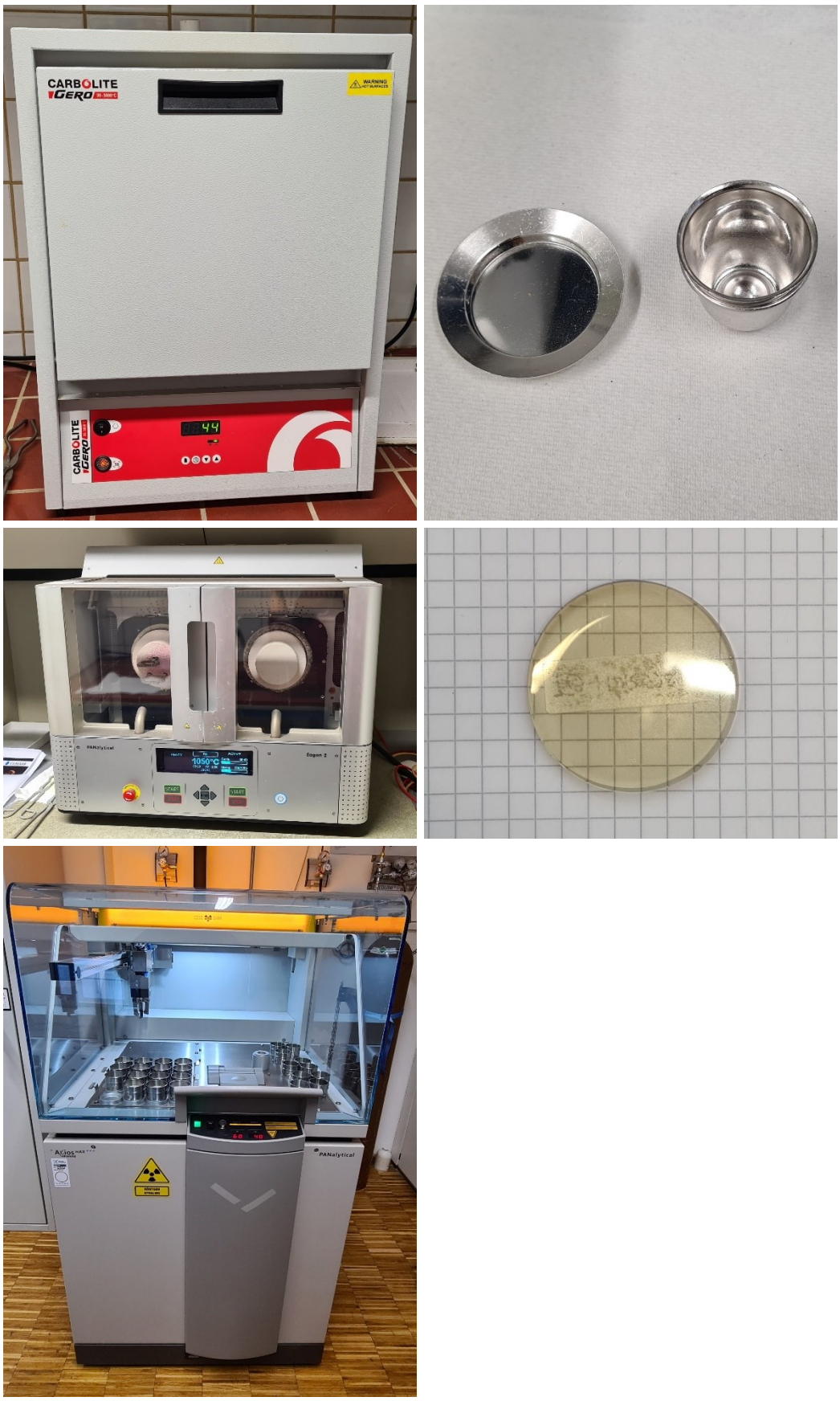


*Figure 7: Oven (determination of the LOI); platinum tigel; Eagon melting furnace; platelet for measurements; PANanalytical Axios X-ray fluorescence spectrometer*

# Chapter 5 – Geochemical pattern

## 1.8 H2O database and Geochemical Atlas

### 1.8.1 Dissolved river water fraction

The following chapters show the data of the respective elements separately (Tab. 2). Measuring point FW61400187 is located in Leoben in the Vordernberger Bach (Figure 8). At this monitoring site, the values of almost every element are slightly to significantly elevated.


*Figure 8: Location measuring points FW6140187 and FW61400097*

| Element | Median [mg/l] | Standard Deviation [mg/l] | Maximum Value [mg/l] | Number of Measurements |
|---|---|---|---|---|
| Al | 0.0112 | 0.0243 | 0.1200 | 2072 |
| Fe | 0.0220 | 0.0239 | 0.1330 | 2211 |
| Mn | 0.0130 | 0.0083 | 0.0580 | 2110 |
| As | <0.0007 | 0.0007 | 0.0025 | 2482 |
| Cd | <0.0001 | 0 | 0.0003 | 2398 |
| Cr | <0.001 | 0.0003 | 0.0020 | 2253 |
| Cu | <0.001 | 0.0014 | 0.0060 | 2271 |
| Hg | <0.0001 | 0 | <0.0001 | 2261 |
| Ni | <0.001 | 0.0005 | 0.0022 | 2253 |
| Pb | <0.001 | 0.0003 | 0.0015 | 2268 |
| Zn | 0.0025 | 0.0104 | 0.0758 | 2262 |

*Table 2: Summary of the F-Parameters considered in the Mur area, values in mg/l*
*The data represent the medians of all 33 measuring points (H2O database) for the respective elements.*

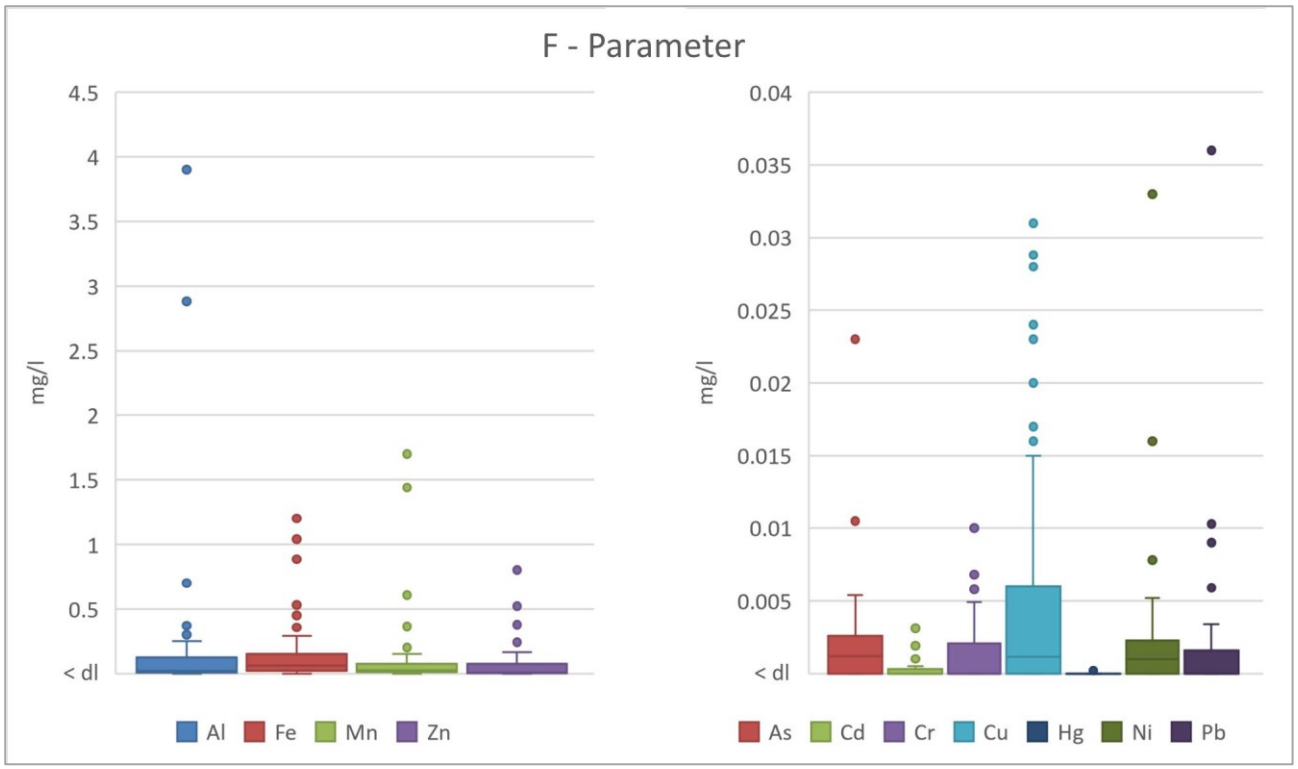


*Figure 9: Summary of the F-Parameters considered in the Mur area, values in mg/l*

### 1.8.2 Sediment

The measuring point FW61499187 is particularly conspicuous - as with the F-parameters, the S-parameters are slightly to significantly elevated in many elements. In addition, measuring point FW61400237 shows slightly to significantly elevated values for almost all elements shown. This monitoring site is located near Kapfenberg in the Thörlbach at the confluence of the Mürz (Figure 10).


*Figure 10: Location measuring point FW6140273*

| Element | Median [mg/kg] | Standard Deviation [mg/kg] | Minimum Value [mg/kg] | Maximum Value [mg/kg] | Number of Measurements |
|---|---|---|---|---|---|
| As | 14.325 | 6.629 | 7.80 | 25.00 | 228 |
| Cd | 0.323 | 0.839 | <0.05 | 2.90 | 228 |
| Cr | 50.550 | 24.631 | 28.50 | 96.15 | 228 |
| Cu | 39.850 | 23.833 | 18.50 | 85.35 | 228 |
| Hg | 0.169 | 0.141 | <0.05 | 0.48 | 228 |
| Ni | 46.925 | 21.121 | 25.00 | 85.50 | 228 |
| Pb | 34.975 | 25.484 | 13.00 | 99.55 | 228 |
| Zn | 122.750 | 67.289 | 59.40 | 232.00 | 228 |

*Table 3: Summary of the S-Parameters considered in the Mur area, values in mg/kg DS*
*The data represent the medians of all 28 measuring points (H2O database) for the respective elements.*

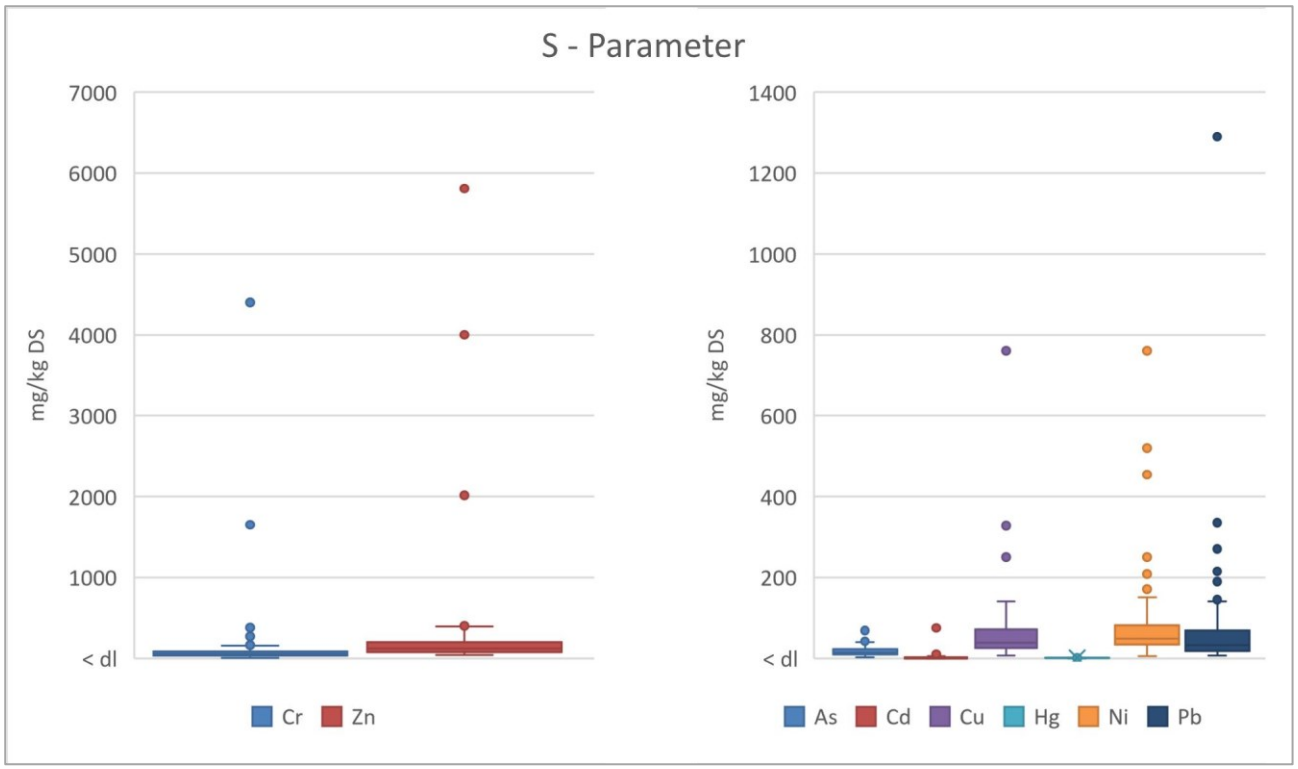


*Figure 11: Summary of the S-Parameters considered in the Mur area, values in mg/kg DS*

## 1.9 Aluminium

*Al* was only recorded in the F parameters. Monitoring sites FW61400097 (Leoben) and FW61400117 (Graz), both located in the Mur River, are particularly prominent. Both the median values (FW61400097 0.1 mg/l; FW61400117 0.06 mg/l), and the maximum values (FW61400097 2.88 mg/l; FW61400117 3.9 mg/l) are clearly above Styrian median and maximum values. The separately considered measuring point FW61499187 in the Vordernbergerbach shows only slightly increased values in relation to the average values of Styria, both in the median, and in the maximum value. Figure 12 - 15

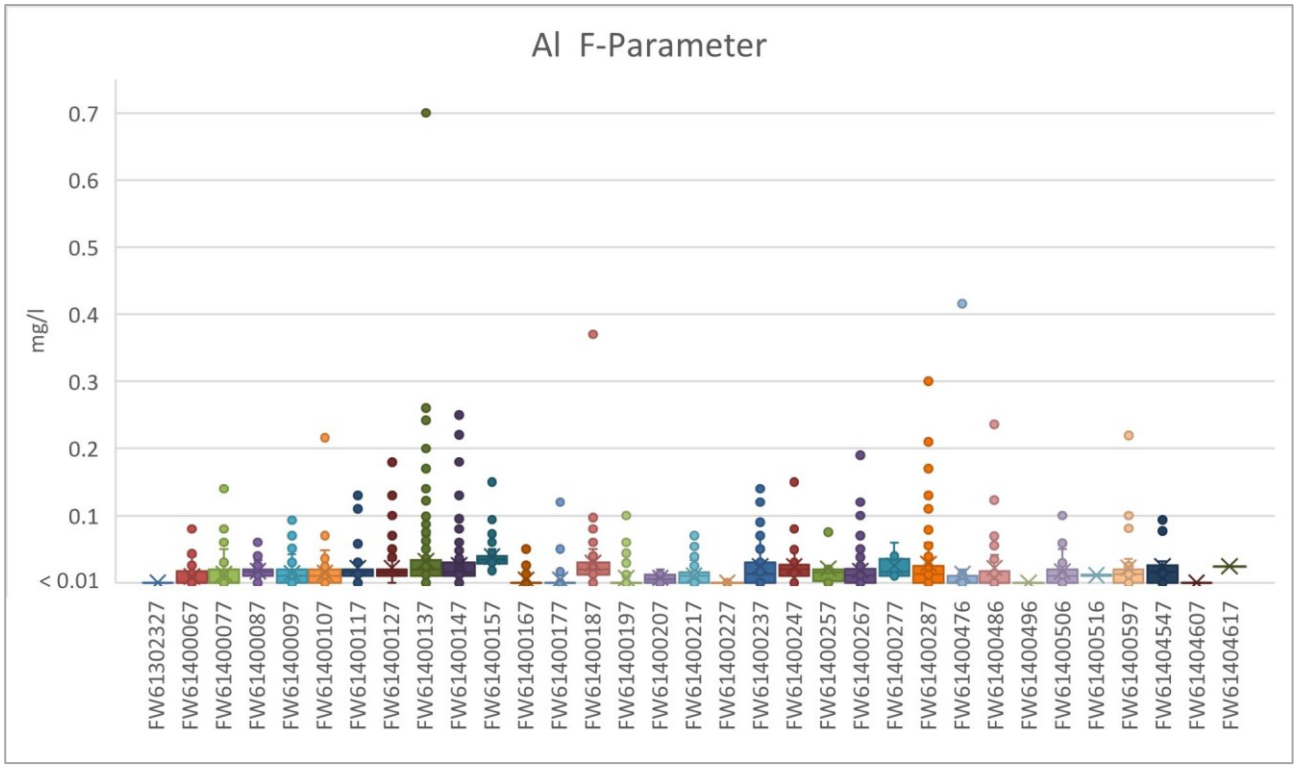


*Figure 12: Al F-Parameter*
*The measuring points were sorted by consecutive number (assigned by the Federal Ministry) in all diagrams.*

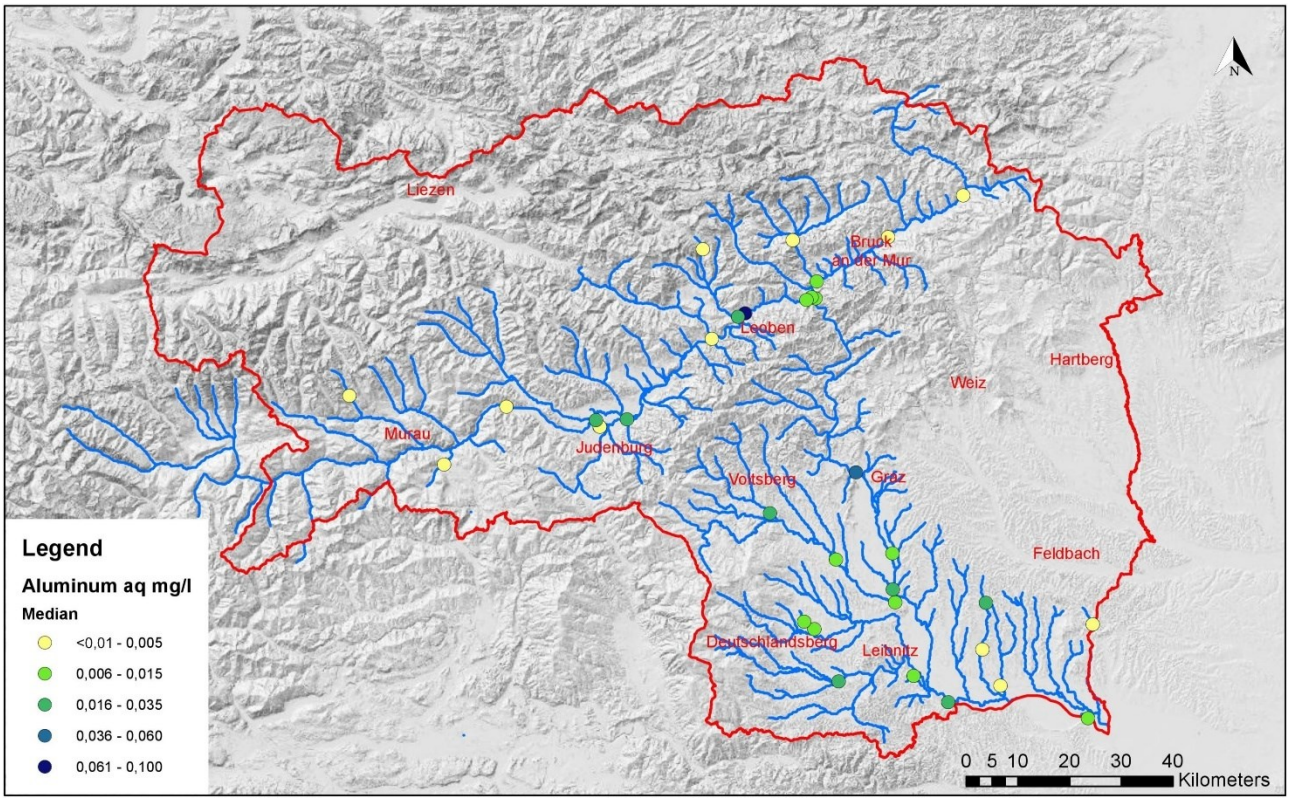


*Figure 13: Aluminum F-Parameter; Median Values*
*Classification in all maps is based on natural breaks (jenks).*

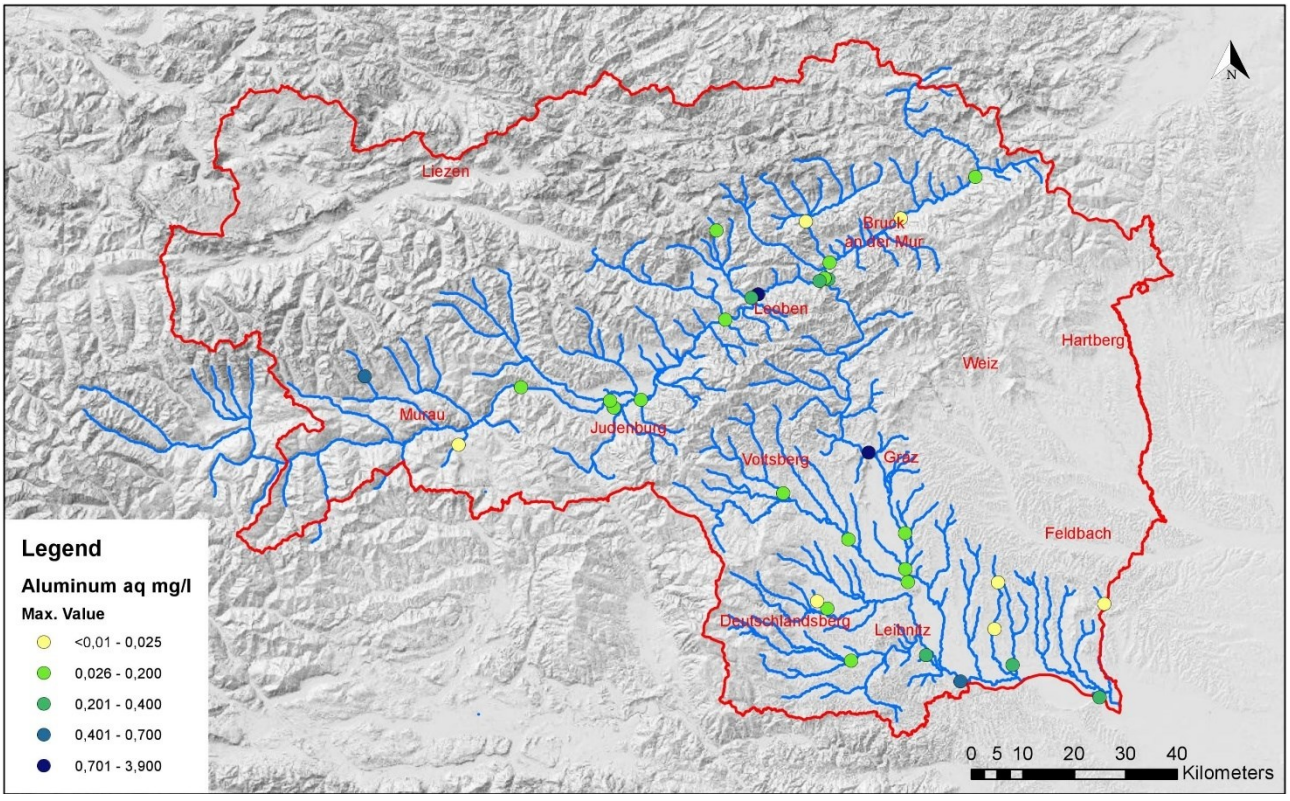


*Figure 14: Aluminum F-Parameter; Maximum Values*


*Figure 15: Detail section measuring point FW61400187, F-Parameter*

## 1.10 Iron

Iron shows a clear peak at the median value, FW61400516 which is located in the Vochera Bach (Gersdorf). However, as only two measurements were taken at this site, this median is not a representative value. Measuring point with the next highest representative median is FW61400287, located in the Sulm. The other monitoring sites fluctuate only slightly around the Styrian median. The highest maximum value was measured at monitoring site FW61400137 (1.2 mg/l). Figure 16 - 19

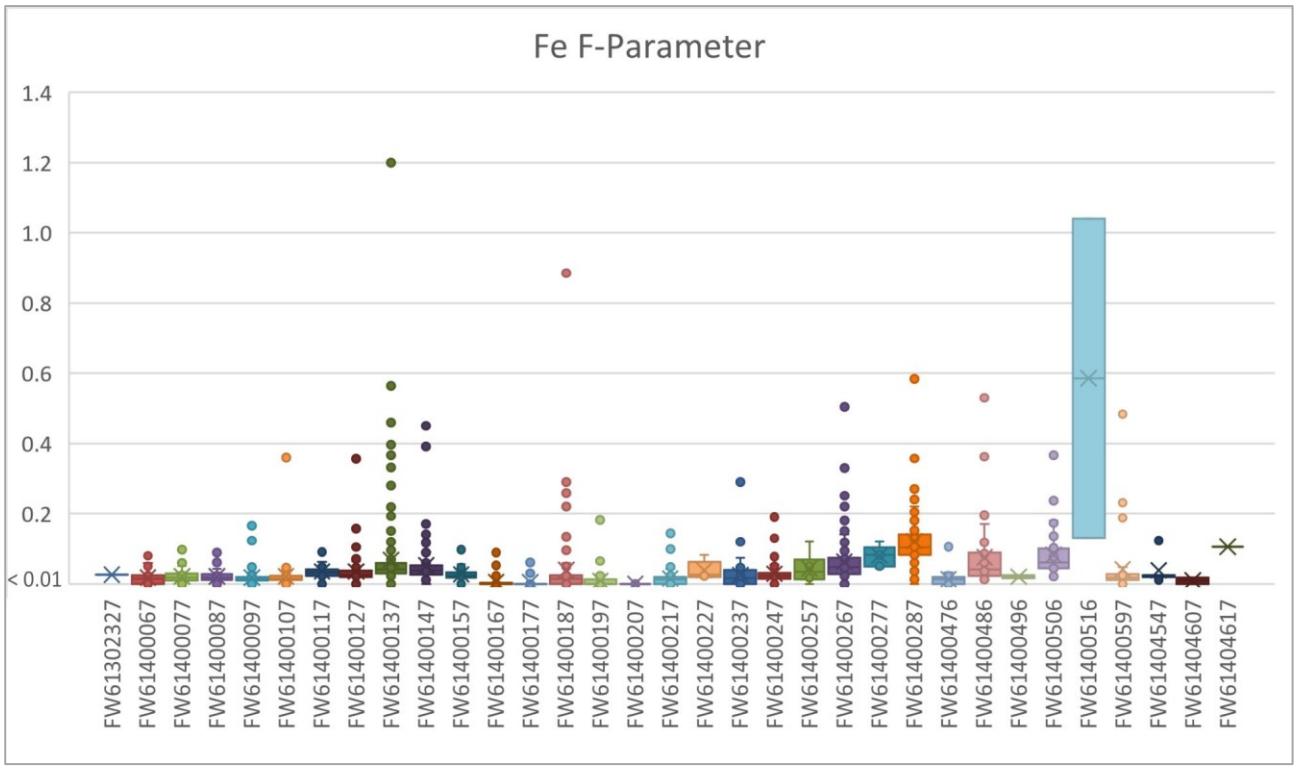


*Figure 16: Fe F-Parameter*

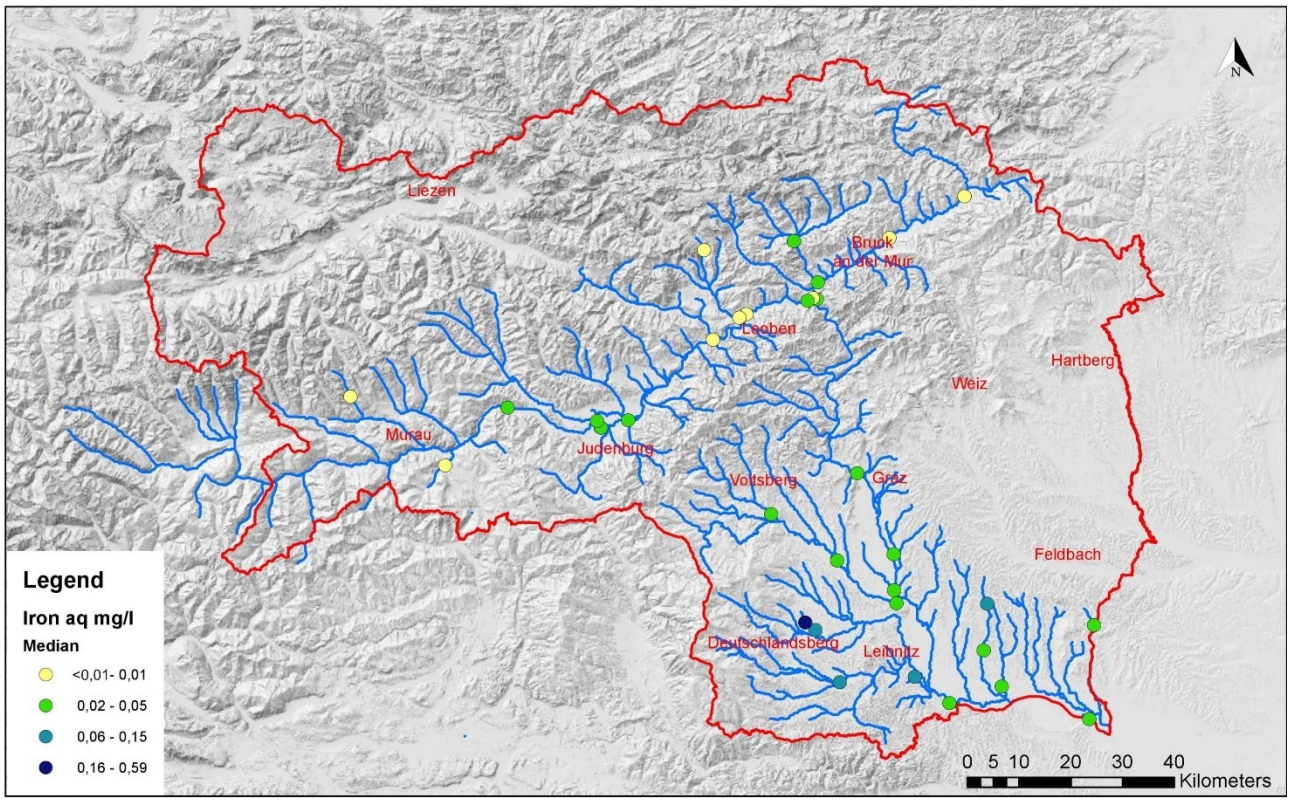


*Figure 17: Iron F-Parameter; Median Values*

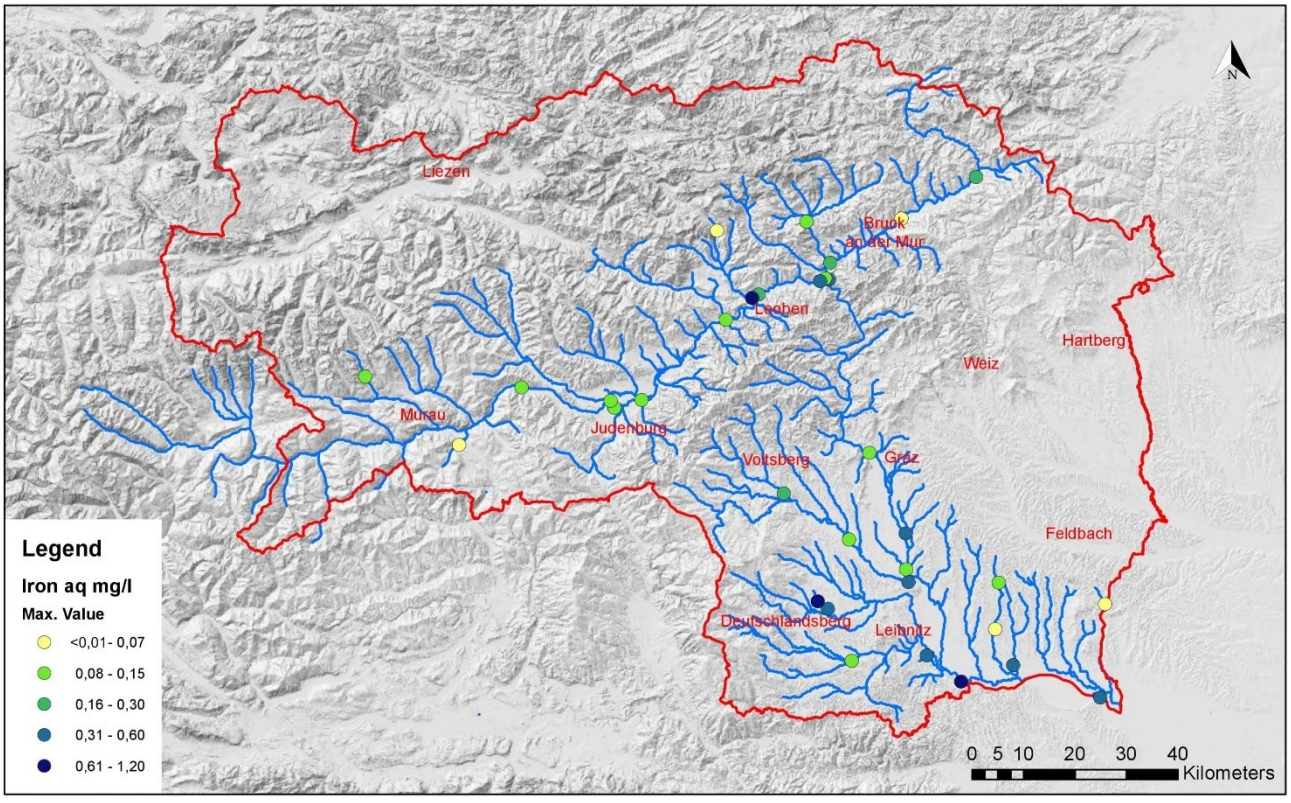


*Figure 18: Iron F-Parameter; Maximum Values*


*Figure 19: Detail section measuring point FW61400187, F-Parameter*

## 1.11 Manganese

Some of the measuring points with the highest peaks do not have representative values. For example, measurement point FW61400516 has the highest median value, but only two measurements. The second highest measured value was recorded in the Saßbach (FW61400496), which also has only two measured values. At monitoring site FW61400187 (1.7 mg/l) the highest maximum value is recorded. Furthermore, the measuring points FW61400486, as well as FW61400516 and FW61400496 have slightly increased values. All other monitoring sites are within a small range of the Styrian maximum value. Figure 20 - 23

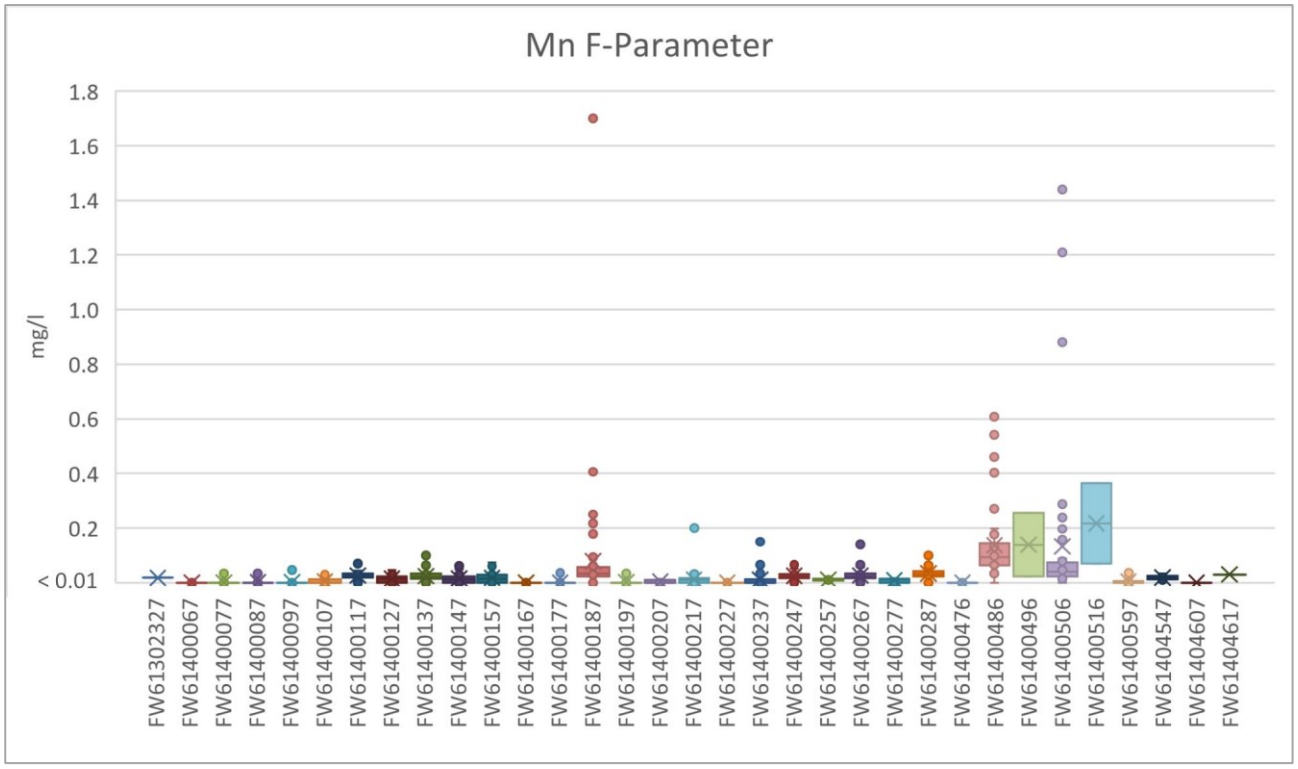


*Figure 20: Mn F-Parameter*

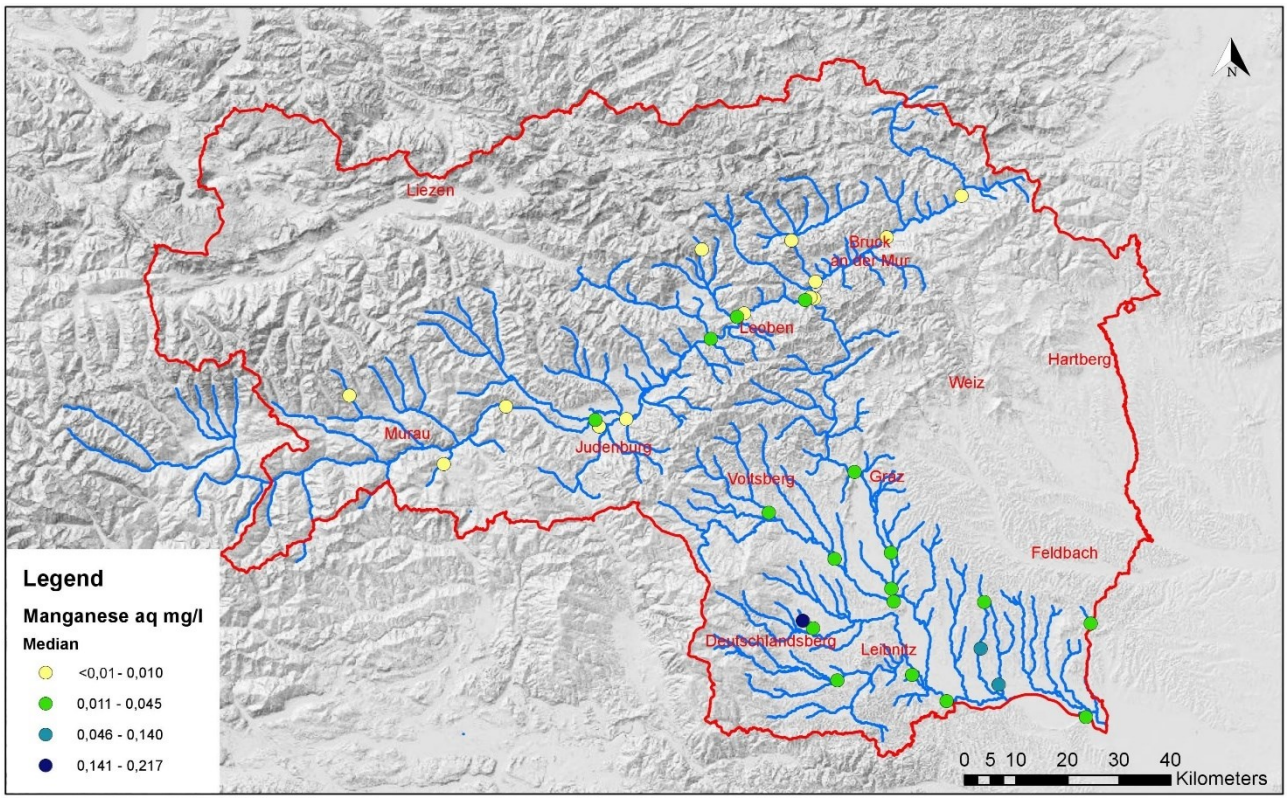


*Figure 21: Manganese F-Parameter; Median Values*

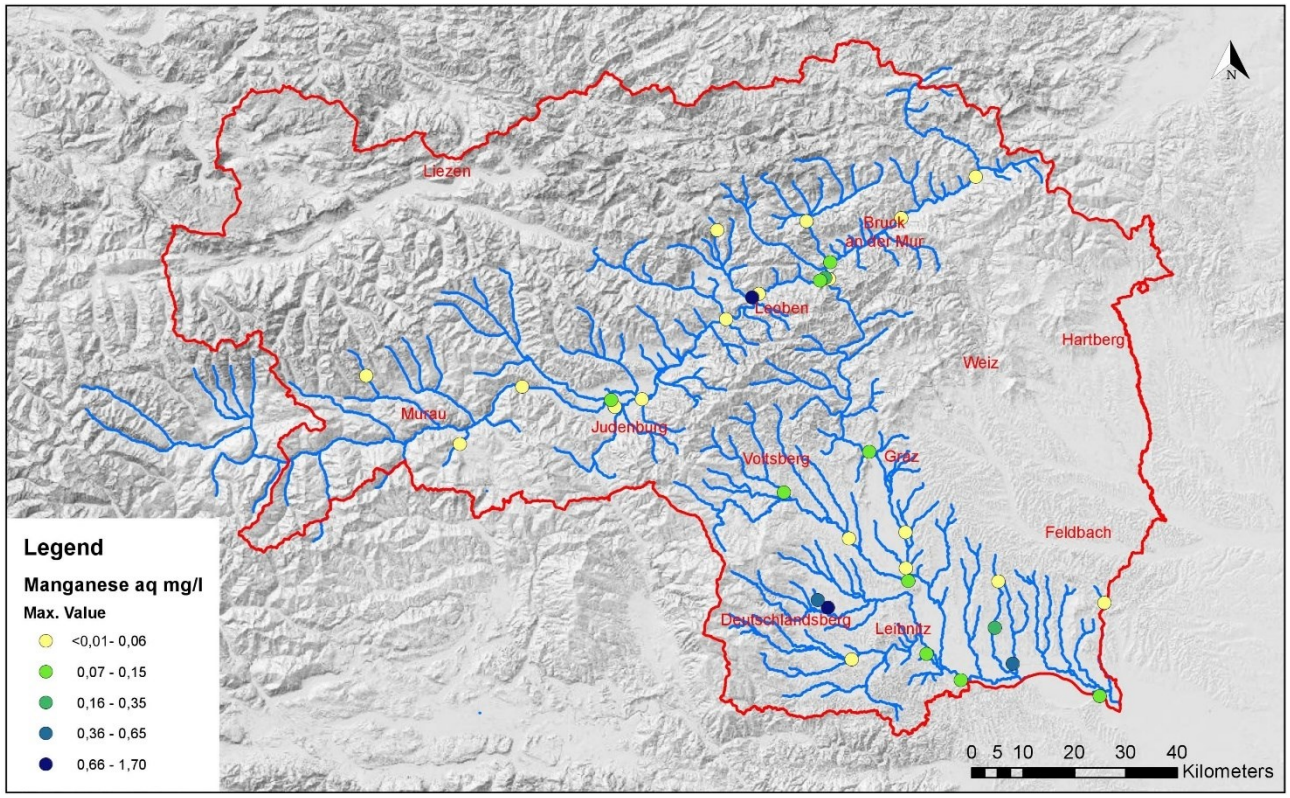


*Figure 22: Manganese F-Parameter; Maximum Values*


*Figure 23: Detail section measuring point FW61400187, F-Parameter*

## 1.12 Arsenic

### 1.12.1 F-Parameters

The measuring point FW61404607 in the Thayabach is a clear outlier (Figure 26 - 27). However, since this monitoring site has only 12 readings, the standard deviation is relatively high and the median value is not representative. All other measuring points are in the range of the Styrian values. Only monitoring site FW1400496 (Saßbach) shows a slightly higher median value. Measuring point FW61400187 is also inconspicuous in terms of *As* values.
Figure 24, 26, 27, 30

### 1.12.2 S-Parameters

The highest deviation from the Styrian median is shown by monitoring site FW61400476 (2 readings; 57.2 mg/kg), followed by monitoring site FW61400197 (9 readings, 46 mg/kg). Maximum values fluctuate very strongly around the Styrian maximum value. Highest value was recorded at monitoring site FW61400197 (88 mg/kg). 79.4 mg/kg were measured at monitoring site FW61400476. The separately considered measuring point FW61400187 shows a maximum value of 69 mg/kg and a median value of 26.45 mg/kg for a total of eight measurements. Figure 25, 28, 29, 31

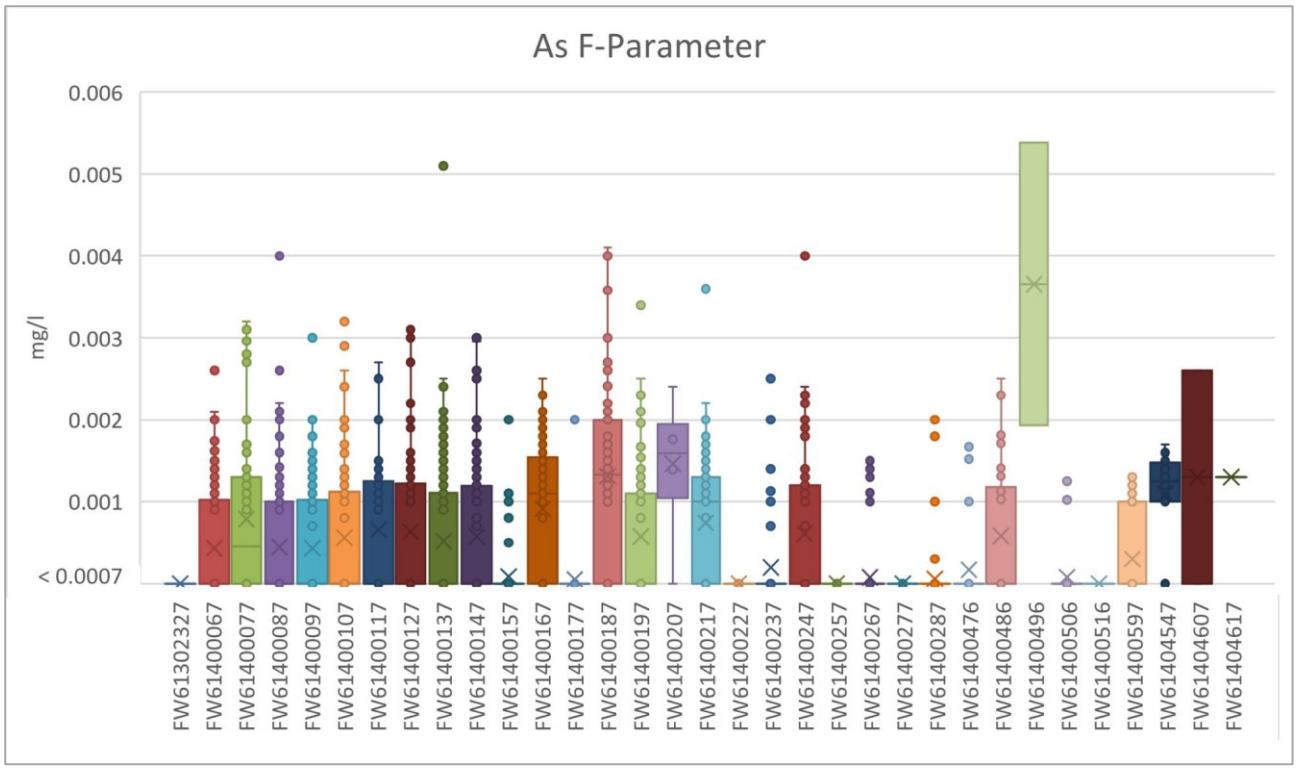


*Figure 24: As F-Parameter*

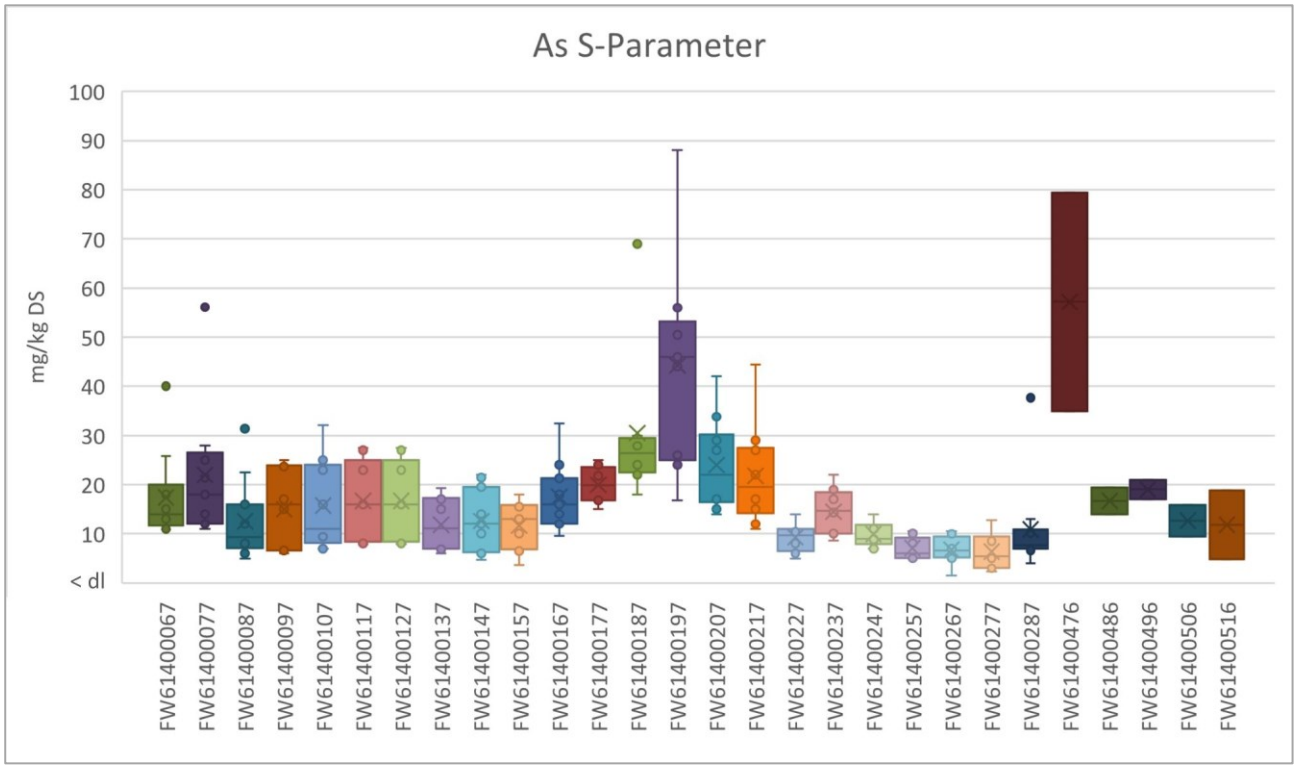


*Figure 25: As S-Parameter*

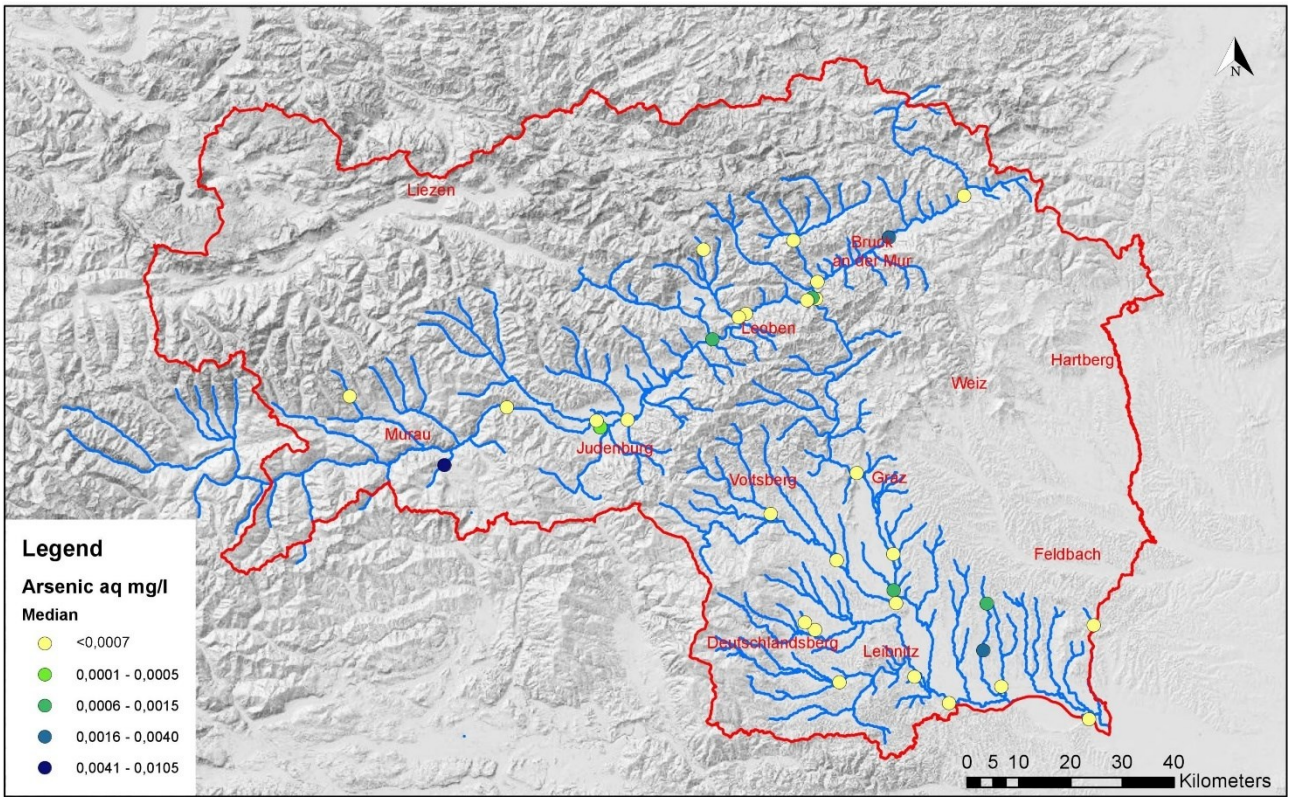


*Figure 26: Arsenic F-Parameter; Median Values*

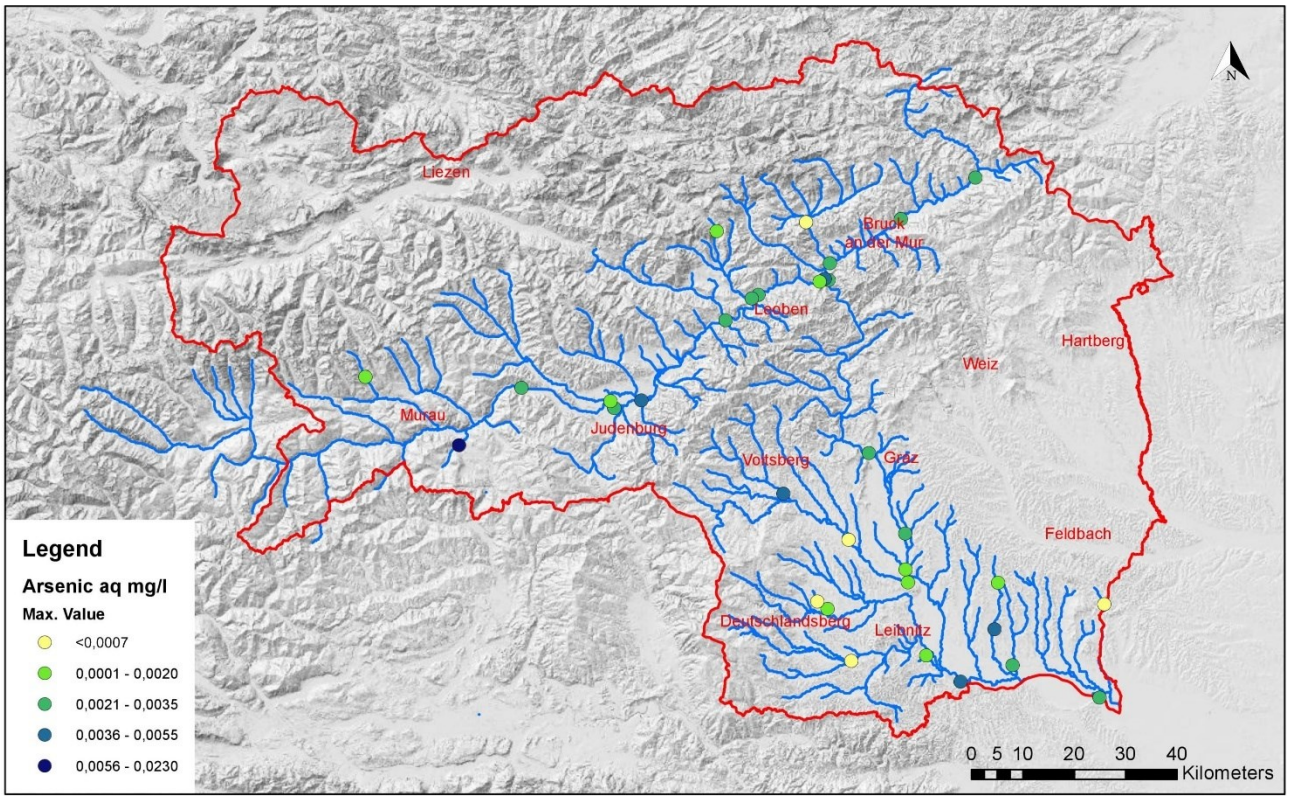


*Figure 27: Arsenic F-Parameter; Maximum Values*

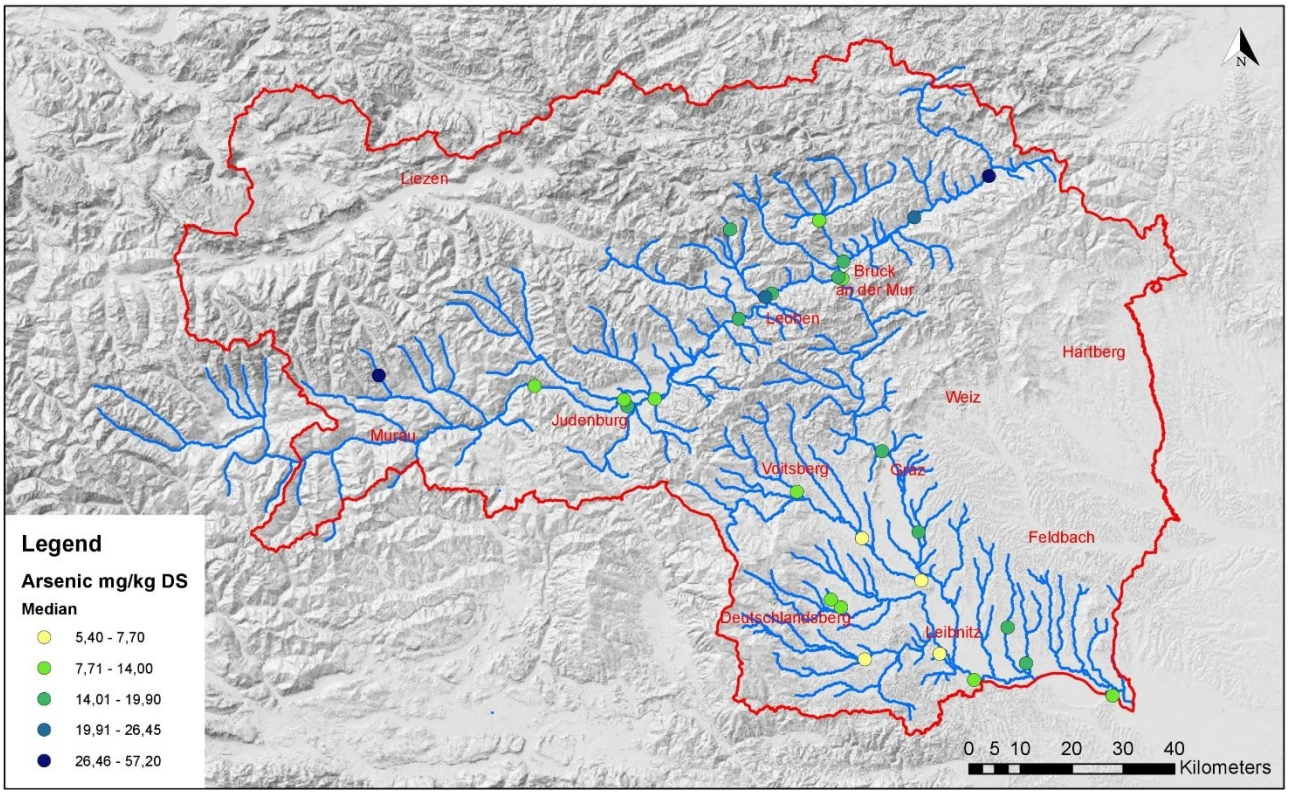


*Figure 28: Arsenic S-Parameter; Median Values*

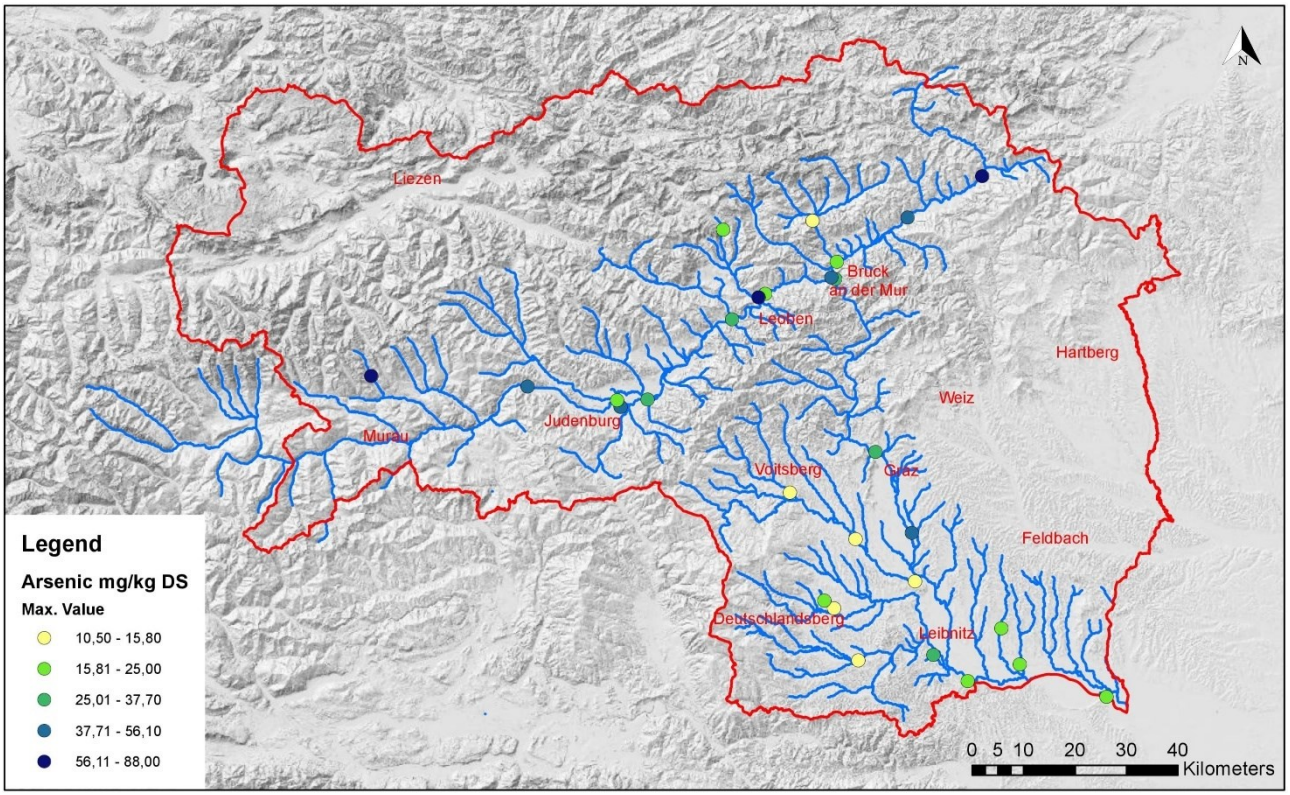


*Figure 29: Arsenic S-Parameter; Maximum Values*


*Figure 30: Detail section measuring point FW61400187, F-Parameter*


*Figure 31: Detail section measuring point FW61400187, S-Parameter*

## 1.13 Cadmium

### 1.13.1 F-Parameters

At all monitoring sites, the median value of the F-parameters is below the detection limit. Measuring point FW61400187 (0.0031 mg/l) shows the highest. Five other monitoring sites exceed the Styrian maximum by a considerable margin (FW61400127, FW61400137, FW61400247, FW61400267, FW61400287). Figure 32, 34, 35, 38

### 1.13.2 S-Parameters

For this element the measuring point FW61400187 shows the only outliers, both in the median value (10.04 mg/kg) and in the maximum value (75.1 mg/kg). All other measured values are around the Styrian median (0.3225 mg/kg) and the maximum value (2.9 mg/kg) with slight fluctuations. Figure 33, 36, 37, 39

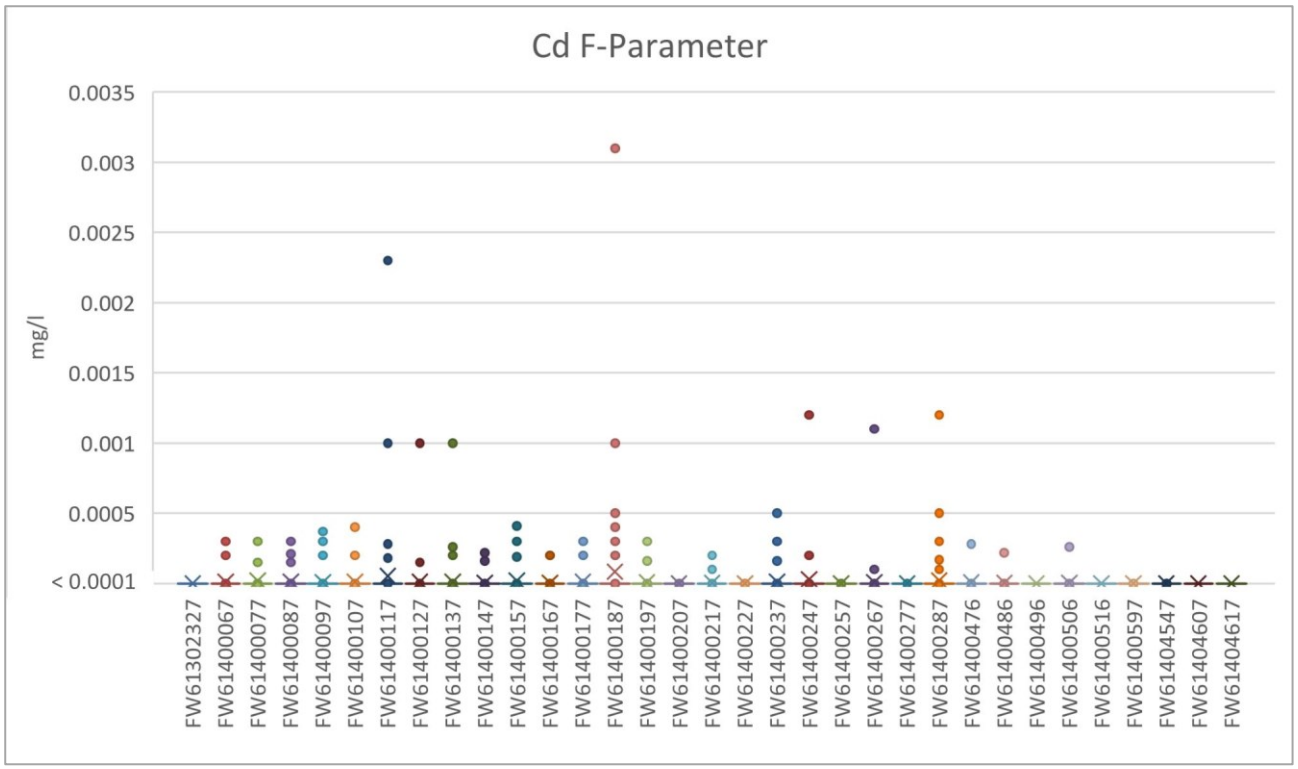


*Figure 32: Cd F-Parameter*

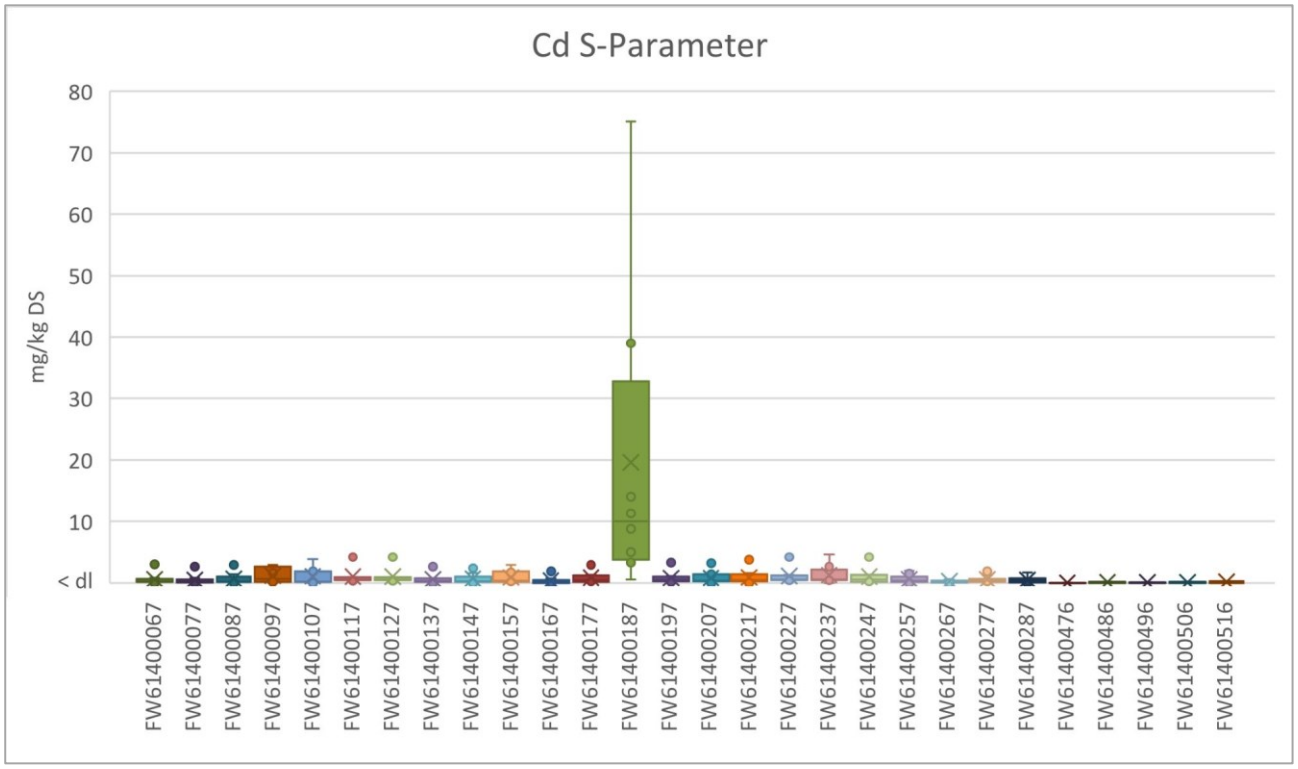


*Figure 33: Cd S-Parameter*

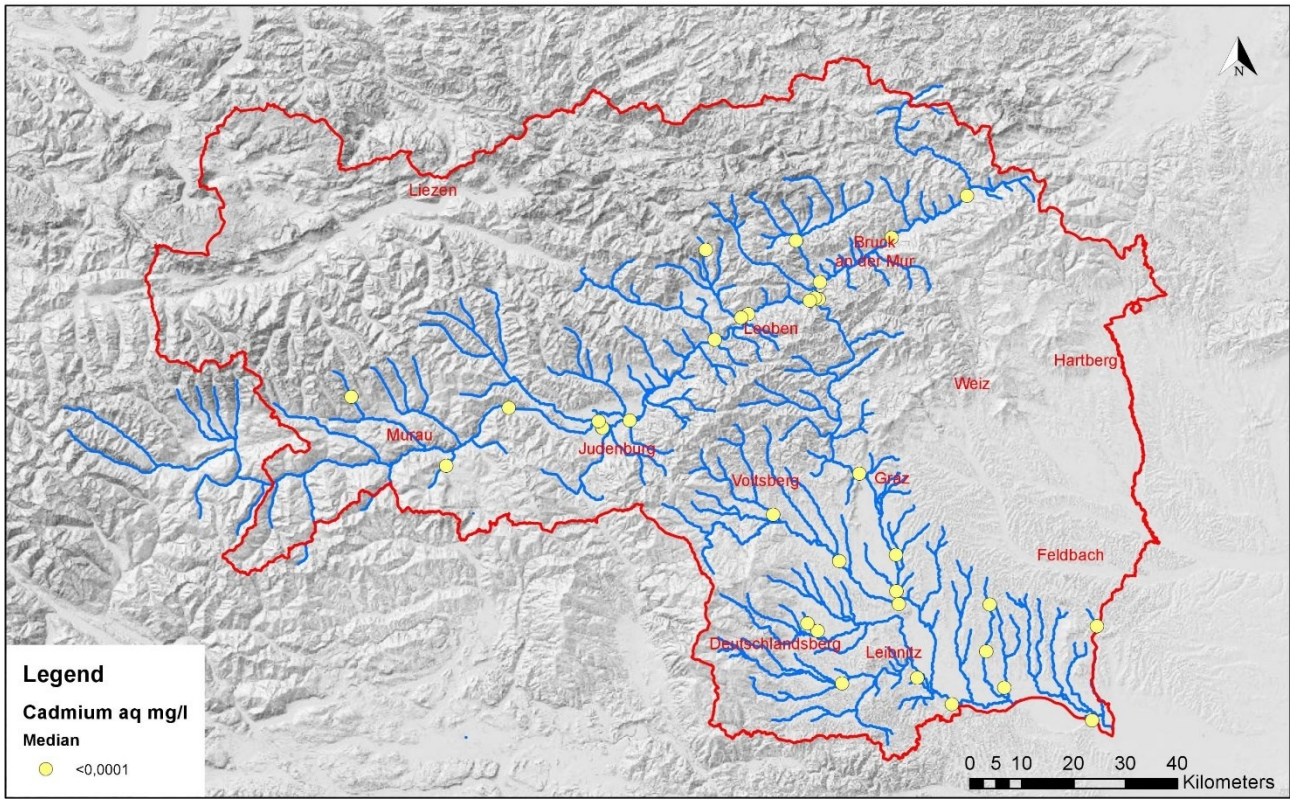


*Figure 34: Cadmium F-Parameter; Median Values*

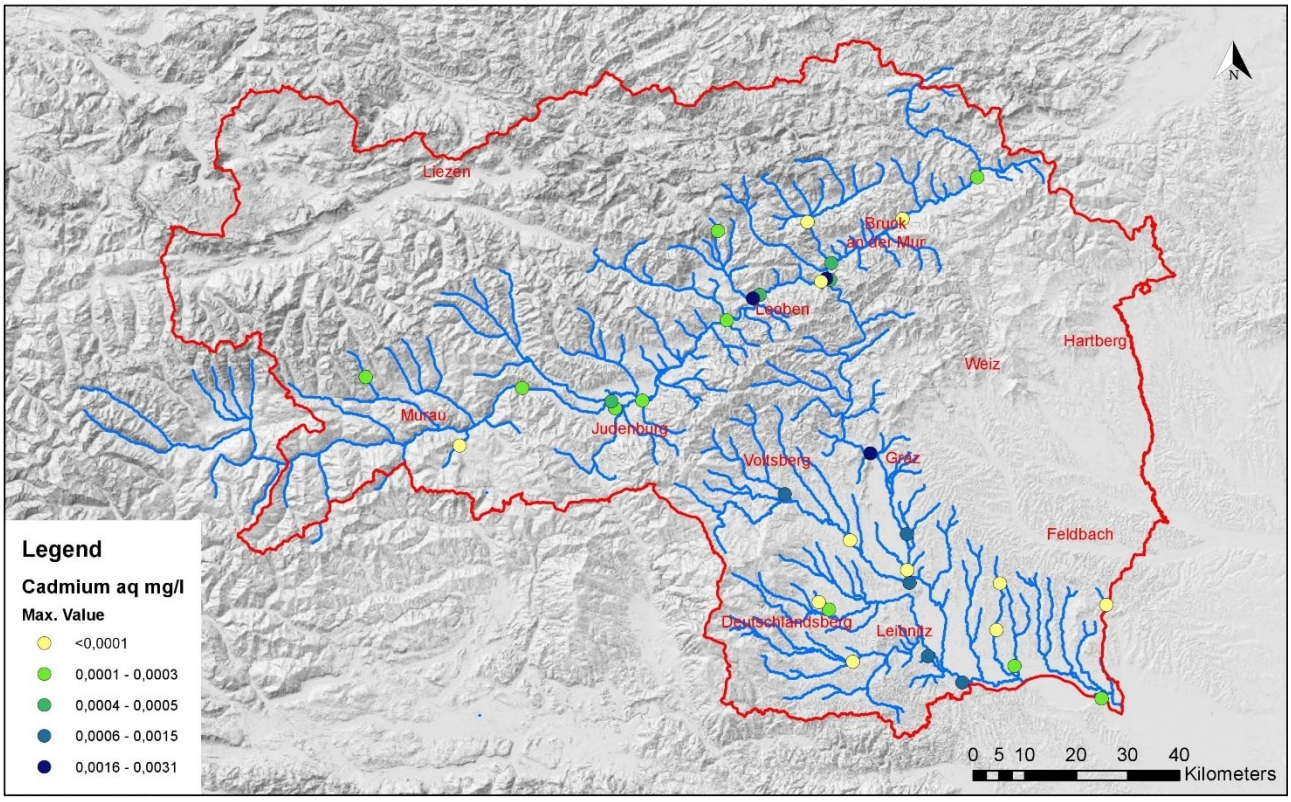


*Figure 35: Cadmium F-Parameter; Maximum Values*

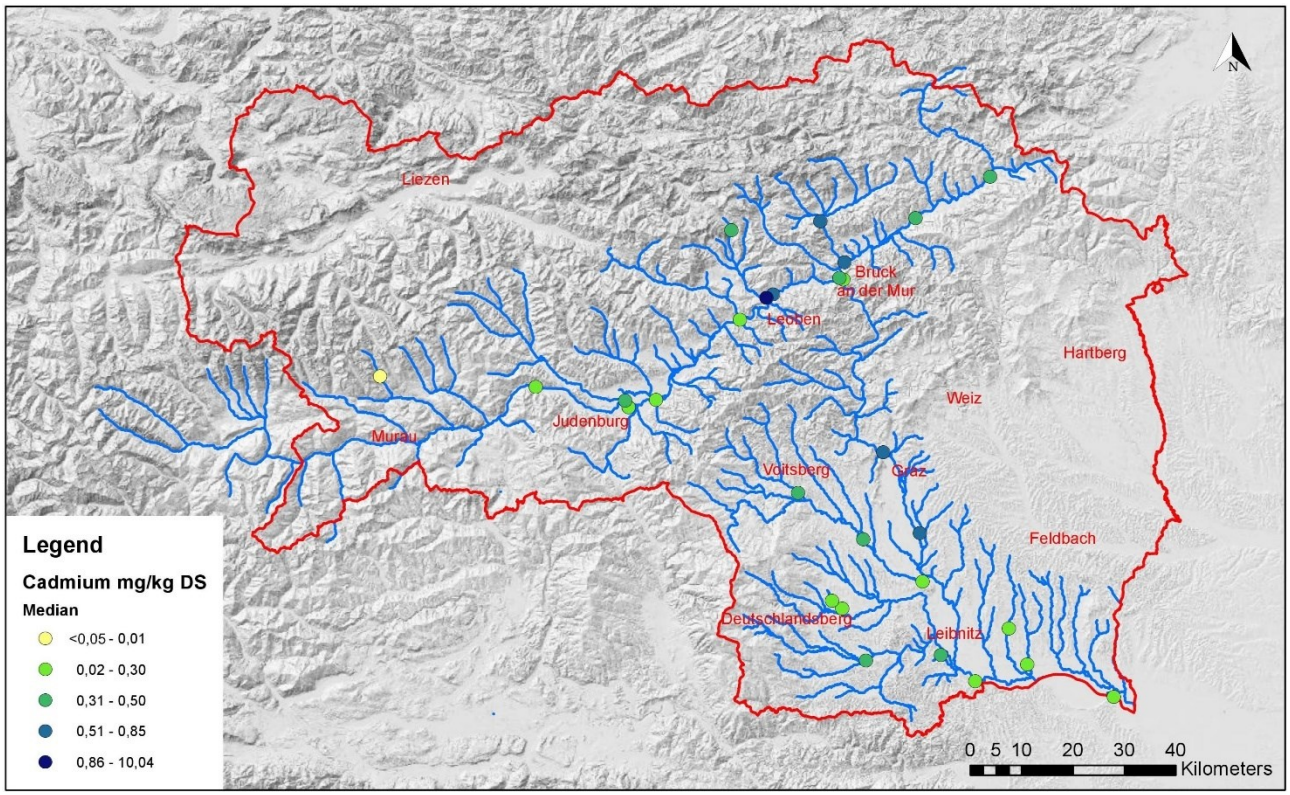


*Figure 36: Cadmium S-Parameter; Median Values*

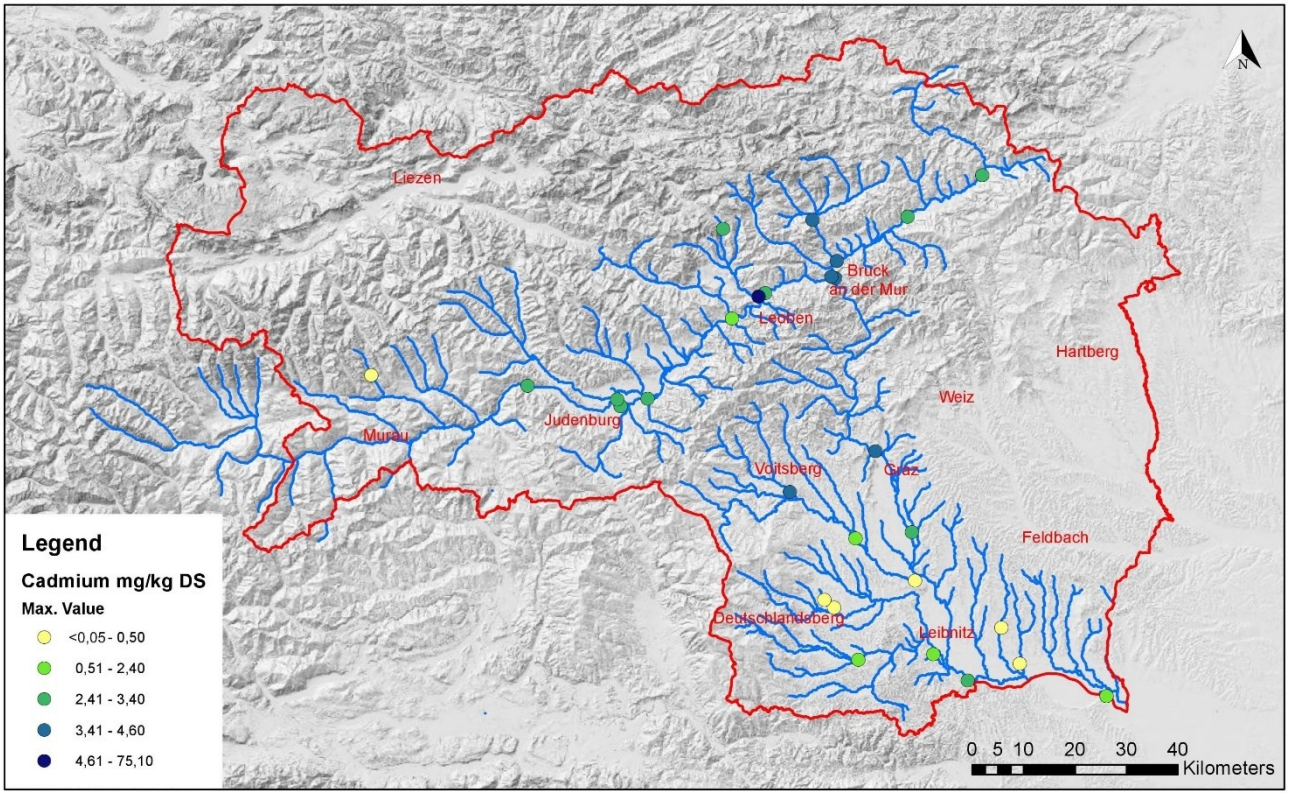


*Figure 37: Cadmium S-Parameter; Maximum Values*


*Figure 38: Detail section measuring point FW61400187, F-Parameter*


*Figure 39: Detail section measuring point FW61400187, S-Parameter*

## 1.14 Chromium

### 1.14.1 F-Parameters

The maximum values varies considerably at very many monitoring sites. Their highest content was measured at monitoring site FW61400207 (Mürz; 0.01 mg/l). All other monitoring sites range between a maximum content of 0.0068 mg/l (FW61400137) and < dl. Measurement point FW61400187 in the Vordernbergerbach, which was considered separately, has a maximum value of 0.0036 mg/l. Figure 40, 42, 43, 46

### 1.14.2 S-Parameters

Analogous to the element cadmium, there is a very clear deviation from the Styrian values at one single measuring point. The measuring point FW61400237 shows a median value of 1650 mg/kg and a maximum value of 4400 mg/kg. Slightly elevated values are also detected at measuring point FW61400217 (median: 160 mg/kg; maximum value: 381 mg/kg). The other measuring points deviate only slightly from the Styrian median (50.55 mg/kg) and maximum value (96.15 mg/kg).
Figure 41, 44, 45, 47

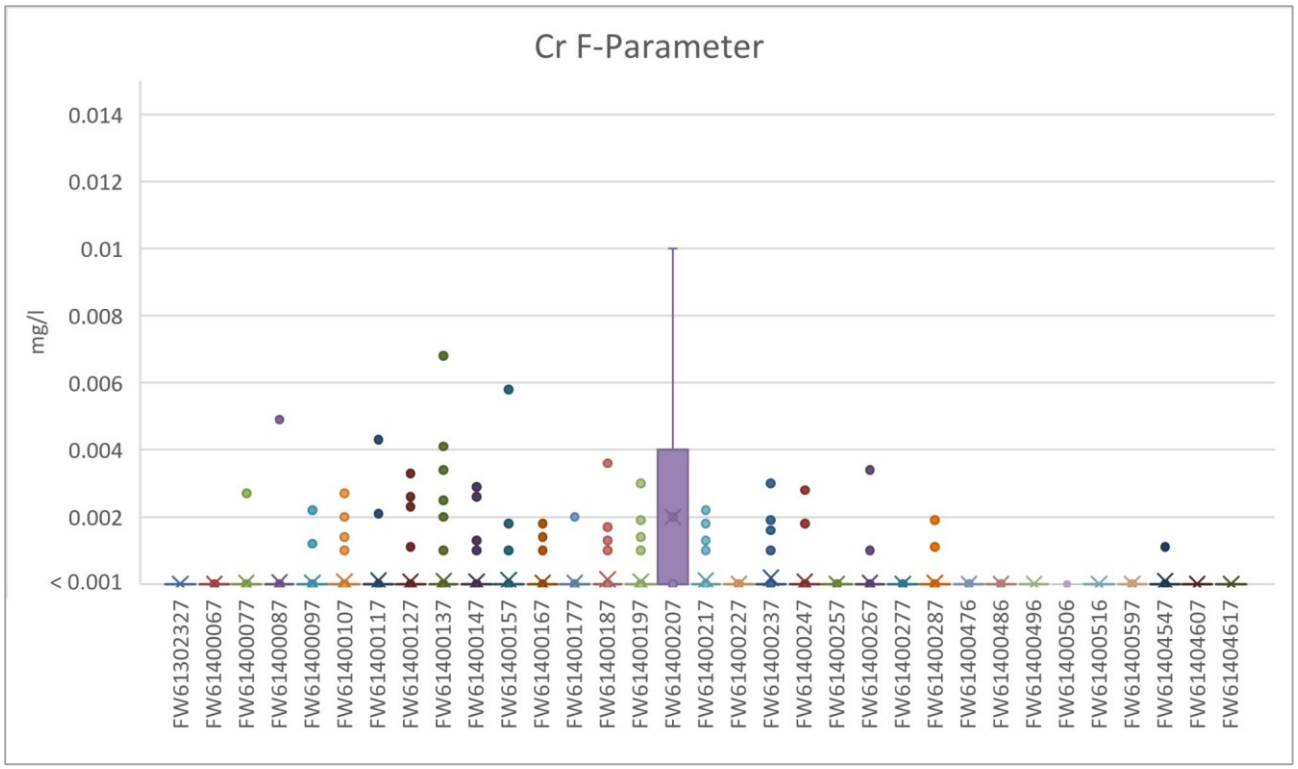


*Figure 40: Cr F-Parameter*

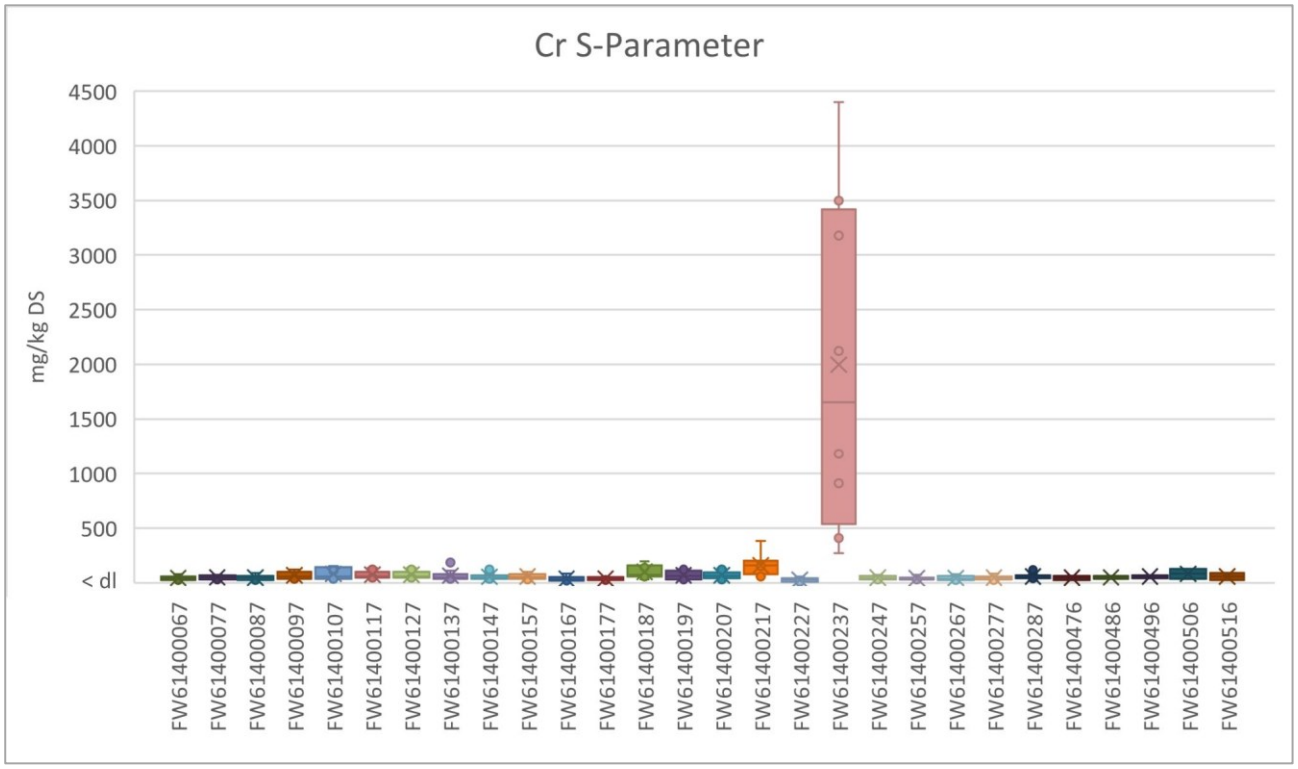


*Figure 41: Cr S-Parameter*

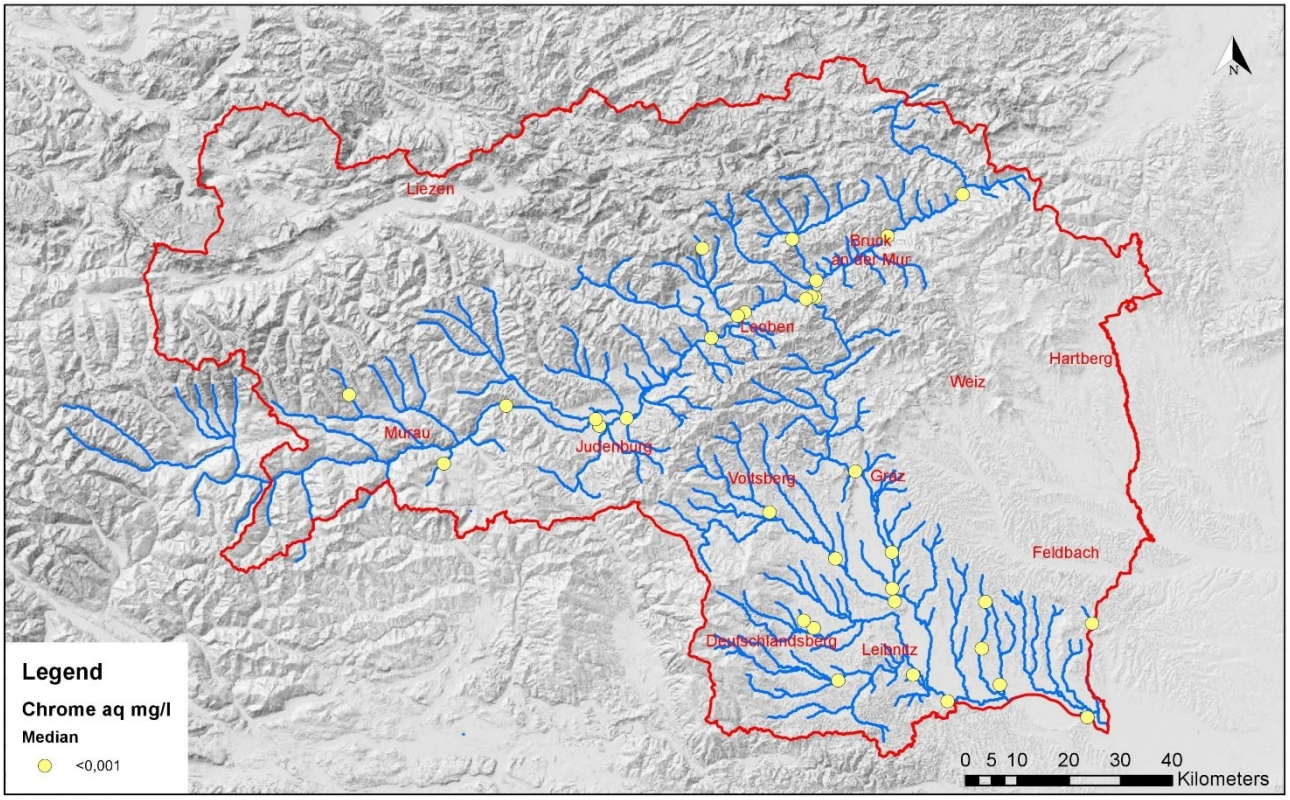


*Figure 42: Chrome F-Parameter; Median Values*

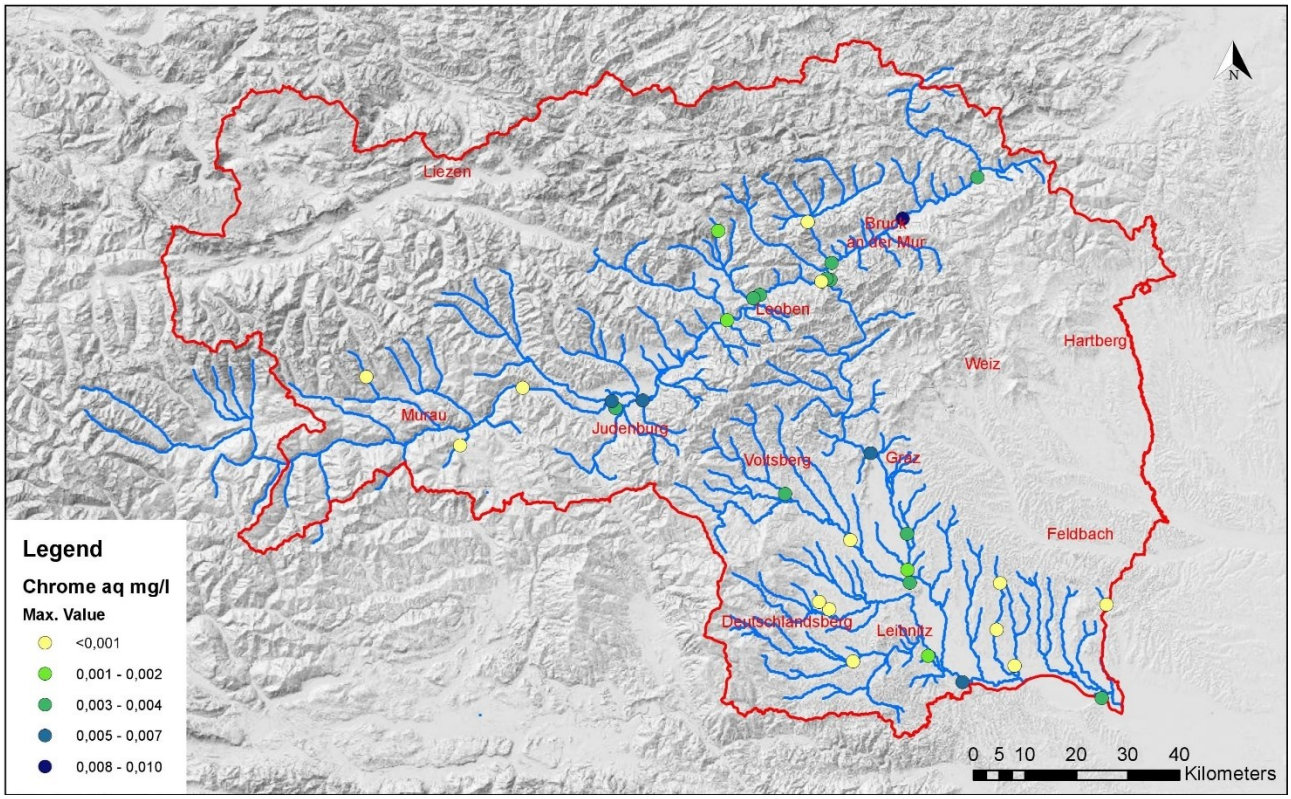


*Figure 43: Chrome F-Parameter; Maximum Values*

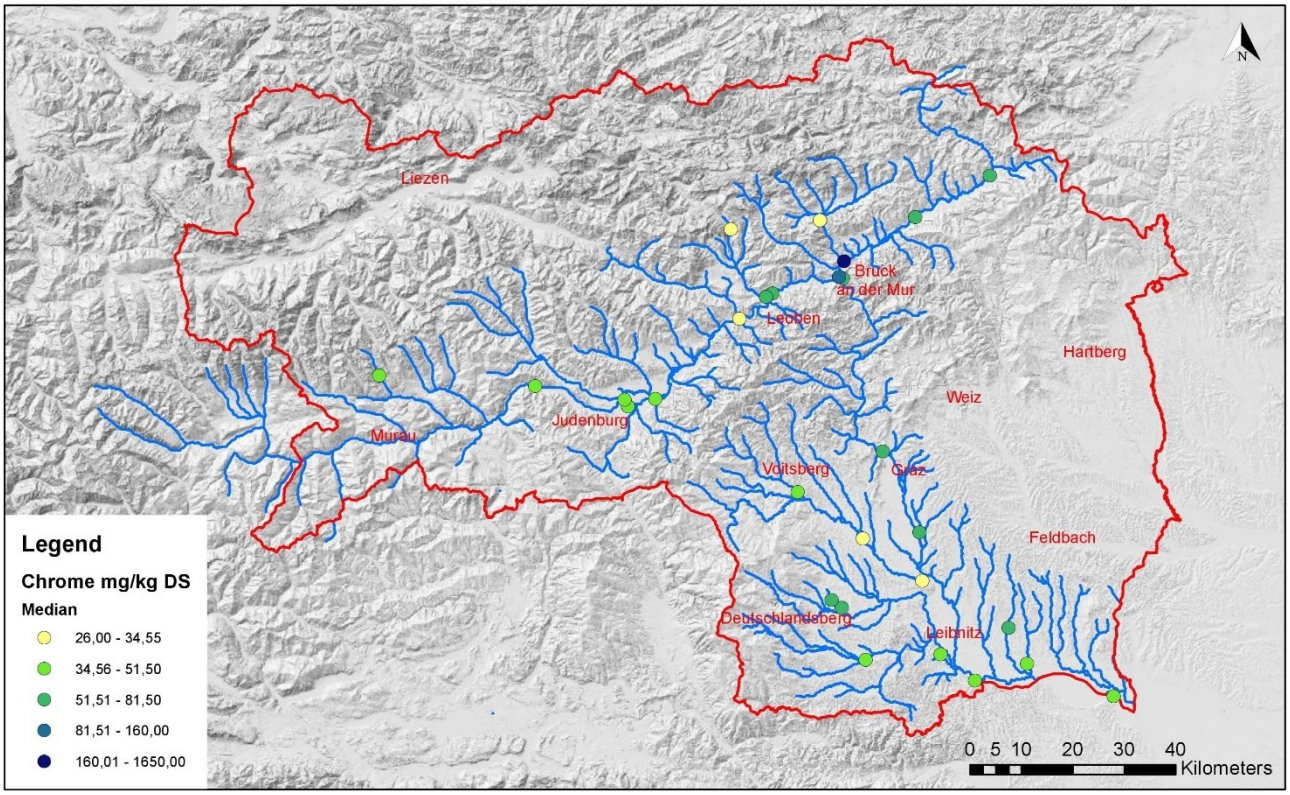


*Figure 44: Chrome S-Parameter; Median Values*

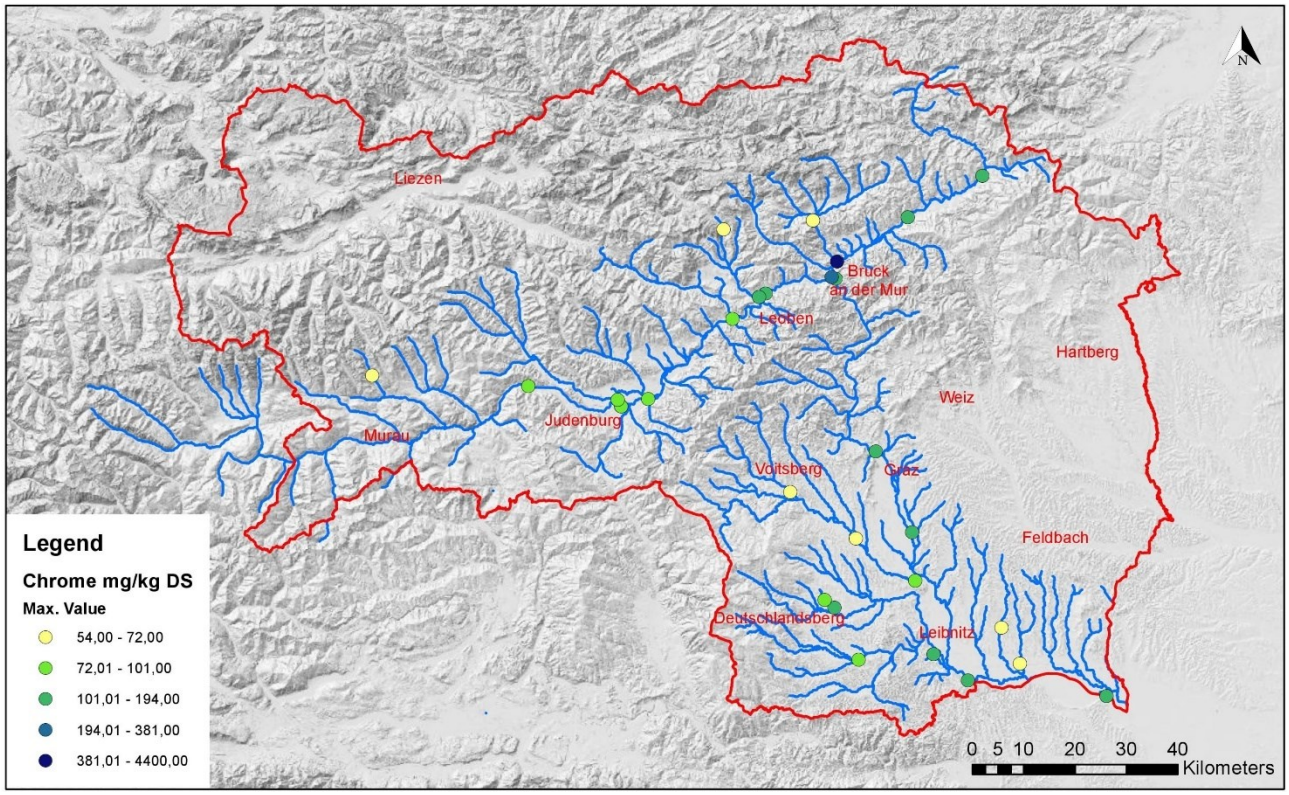


*Figure 45: Chrome S-Parameter; Maximum Values*


*Figure 46: Detail section measuring point FW61400187, F-Parameter*


*Figure 47: Detail section measuring point FW61400187, S-Parameter*

## 1.15 Copper

### 1.15.1 F-Parameters

Compared to the other elements, copper shows the greatest variation between the individual measuring points. There are four levels of medians with similar readings. This is controlled by the analytical constraints. Measuring point FW61400247 forms one tier with the highest median of 0.003 mg/l. Measuring point FW61400187 shows a maximum value of 0.02 mg/l. Figure 48, 50, 51, 54

### 1.15.2 S-Parameters

For copper, too, the two measuring points FW61400187 and FW61400237 stand out. FW61400237 shows a clearly increased median value of 250 mg/kg, the measuring point FW61400187 only a slightly increased median value of 70.8 mg/kg. In the map of maximum values these two sampling points also distinguish (FW61400187: 328 mg/kg; FW61400237: 760 mg/kg). The other measured values are again in the range of the Styrian values (median: 39.85 mg/kg; maximum: 85.35 mg/kg).
Figure 49, 52, 53, 55

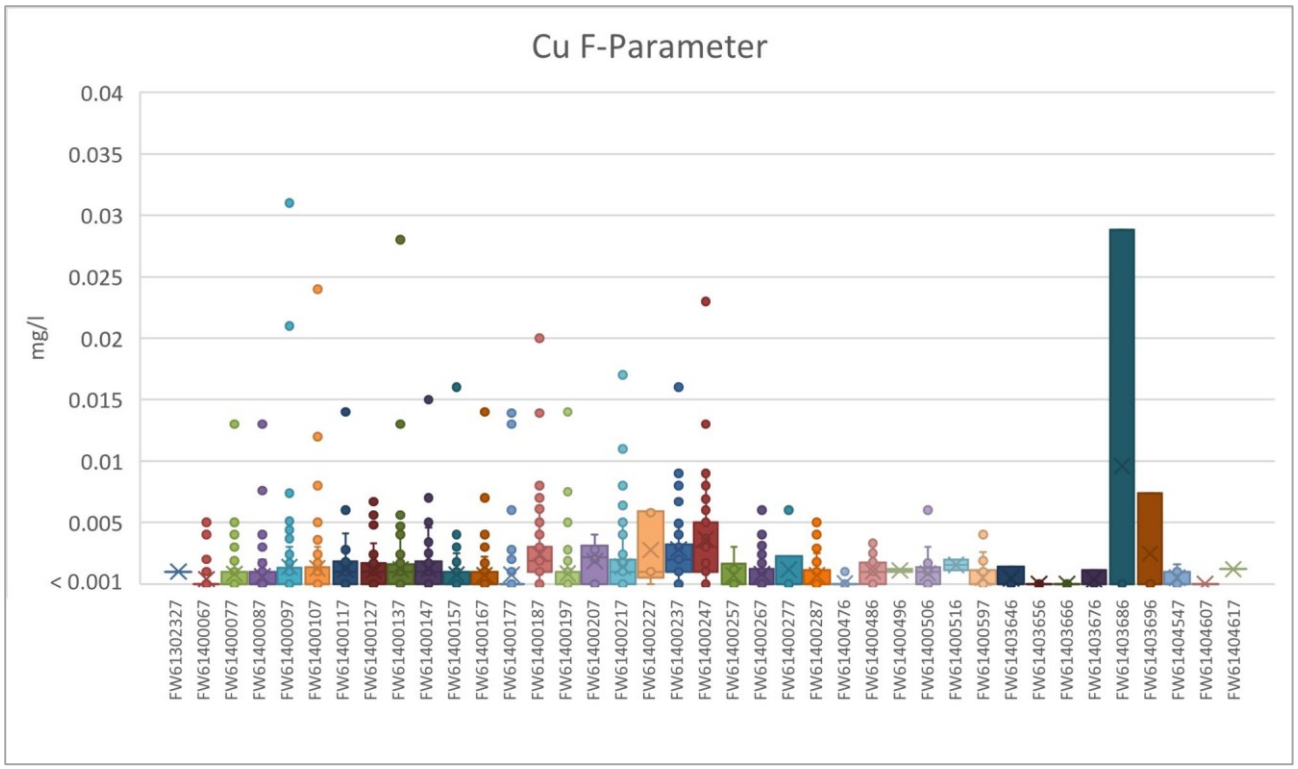


*Figure 48: Cu F-Parameter*

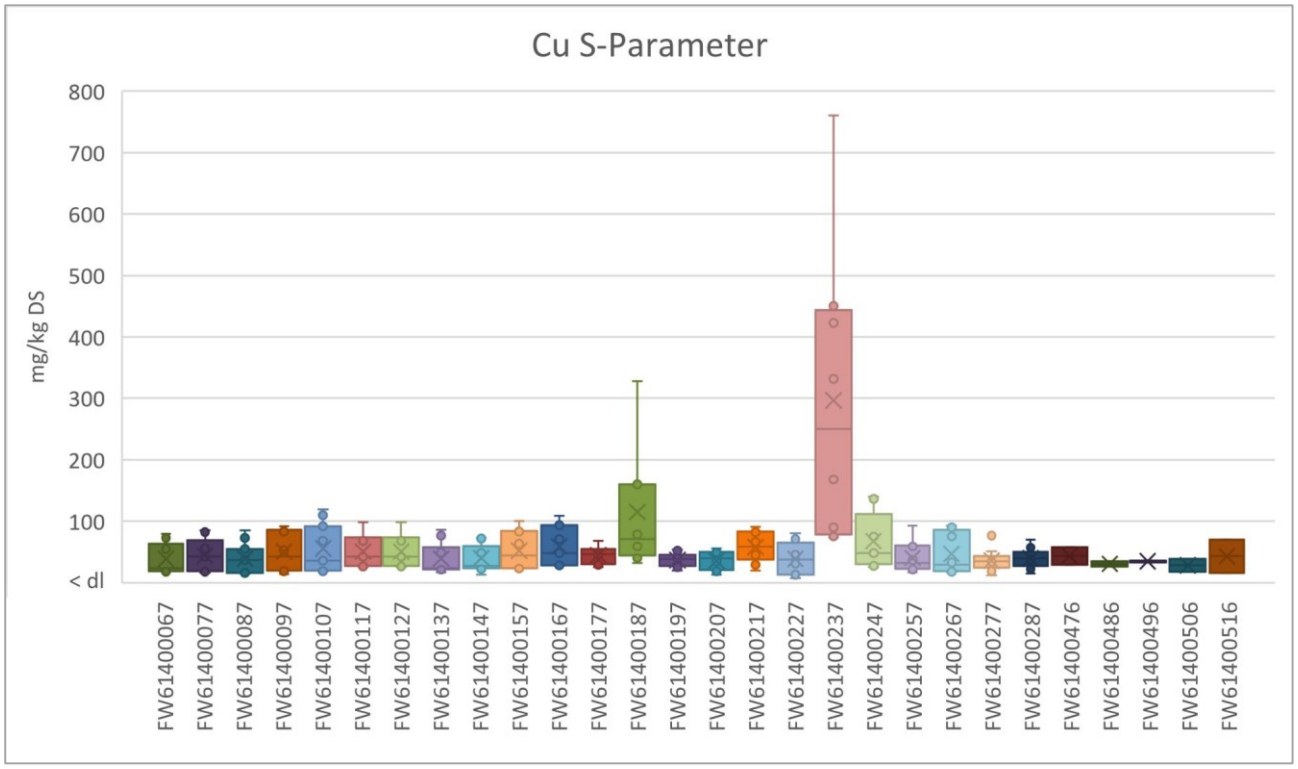


*Figure 49: Cu S-Parameter; Maximum*

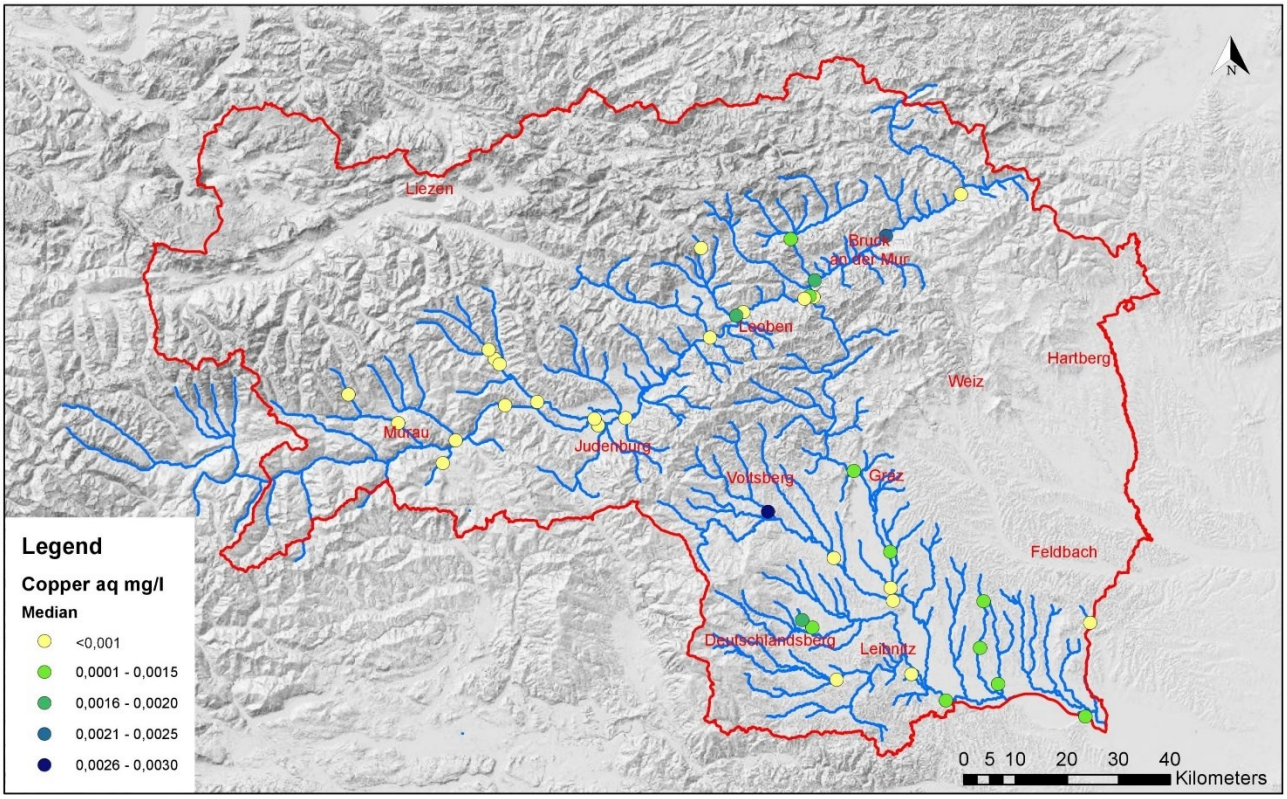


*Figure 50: Copper F-Parameter; Median Values*

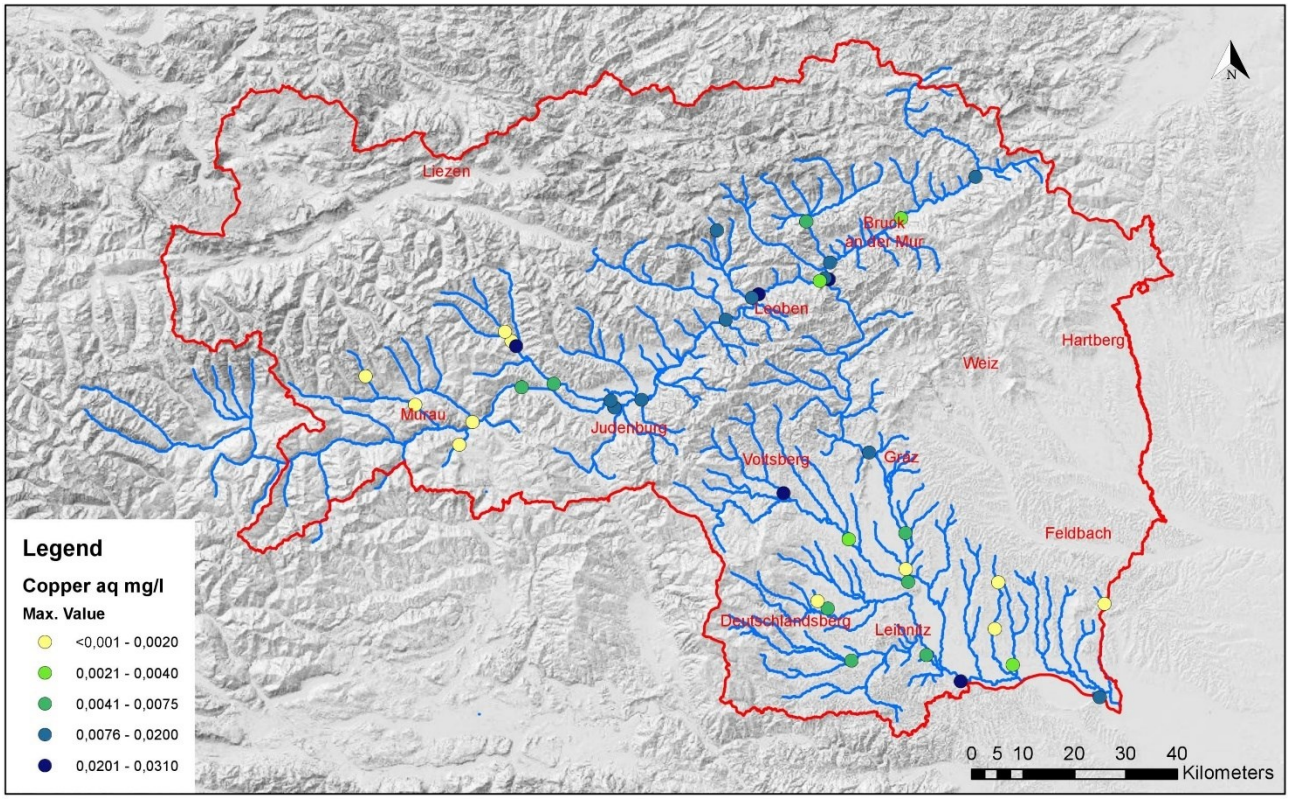


*Figure 51: Copper F-Parameter; Maximum Values*

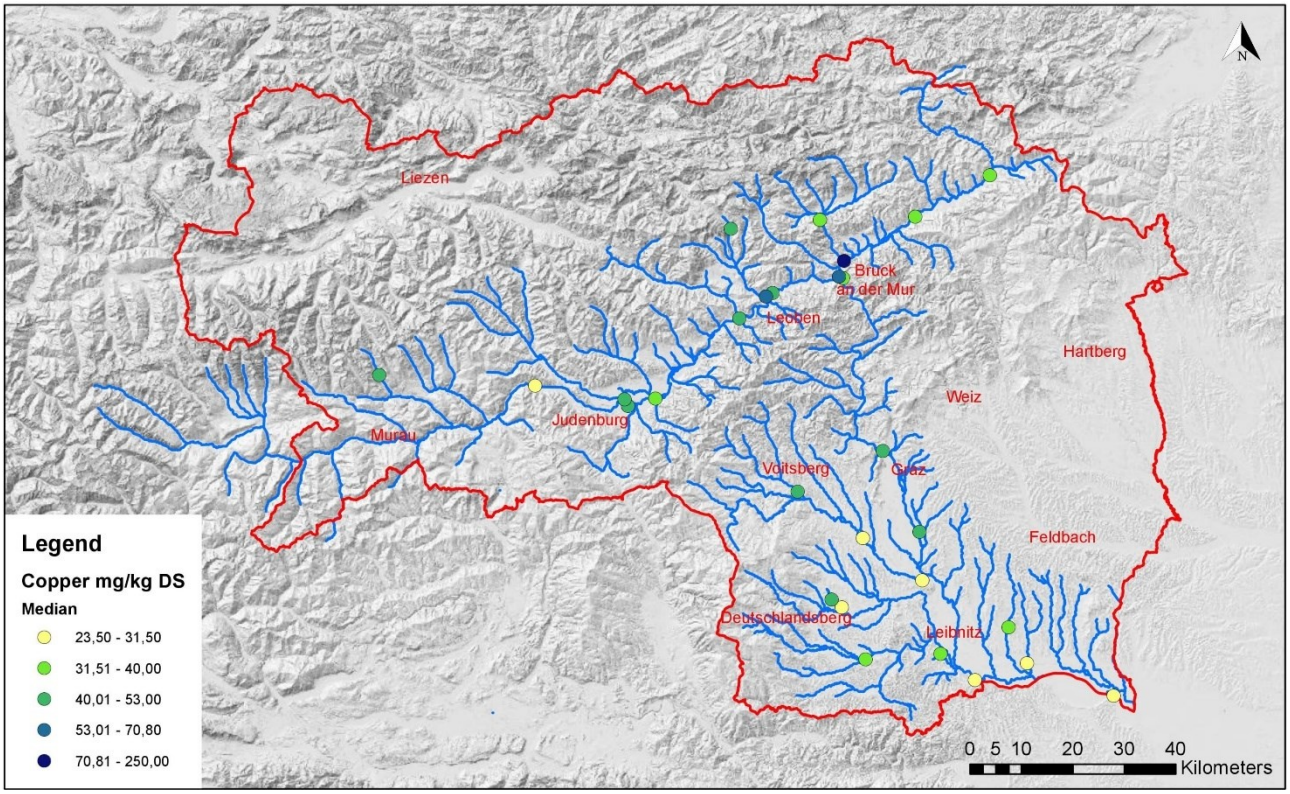


*Figure 52: Copper S-Parameter; Median Values*

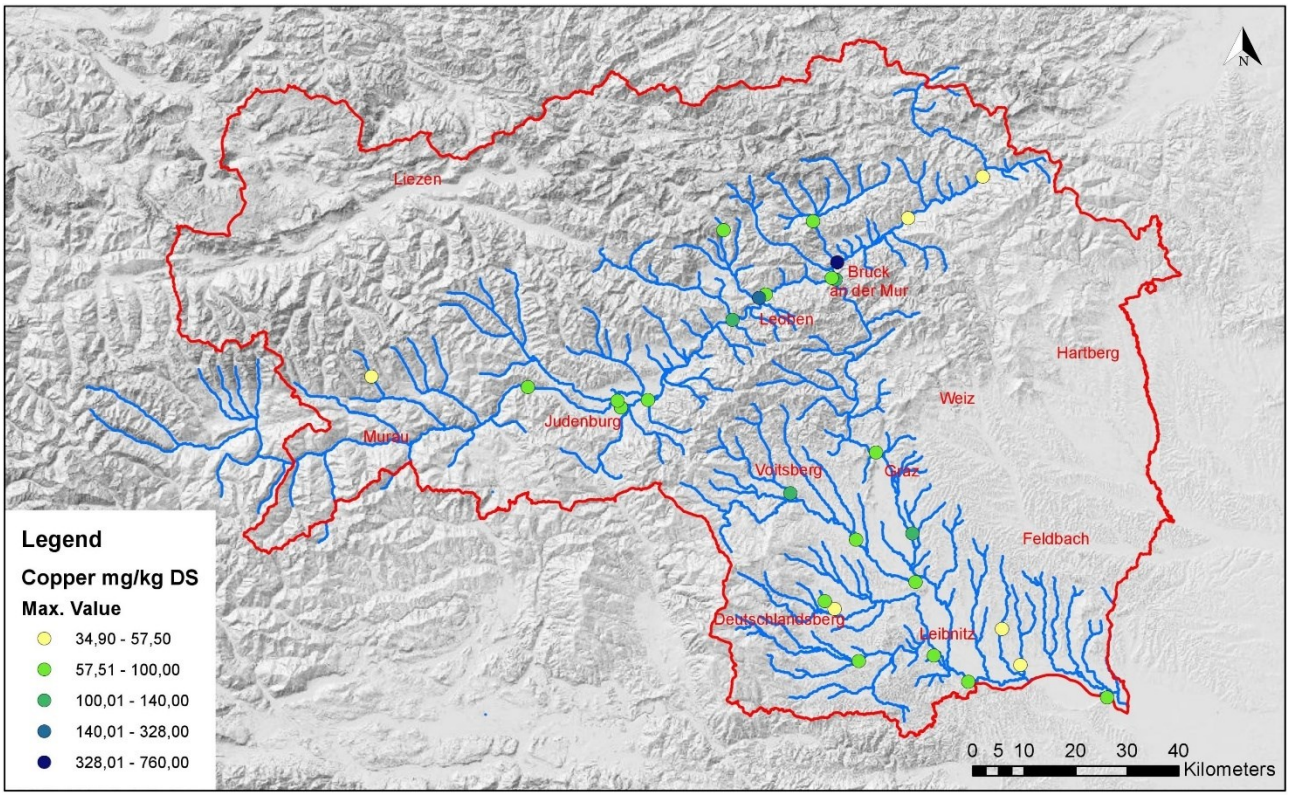


*Figure 53: Copper S-Parameter; Maximum Values*


*Figure 54: Detail section measuring point FW61400187, F-Parameter*


*Figure 55: Detail section measuring point FW61400187, S-Parameter*

## 1.16 Mercury

### 1.16.1 F-Parameters

Mercury concentrations were measured at five monitoring sites. The highest maximum value occurred at FW61400287 (0.0004 mg/l). Furthermore, the monitoring sites FW61400097, FW61400137, FW61400147 and FW61400187 show measured values >dl. Figure 56, 58, 59, 62

### 1.16.2 S-Parameters

The measuring point FW61400187 shows a particular conspicuousness. With a median value of 1.97 mg/kg and a maximum value of 10.8 mg/kg, there is a clear divergence. FW61400177 (0.50825 mg/kg) and FW61400227 (0.58425 mg/kg) show a slight deviation from the other measuring points. In addition to FW61400187, FW61400147 (1.8 mg/kg) and FW61400227 (1.5 mg/kg) show a slightly higher deviation of the maximum. Figure 57, 60, 61, 63

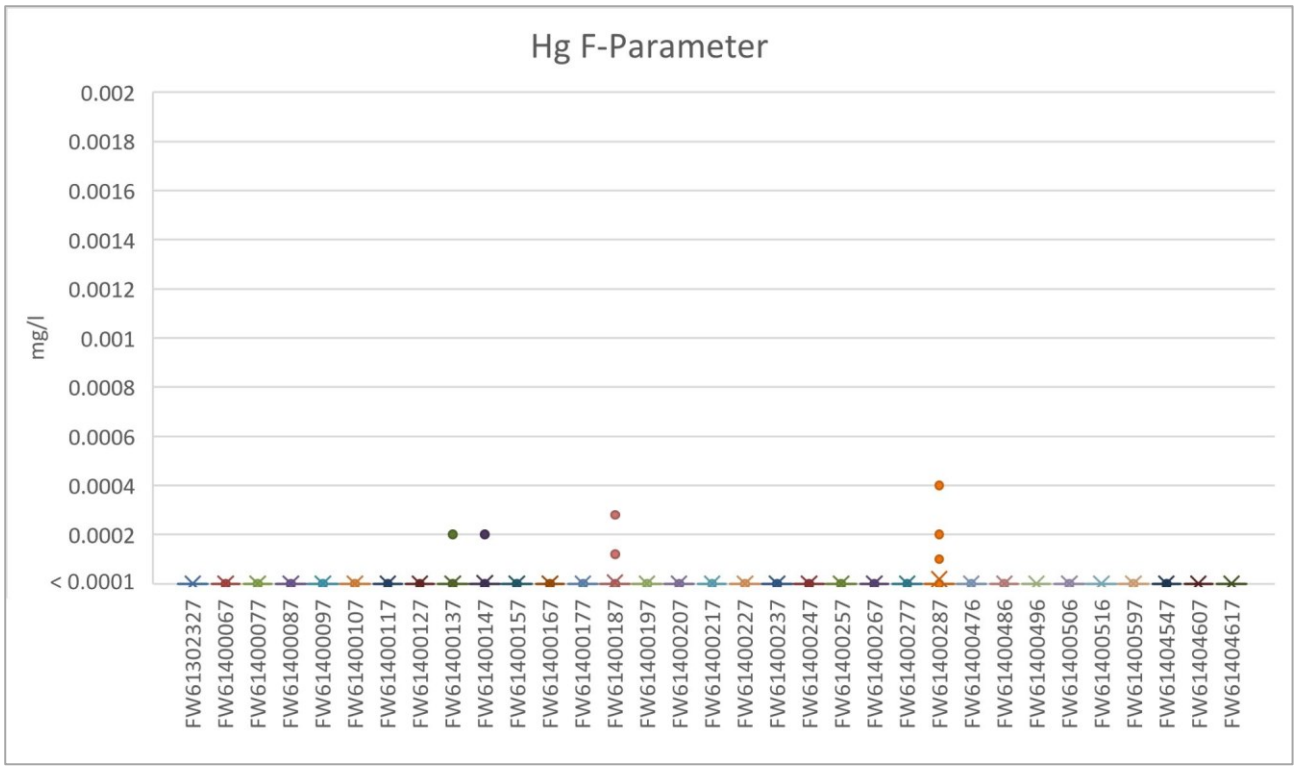


*Figure 56: Hg F-Parameter*

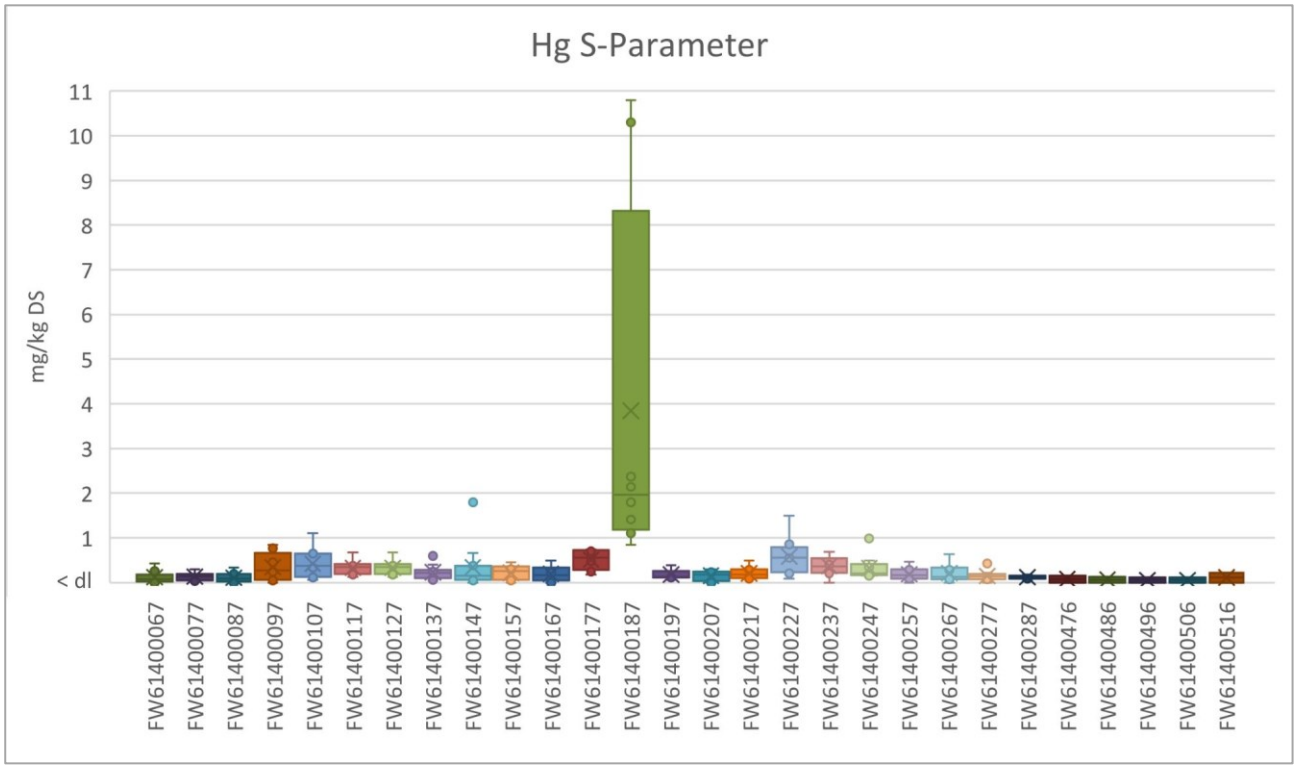


*Figure 57: Hg S-Parameter*

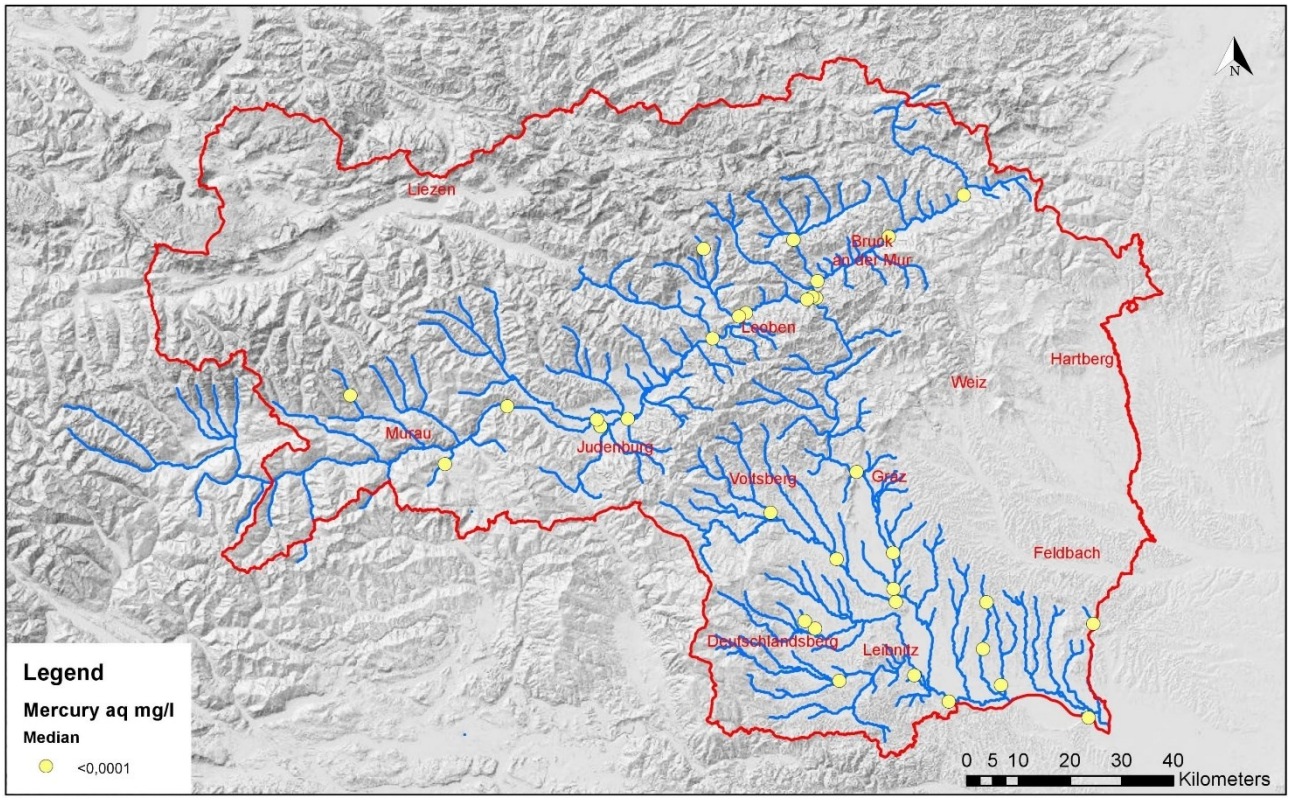


*Figure 58: Mercury F-Parameter; Median Values*

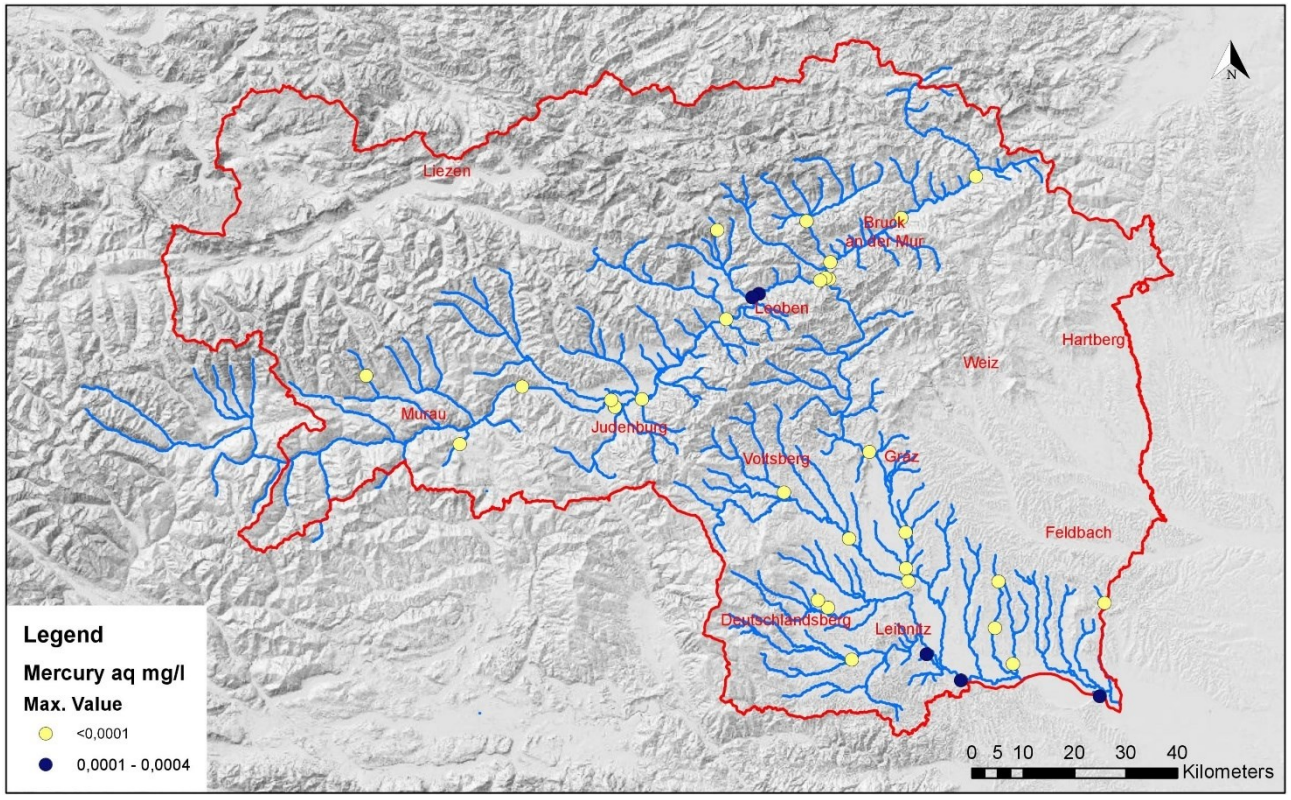


*Figure 59: Mercury F-Parameter; Maximum Values*

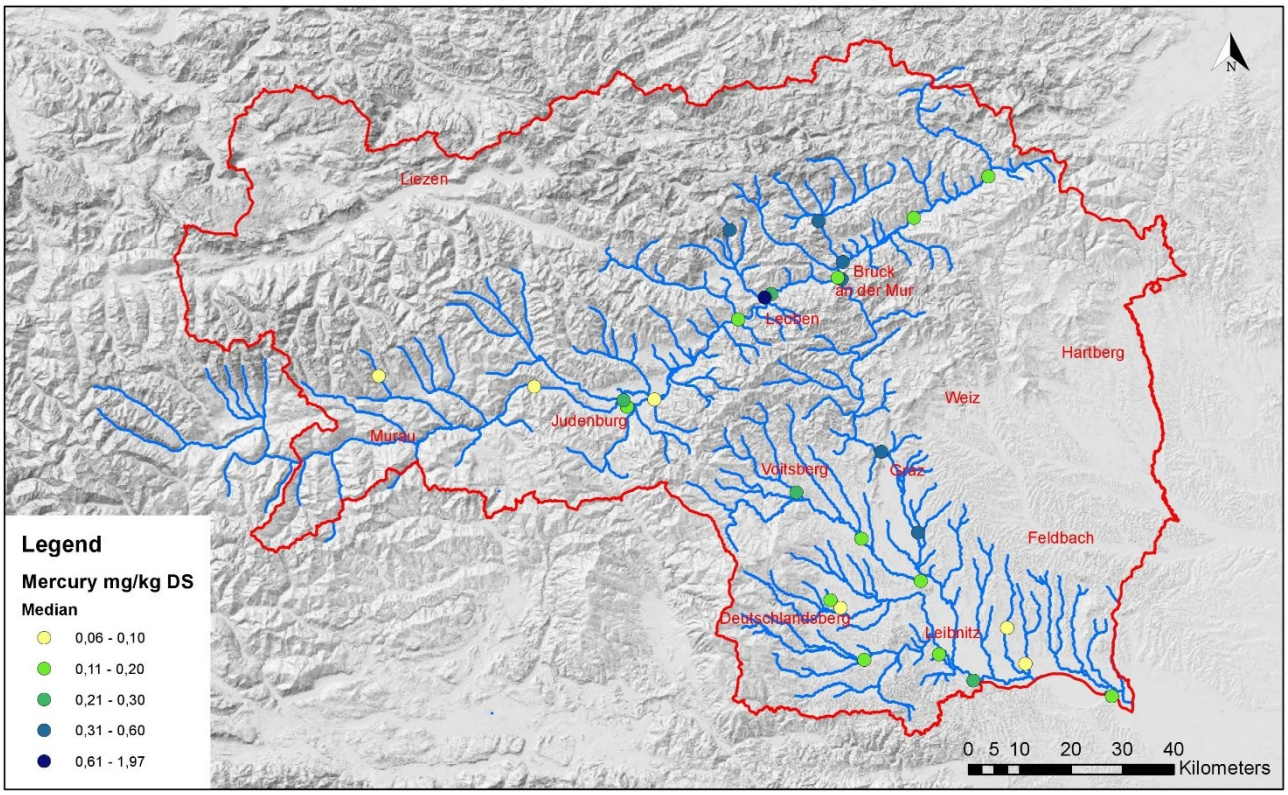


*Figure 60: Mercury S-Parameter; Median Values*

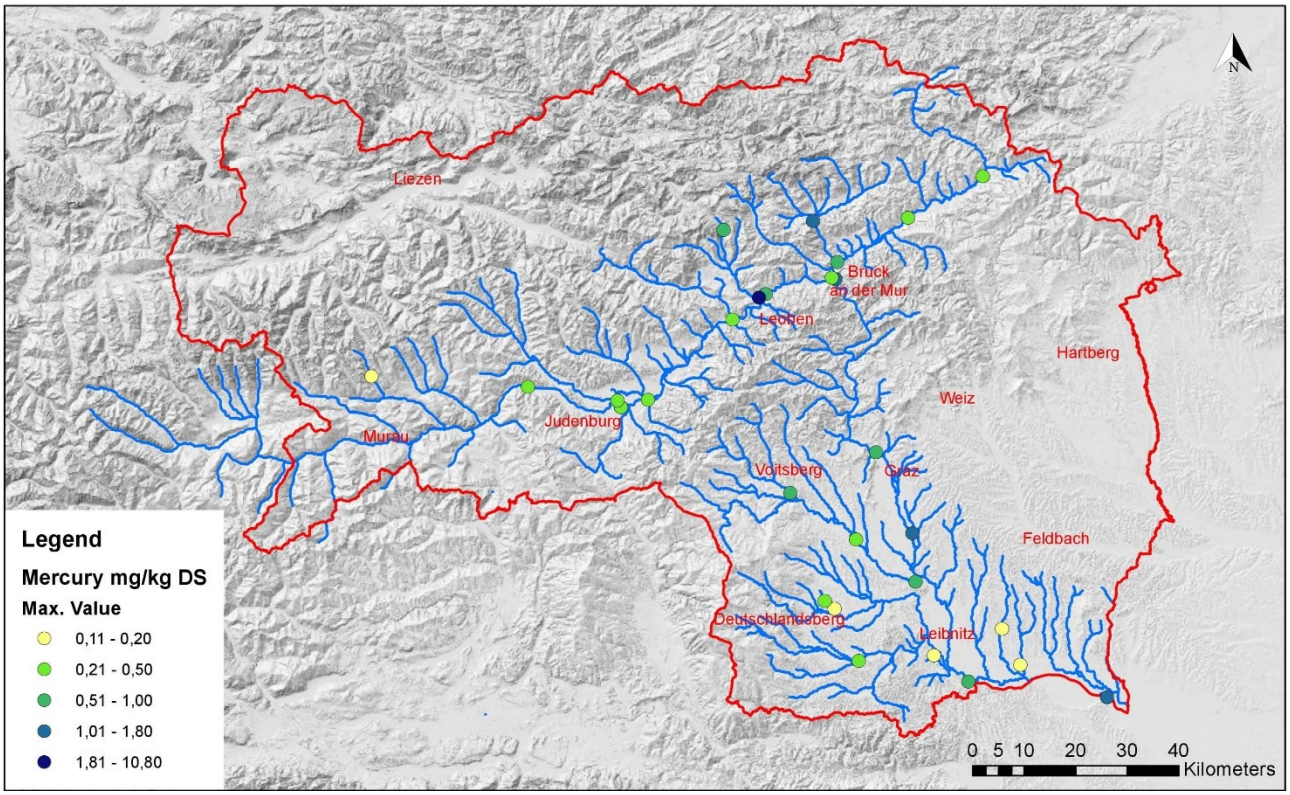


*Figure 61: Mercury S-Parameter; Maximum Values*


*Figure 62: Detail section measuring point FW61400187, F-Parameter*


*Figure 63: Detail section measuring point FW61400187, S-Parameter*

## 1.17 Nickel

### 1.17.1 F-Parameters

The largest deviation from the Styrian median is at monitoring site FW61400187 (0.002 mg/l). Measuring point FW61400506 has the second highest value (0.0018 mg/l). Measuring point FW61400516 has only a slightly lower median value, which again is not representative. Another four monitoring sites have a higher median value of 0.01 mg/l (FW61400147, FW61400217, FW61400237, FW61400496). By contrast, the highest nickel content was measured at monitoring site FW61400207 (0.033 mg/l). The measuring points FW61400137 and FW61400187 show slightly increased values compared to the Styrian maximum value. All other measuring points are in the low fluctuation range. Figure 64, 66, 67, 70

### 1.17.2 S-Parameters

The most striking deviation in the median value is shown by the measuring point FW61400237 with 250 mg/kg. Another deviation worth mentioning is shown by the measuring points FW61400177 (84.85 mg/kg), FW61400187 (82 mg/kg), FW61400217 (108.5 mg/kg) and FW61400506 (only 2 measured values, 78 mg/kg). The maximum values show clearer deviations from the Styrian maximum value. The three monitoring sites with the highest measured values are FW61400237 (760 mg/kg), FW61400187 (520 mg/kg) and FW61400217 (454 mg/kg). Figure 65, 68, 69, 71

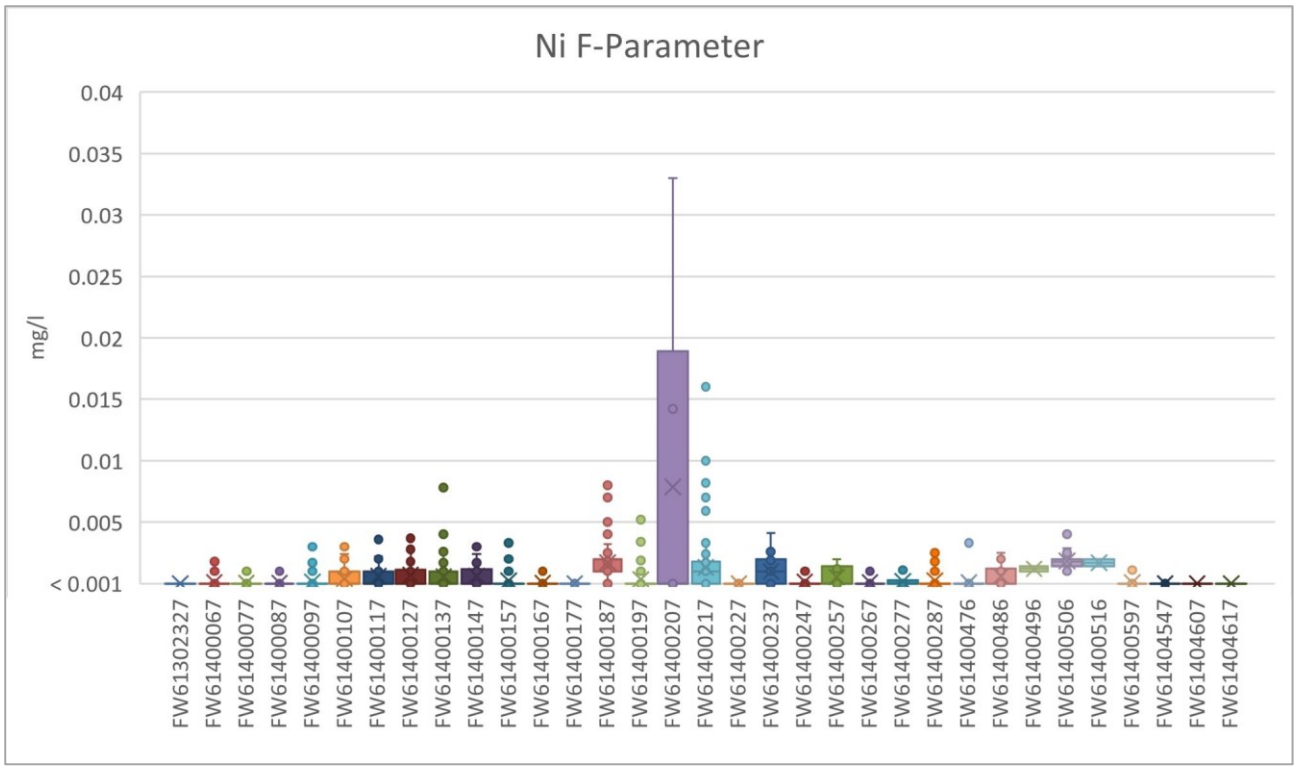


*Figure 64: Ni F-Parameter*

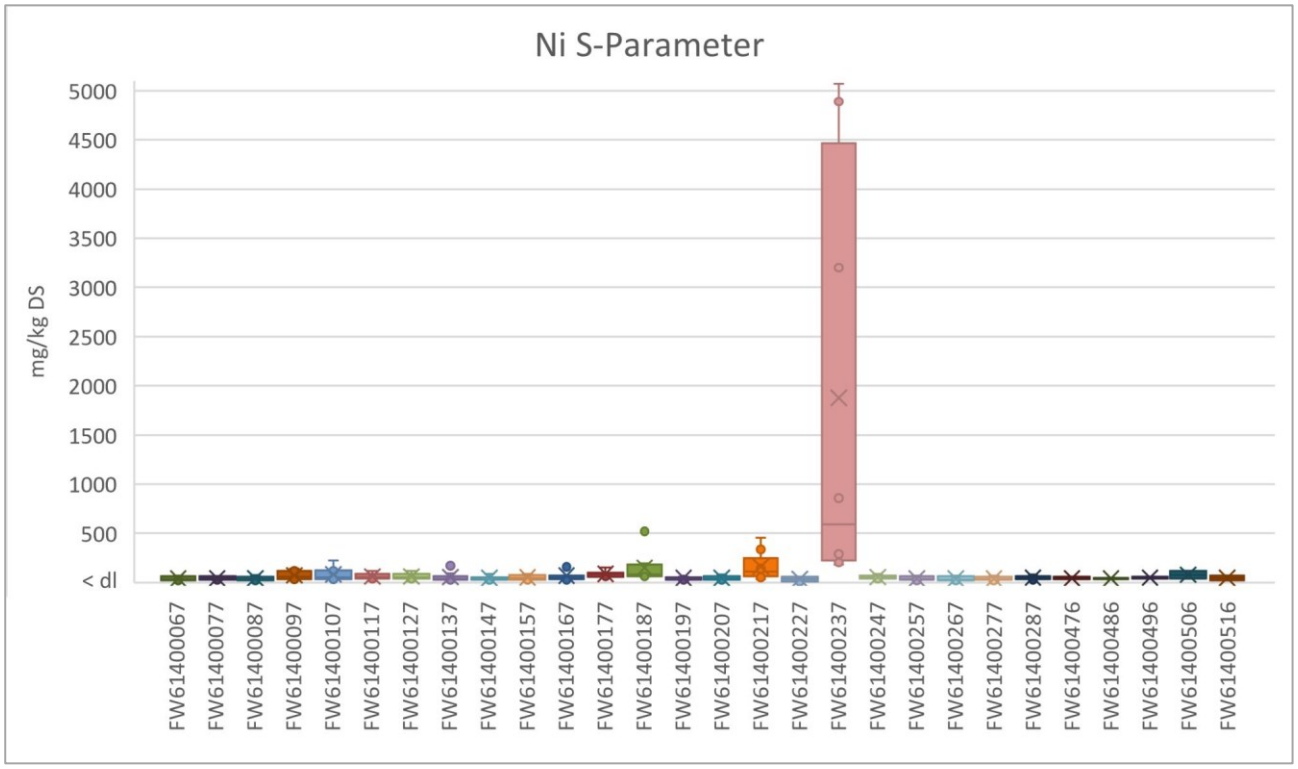


*Figure 65: Ni S-Parameter*

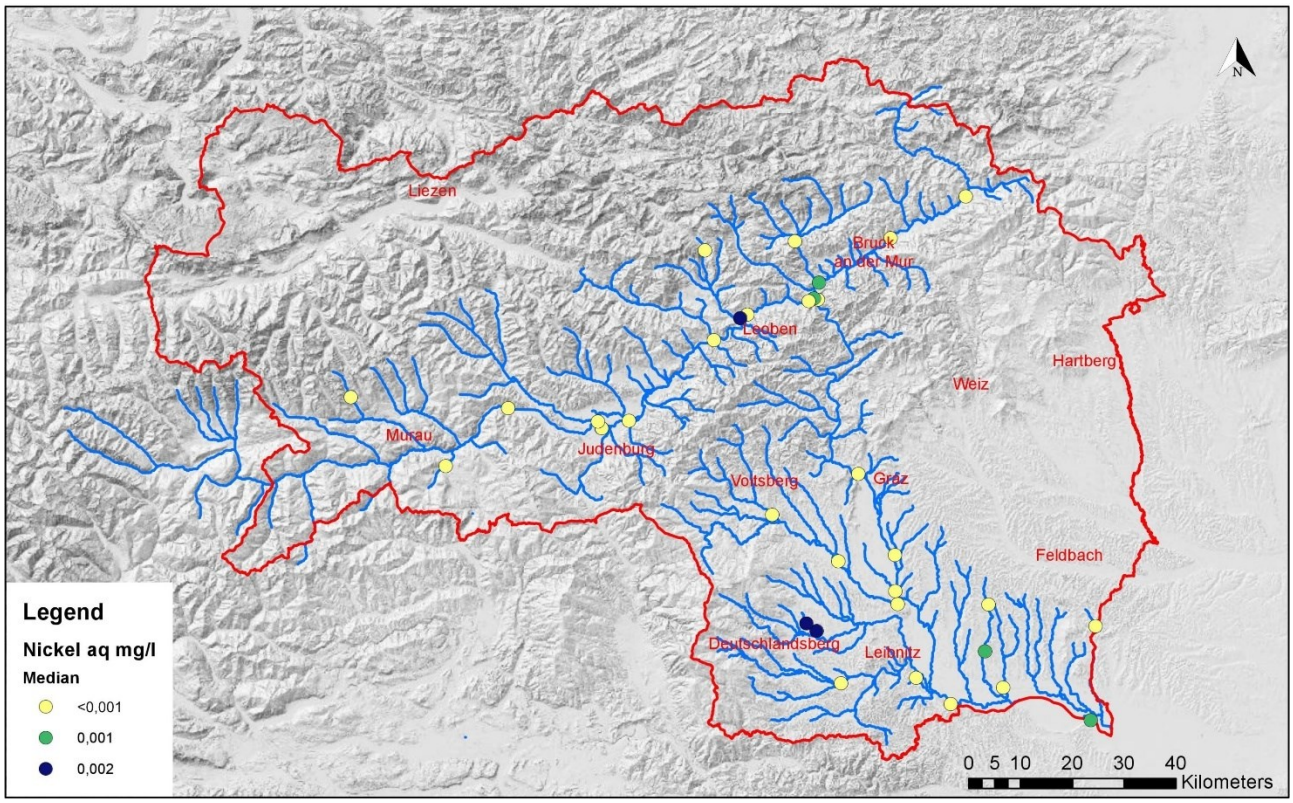


*Figure 66:Nickel F-Parameter; Median Values*

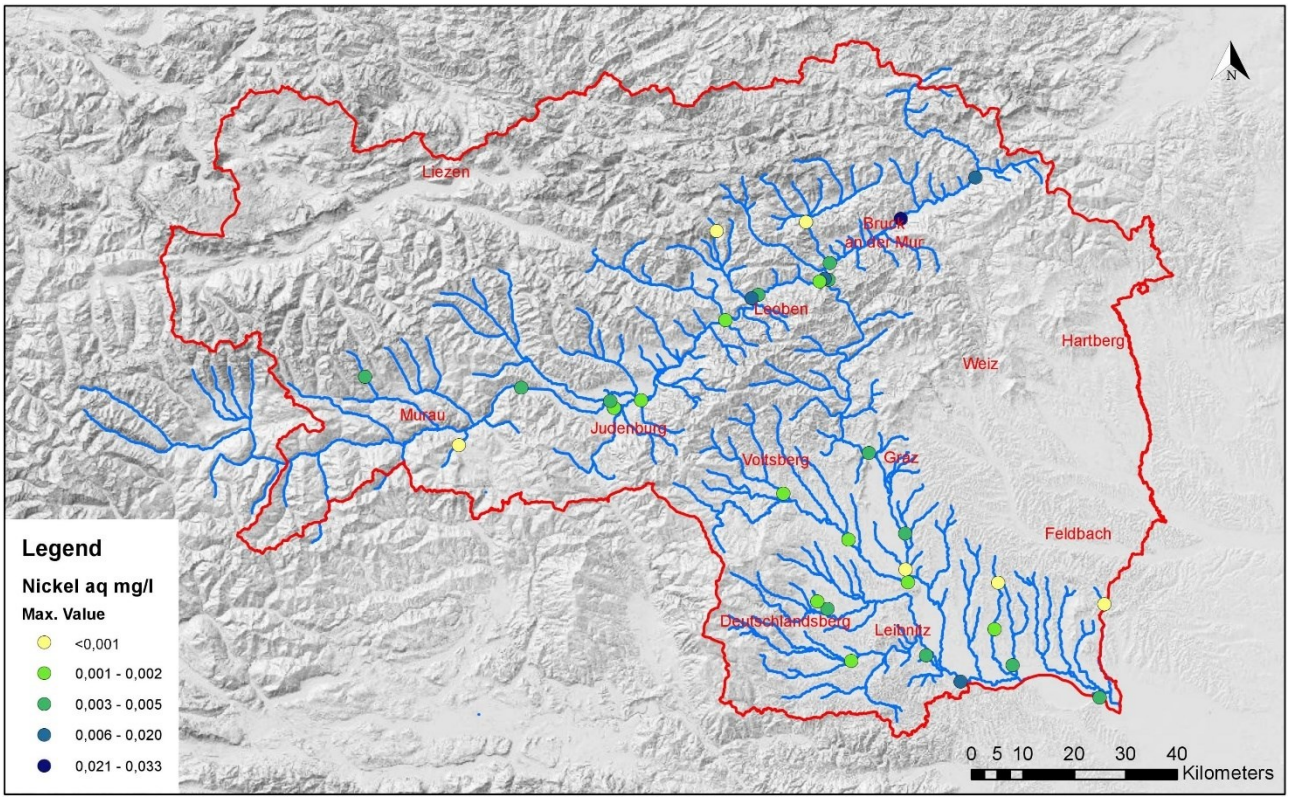


*Figure 67: Nickel F-Parameter; Maximum Values*

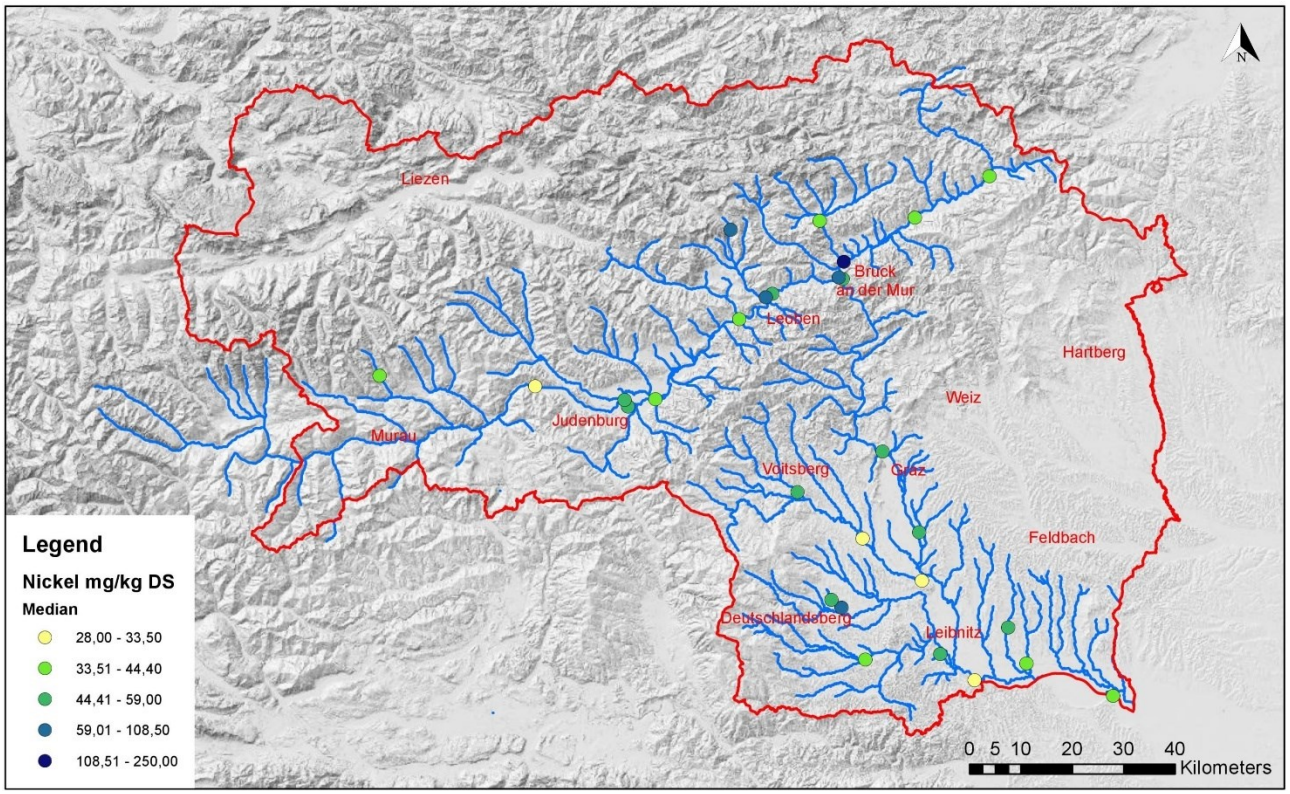


*Figure 68: Nickel S-Parameter; Median Values*

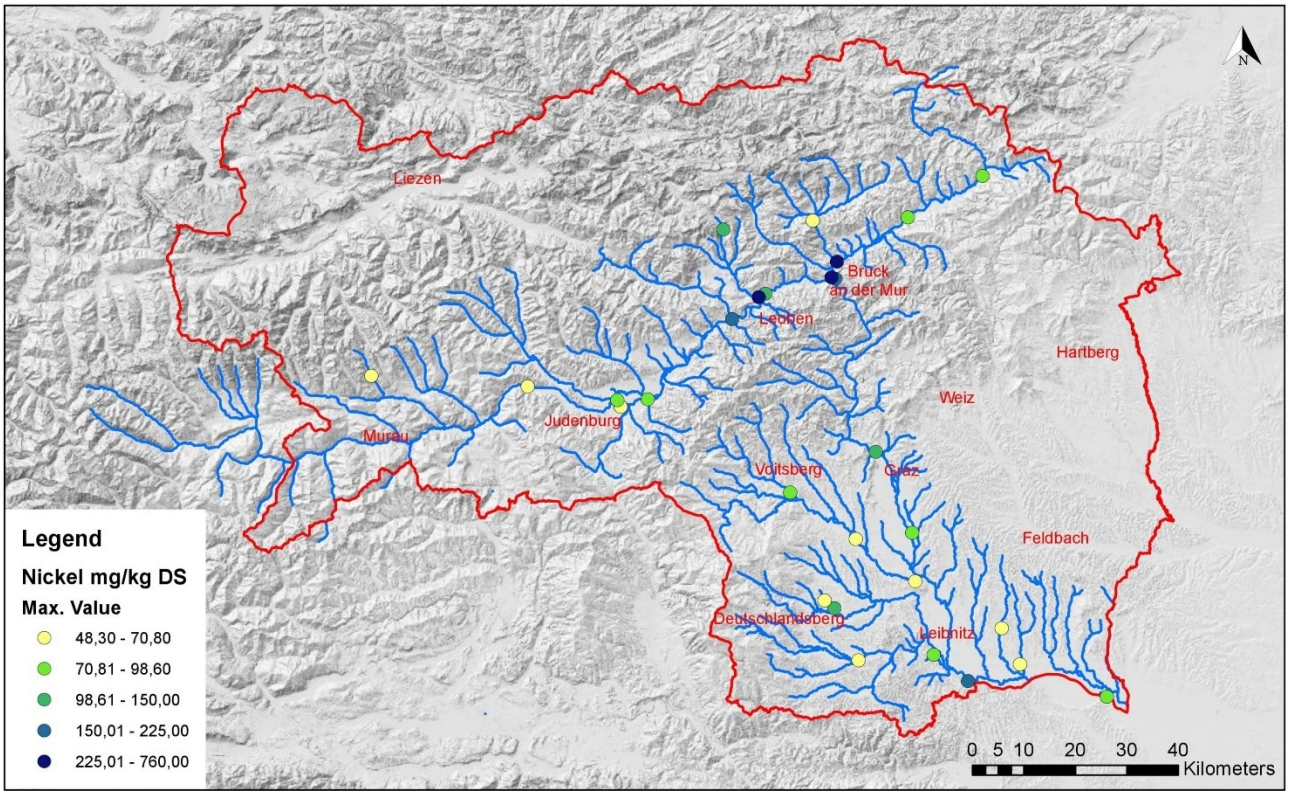


*Figure 69: Nickel S-Parameter; Maximum Values*


*Figure 70: Detail section measuring point FW61400187, F-Parameter*


*Figure 71: Detail section measuring point FW61400187, S-Parameter*

## 1.18 Lead

### 1.18.1 F-Parameters

The only outlier in the median values is monitoring site FW61400187 in the Vordernbergerbach. This median is 0.00115 mg/l with 80 measurements, all other monitoring sites are in the Styrian median (< dl). In the case of the maximum values, two monitoring sites show a significantly increased deviation. These are again the measuring point FW61400187, as well as the measuring point FW61400247 in the Kainach in Voitsberg. The value at both measuring points is 0.036 mg/l. Slightly elevated values were also recorded at monitoring sites FW61400137 (Mur; 0.0094 mg/l), FW61400227 (Thörlbach; 0.009 mg/l) and FW61400237 (Thörlbach; 0.0103 mg/l). Figure 72, 74, 75, 78

### 1.18.2 S-Parameters

Measuring point FW61400187 stands out particularly in both the median value and the maximum value. The median value is 335.5 mg/kg, the maximum value 1290 mg/kg. Two other monitoring sites also exhibit larger discrepancies in the median value from the Styrian median, site FW61400237 (270 mg/kg), which also shows a significant deviation in the maximum value (129.5 mg/kg), and site FW61400127 (median value: 101 mg/kg). Figure 73, 76, 77, 79

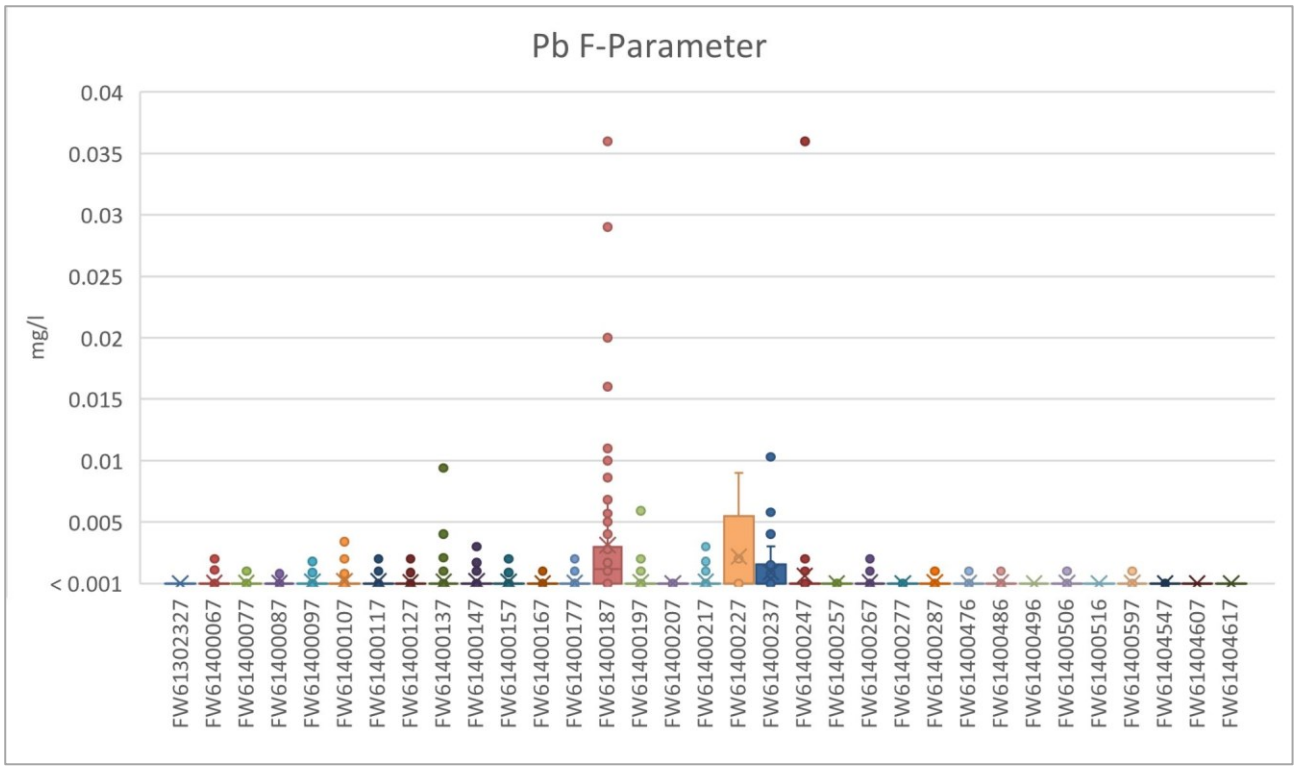


*Figure 72: Pb F-Parameter*

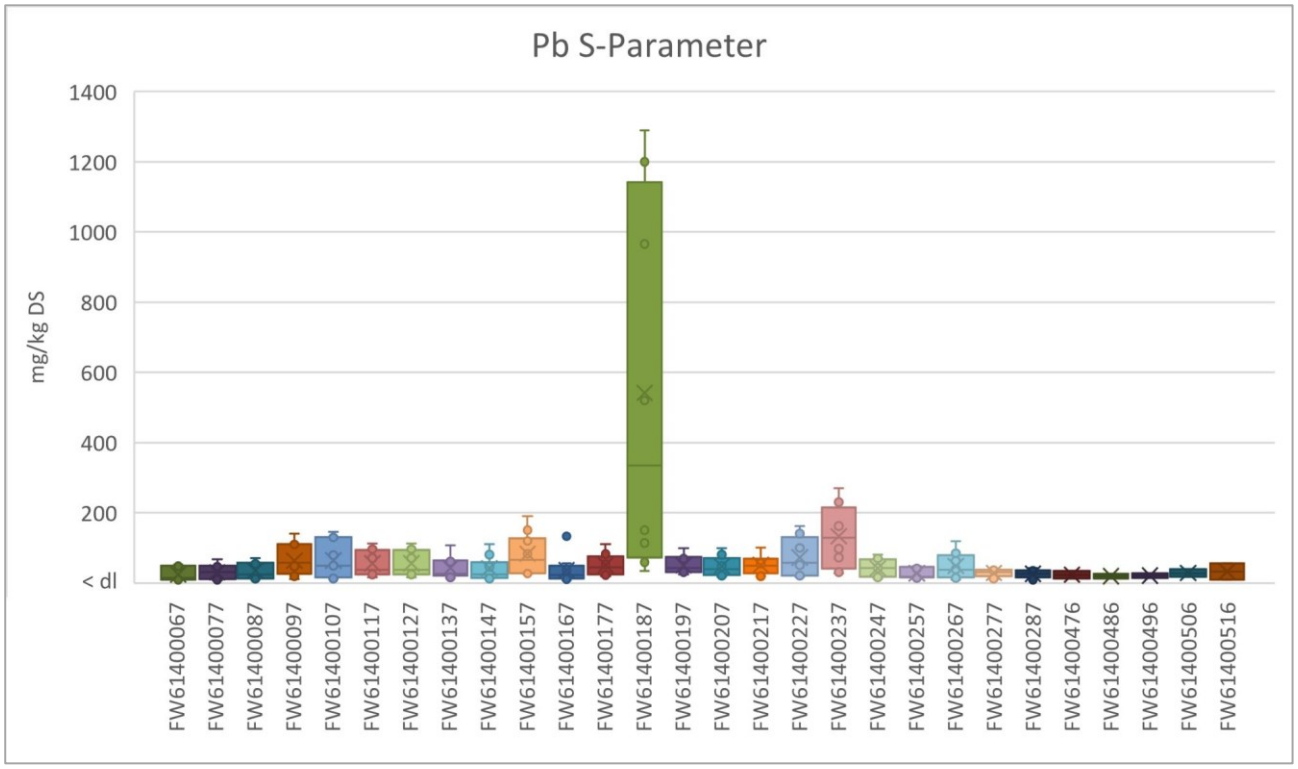


*Figure 73: Pb S-Parameter; Maximum*

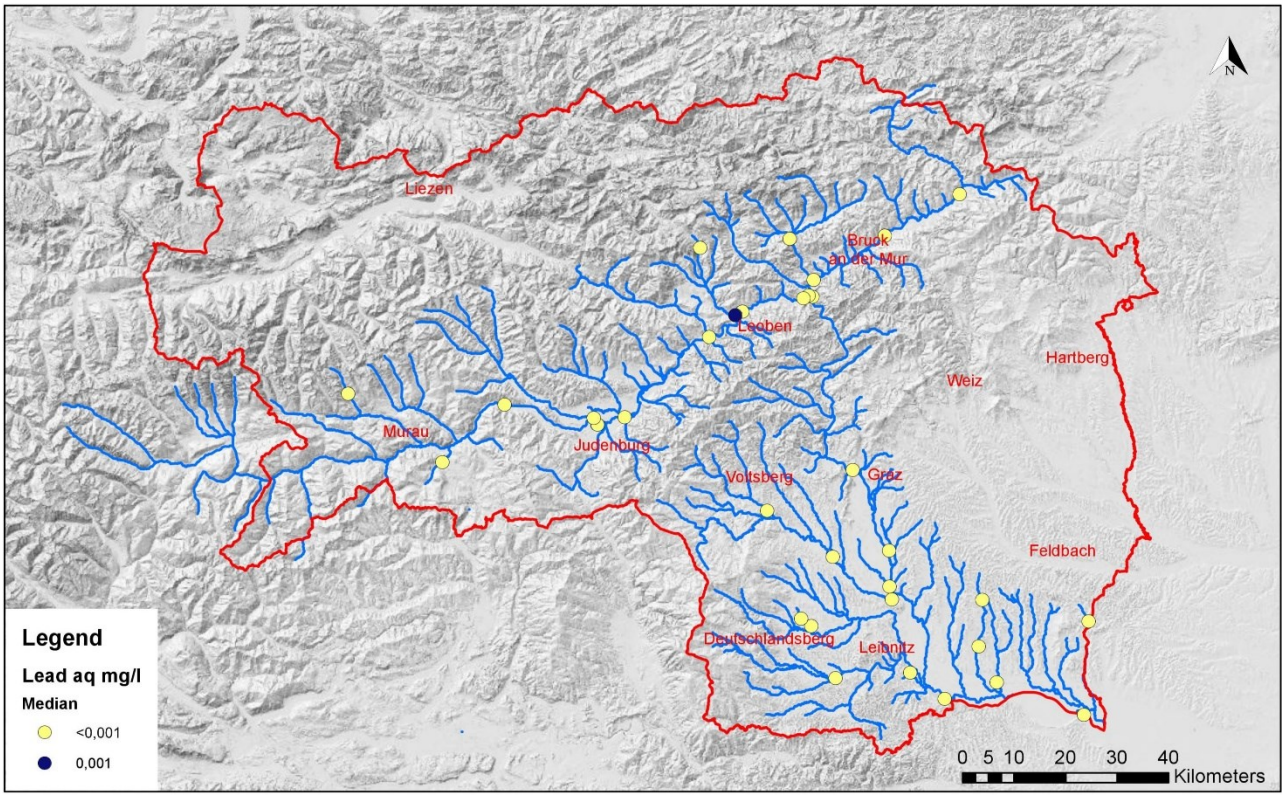


*Figure 74: Lead F-Parameter; Median Values*

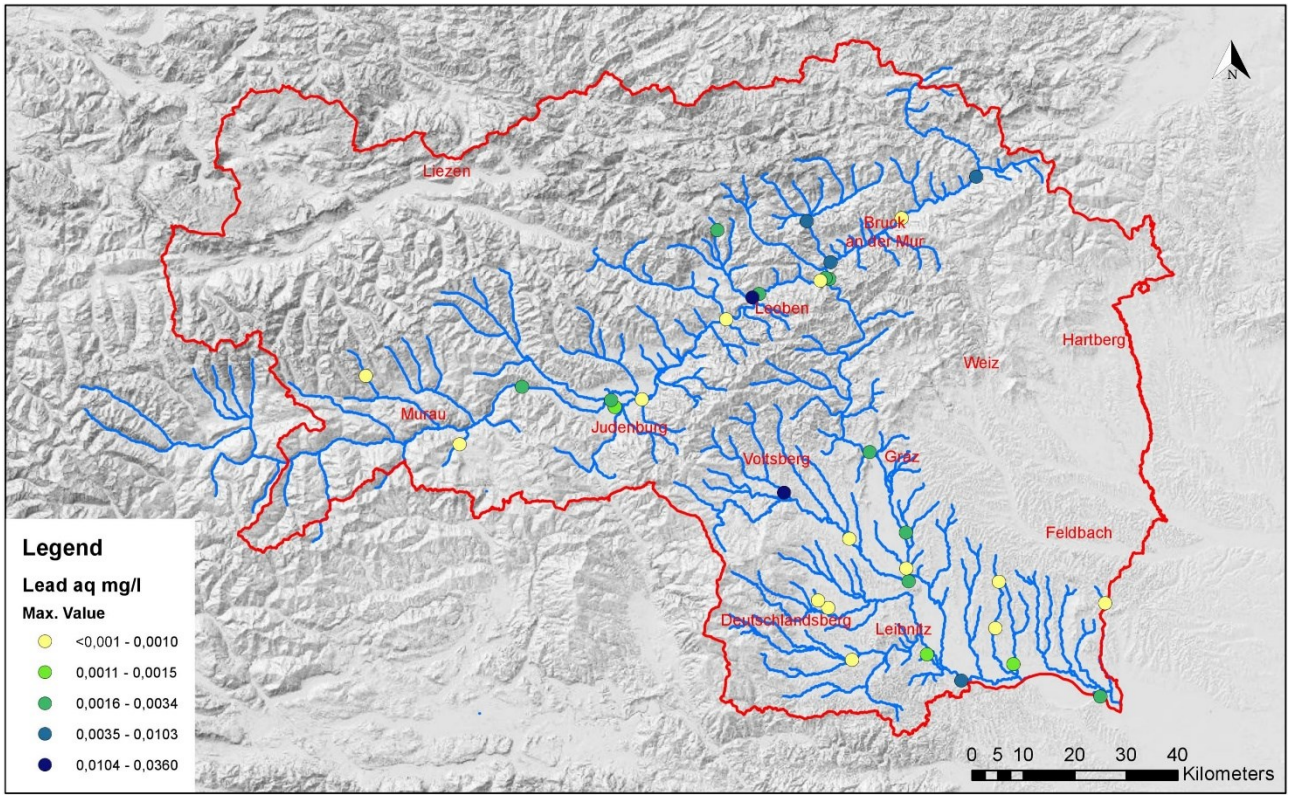


*Figure 75: Lead F-Parameter; Maximum Values*

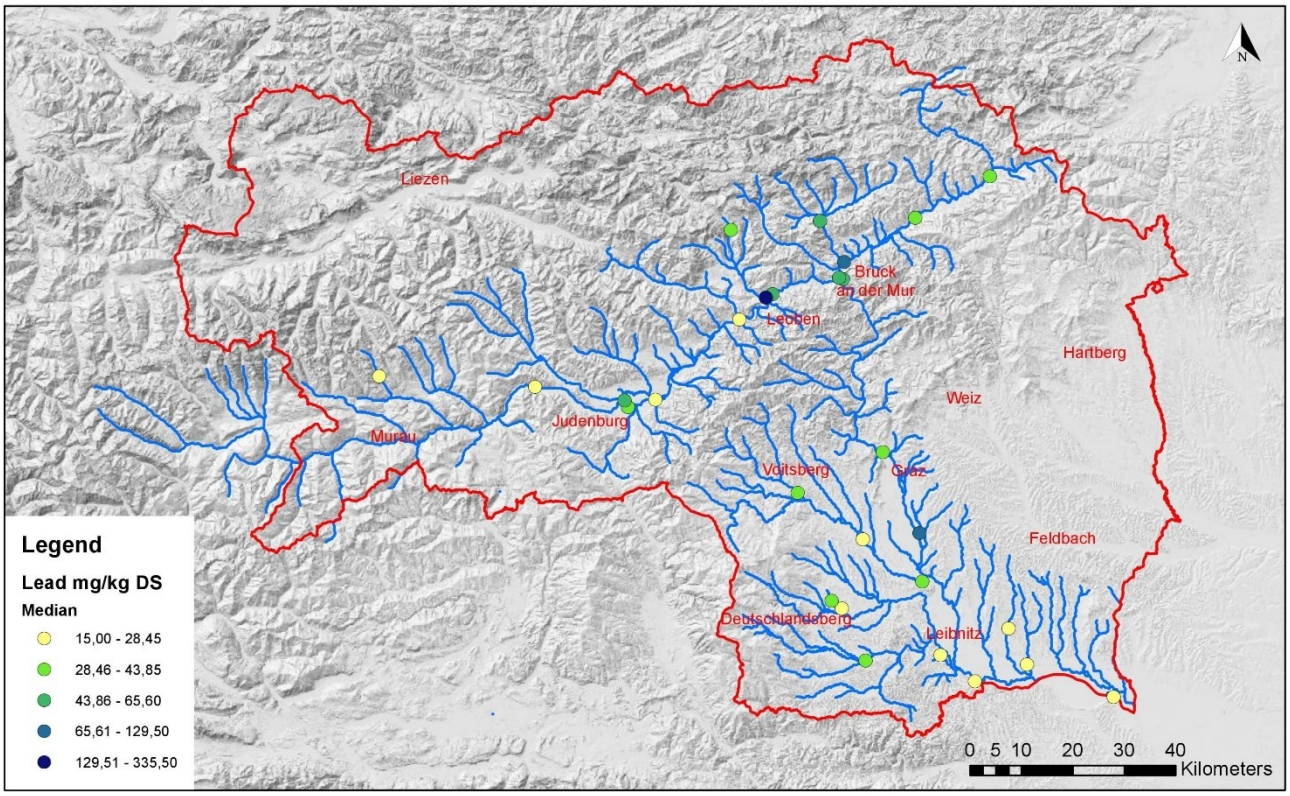


*Figure 76: Lead S-Parameter; Median Values*

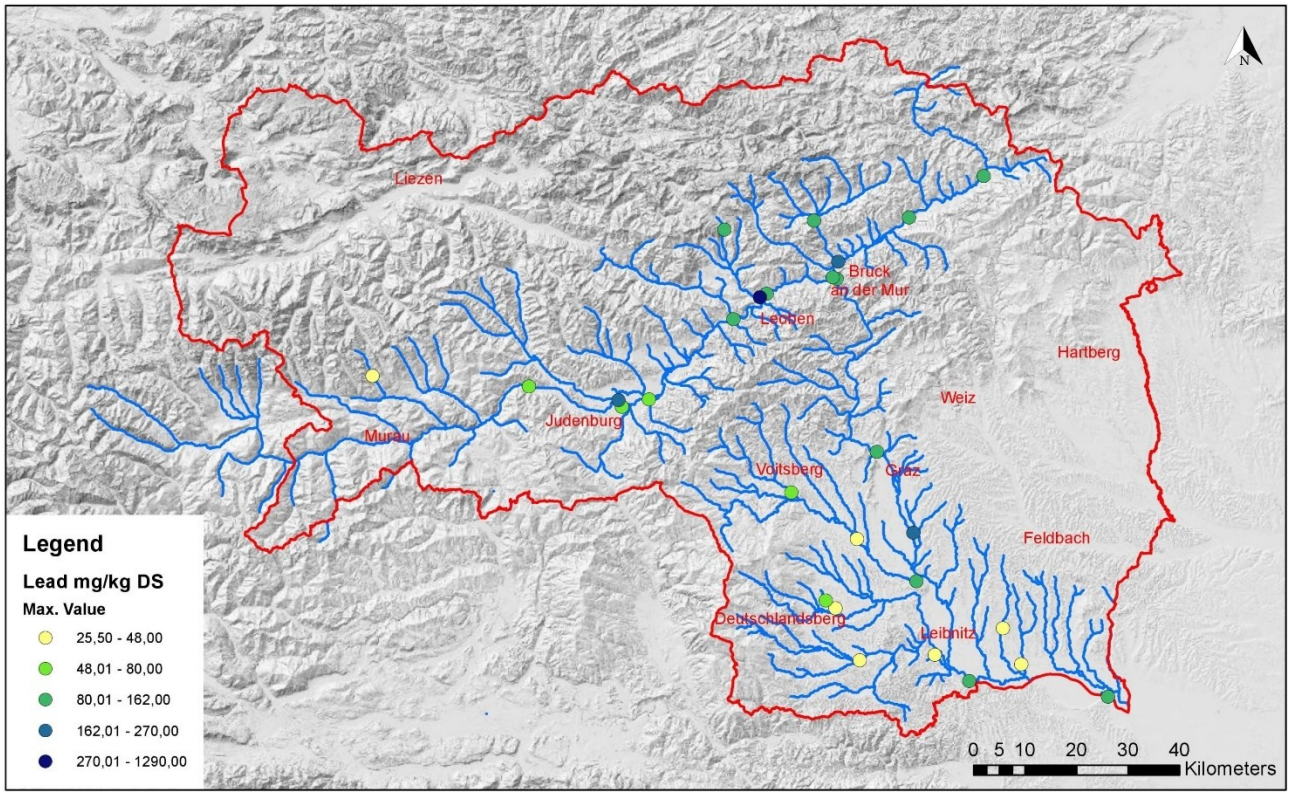


*Figure 77: Lead S-Parameter; Maximum Values*


*Figure 78: Detail section measuring point FW61400187, F-Parameter*


*Figure 79: Detail section measuring point FW61400187, S-Parameter*

## 1.19 Zinc

### 1.19.1 F-Parameters

The highest median value for this element is at monitoring site FW61400187 (0.051 mg/l). Also the maximum value is highest at this site (0.8 mg/l). Five other monitoring sites have a slightly higher median value compared to the Styrian median (FW61400097, FW61400227, FW61400237, FW61404547, FW61404607). Except for the measuring points FW61400097 and FW61400237, none of the mentioned points has enough measured values to be able to represent a resilent median. In addition to the measuring point FW61400187, the points FW61400117 (0.52 mg/l), FW61400147 (0.378 mg/l) and FW61400237 (0.24 mg/l) have clearly elevated maximum values.
Figure 80, 82, 83, 86

### 1.19.2 S-Parameters

The measuring point FW61400187 displays a clear deviation in both diagrams. The median value is 2015 mg/kg, the maximum value 5810 mg/kg. A second measuring point with anomalies is FW61400237. It shows a slightly increased median value of 344.5 mg/kg and a significantly increased maximum value of 4000 mg/kg. All other sample values are in the low fluctuation range around the Styrian values.
Figure 81, 84, 85, 87

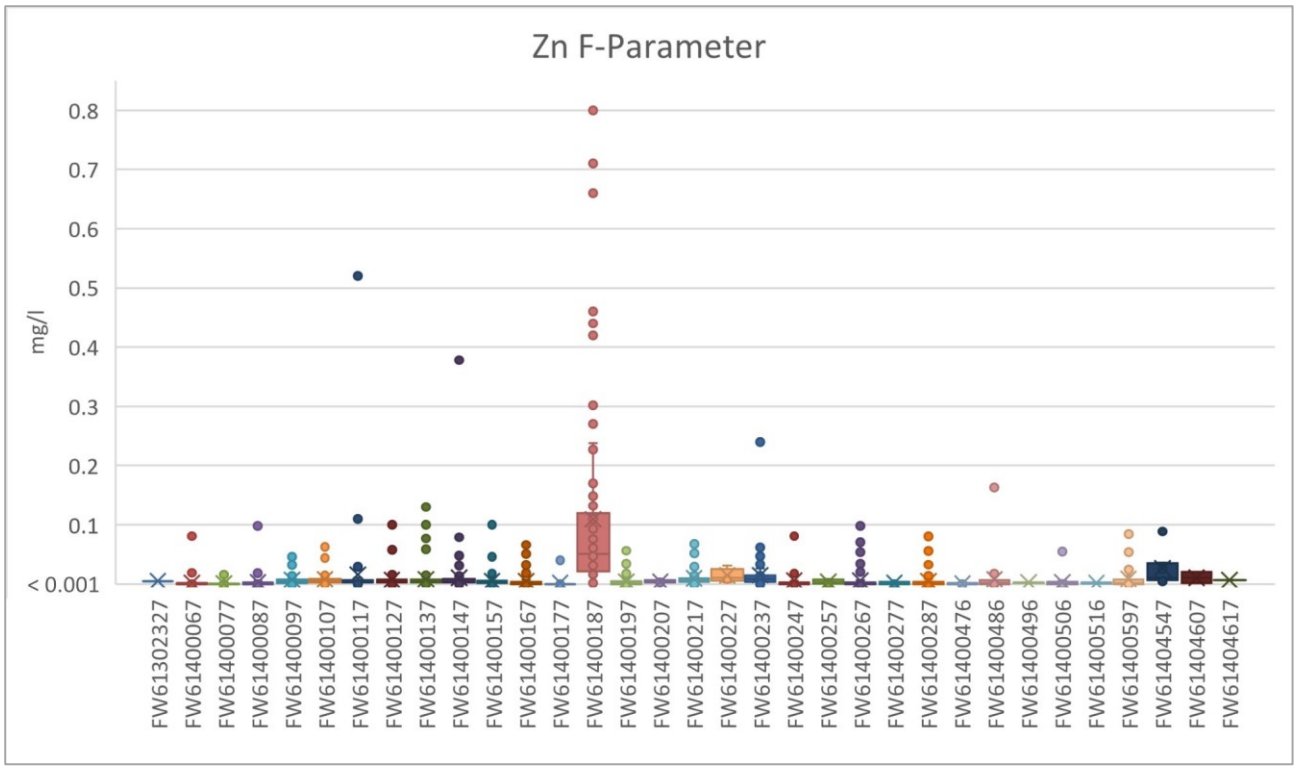


*Figure 80: Zn F-Parameter*

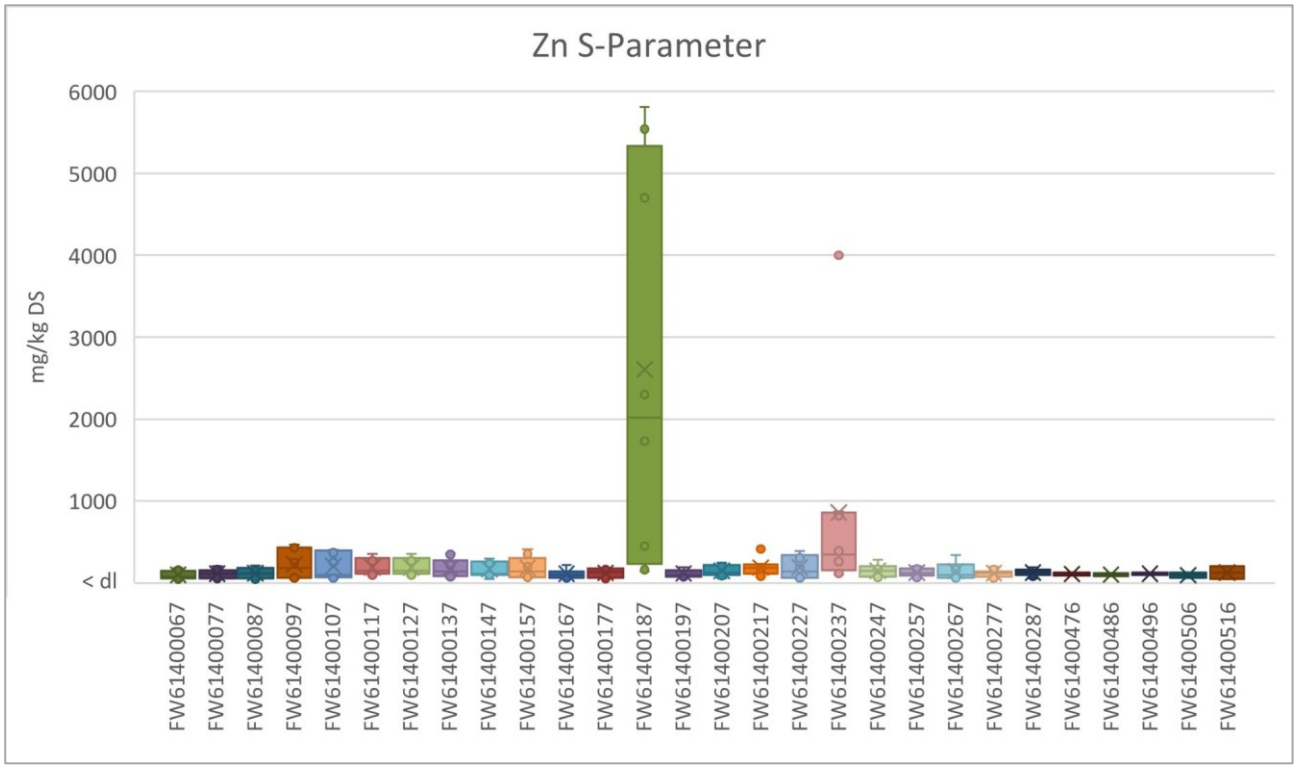


*Figure 81: Zn S-Parameter*

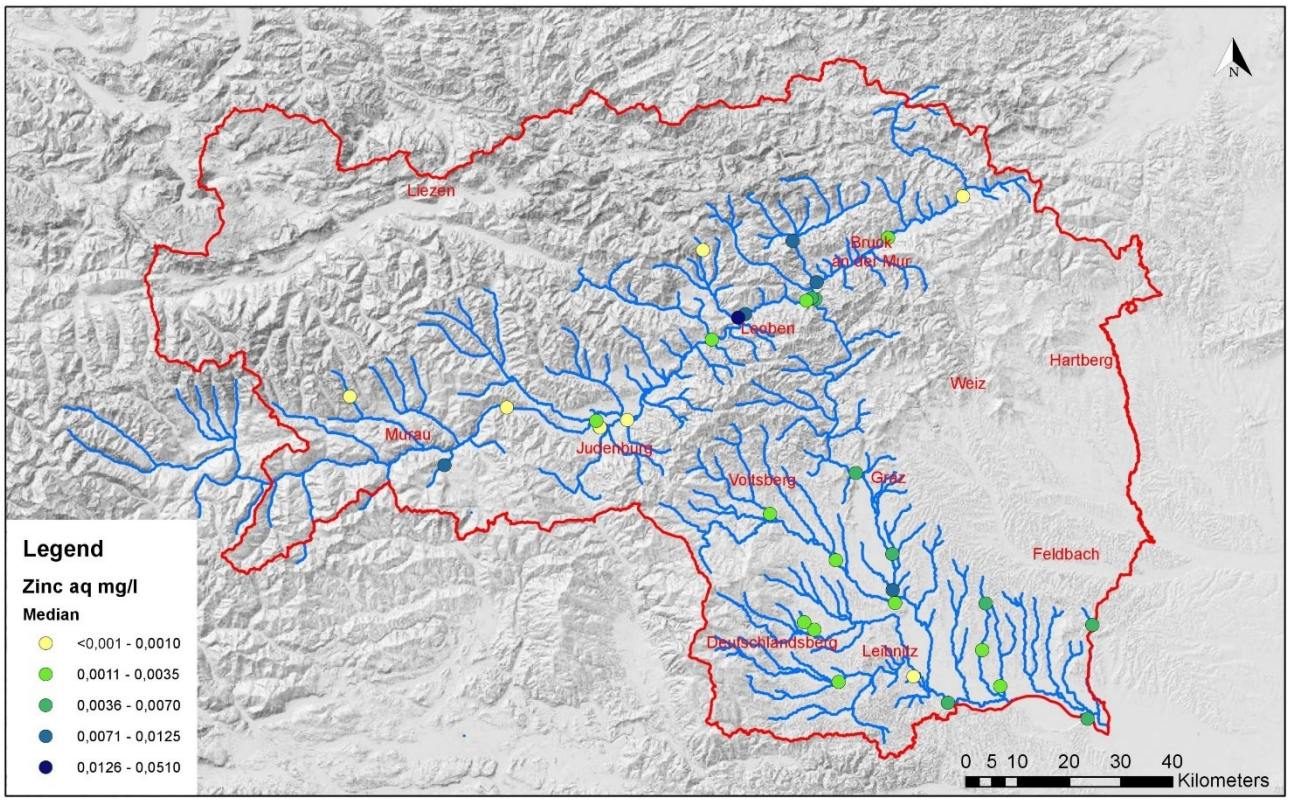


*Figure 82: Zinc F-Parameter; Median Values*

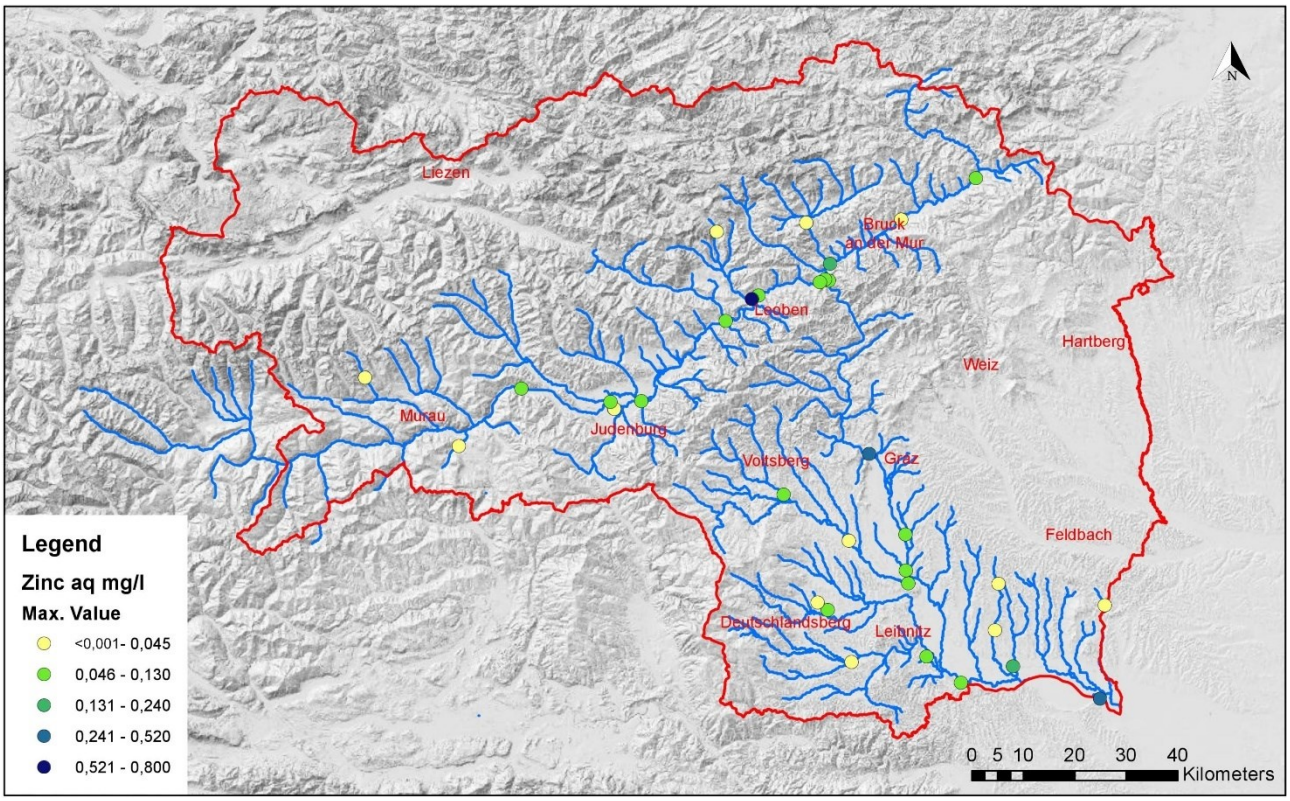


*Figure 83: Zinc F-Parameter; Maximum Values*

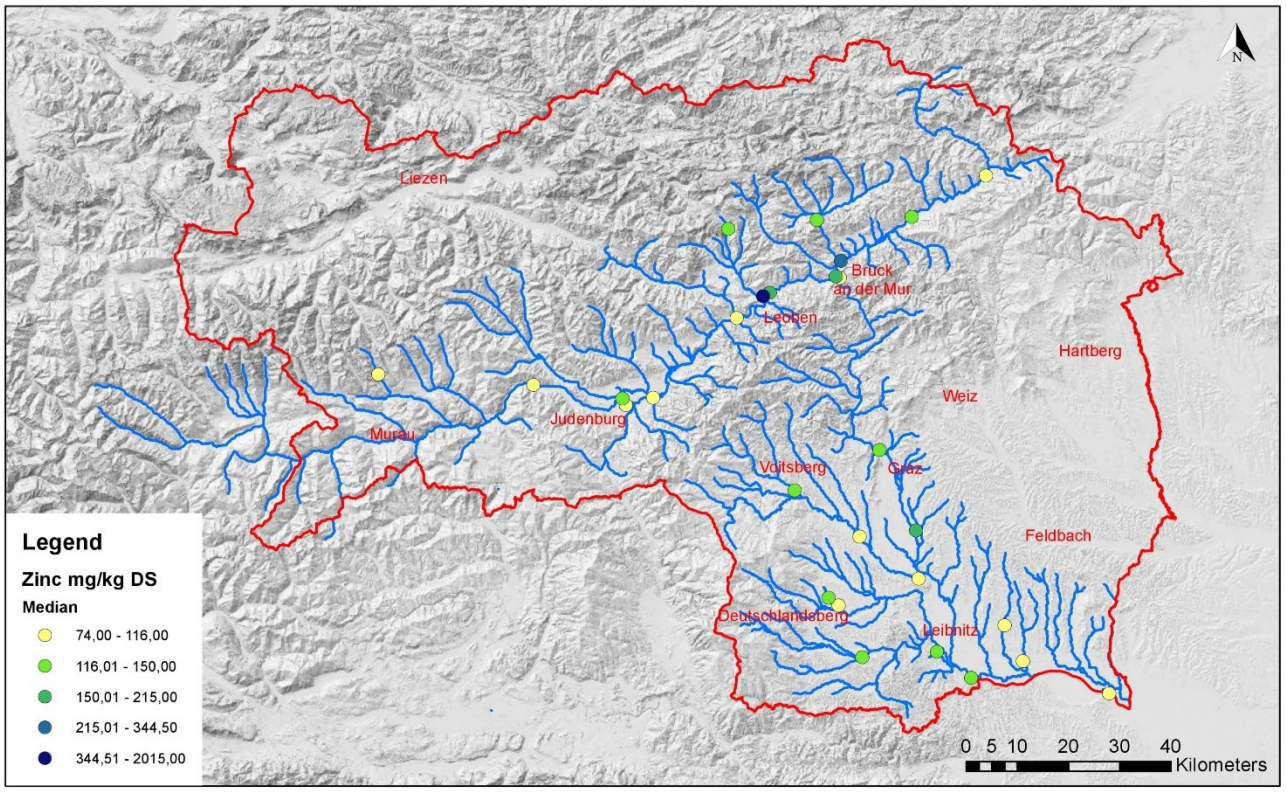


*Figure 84: Zinc S-Parameter; Median Values*

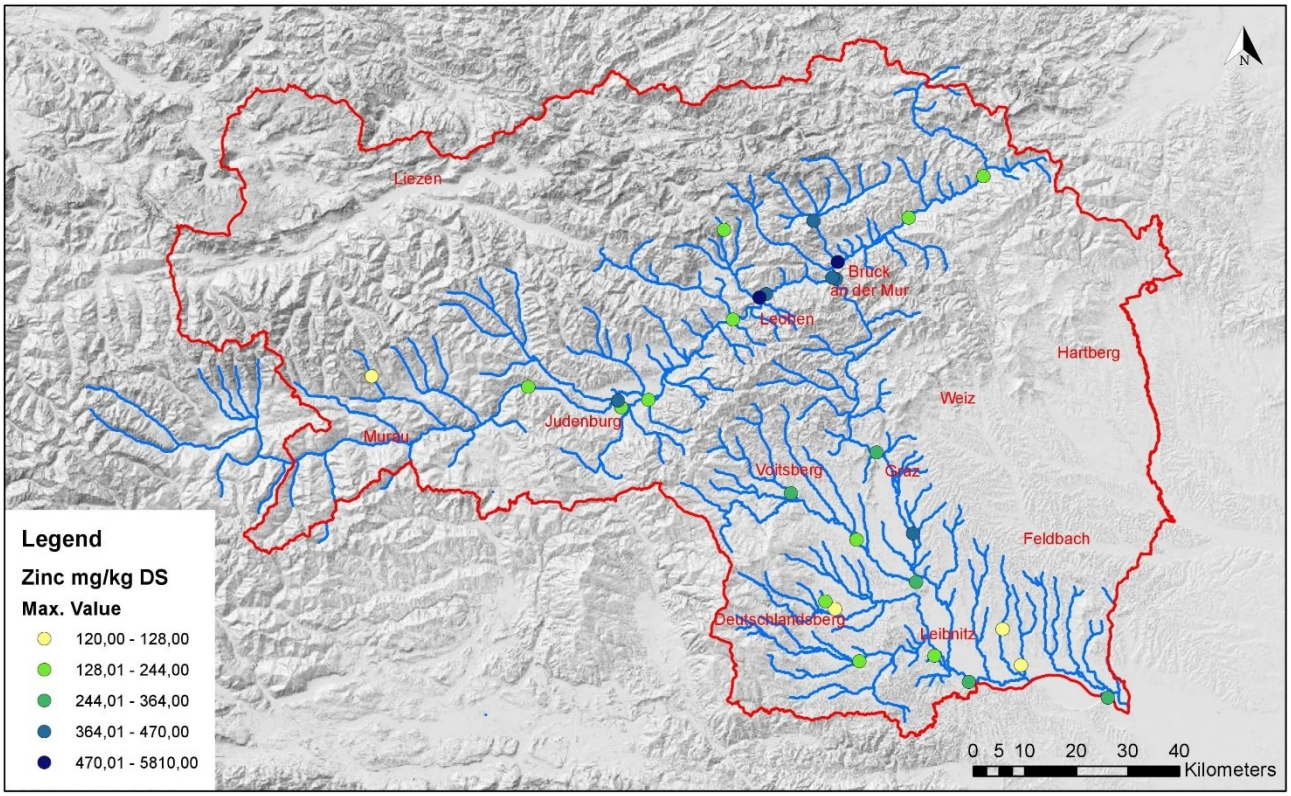


*Figure 85: Zinc S-Parameter; Maximum Values*


*Figure 86: Detail section measuring point FW61400187, F-Parameter*


*Figure 87: Detail section measuring point FW61400187, F-Parameter*

## 1.20 Time-dependent comparison of heavy metal concentration and flow rate

For the following two monitoring sites, continuous flow rate measurements as well as heavy metal measurements from July 1996 to July 1997 are available (for data basis, see Appendix 2). Both are located in Leoben.

### 1.20.1 Measuring point FW61400097 (Leoben)

In Figures 88 - 89 the flow rate (measured in $m^3/s$) and the heavy metal concentrations (in mg/l) are correlated. No direct correlation is found. This is particularly evident for the element copper, where the concentration decreases from July to August 1996. At the same time, however, the flow rate increases significantly (dilution effect). Afterwards, from October 1996 to February 1997 the flow rate decreases constantly. Copper, on the other hand, increases until November 1996 and then decreases until December 1996. This would indicate a delayed response of the heavy metals to the flow, but from December onwards the copper content in the water increases significantly without any increase in flow. From February 1997 to April 1997 copper and flow show an almost parallel increase, from April 1997 the flow value again increases strongly, but the copper content decreases instead.

The situation is similar for the element zinc. Here, too, a delayed reaction of the metal concentration to the flow rate can be assumed (until November 1996). From then on, however, the zinc concentrations jump significantly in comparison to the constantly falling flow rate. Similarly, the kink in the flow line in April 1997 is not shown in the zinc.

If the heavy metal lines are compared, no correlation can be found. If the concentration of one element increases, an increase in the other heavy metal concentrations is not necessarily to be expected.

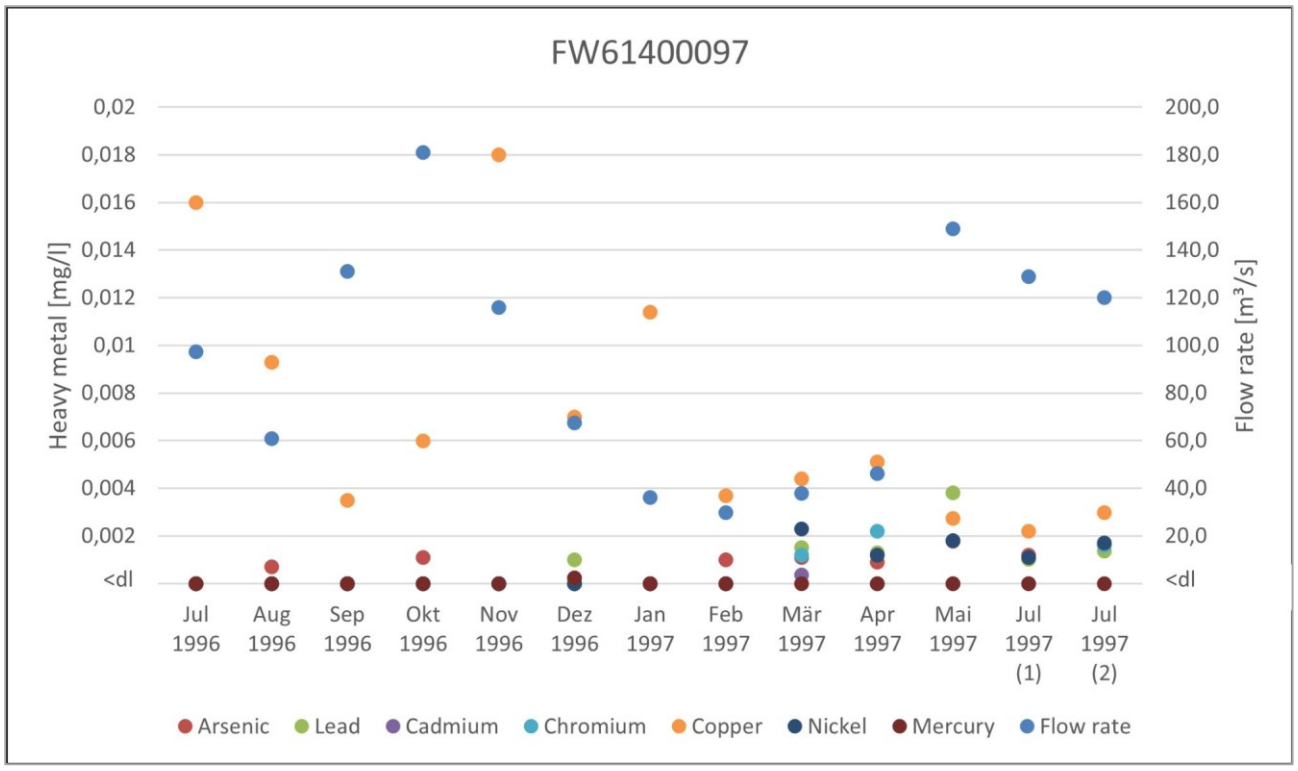


*Figure 88: Flow rate and heavy metal concentrations FW61400097, pt. 1*

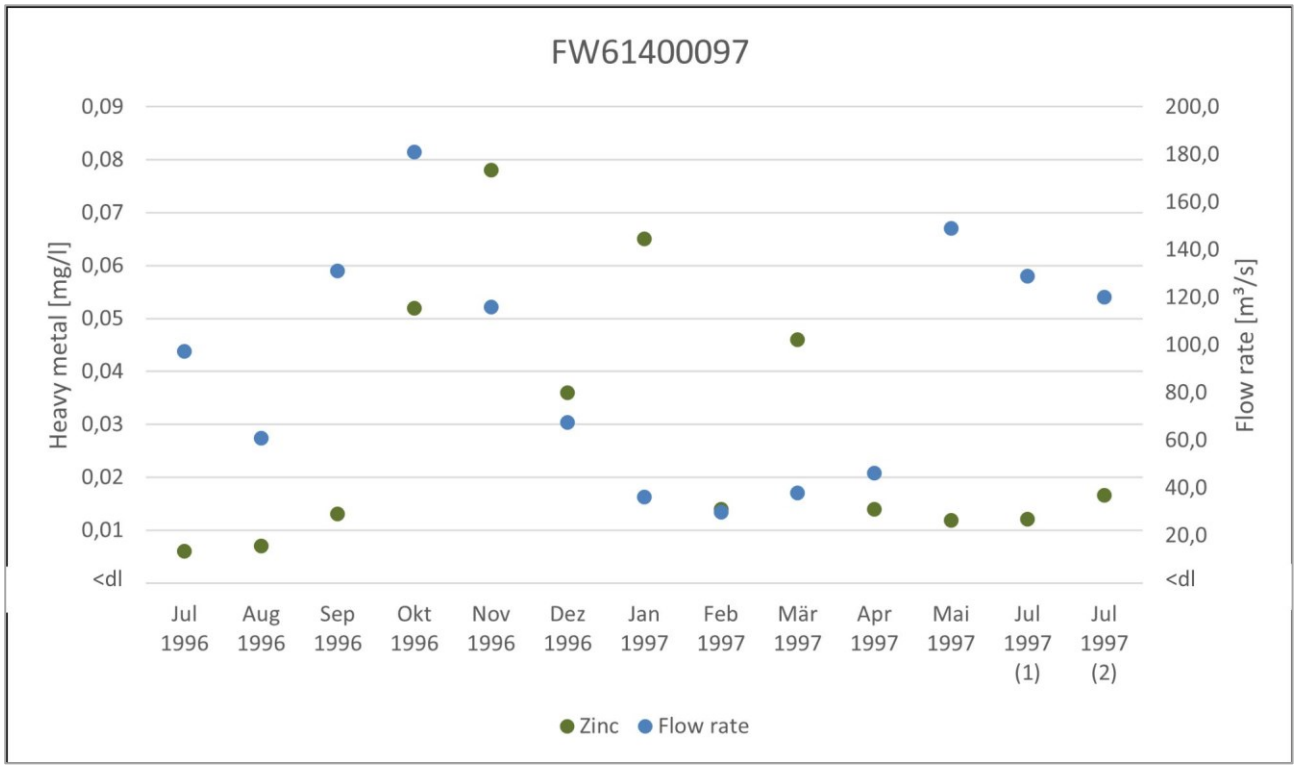


*Figure 89: Flow rate and heavy metal concentrations FW61400097, pt. 2*

### 1.20.2 Measuring point FW61400187 (Leoben)

The data of the curves shown in Figures 90 - 91 (flow rate, measured in m³/s and heavy metal content, in mg/l) were measured at the same times. Analogous to measuring point FW61400097, no direct correlations between flow and heavy metal concentration can be established here either. Figure 90 shows a similar development of the copper content as at monitoring site FW61400097. After the flow peak in October 1996, there is an increase in copper content in November 1996. Flow decreases constantly until March and increases again from March 1997 until May 1997. It decreases again until July but increases again in the same month. Copper levels drop to an interim low in January 1997, rise again briefly in February, drop again in March 1997 and reach another peak in April 1997. Noticeable is that at the measuring point FW61400097 a similar development of the copper concentration can be read (partly slightly delayed). Same applies to the zinc content between September 1996 and April 1997. Here, too, the contents of both measuring points show a similar, partly somewhat time-delayed development of the curve. Concentrations of zinc at monitoring site FW61400187 show peaks in November 1996, January 1997 and March 1997. In contrast to the measuring point FW61400097, the zinc content rises sharply from April 1997 until the peak is reached at the beginning of July 1997. At the second measurement in July the zinc concentration in the water has clearly decreased.

If the heavy metal concentrations of the different elements are also compared with each other here, no correlation between them is discernible. However, if the data are considered across measuring sites, at least a correlation between the respective element concentrations can be established, as already mentioned.

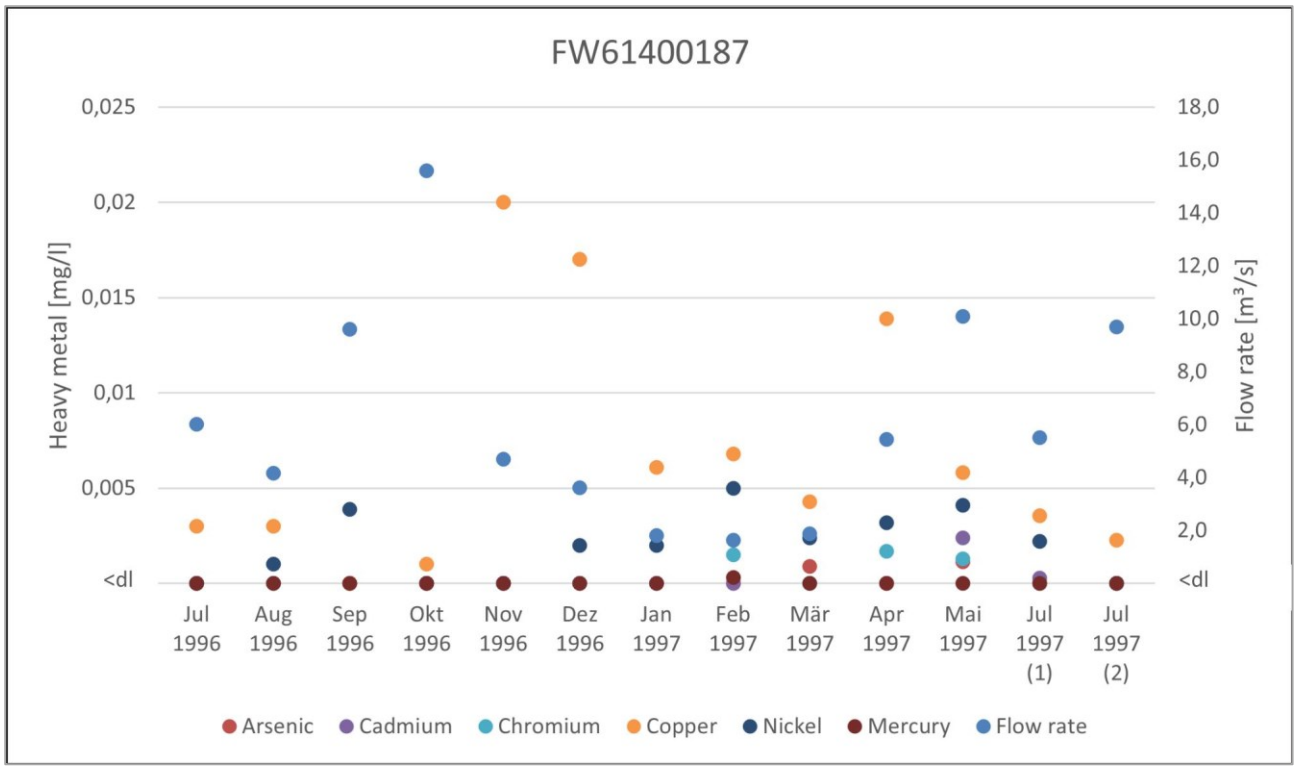


*Figure 90: Flow rate and heavy metal concentrations FW61400187, pt. 1*

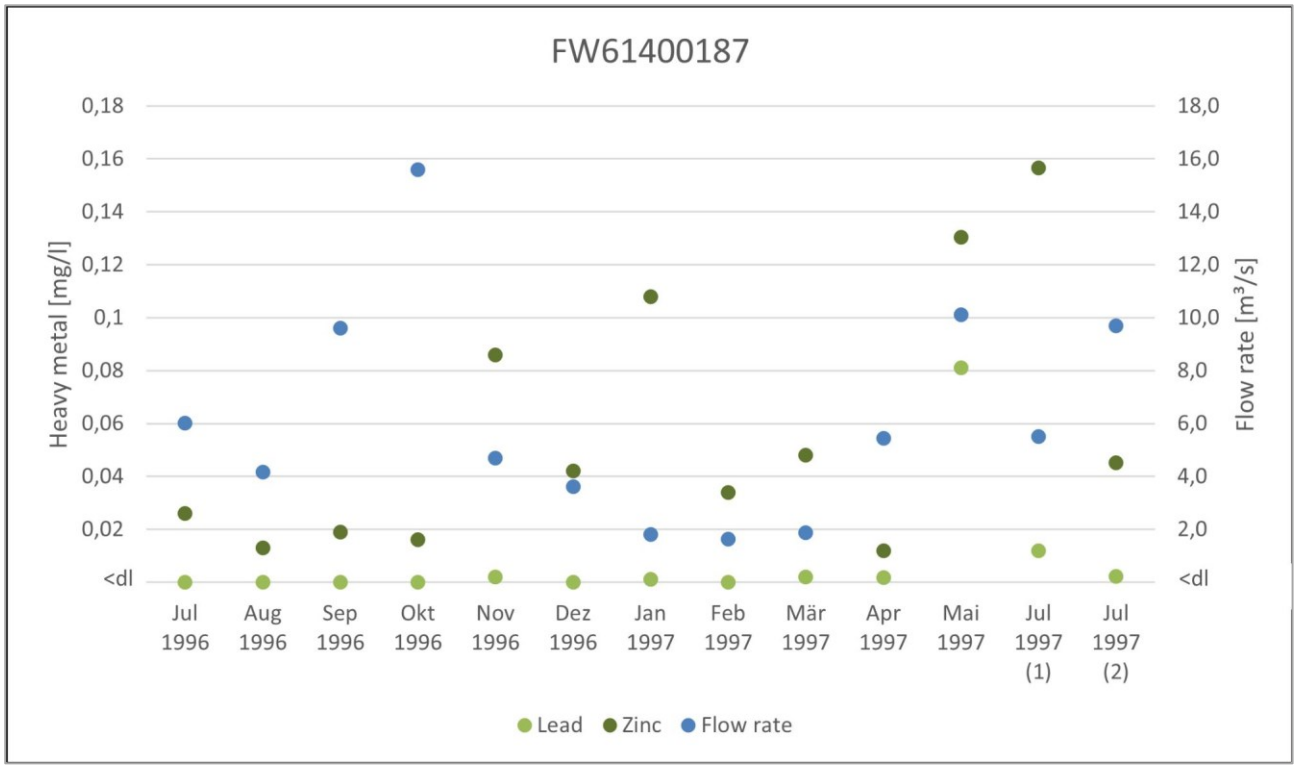


*Figure 91: Flow rate and heavy metal concentrations FW61400187, pt. 2*

## 1.21 Area of Leoben

Table 4 shows the results from the XRF measurements for the sampling in Leoben. The following chapters refer to this Table.

| Sample | Total | LOI | SiO2 | TiO2 | Al2O3 | Fe2O3 | MnO | CaO | MgO | Na2O | K2O | P2O5 |
|---|---|---|---|---|---|---|---|---|---|---|---|---|
| Nr. | % | % | % | % | % | % | % | % | % | % | % | % |
| Mur1 | 100.87 | 5.31 | 61.94 | 0.99 | 15.47 | 6.36 | 0.09 | 2.68 | 2.79 | 2.37 | 2.39 | 0.17 |
| Mur2 | 99.67 | 12.94 | 51.41 | 0.69 | 9.27 | 10.16 | 0.43 | 8.48 | 3.08 | 0.95 | 1.89 | 0.22 |
| Mur3 | 99.77 | 10.48 | 53.17 | 1.16 | 15.74 | 7.35 | 0.12 | 3.32 | 3.42 | 2.01 | 2.55 | 0.26 |
| Mur4 | 100.27 | 3.24 | 62.06 | 1.62 | 13.84 | 8.65 | 0.20 | 3.82 | 2.67 | 2.19 | 1.53 | 0.27 |
| Mur5 | 100.06 | 1.37 | 52.34 | 2.78 | 14.85 | 17.65 | 0.54 | 4.81 | 2.84 | 1.43 | 0.80 | 0.29 |
| Mur6 | 100.87 | 4.72 | 60.41 | 1.54 | 14.52 | 8.38 | 0.18 | 3.74 | 2.83 | 2.18 | 1.82 | 0.27 |
| Mur7 | 100.55 | 0.17 | 65.90 | 1.34 | 14.73 | 7.32 | 0.14 | 3.44 | 2.67 | 2.41 | 1.89 | 0.24 |
| Mur8 | 99.85 | 4.97 | 54.30 | 1.85 | 14.56 | 12.44 | 0.36 | 4.47 | 3.19 | 1.69 | 1.43 | 0.26 |
| Mur9 | 100.90 | 2.96 | 62.93 | 1.67 | 14.13 | 7.94 | 0.17 | 3.77 | 2.65 | 2.32 | 1.68 | 0.30 |
| Mur10 | 100.88 | 2.73 | 62.07 | 1.94 | 13.98 | 9.30 | 0.22 | 3.85 | 2.63 | 2.20 | 1.44 | 0.31 |

| Sample | Ba | Ce | Co | Cr | Cu | Ga | La | Nb | Ni | Pb |
|---|---|---|---|---|---|---|---|---|---|---|
| Nr. | ppm | ppm | ppm | ppm | ppm | ppm | ppm | ppm | ppm | ppm |
| Mur1 | 551.07 | 75.00 | 10.59 | 108.99 | 25.82 | 24.26 | 0.00 | 18.41 | 42.69 | 1430.06 |
| Mur2 | 343.92 | 55.77 | 22.95 | 197.30 | 35.74 | 11.75 | 51.49 | 12.41 | 99.35 | 53.52 |
| Mur3 | 542.59 | 98.58 | 18.88 | 128.62 | 44.27 | 22.95 | 58.31 | 21.44 | 57.87 | 84.38 |
| Mur4 | 369.22 | 91.36 | 16.54 | 131.93 | 23.00 | 17.01 | 59.57 | 28.96 | 36.87 | 242.24 |
| Mur5 | 190.67 | 153.54 | 23.44 | 831.06 | 20.89 | 13.31 | 0.00 | 48.79 | 27.54 | 1185.92 |
| Mur6 | 412.51 | 50.54 | 18.52 | 162.70 | 26.46 | 23.24 | 0.00 | 29.14 | 39.72 | 1013.77 |
| Mur7 | 442.34 | 100.98 | 13.17 | 113.97 | 17.68 | 23.68 | 0.00 | 23.36 | 40.17 | 1457.66 |
| Mur8 | 334.87 | 111.95 | 21.90 | 245.22 | 27.40 | 16.41 | 45.26 | 32.20 | 50.77 | 1616.19 |
| Mur9 | 342.57 | 100.25 | 17.46 | 119.57 | 21.18 | 20.38 | 52.75 | 30.91 | 33.87 | 2190.16 |
| Mur10 | 378.16 | 101.02 | 14.87 | 145.10 | 19.64 | 18.48 | 51.82 | 33.72 | 33.07 | 290.16 |

| Sample | Rb | Sr | Th | V | Y | Zn | Zr |
|---|---|---|---|---|---|---|---|
| Nr. | ppm | ppm | ppm | ppm | ppm | ppm | ppm |
| Mur1 | 94.19 | 200.53 | 29.12 | 125.50 | 25.66 | 106.72 | 185.69 |
| Mur2 | 60.93 | 82.82 | 11.46 | 93.67 | 21.30 | 161.64 | 171.92 |
| Mur3 | 97.68 | 188.05 | 19.19 | 146.73 | 34.77 | 139.57 | 221.19 |
| Mur4 | 60.34 | 199.30 | 15.15 | 167.65 | 36.01 | 97.52 | 267.47 |
| Mur5 | 31.72 | 158.09 | 25.42 | 261.08 | 84.61 | 119.67 | 355.66 |
| Mur6 | 69.26 | 200.99 | 19.96 | 164.78 | 35.64 | 106.25 | 302.51 |
| Mur7 | 74.64 | 213.36 | 29.46 | 147.35 | 30.02 | 95.19 | 240.22 |
| Mur8 | 52.42 | 172.28 | 22.89 | 188.25 | 57.84 | 123.53 | 255.94 |
| Mur9 | 65.59 | 209.13 | 39.30 | 174.85 | 36.44 | 88.09 | 262.22 |
| Mur10 | 54.87 | 204.46 | 19.64 | 194.88 | 40.34 | 89.53 | 342.05 |

*Table 4: Processed data from XRF results; measurements in Leoben*

### 1.21.1 Loss on ignition (LOI)

A very high LOI is observed at sample Mur2 (12.94%), as well as at sampling point Mur3 (10.48%). The loss on ignition is particularly low at sampling point Mur7, where the LOI is only 0.17%. (Figure 92)

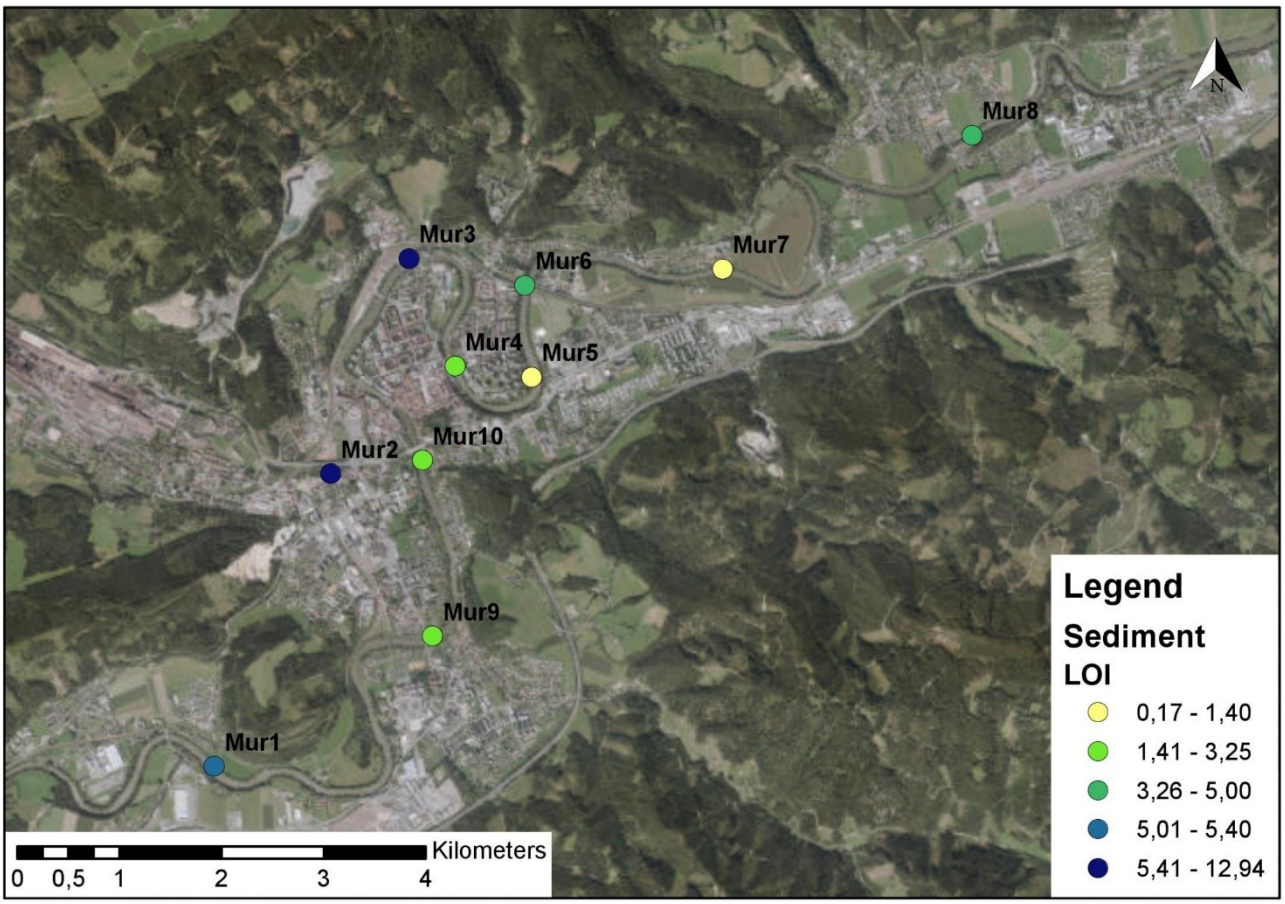


*Figure 92: Loss on ignition of the Leoben samples*

### 1.21.2 $SiO_2$

As shown in Figure 60, the $SiO_2$ contents of the individual sampling points lie within a small range of variation. The values vary between 51.41% (Mur2) and 65.90% (Mur7). (Figure 93)

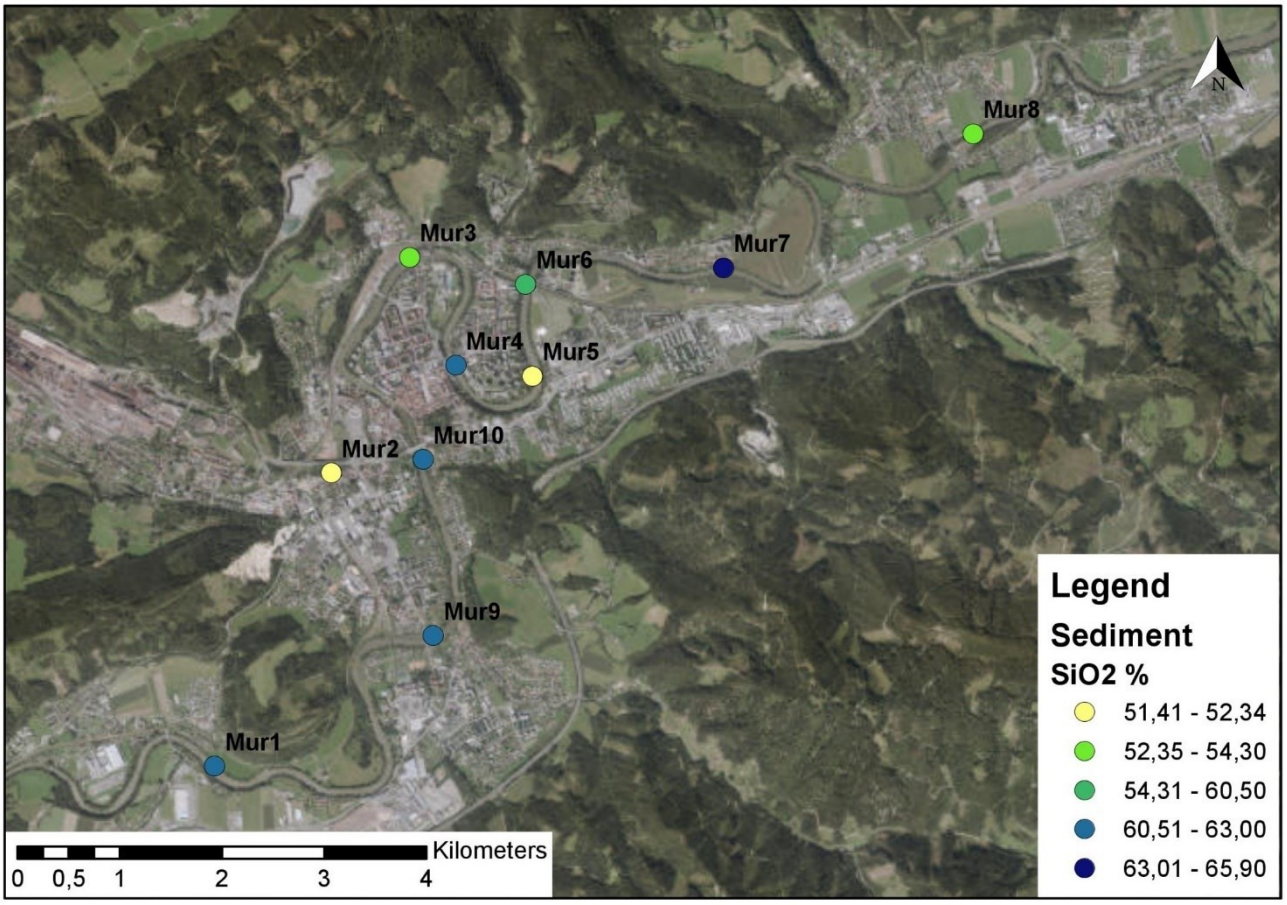


*Figure 93: SiO2 content of the Leoben samples*

### 1.21.3 $Fe_2O_3$

With an Fe2O3 content of 17.65%, this sampling point shows a clearly increased value. The content of the sediment sample from Mur8 is slightly increased (12.44%). The measuring point Mur2 has an $Fe_2O_3$ content of 10.16%. (Figure 94)

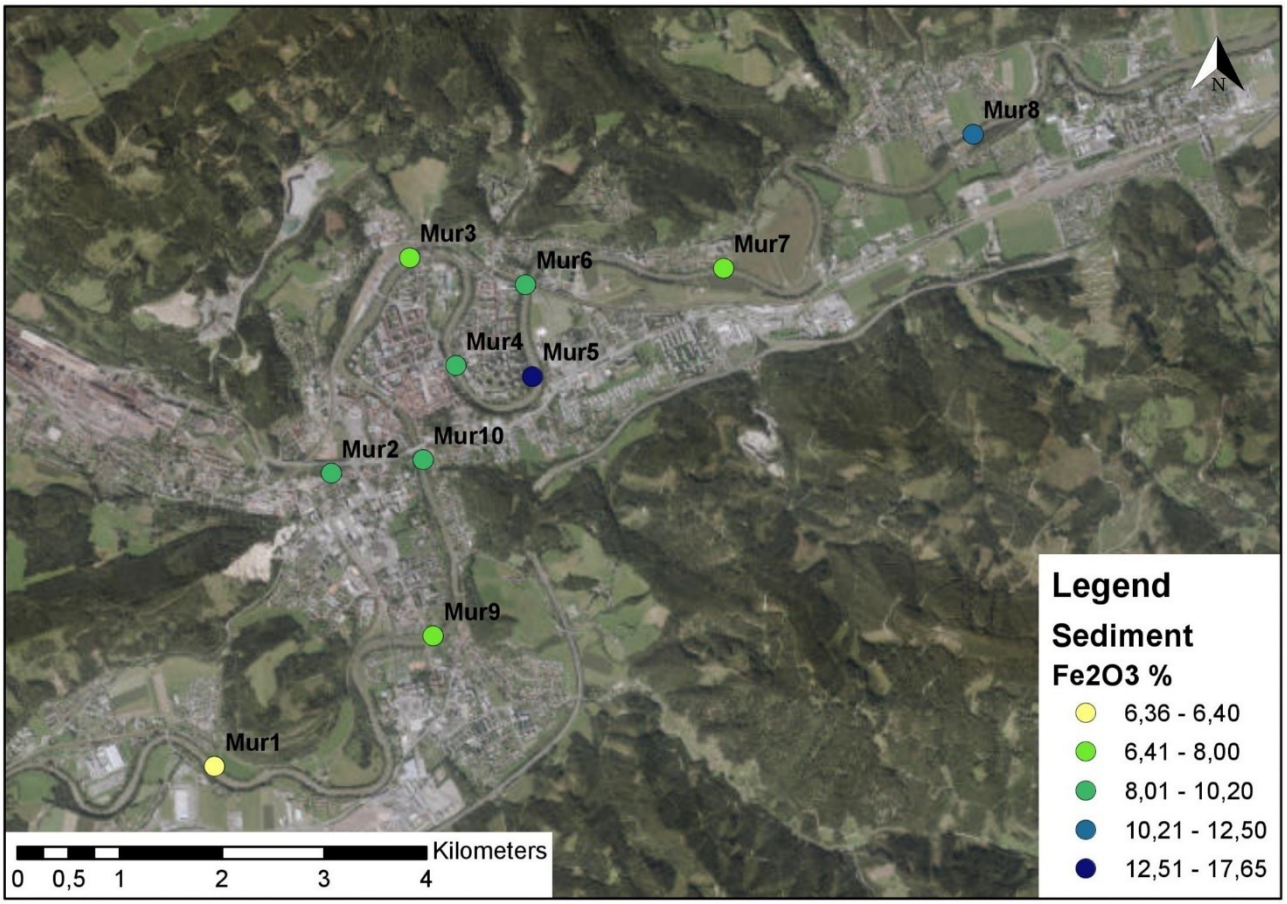


*Figure 94: Fe2O3 content of the Leoben samples*

### 1.21.4 CaO

The measuring point Mur2 shows a clearly increased *CaO* value of 8.48%. (Figure 95)

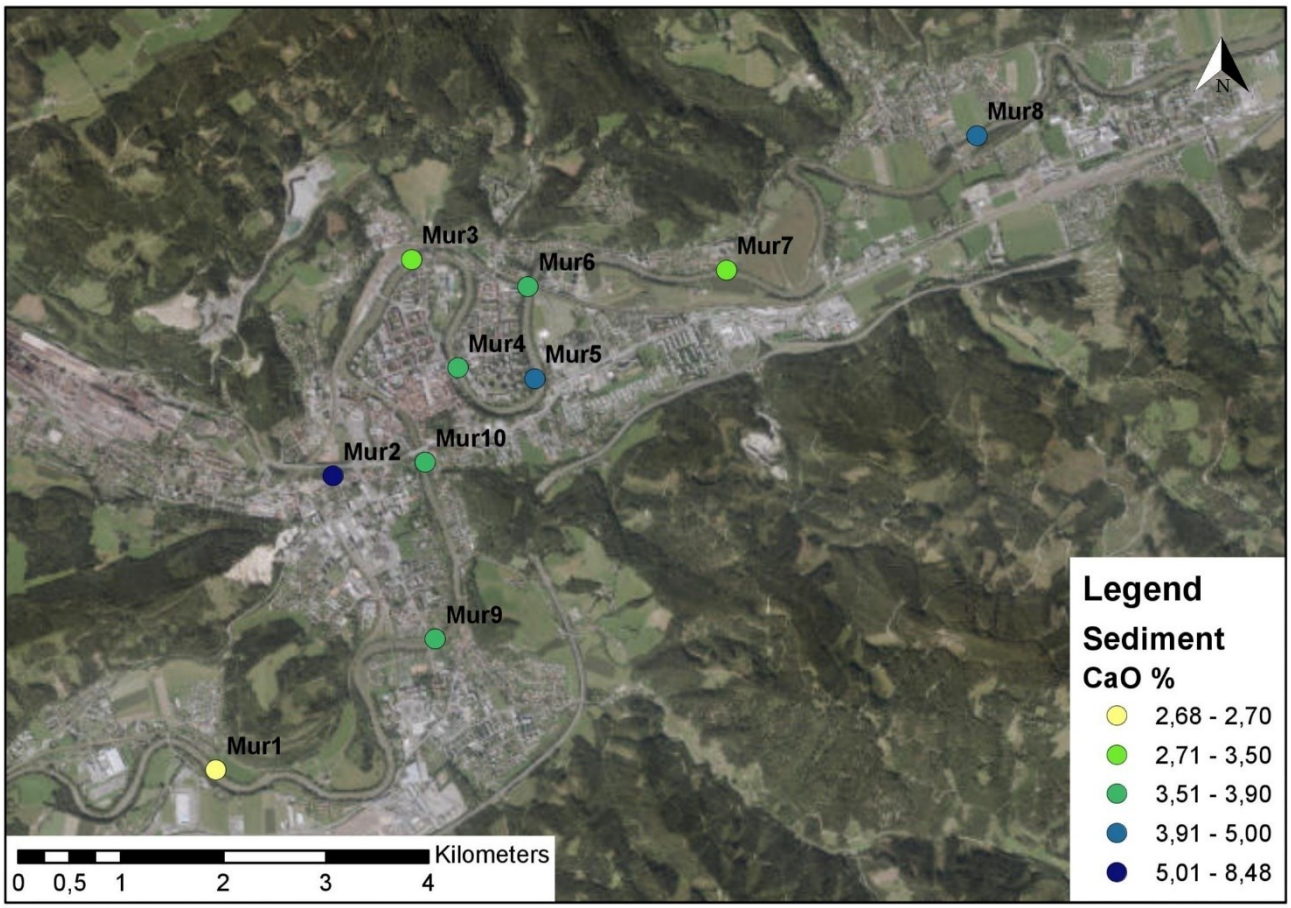


*Figure 95: CaO content of the Leoben samples*

### 1.21.5 Barium

All measurements are within the usual fluctuation range. The measuring points Mur1 (551 ppm) and Mur3 (542 ppm) show slightly higher values, the measuring point Mur5 (190 ppm) slightly lower. (Figure 96)

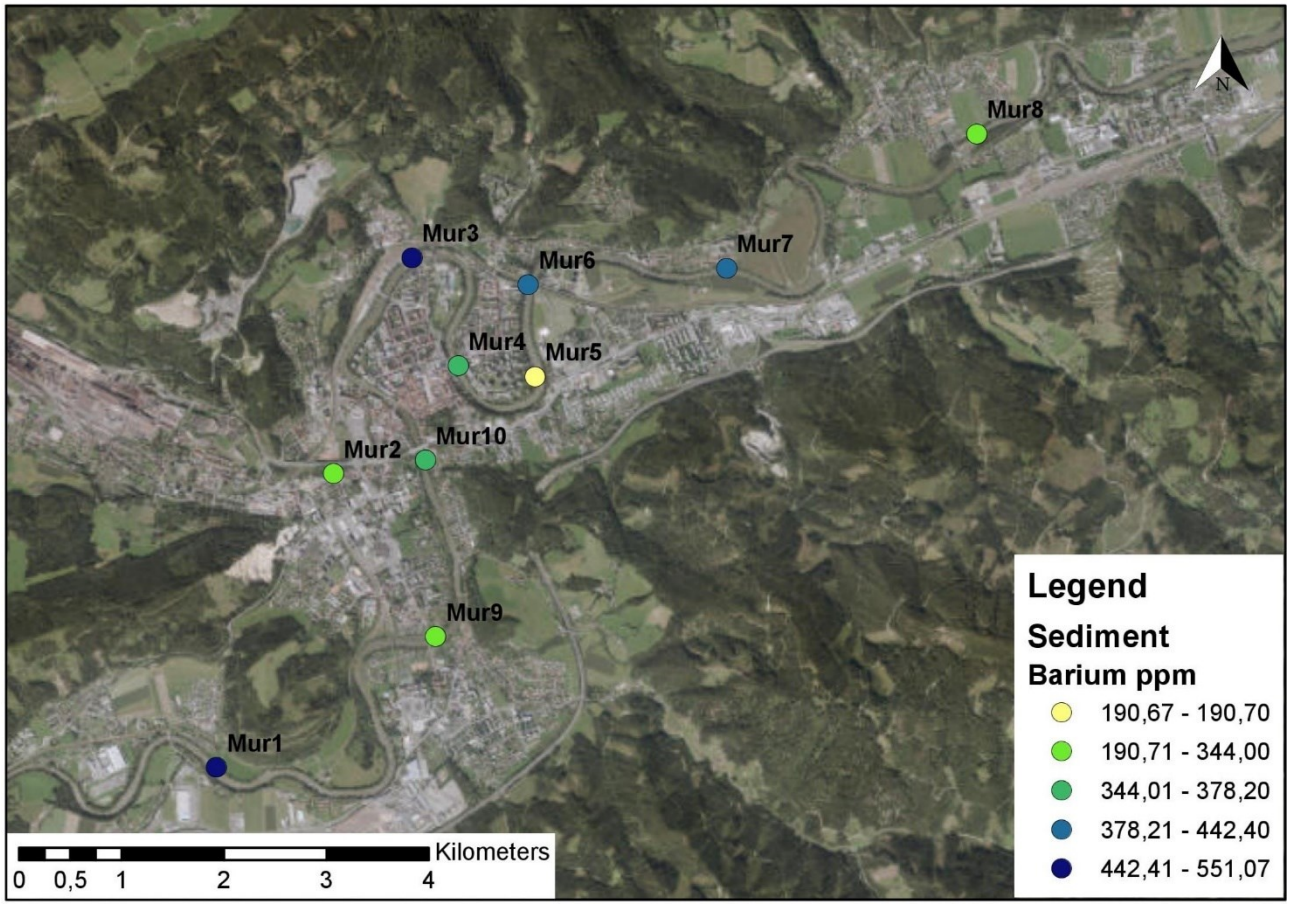


*Figure 96: Ba content of the Leoben samples*

### 1.21.6 Cobalt

All measuring points have a *Co* content between 10 ppm and 23 ppm. The separately considered measuring point Mur2 has a *Co* value of 22 ppm. (Figure 97)

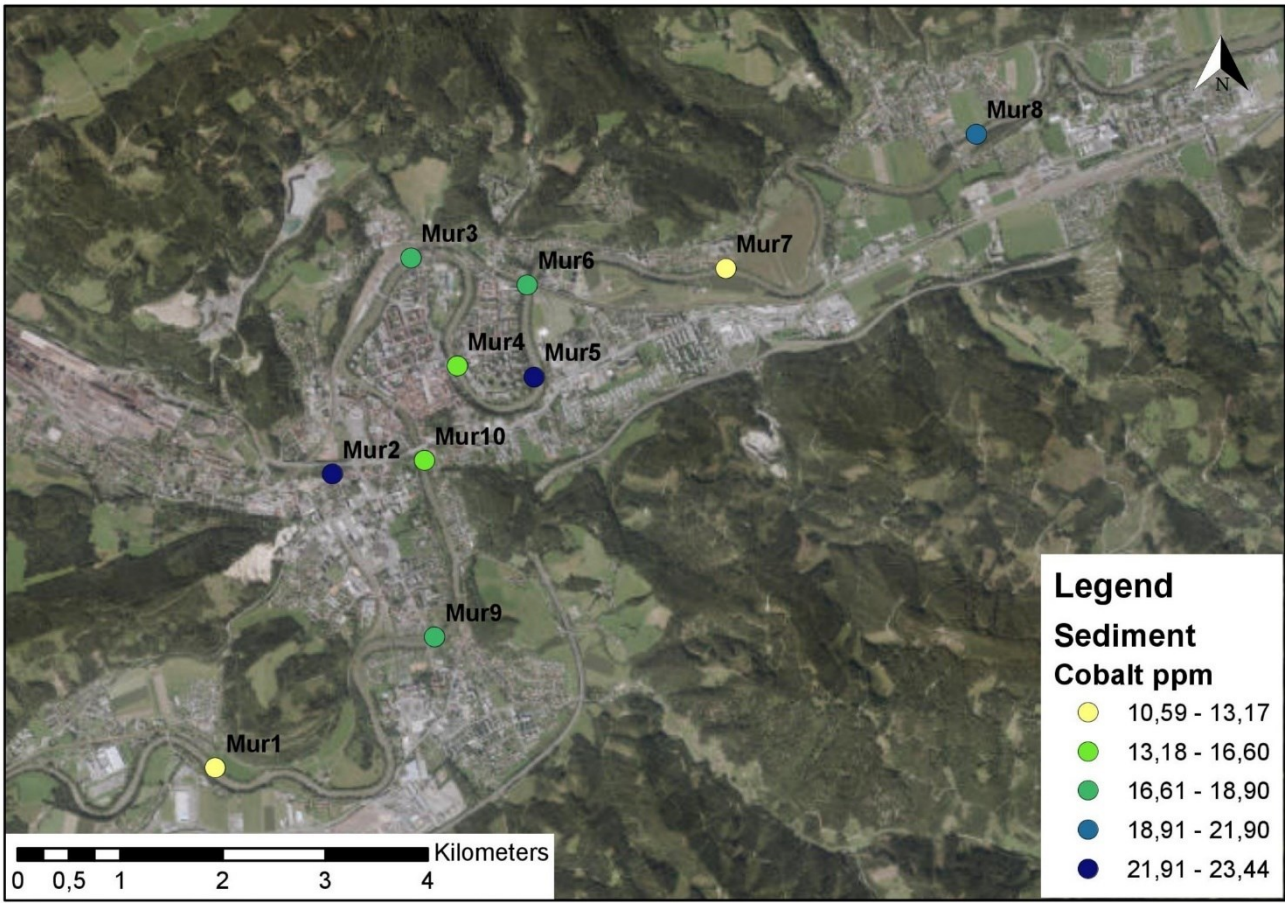


*Figure 97: Co content of the Leoben samples*

### 1.21.7 Chromium

Measuring point Mur5 shows a significantly increased chromium content. At 831 ppm, this value is significantly higher than those of the other measuring points. The measuring point Mur2 shows a value of 197 ppm. (Figure 98)

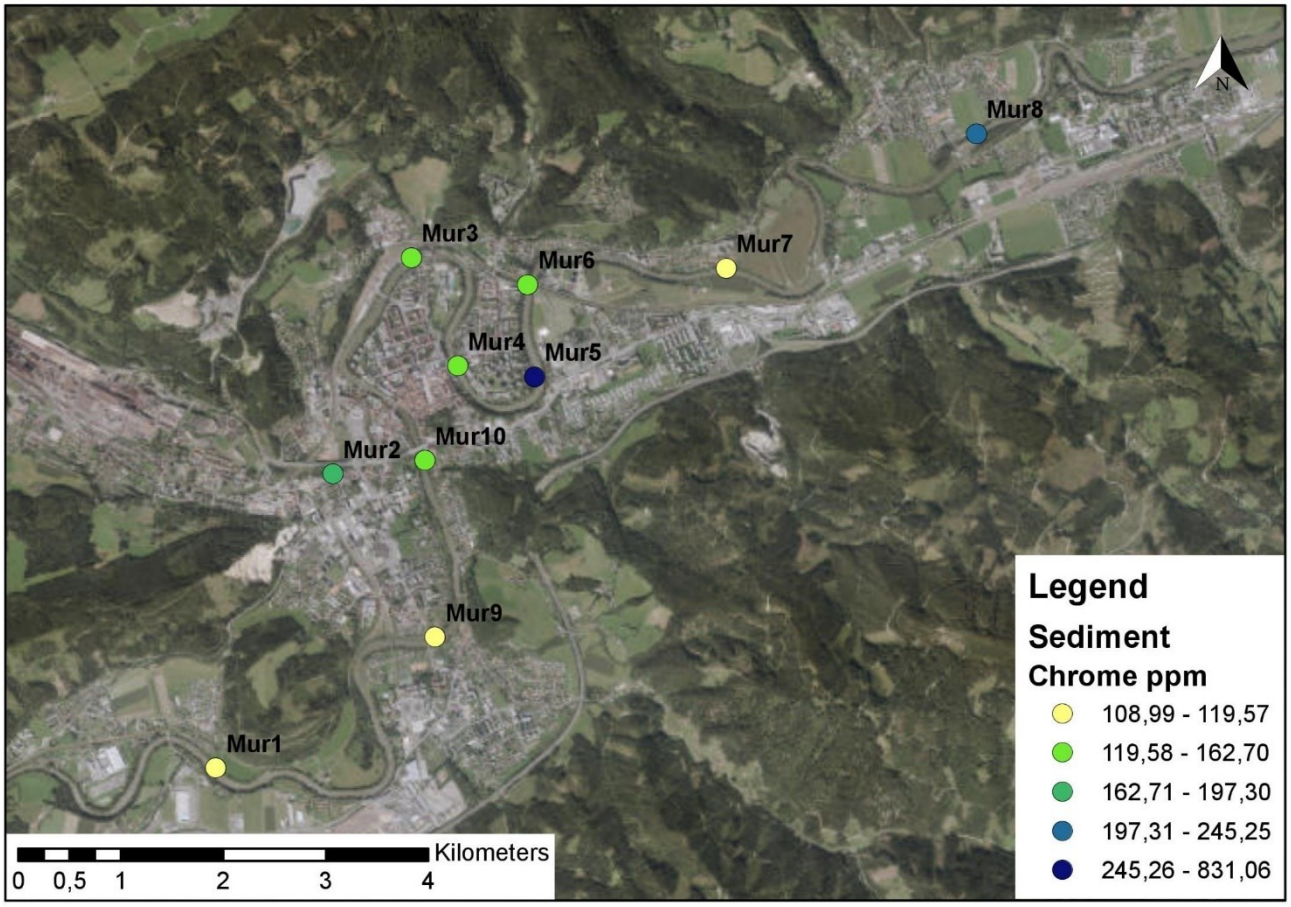


*Figure 98: Cr content of the Leoben samples*

### 1.21.8 Copper

None of the samples has an above-average value. In a comparison of the measuring points, Mur3 (44 ppm) has the highest and Mur7 (17 ppm) the lowest measured value. The measuring point Mur2 has a *Cu* content of 35 ppm. (Figure 99)

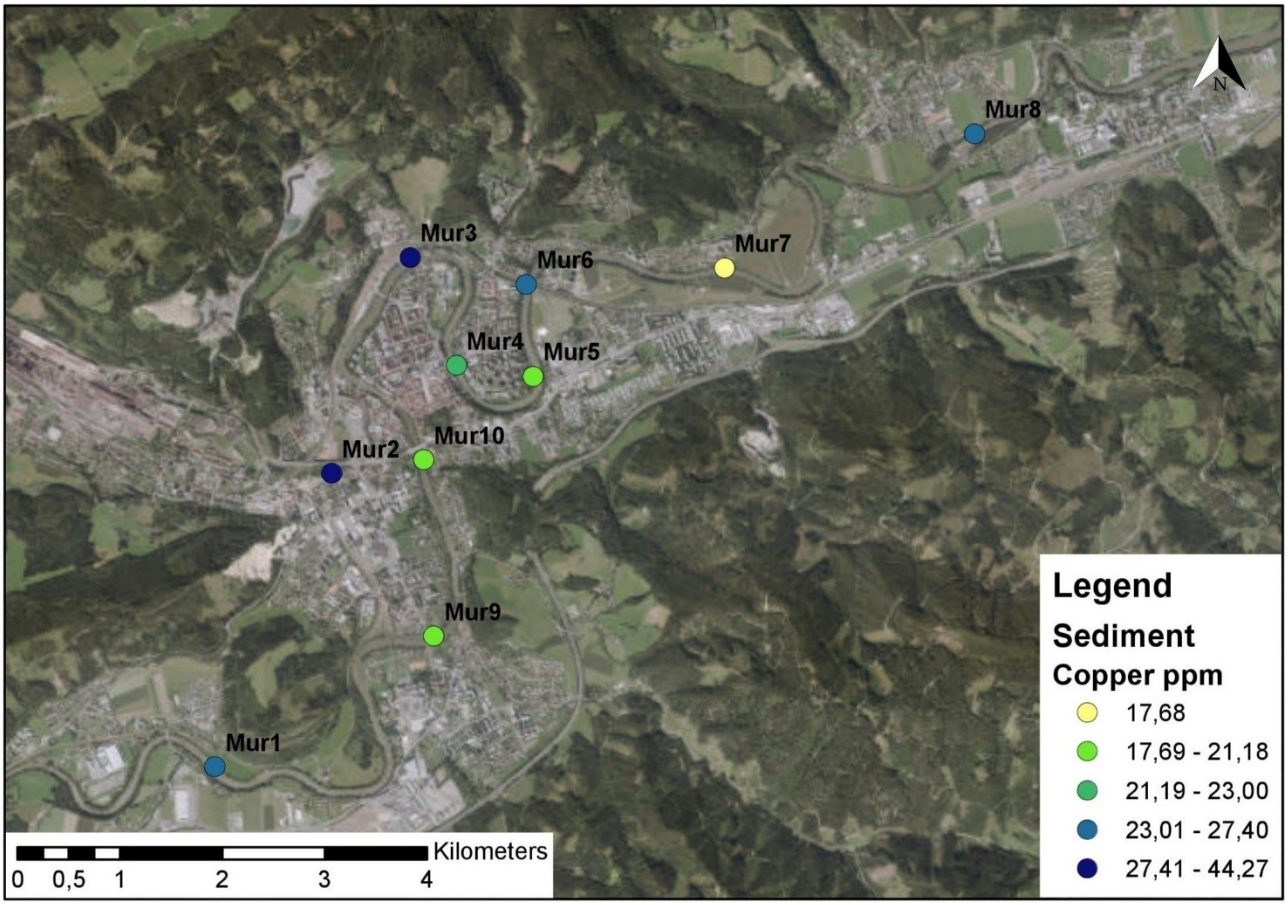


*Figure 99: Cu content of the Leoben samples*

### 1.21.9 Gallium

All measuring points are also within the usual fluctuation range for gallium values. Values between 11 ppm (Mur2) and 24 ppm (Mur1) were recorded. (Figure 100)

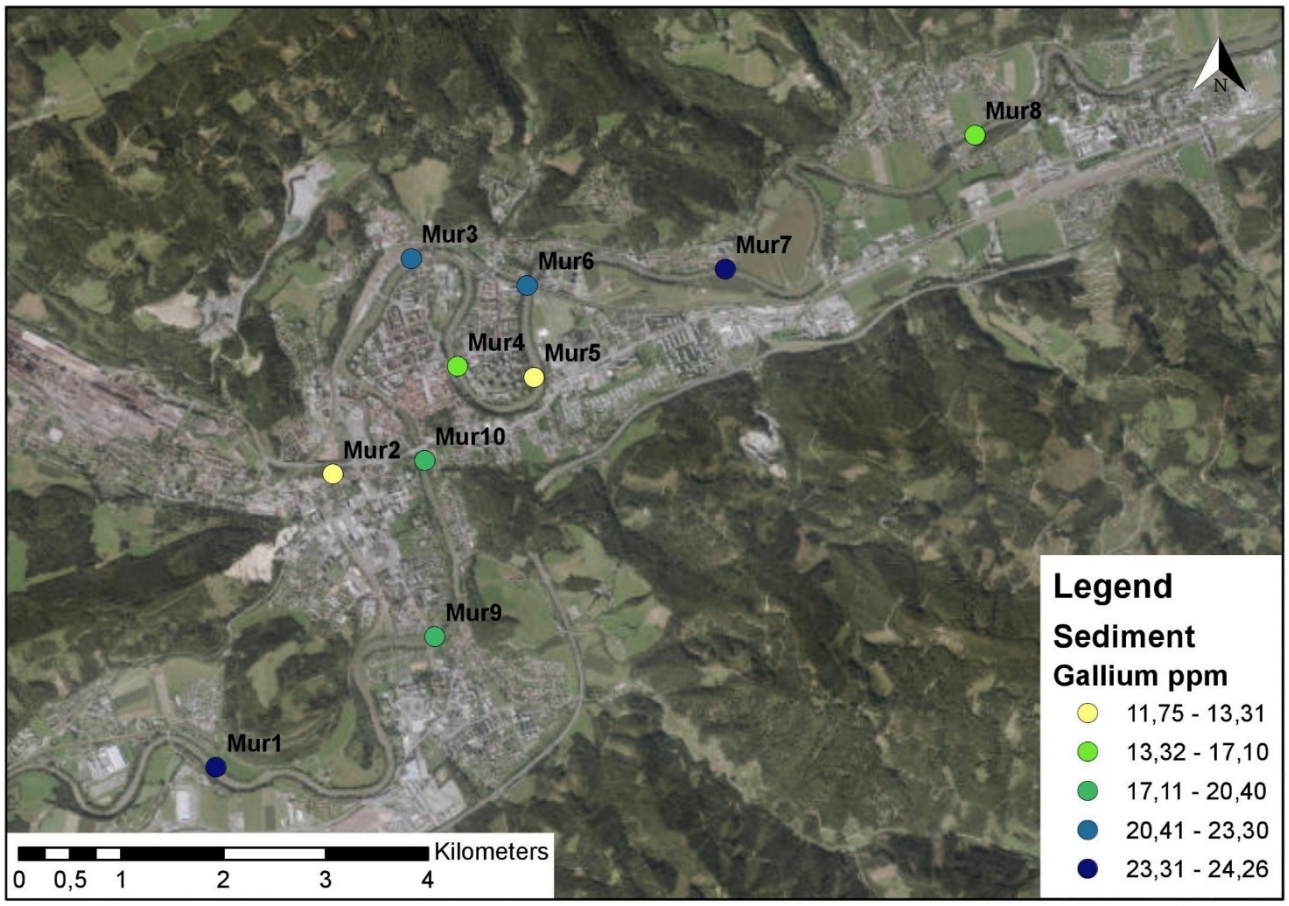


*Figure 100: Ga content of the Leoben samples*

### 1.21.10 Lanthanum

At four measuring points the lanthanum content falls below the detection limit. All other monitoring sites also have no conspicuous values. Measuring point Mur2 has a lanthanum content of 51 ppm. (Figure 101)

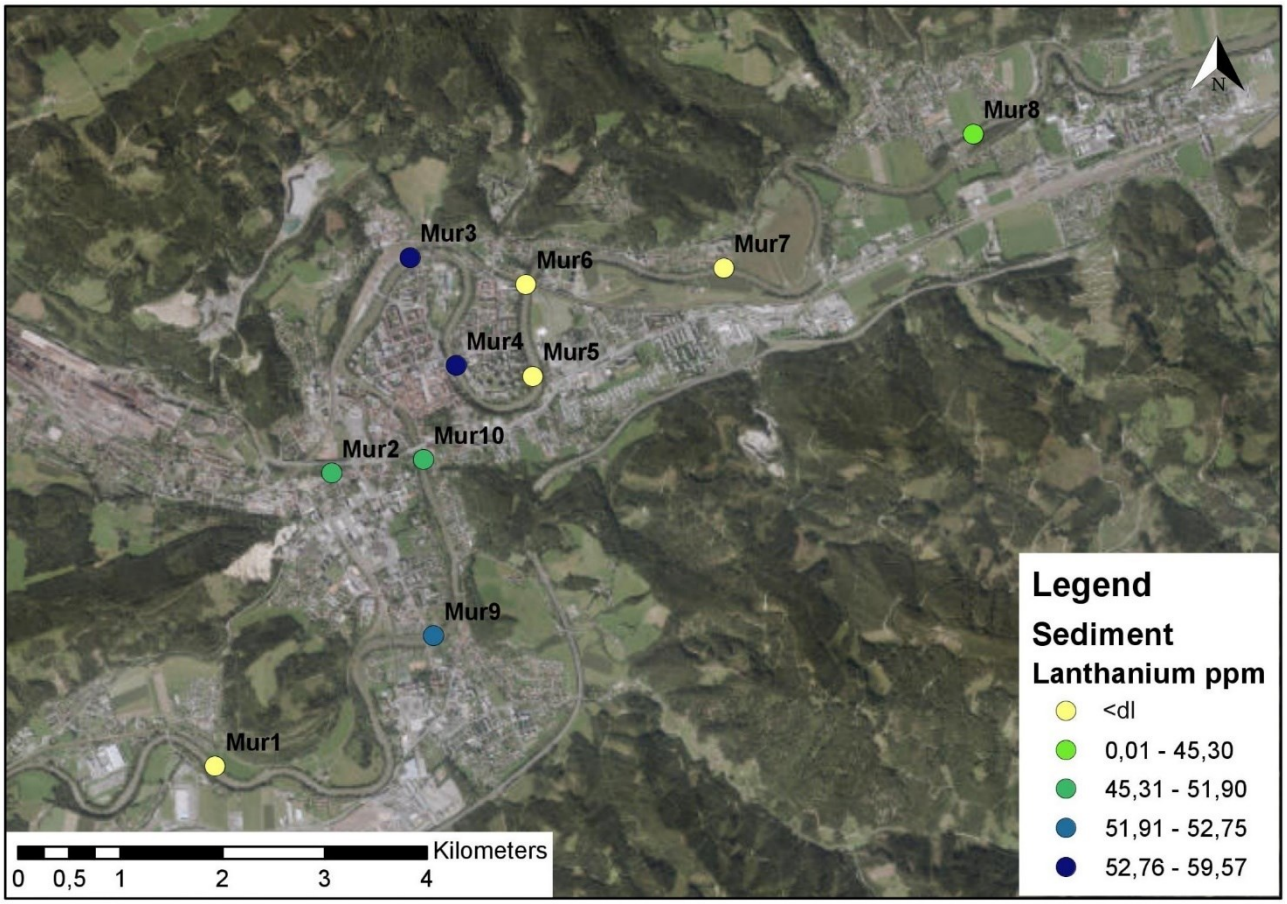


*Figure 101: La content of the Leoben samples*

### 1.21.11 Nickel

None of the samples shows an above-average *Ni* value. In a comparison of the measuring points with each other, the Mur2 measuring point shows a significantly higher concentration of 99 ppm (see Figure 71). All other measuring points are in a fluctuation range between 27 ppm (Mur5) and 57 ppm (Mur3). (Figure 102)

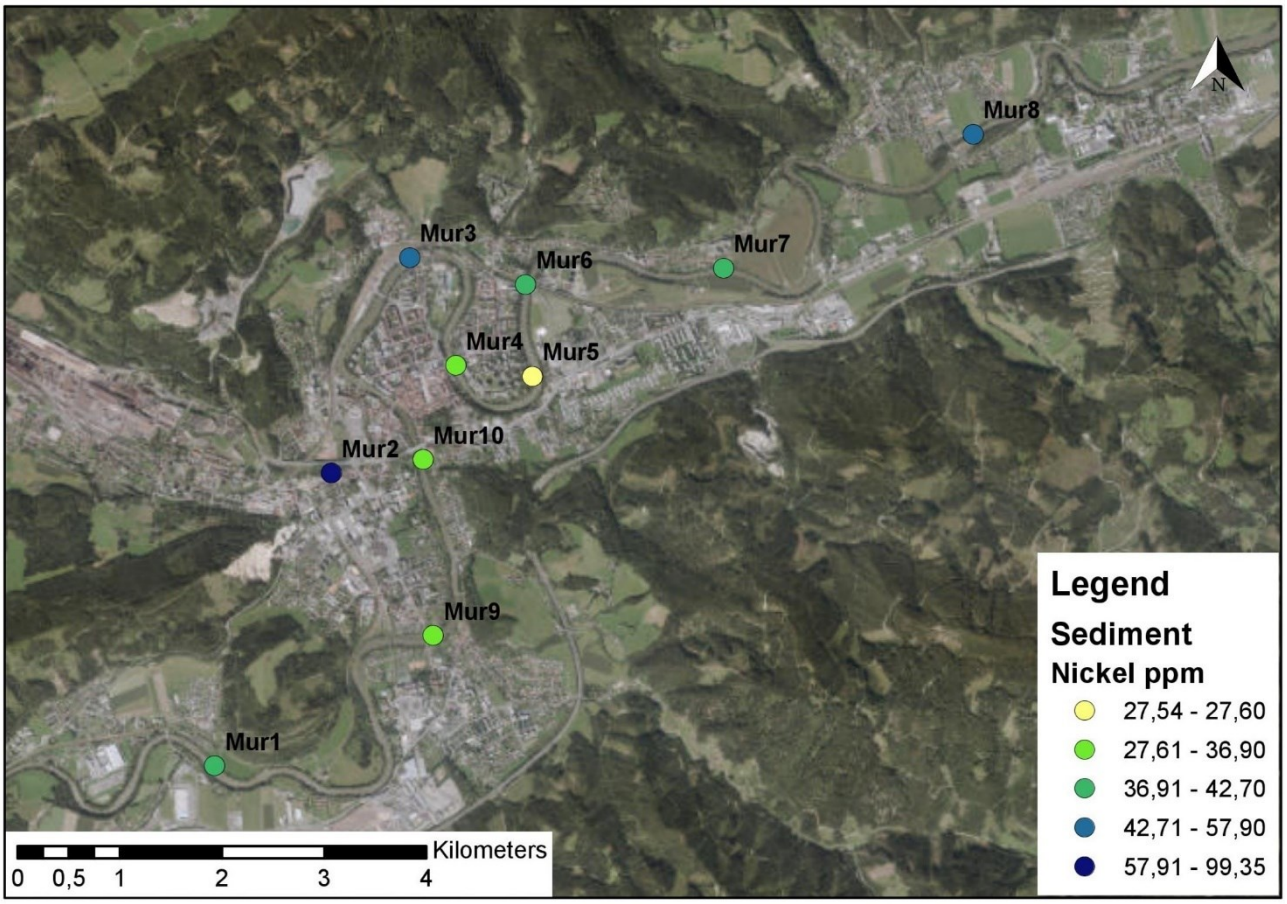


*Figure 102: Ni content of the Leoben samples*

### 1.21.12 Lead

Five sampling points show extraordinary high values. Points Mur1 (1430 ppm), Mur5 (1185 ppm), Mur6 (1013 ppm), Mur7 (1457 ppm), Mur8 (1616 ppm) and Mur9 (2190 ppm) show significantly elevated values. (Figure 103)

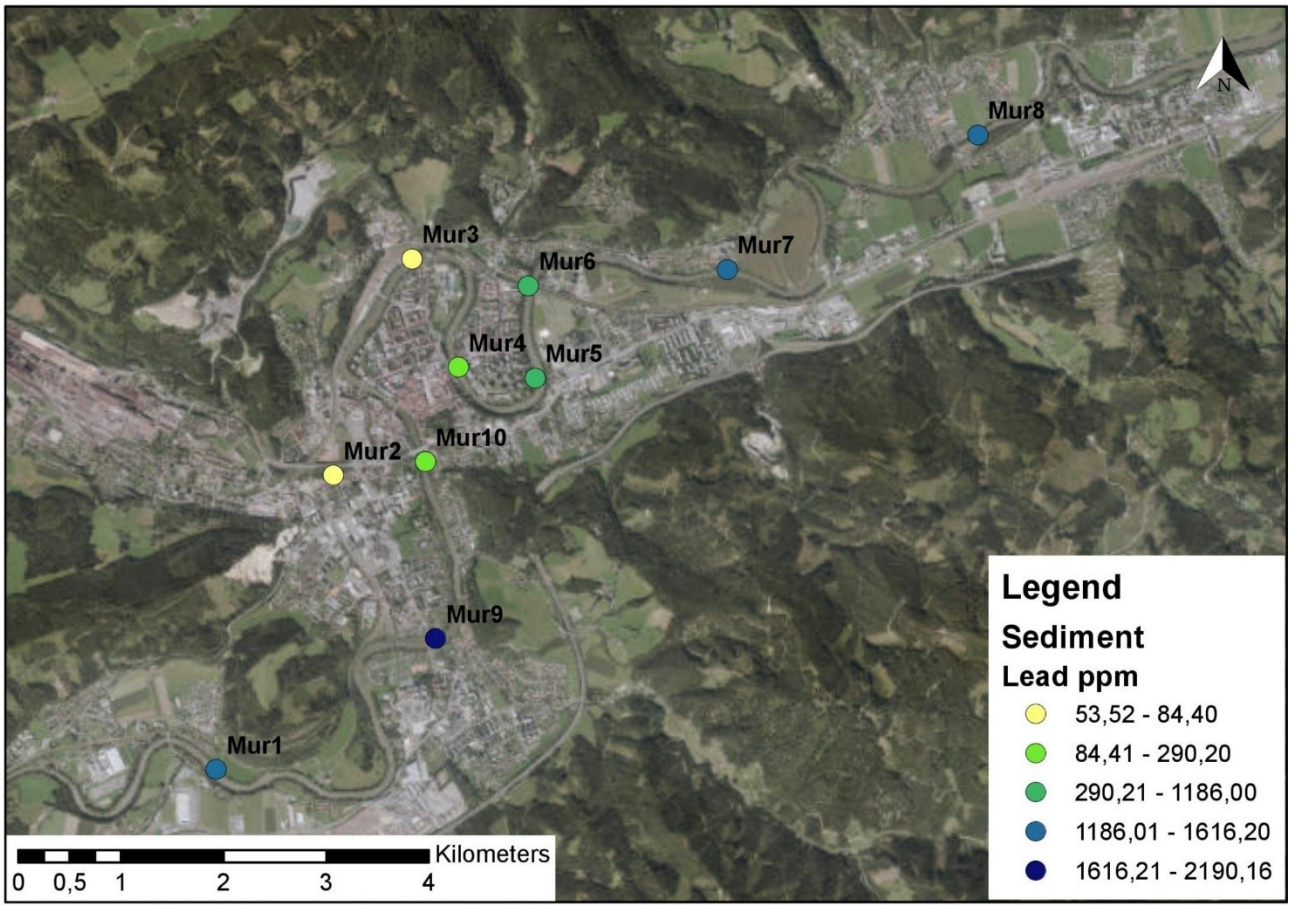


*Figure 103: Pb content of the Leoben samples*

### 1.21.13 Rubidium

The measured values of all sample points are also within the usual fluctuation range. With 31 ppm, the Mur5 measuring point shows the lowest value and with 97 ppm, the Mur3 measuring point shows the highest value. Measuring point Mur2 has a rubidium content of 60 ppm. (Figure 104)

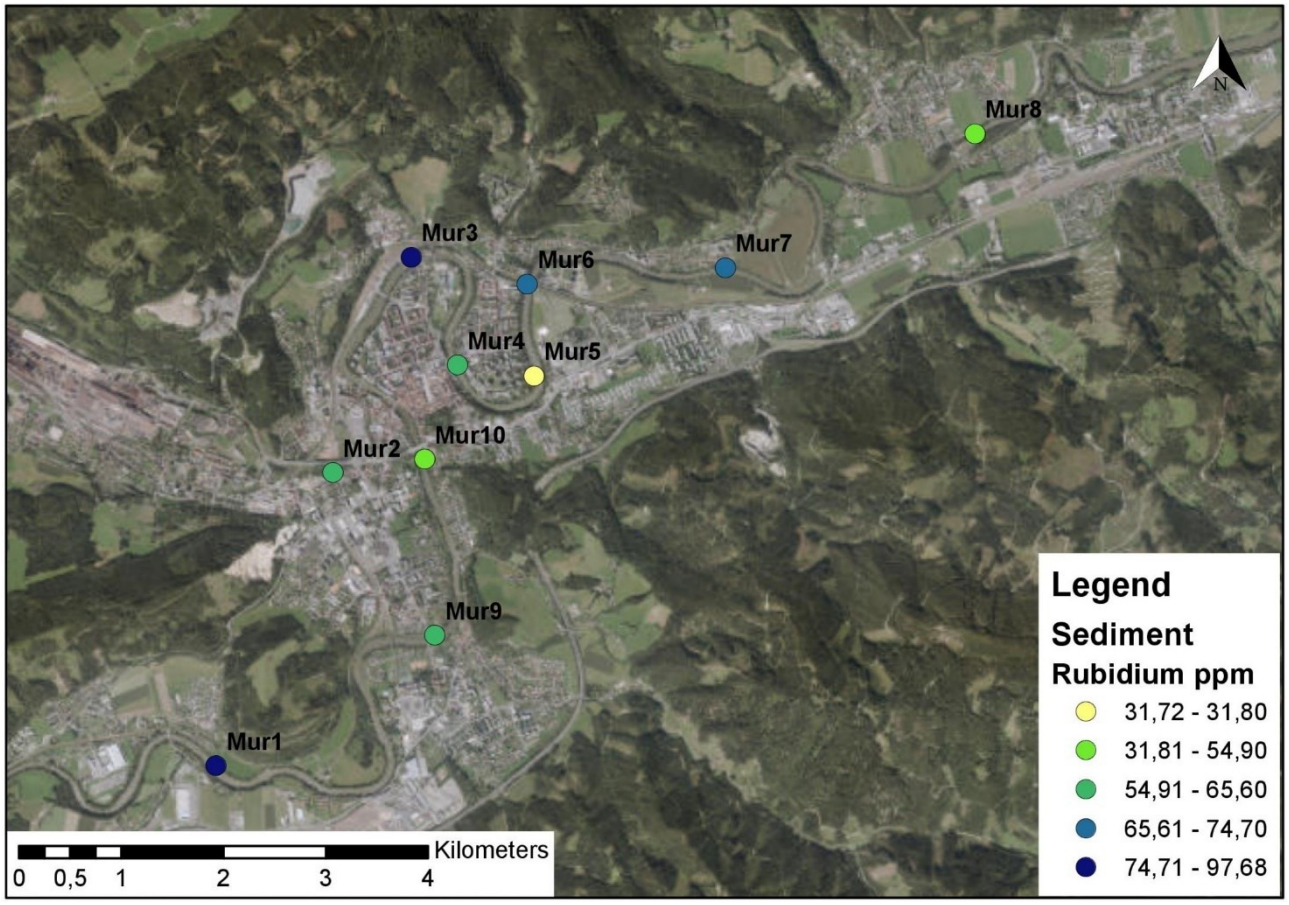


*Figure 104: Rb content of the Leoben samples*

### 1.21.14 Strontium

Figure 74 shows that there is also no significant higher value. Only the measuring point Mur2 has a lower Sr content in comparison (82 ppm). (Figure 105)

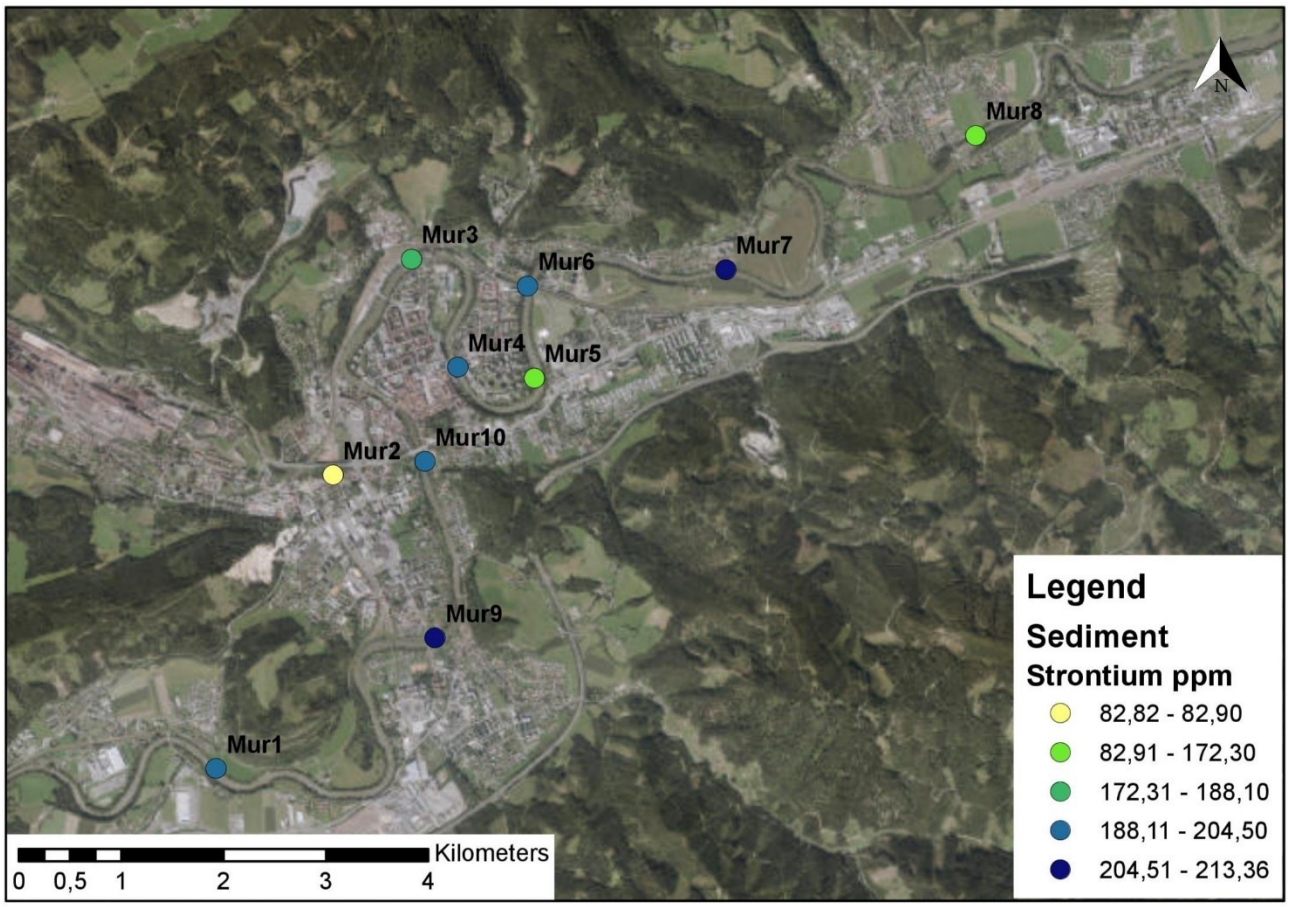


*Figure 105: Sr content of the Leoben samples*

### 1.21.15 Thorium

None of the *Th* readings obtained from this analysis are elevated. The range of variation is between Mur2 (11 ppm) and Mur9 (39 ppm). (Figure 106)

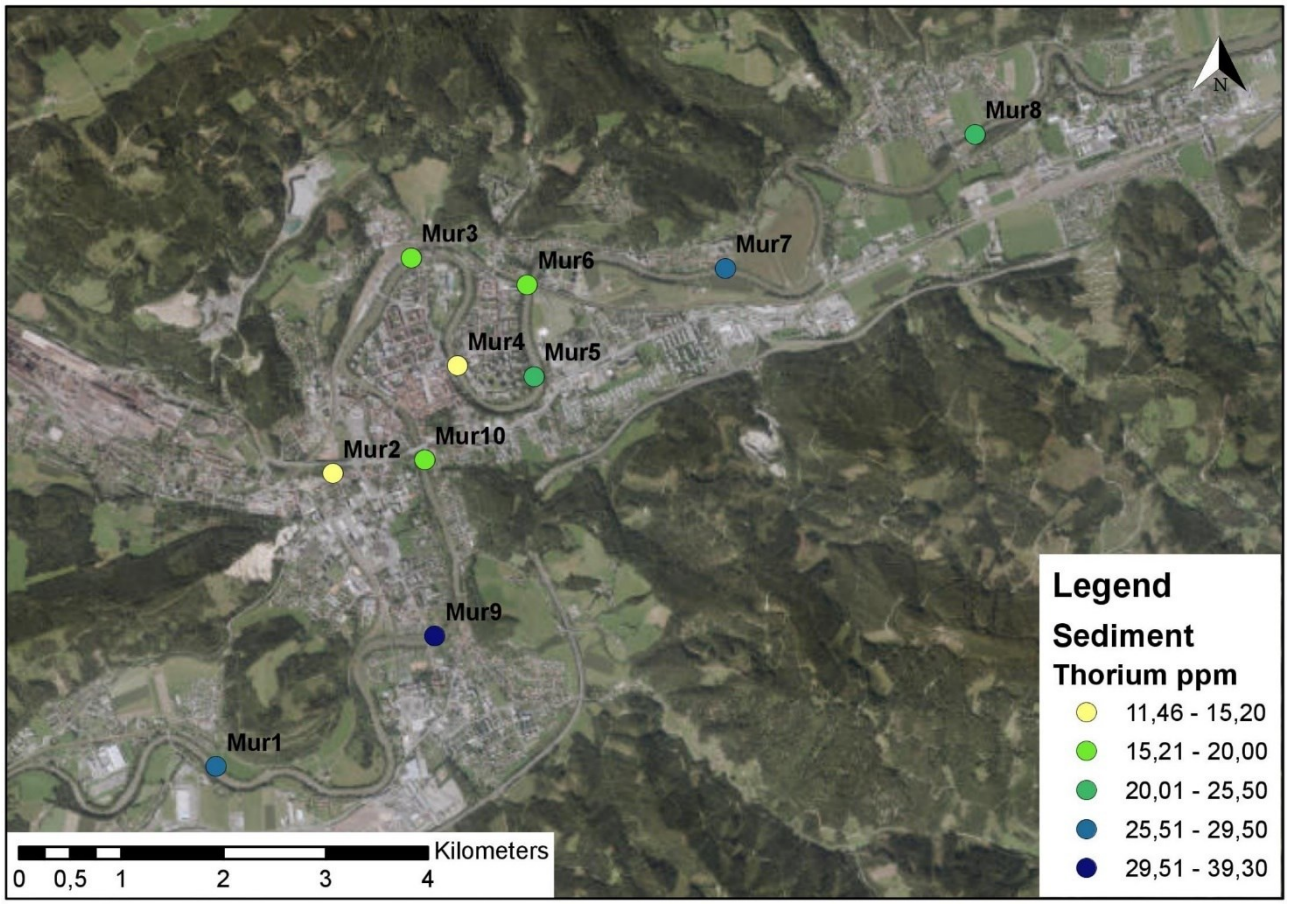


*Figure 106: Th content of the Leoben samples*

### 1.21.16 Vanadium

A comparison of the ten samples taken for this work shows an elevated vanadium value of 261 ppm at monitoring site Mur5. However, this and all other measured values are within the usual measuring range. The measuring point Mur2 shows a vanadium content of 93 ppm. (Figure 107)

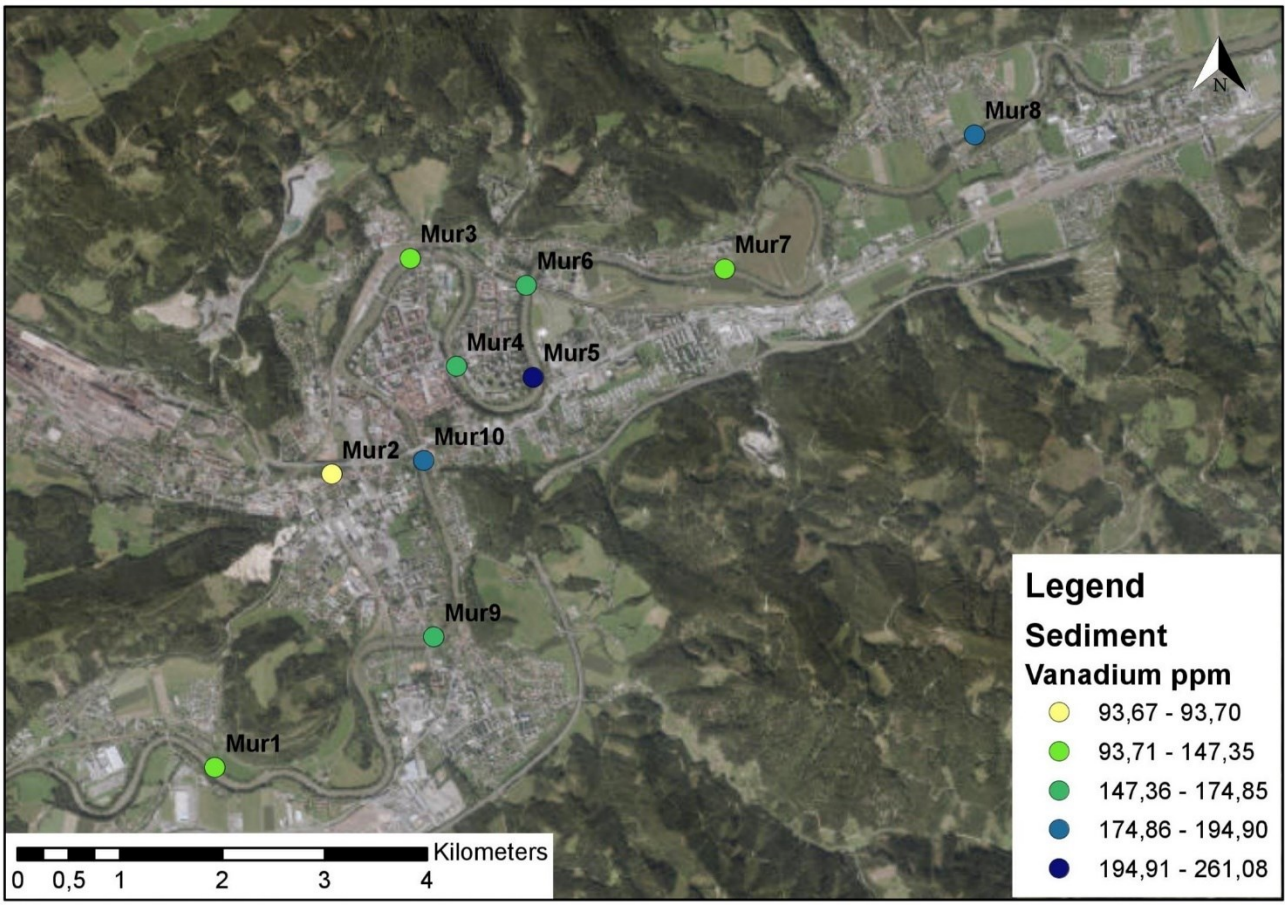


*Figure 107: V content of the Leoben samples*

### 1.21.17 Yttrium

Here, too, no conspicuous values can be detected. A comparison of the measuring points shows an increased *Y* content at sample point Mur5 (84 ppm). Measuring value at point Mur8 is also slightly elevated (57 ppm). The separately considered measuring point Mur2 shows a value of 21 ppm. (Figure 108)

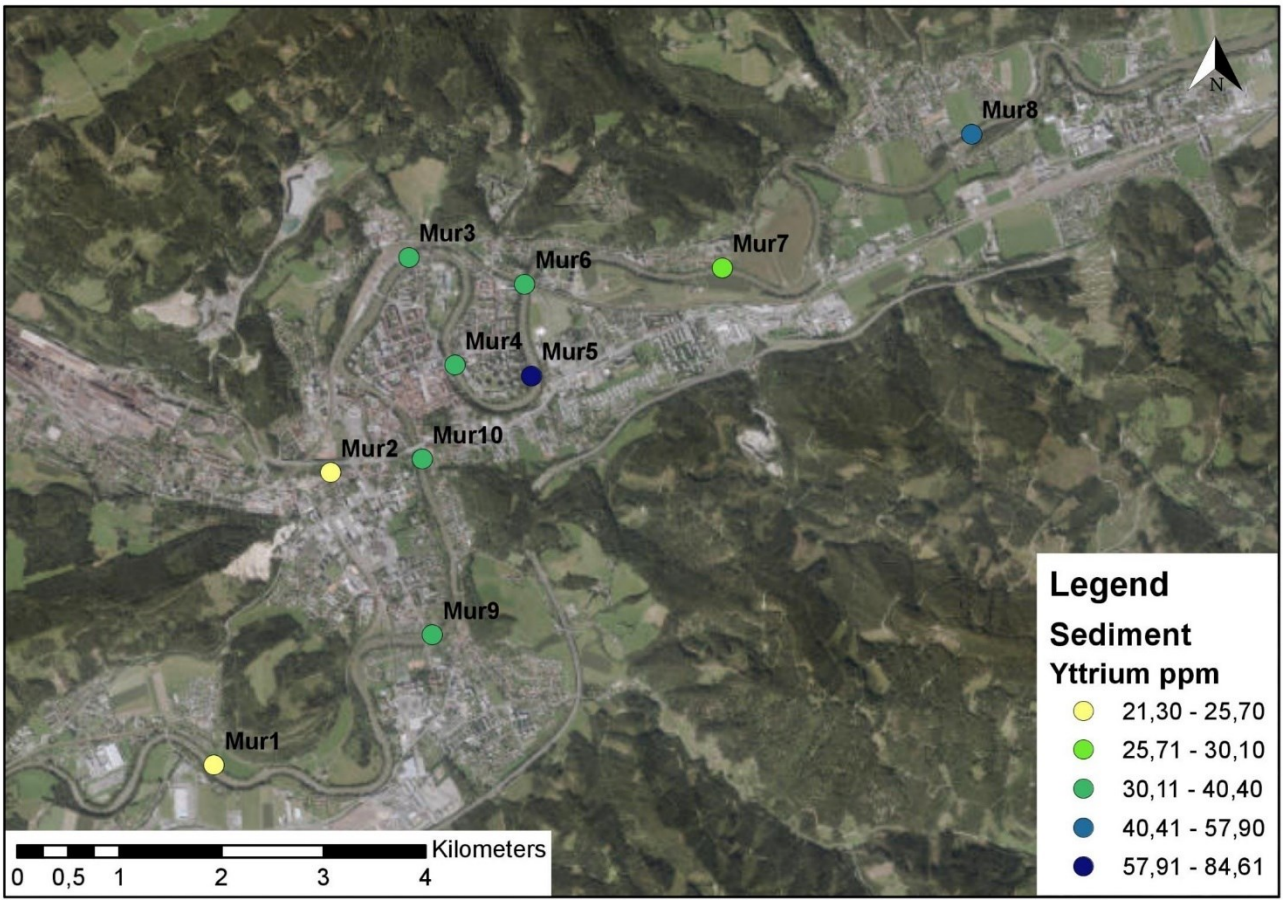


*Figure 108: Y content of the Leoben samples*

### 1.21.18 Zinc

None of the samples shows an above-average *Zn* value. The measured range of variation is between 161 ppm (Mur2) and 88 ppm (Mur9). (Figure 109)

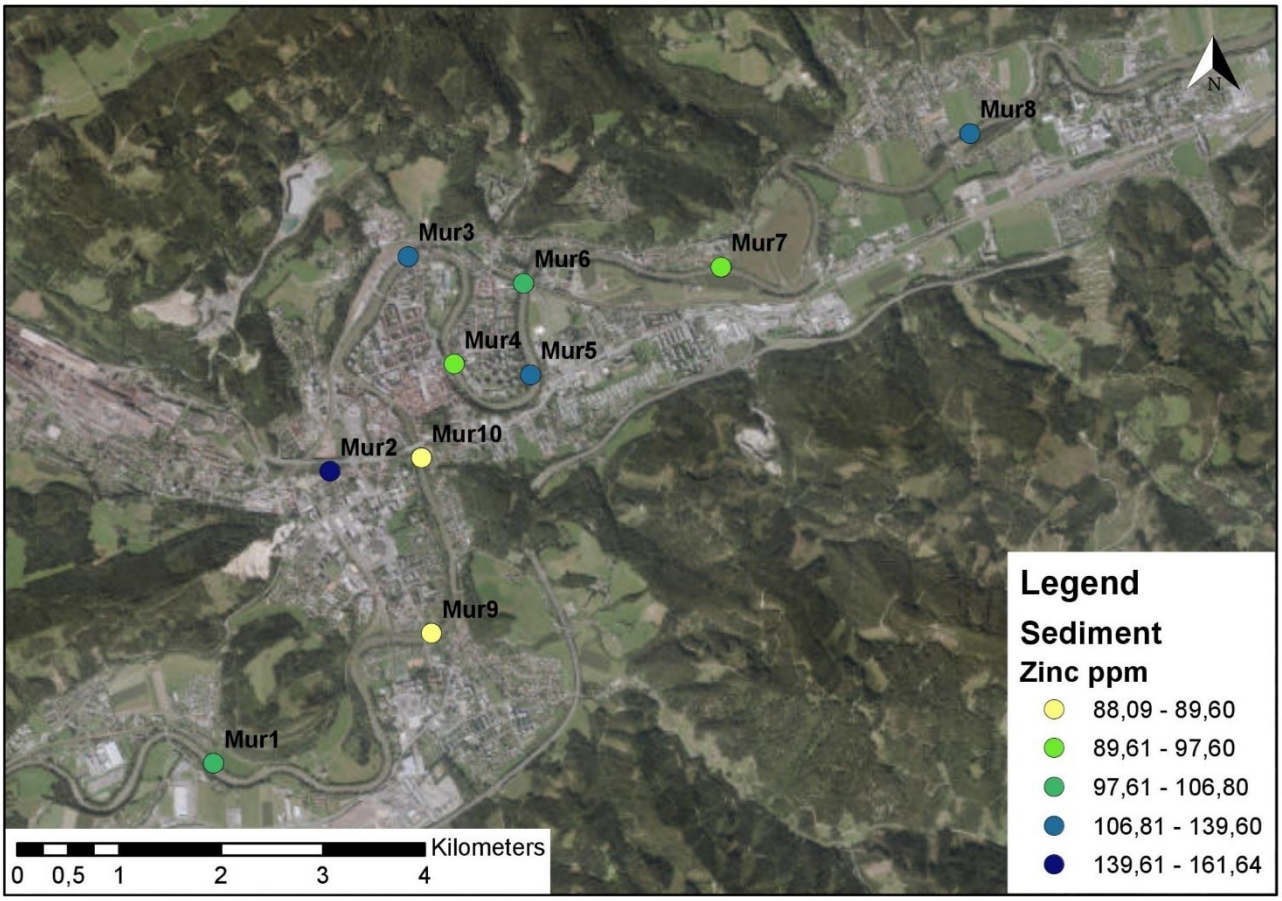


*Figure 109: Zn content of the Leoben samples*

### 1.21.19 Zirconium

As with most of the previous element contents, the zirconium value is not elevated at any measurement point. The highest measured value is found at sampling point Mur5 (355 ppm). The lowest *Zr* content was found at sample point Mur2 (171 ppm). (Figure 110)

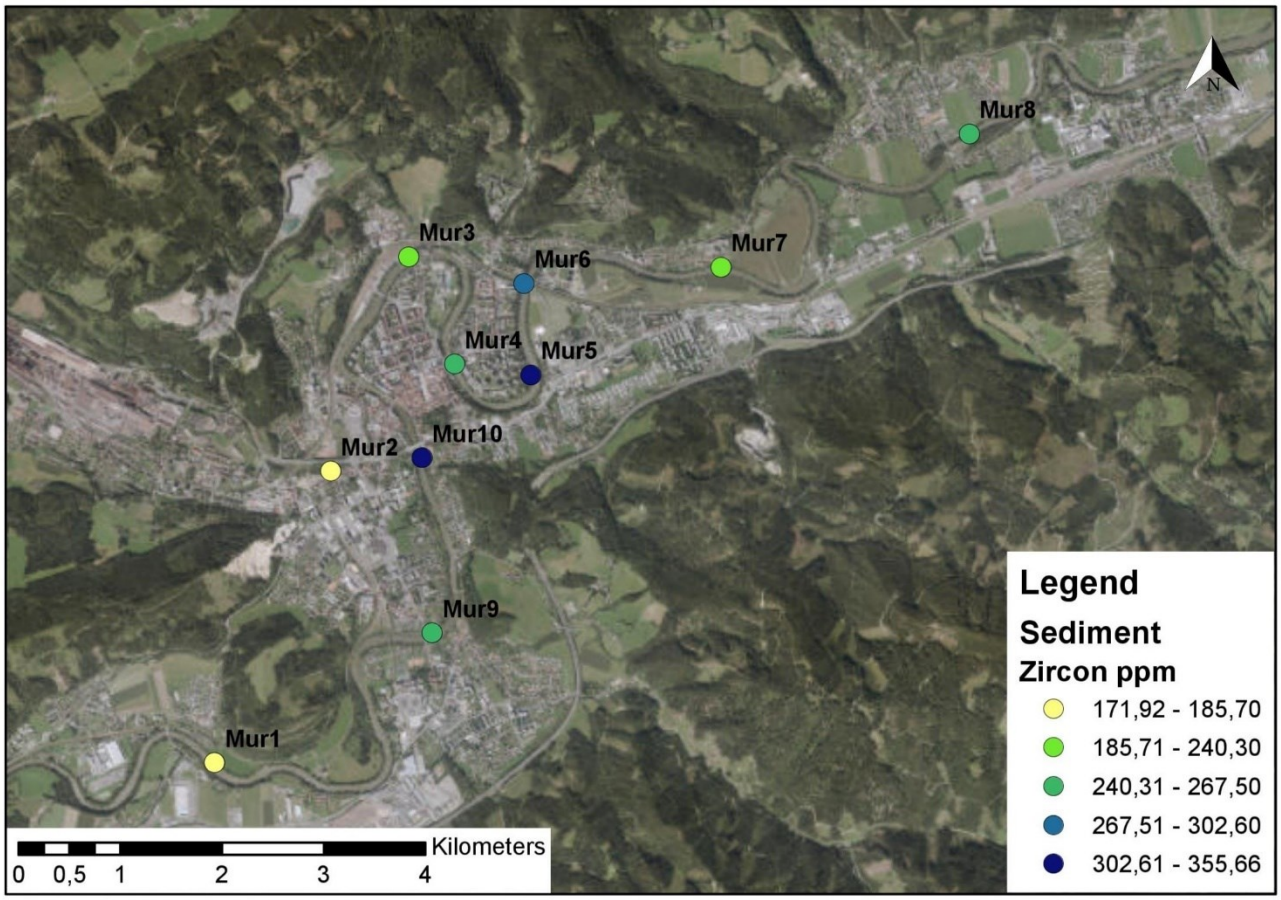


*Figure 110: Zr content of the Leoben samples*

### 1.21.20 Summary

Compared to the other measuring points, the measuring point Mur5 often shows higher contents of the measured element concentrations. At the Mur2 monitoring site, there are no particular anomalies with regard to a significantly higher heavy metal content in comparison. Lead is particularly conspicuous. Six monitoring sites show significantly higher concentrations of this heavy metal.

# Discussion and Interpretation

## 1.22 Comparison of river sediment to the Geochemical Atlas data

In the following, the F- and S-parameters of three elements are compared, followed by a comparison with the Geochemical Atlas. For this purpose, elements and measuring points are used which have both F and S parameters. Some elements were selected as representatives.

### 1.22.1 Arsenic

If the overall picture of the *As* concentration in the Austrian territory is considered, it suggests that the arsenic distribution in the entire Austrian territory is practically completely geogenically determined (Pirkl et al., 2015). Ore, tailings and soil analyses from old mining areas suggest that *As*-bearing minerals are involved in polysulphide mineralisations. In the Austroalpine crystalline units, concentrations significantly greater than 100 ppm are sometimes found in the stream sediments. All these areas with higher As concentrations can either be directly attributed to local mineralisation with high arsenic contents or to areal, finely distributed sulphide mineralisation in certain rock series (Pirkl et al., 2015).

The anomalies south of Saurau near the Thajabach as well as those near Gasen and near Mürzzuschlag can be directly attributed to arsenic mineralisation by comparison with the Geochemical Atlas deposit layer (Geologische Bundesanstalt, 2018).

If the data of the H2O database are compared with those of the Geochemical Atlas, the anomaly at Thajabach (FW61404607) is clearly evident both in the data of the stream sediments of the Geochemical Atlas and in the F parameters of the H2O database. The S-parameters also agree relatively well with those of the stream sediment layer (Geochemical Atlas). Only at Leoben is there a deviation in the S-parameters, as the value of the measuring point FW61400187 of the Vordernbergbach is clearly elevated. However, since there are almost no sampling points around Leoben in the Geochemical Atlas, the values of the stream sediment layer around Leoben should be viewed with caution. The outliers referred to above at the FW61400197 measuring point (Leoben) can be explained by mineralisation in the hinterland (*As* is enriched in Fe-(hydr-)oxides during pedogenic processes (Schedl et al., 2010)) when compared with the Geochemical Atlas. In contrast to the Thajabach, this mineralisation is not clearly visible in the F-parameters. At monitoring site FW61400476, no clear background contamination is evident in the Geochemical Atlas layer.

Comparing the data of the median values of the F- and S-parameters, as well as the maximum values of these among each other, no clear correlation of an increased dissolved arsenic with one deposited in the sediment is identified. An example of this is monitoring site FW61400476, which is located in the Katschbach. The median and maximum values in the sediment are significantly higher than the values that occur on average in Styria. The median value at this monitoring site is 57.2 mg/kg and the maximum value 79.4 mg/kg. The median value of the F-parameters is <dl, the maximum value is 0.00167 mg/l. The values of the F-parameters are exactly the same as in Styria. The values of the F-parameters are in the average (median value) of Styria, or even below (maximum value). However, since only two sediment samples and 43 water samples were taken at this monitoring site, it is difficult to judge whether the values of the S-parameters are outliers. The same applies to monitoring site FW61400197, which is located in the Mürz. Nine sediment samples were taken and determined here. Compared to the Styrian median, the value is significantly higher (median 46 mg/kg; maximum 88 mg/kg). However, no clear outlier could be found in the water samples. With 109 measurements and a standard deviation of 0.000753 the median is <dl and the maximum value 0.0034 mg/l and thus within the Styrian median or only slightly above it. The sediment samples show the greatest deviations from the Styrian median of all measured arsenic contents at this measuring point.
Figure 111 - 116

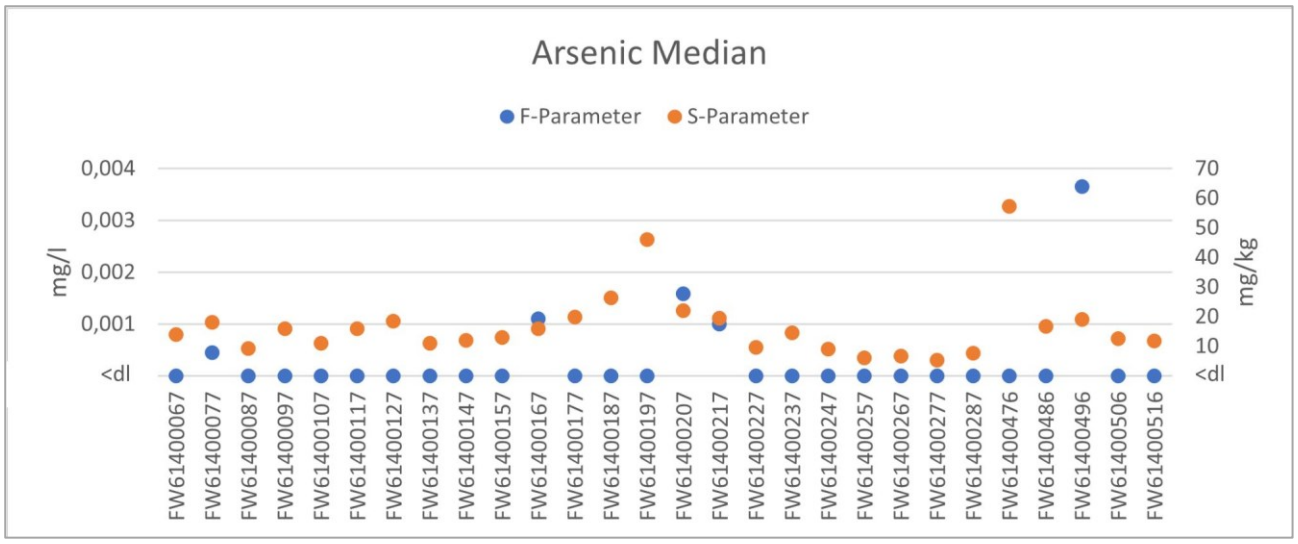


*Figure 111: Arsenic - Comparison F-Parameters and S-Parameters – Median*

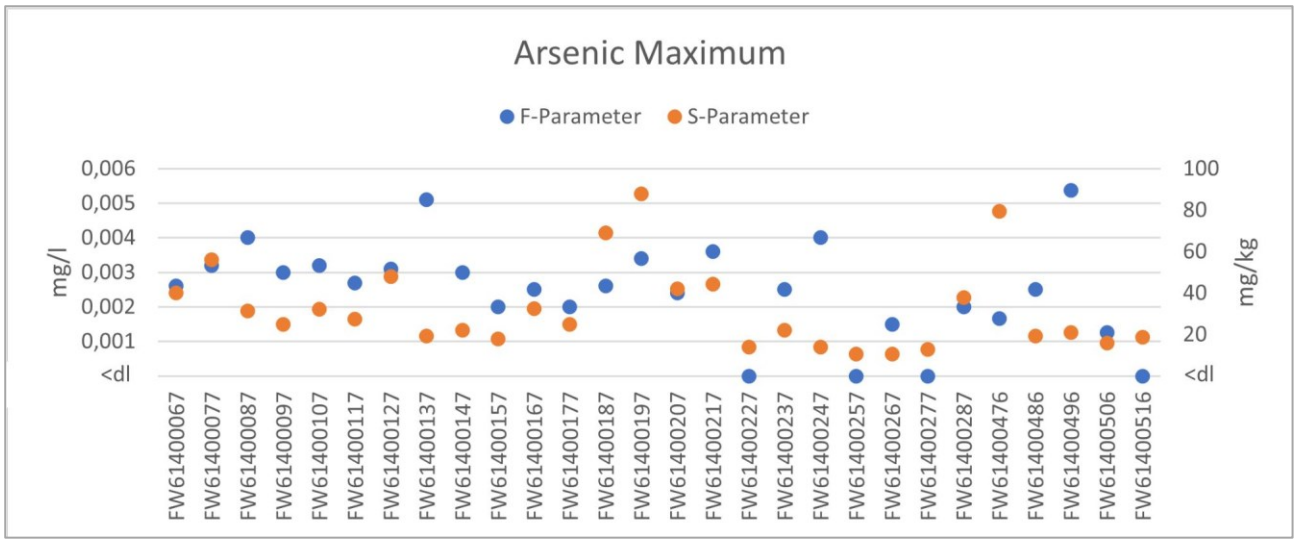


*Figure 112: Arsenic - Comparison F-Parameters and S-Parameters - Maximum*

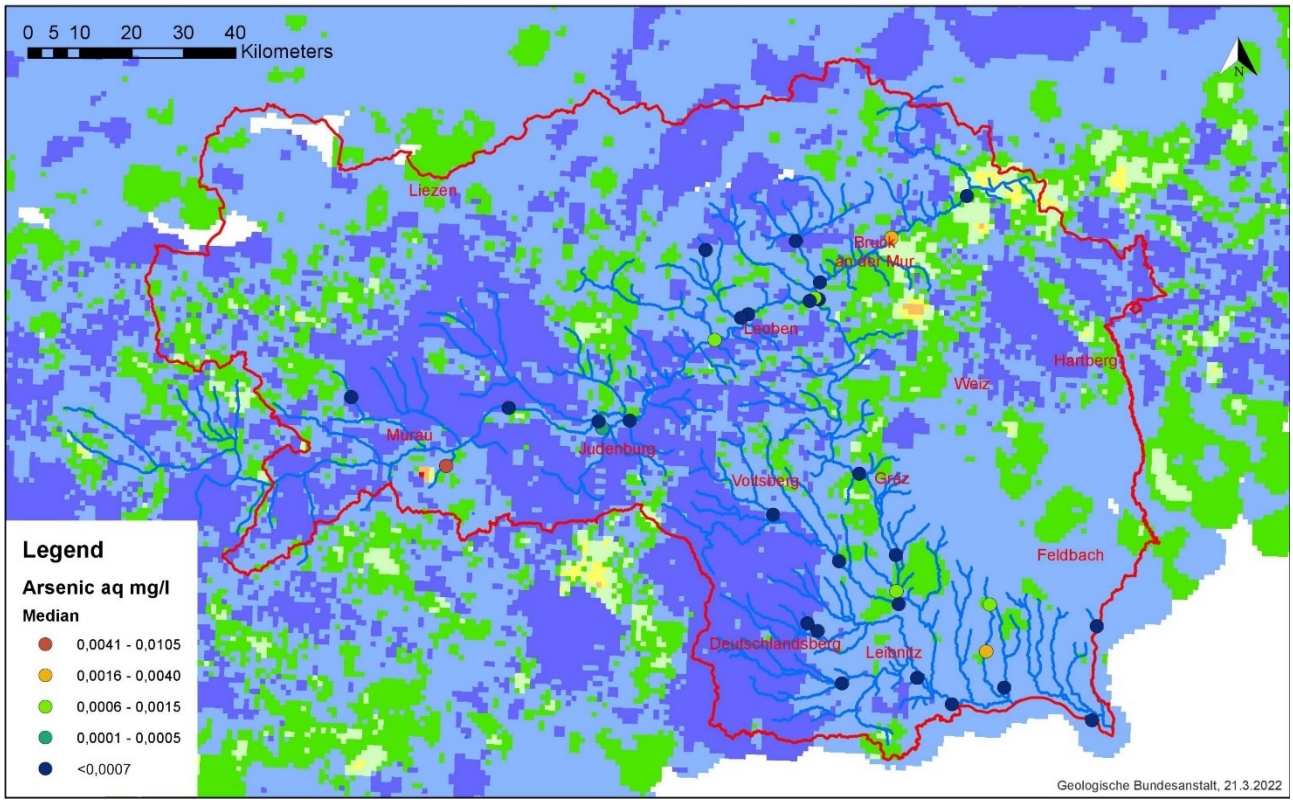


*Figure 113: Comparison of Geochemical Atlas and H2O database - As F-Parameter Median Values; (Geologische Bundesanstalt, 2018)*

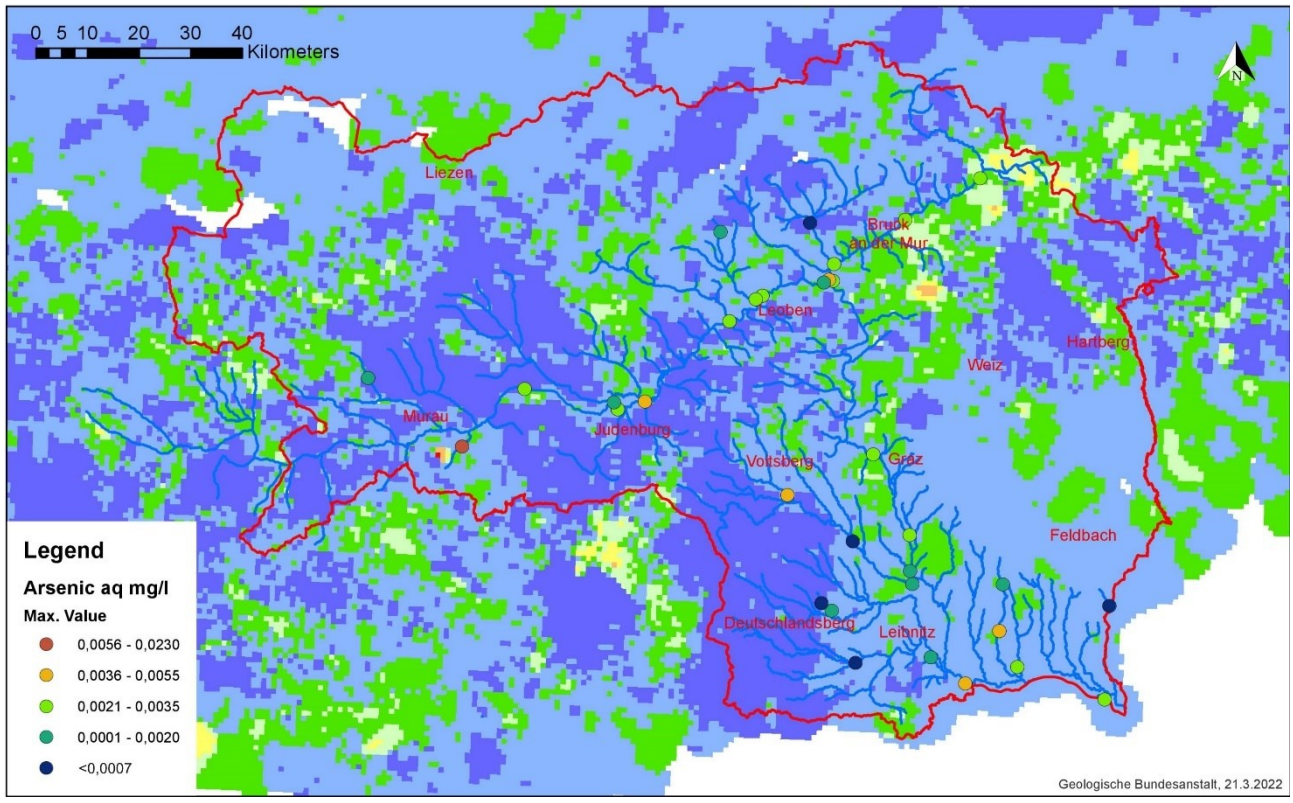


*Figure 114: Comparison of Geochemical Atlas and H2O database - As F-Parameter Maximum Values; (Geologische Bundesanstalt, 2018)*

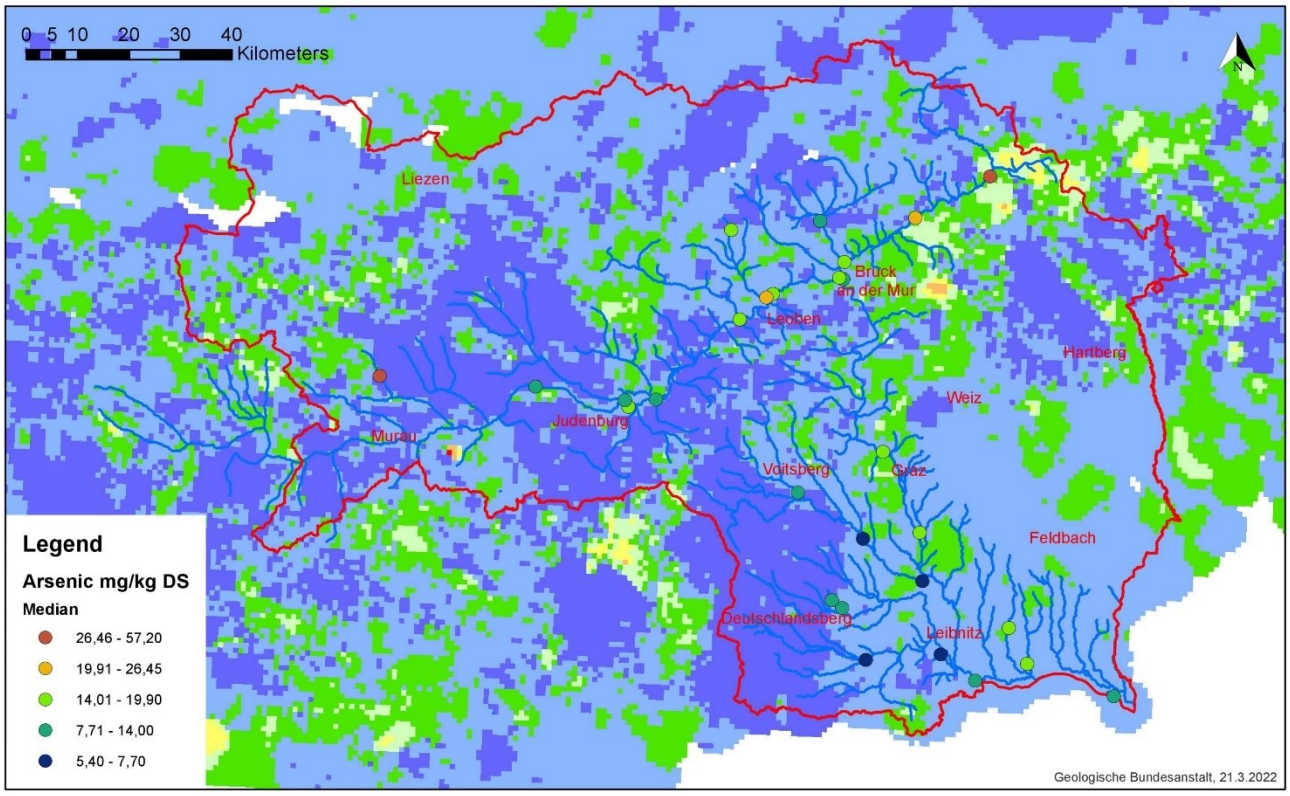


*Figure 115: Comparison of Geochemical Atlas and H2O database - As S-Parameter Median Values; (Geologische Bundesanstalt, 2018)*

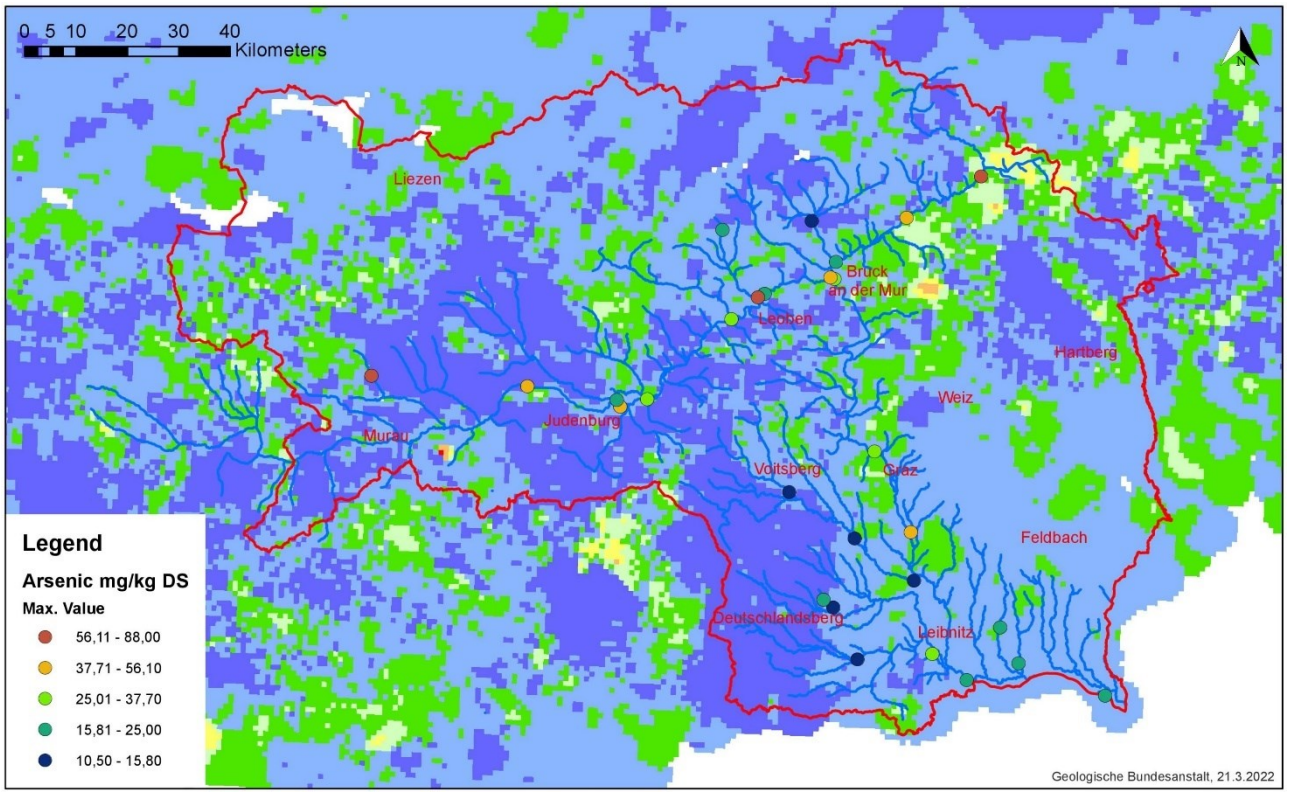


*Figure 116: Comparison of Geochemical Atlas and H2O database - As S-Parameter Maximum Values; (Geologische Bundesanstalt, 2018)*

### 1.22.2 Chromium

The spatial distribution of chromium in stream sediments is closely related to the distribution of basic and ultrabasic rock series. This is particularly evident in the rather small-scale occurrences of serpentinites, which are marked by very high *Cr* concentrations (e.g. Preg-Kraubath). In basic rock series, the chromium content is between 100 and 250ppm. Local areas with very high *Cr* concentrations (> 600ppm) in the Northern Calcareous Alps are striking. These small-scale "anomalies" are linked to occurrences of Cretaceous sediments (Gosau Formation). The associated *Cr* content is due to chromite conduction in these sediment series. There is probably additional local enrichment due to transport processes in the streams (Pirkl et al., 2015; Geologische Bundesanstalt, 2018).

A comparison with the Geochemical Atlas shows a similar picture. Measuring point FW6140016 shows no anomaly in either the F or the S parameters. However, this measuring point is located just downstream Kraubath, where the ultramafite complex is clearly evident in the Geochemical Atlas. The elevated measured values at Mürzzuschlag are not shown in the Geochemical Atlas.

For chromium, too, the low values coincide to a certain extent. As with the previous elements, an anomaly in the F or S parameter not automatically leads to an anomaly in the other parameter. An example of this is measuring point FW61400237 for the median and maximum values, where there is a clear anomaly in the S-parameter, but this is not measurable in the F-parameters. In the case of the maximum values, a similar situation is also seen at the FW61400207 and FW61400217 measuring points. Figure 117 - 122

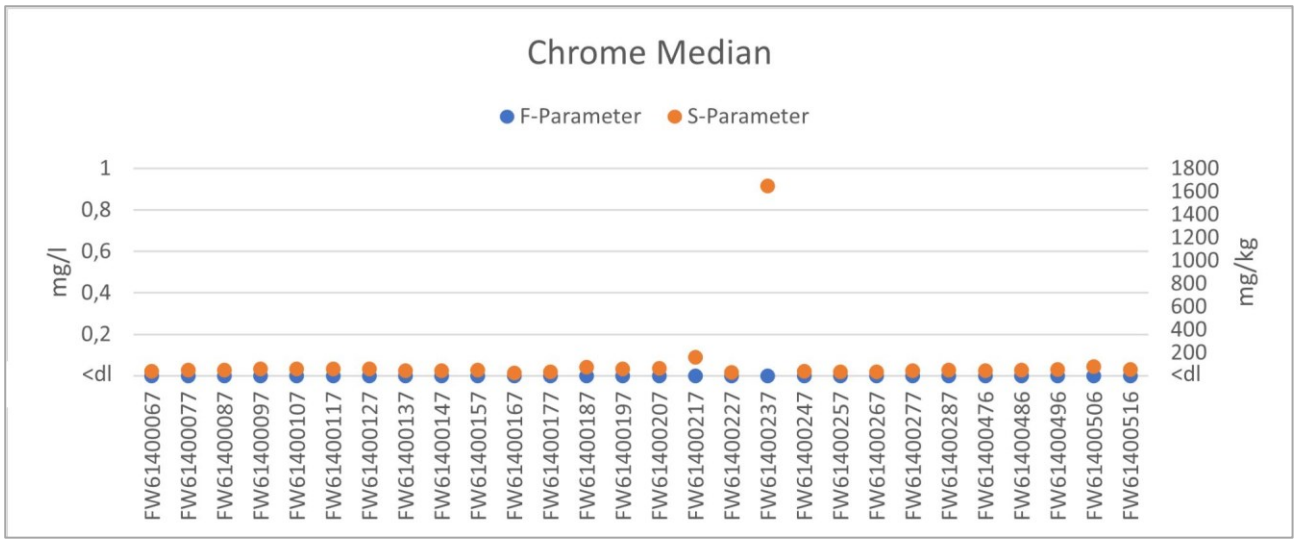


*Figure 117: Chrome - Comparison F-Parameters and S-Parameters – Median*

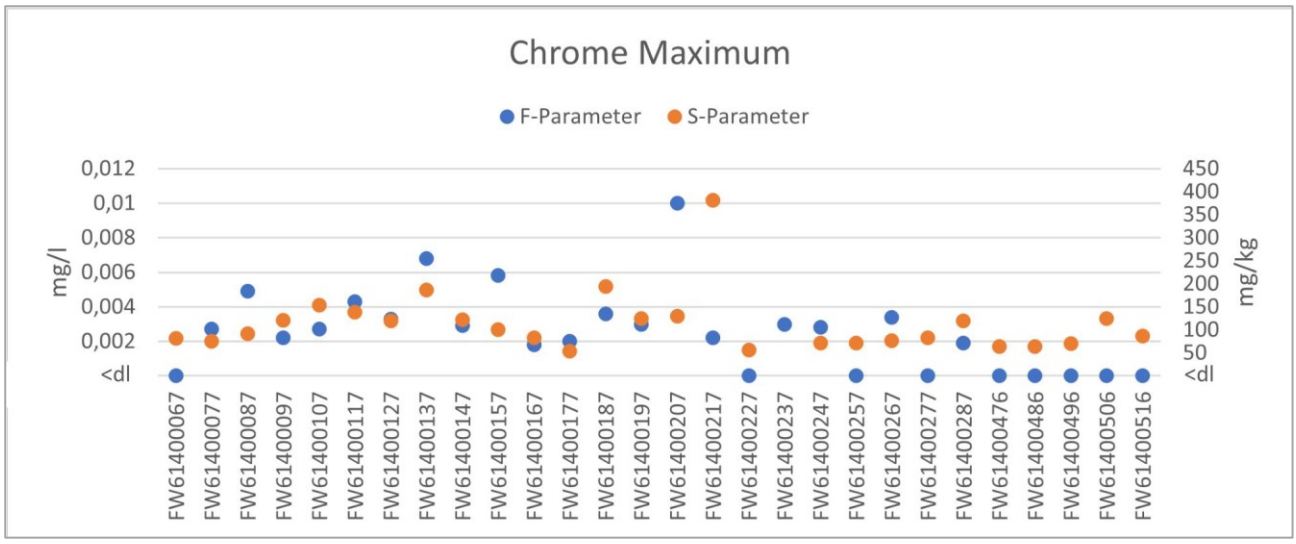


*Figure 118: Chromium - Comparison F-Parameters and S-Parameters - Maximum*

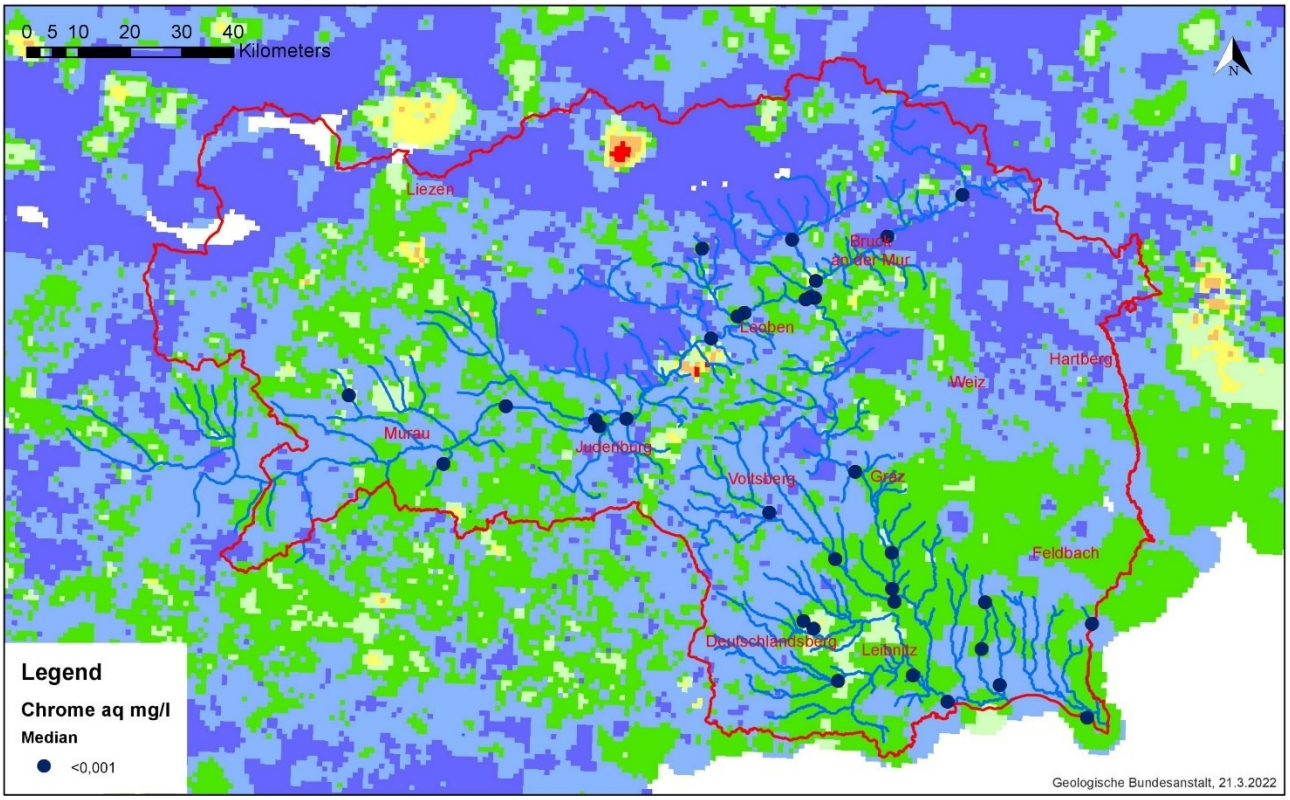


*Figure 119: Comparison of Geochemical Atlas and H2O database - Cr F-Parameter Median Values; (Geologische Bundesanstalt, 2018)*

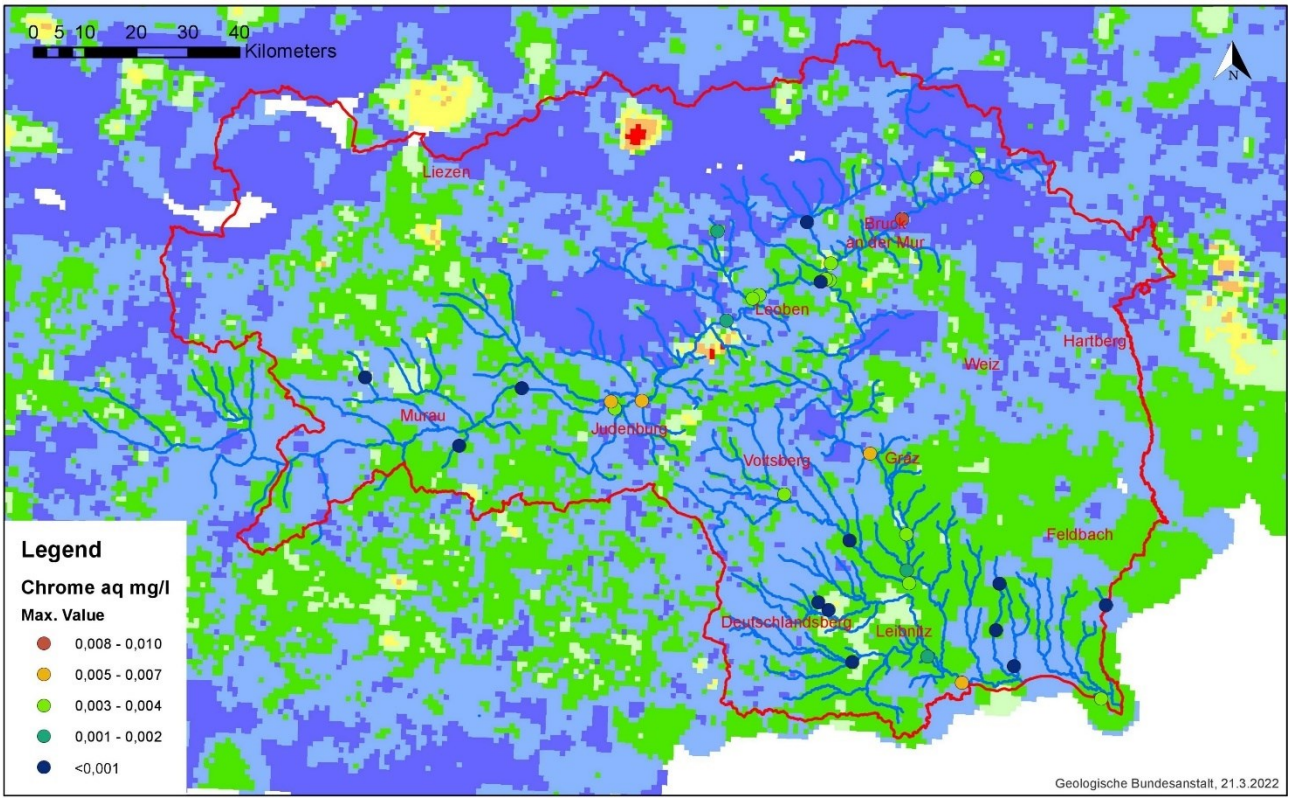


*Figure 120: Comparison of Geochemical Atlas and H2O database - Cr F-Parameter Maximum Values; (Geologische Bundesanstalt, 2018)*

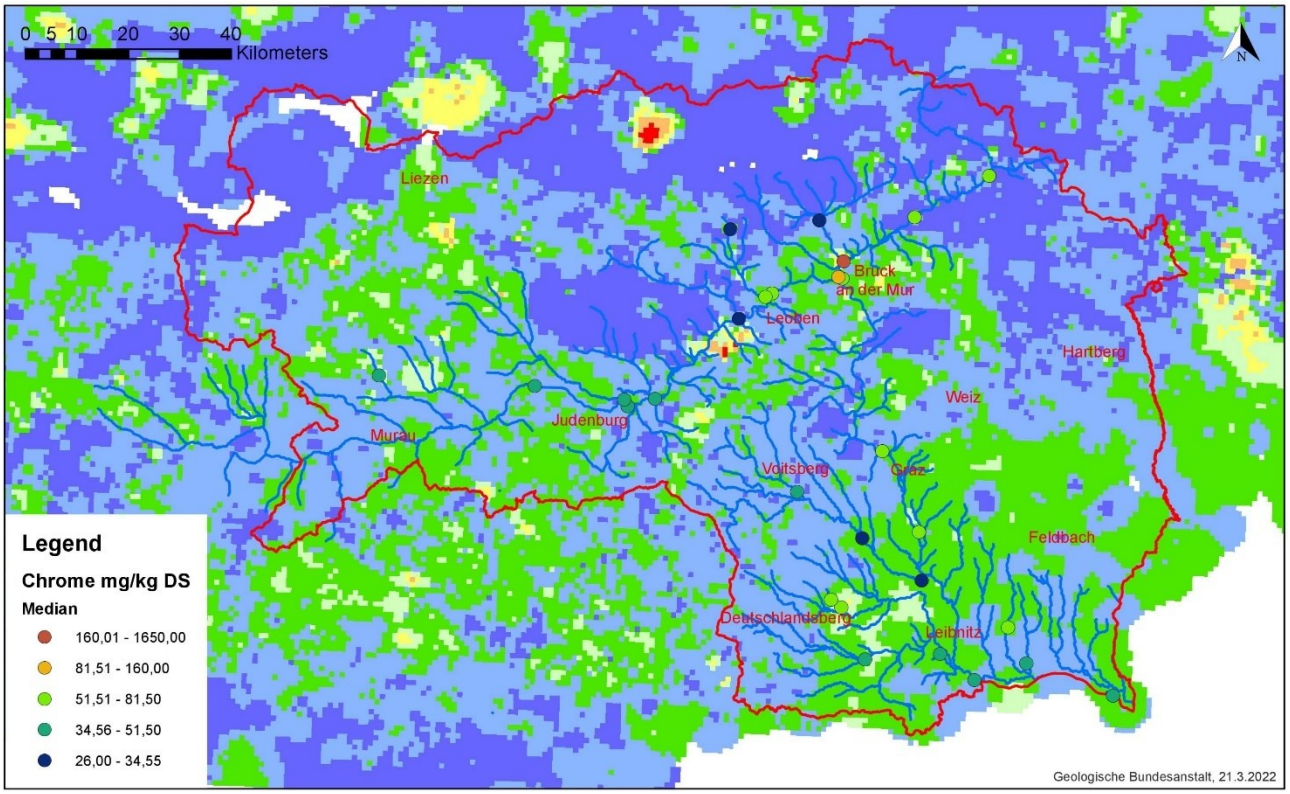


*Figure 121: Comparison of Geochemical Atlas and H2O database - Cr S-Parameter Median Values; (Geologische Bundesanstalt, 2018)*

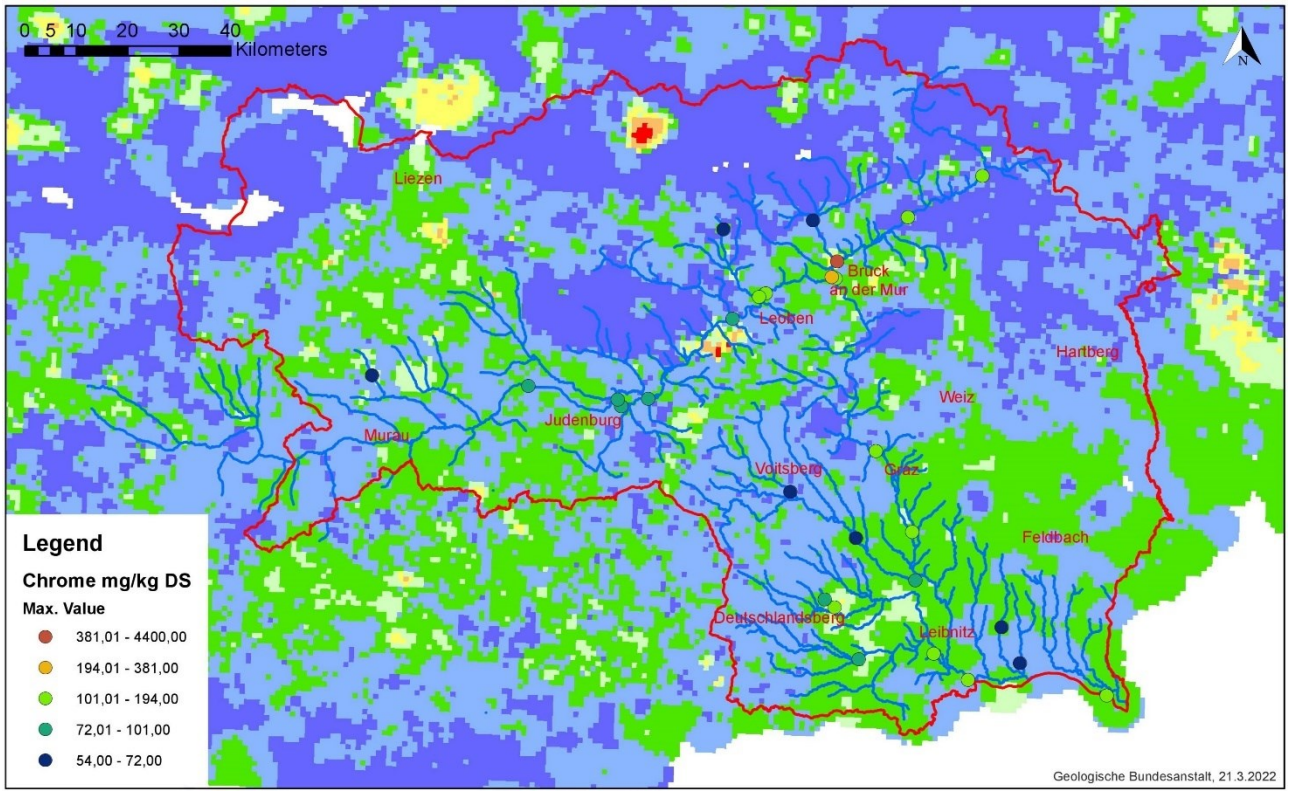


*Figure 122: Comparison of Geochemical Atlas and H2O database - Cr S-Parameter Maximum Values; (Geologische Bundesanstalt, 2018)*

### 1.22.3 Copper

According to Pirkl et al. (2015), the spatial distribution of copper concentrations is likely to have three causes: (small-) regionally slightly elevated basic contents in basic and ultrabasic rock series, "anomalies" of higher concentrations in direct connection with chalcopyrite or polysulphide mineralisations and possibly occurring in connection with viticulture, but in any case anthropogenically caused elevated concentrations (Vienna Basin). It is striking that numerous *Cu* mineralisations or old mining areas with copper as a target raw material are not or only indistinctly detectable by stream sediment geochemistry. The reason for this is the high mobility of copper in the natural systems, which leads to the fact that dissolution processes predominate over transport processes in the sediment. The two anomalies in Styria are also due to mineralisation (Pirkl et al., 2015; Geologische Bundesanstalt, 2018).

For this element, the two databases match only slightly. Significant anomalies are again seen in the H2O database around Leoben and Bruck an der Mur in the F median. These are also shown in the S-parameter median. However, a significantly increased background copper load is not shown in the Geochemical Atlas layer. Measuring point FW61400247 is particularly striking. Here there is a clear copper load in the F-parameters, in the S-parameters the values are in line with the Styrian average, and in the Geochemical Atlas no anomalies are detected in the immediate vicinity.

In the case of copper, no clear correlation between the measured F- and S-parameters is found. In the case of the F-parameters, a total of 15 measuring points show values that are in part significantly elevated. In the sediment, however, a significantly higher median value can only be determined at measuring point FW61400237. The same picture emerges when comparing the maximum values. Here, too, there are large differences between the individual monitoring sites in the range of the F-parameters. However, the S-parameters show larger deviations from the Styria maximum values at only two sites (FW61400187 and FW61400237).

Figure 123 - 128

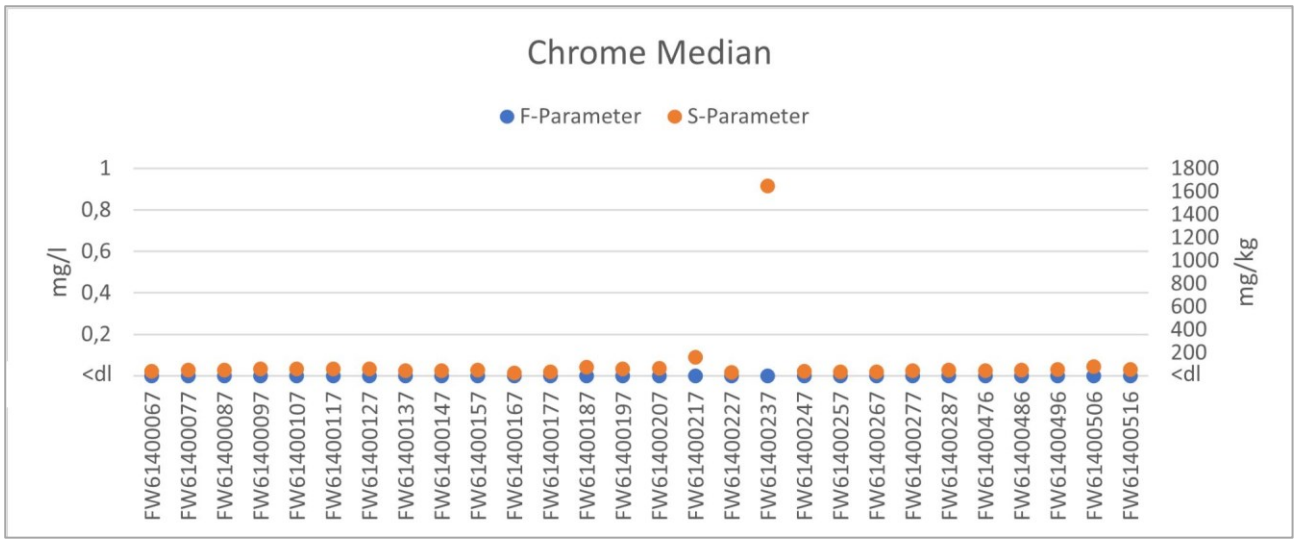


*Figure 123: Copper - Comparison F-Parameters and S-Parameters – Median*

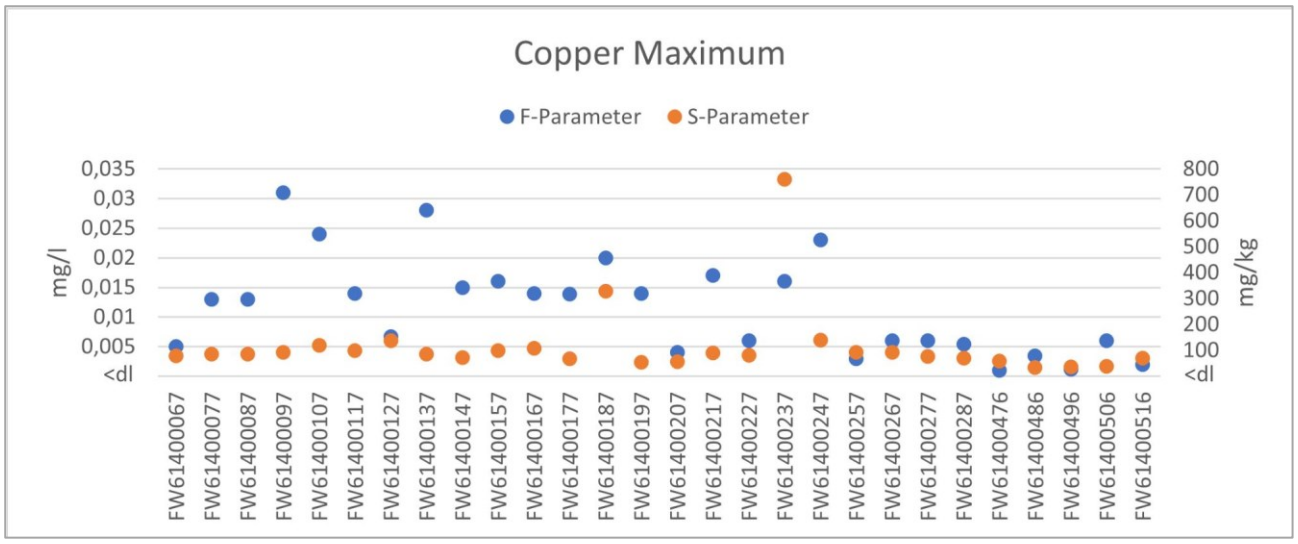


*Figure 124: Copper - Comparison F-Parameters and S-Parameters - Maximum*

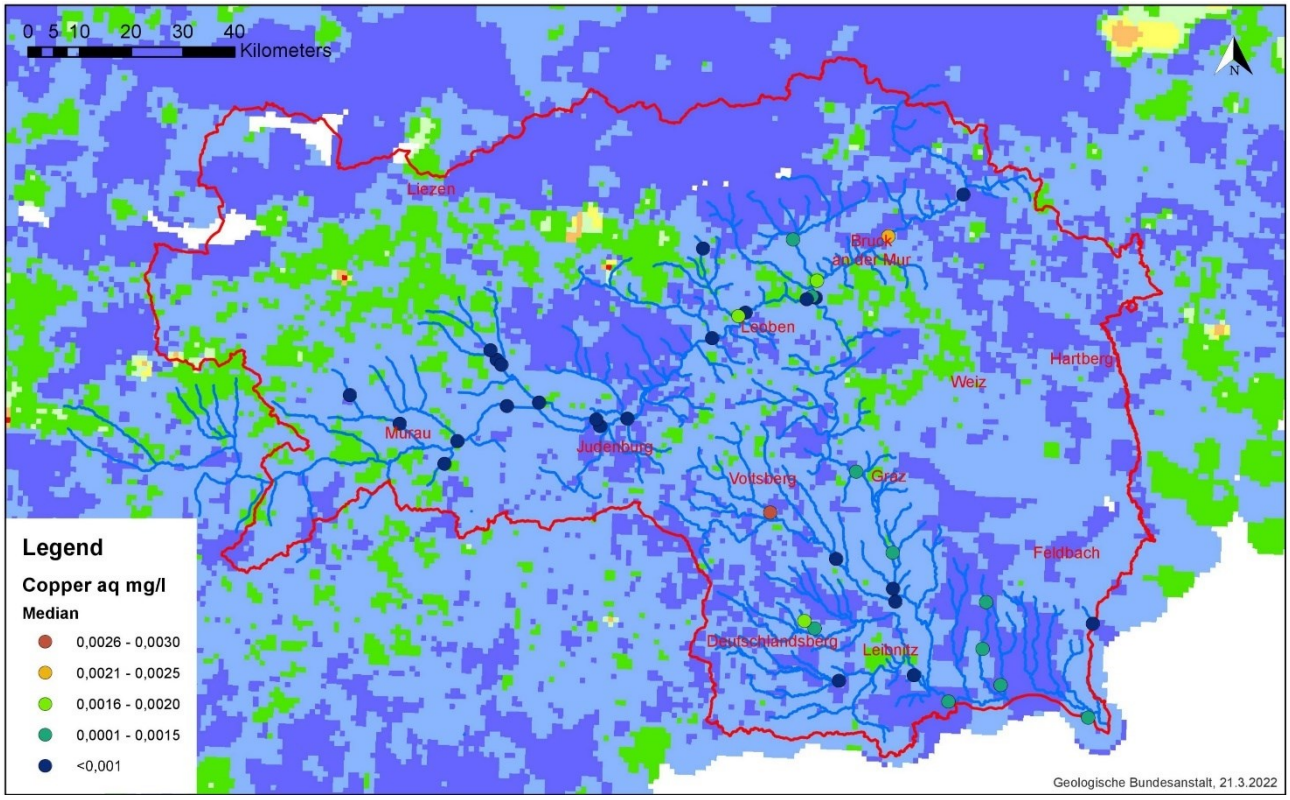


*Figure 125: Comparison of Geochemical Atlas and H2O database - Cu F-Parameter Median Values; (Geologische Bundesanstalt, 2018)*

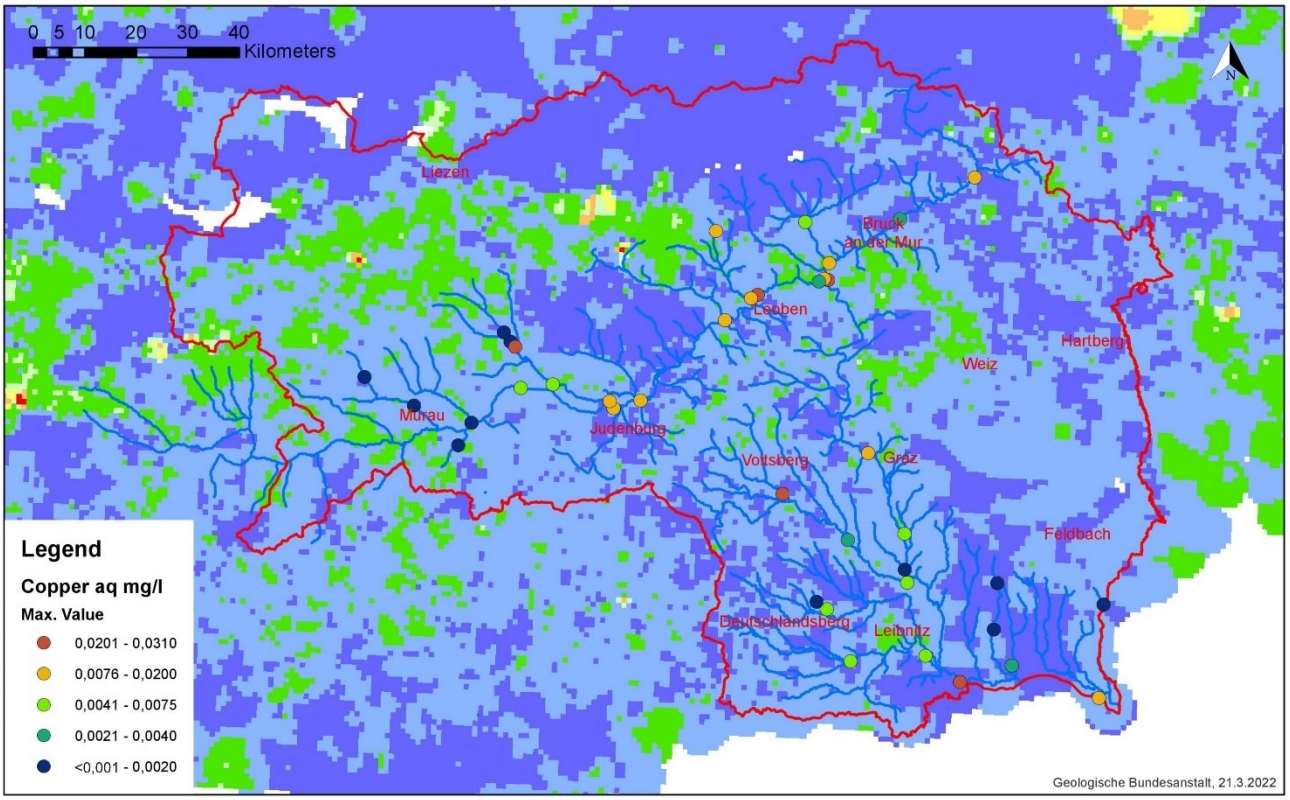


*Figure 126: Comparison of Geochemical Atlas and H2O database - Cu F-Parameter Maximum Values; (Geologische Bundesanstalt, 2018)*

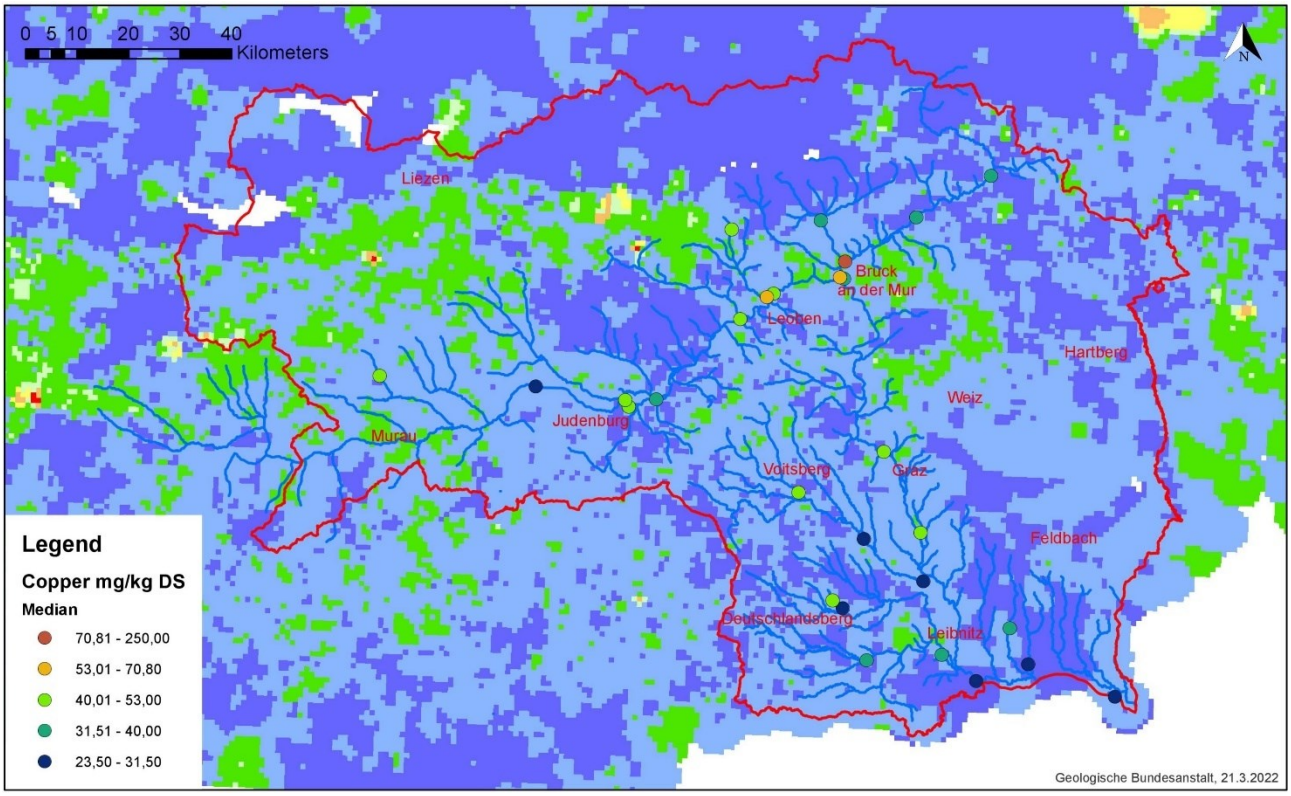


*Figure 127: Comparison of Geochemical Atlas and H2O database - Cu S-Parameter Median Values; (Geologische Bundesanstalt, 2018)*

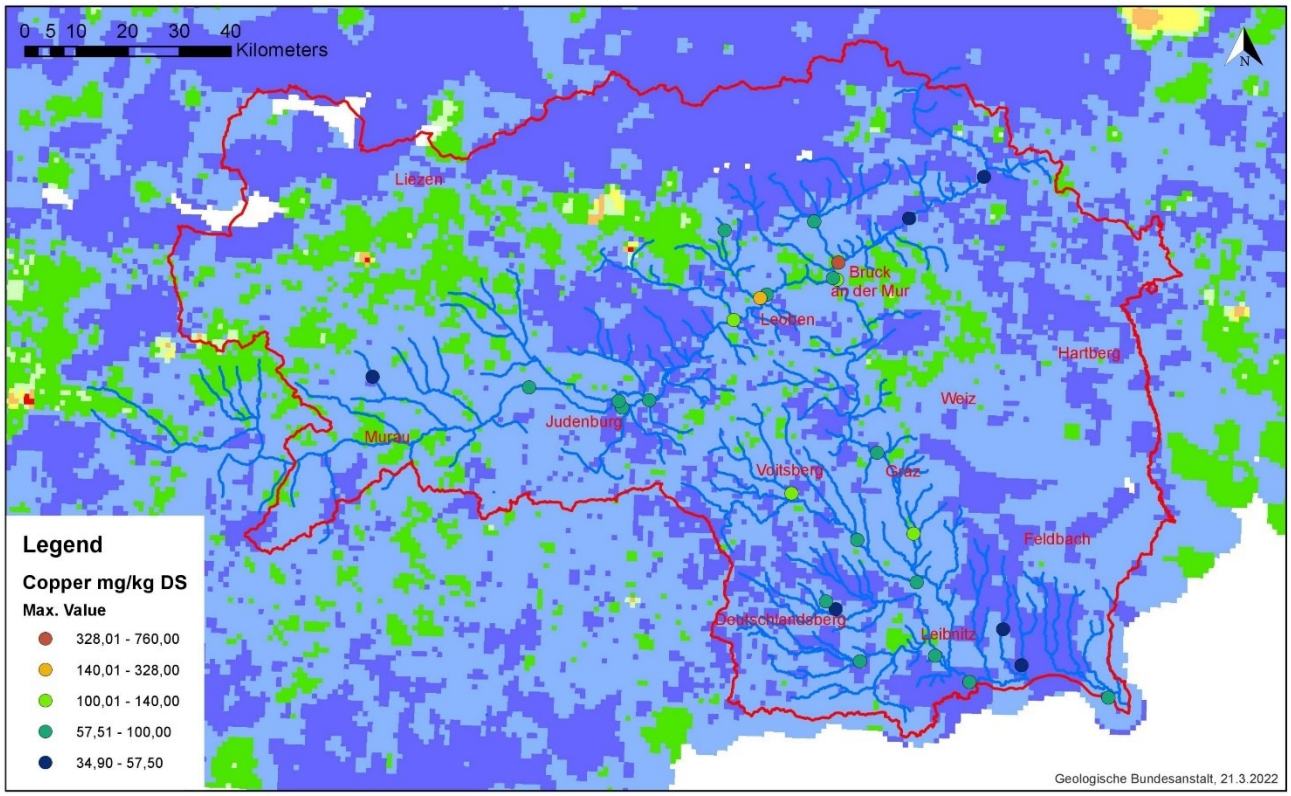


*Figure 128: Comparison of Geochemical Atlas and H2O database - Cu S-Parameter Maximum Values; (Geologische Bundesanstalt, 2018)*

### 1.22.4 Nickel

The spatial distribution of *Ni* resembles to that of chromium. It is closely related to the distribution of basic and ultrabasic rock series. This is evident in the serpentinite in Kraubath. Basic rock series are characterised by large-scale, relatively uniform *Ni* concentration distributions between about 50 and 200 ppm (Pirkl et al., 2015). In the sediments of the Gosau Formation in the Northern Calcareous Alps there are local very high nickel anomalies (up to >> 250 ppm) due to chromite conduction. There is probably an additional local enrichment due to the transport processes in the streams (Pirkl et al., 2015; Geologische Bundesanstalt, 2018).

In comparison, no correlation is seen between the Geochemical Atlas and the H2O database. The area around Kraubath, which is elevated with *Ni*, does not appear in the data of the H2O database. On the other hand, the significantly elevated values in the H2O database around Leoben, Bruck an der Mur and Frauental an der Lassnitz are not represented in the stream sediment layer of the Geochemical Atlas.

For nickel, too, there is no clear correlation between S and F parameters. As already mentioned for other elements, it is also true here that at low measured values both parameters are basically in a similar range. However, anomalies often show up in only one of the two parameters. Figure 129 shows a clearly elevated F-value at measuring point FW61400187, whereas the S-value has a background value. The opposite is true for measuring point FW61400237. Here the S-parameter is anomalous, but the F-parameter is only slightly elevated. In the illustration of the maximum values (see Figure 99), measuring point FW61400207 shows a clear deviation in the F-parameter, but the S-parameter is not increased at this measuring point. At sampling point FW61400237, on the other hand, the S-parameter is clearly elevated, but no elevated value is detected in the water sample (F-parameter).

Figure 129 – 134

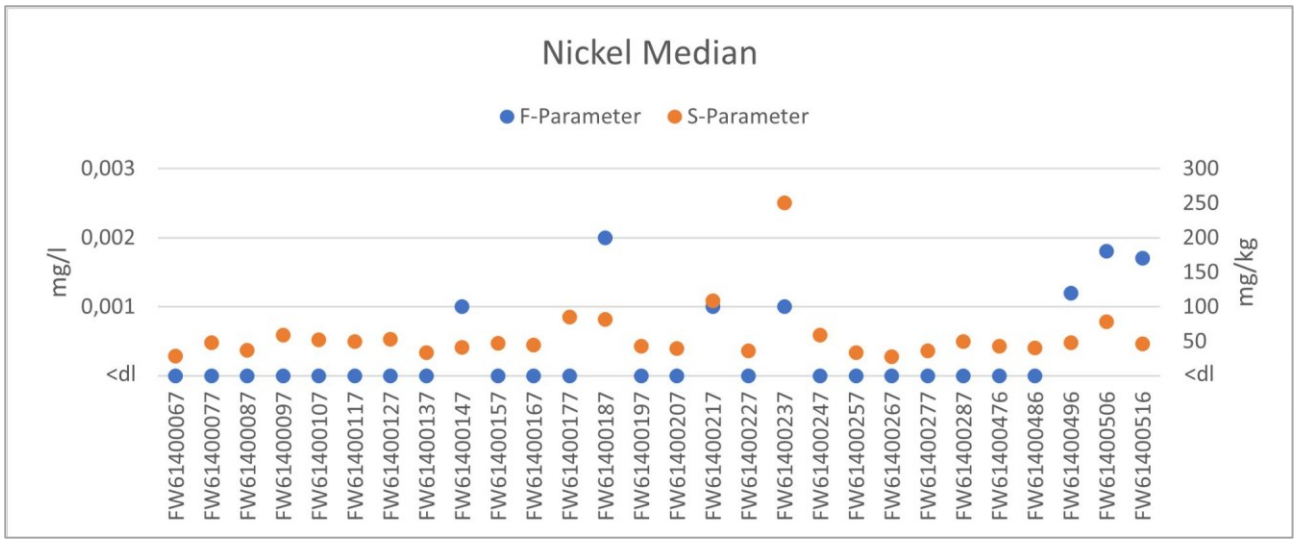


*Figure 129: Nickel - Comparison F-Parameters and S-Parameters – Median*

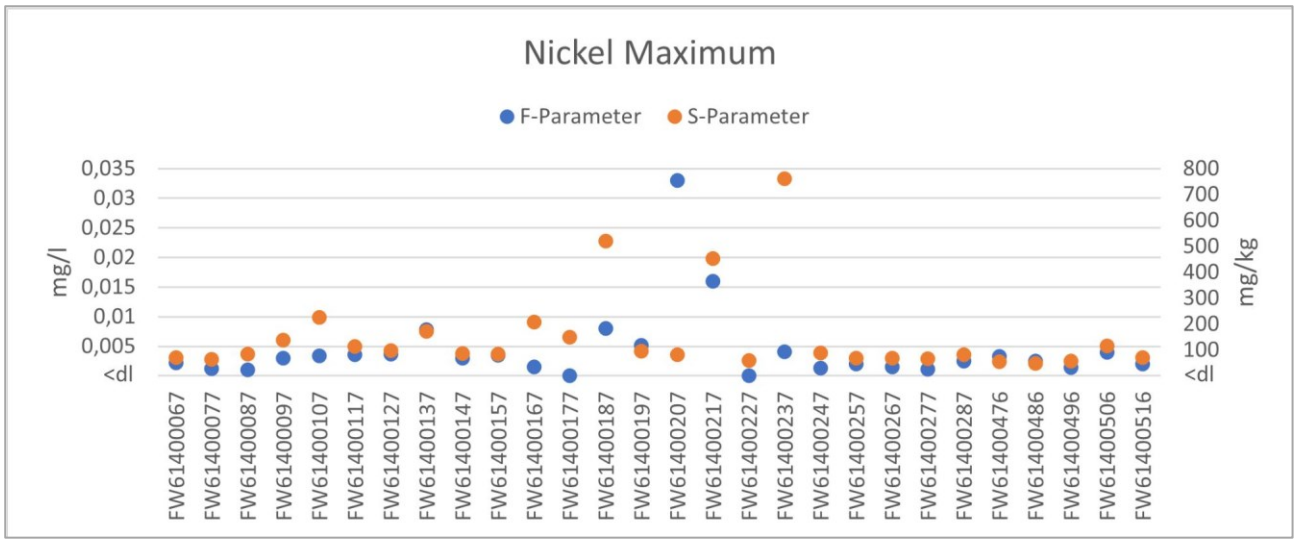


*Figure 130: Nickel - Comparison F-Parameters and S-Parameters – Maximum*

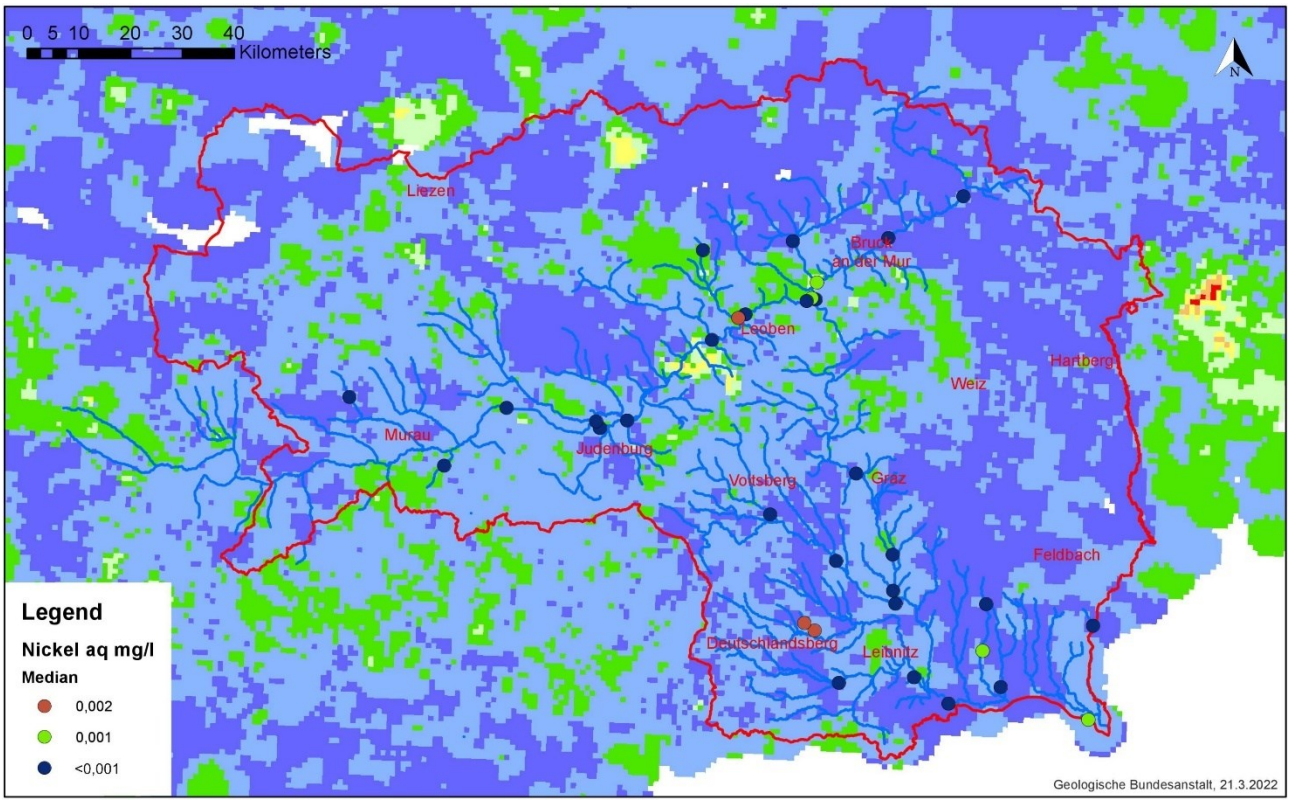


*Figure 131: Comparison of Geochemical Atlas and H2O database - Ni F-Parameter Median Values; (Geologische Bundesanstalt, 2018)*

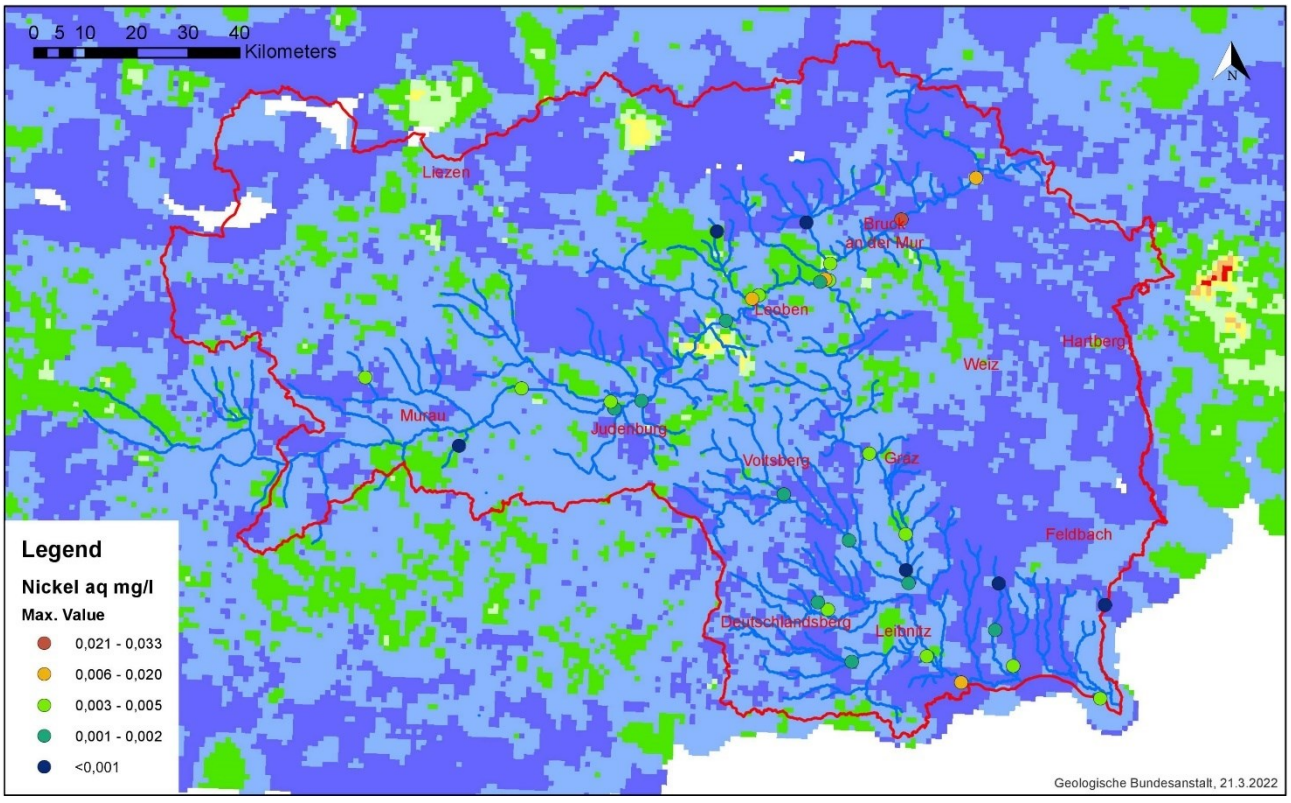


*Figure 132: Comparison of Geochemical Atlas and H2O database - Ni F-Parameter Maximum Values; (Geologische Bundesanstalt, 2018)*

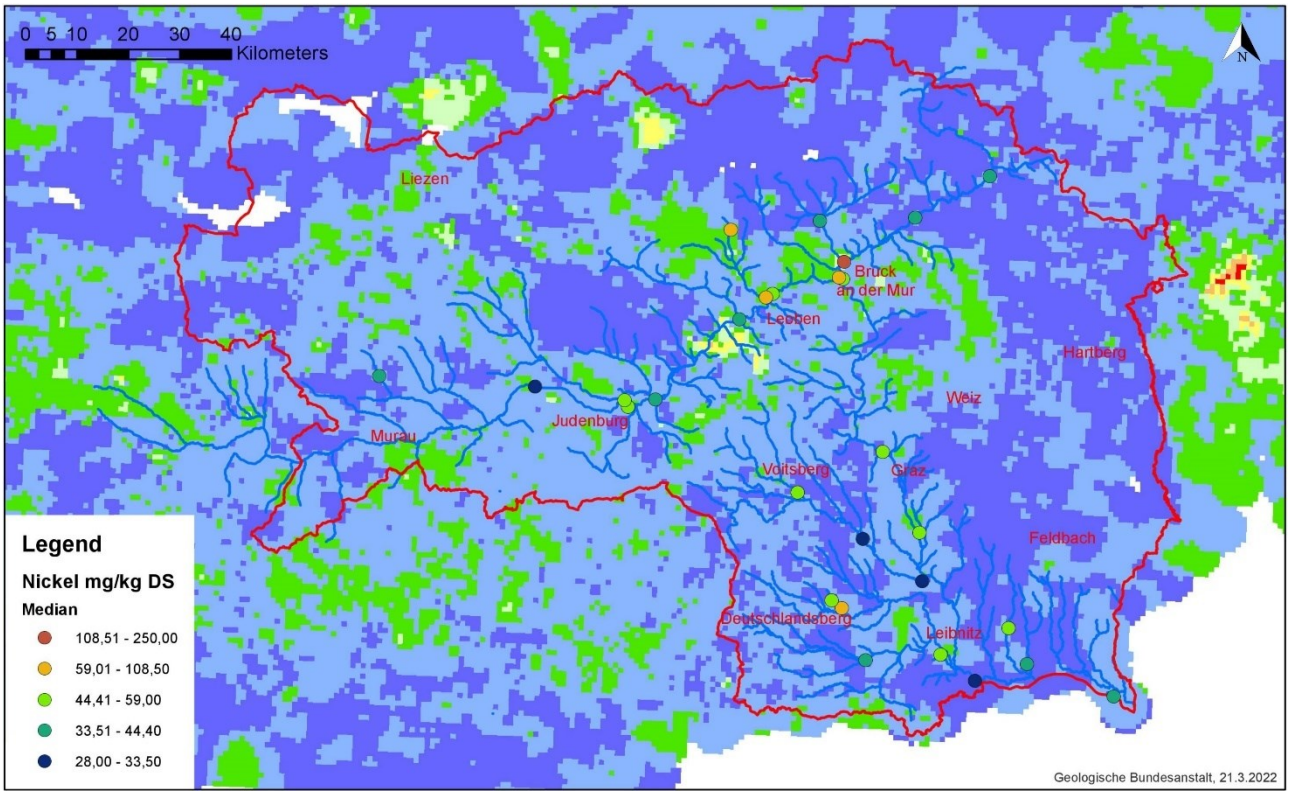


*Figure 133: Comparison of Geochemical Atlas and H2O database - Ni S-Parameter Median Values; (Geologische Bundesanstalt, 2018)*

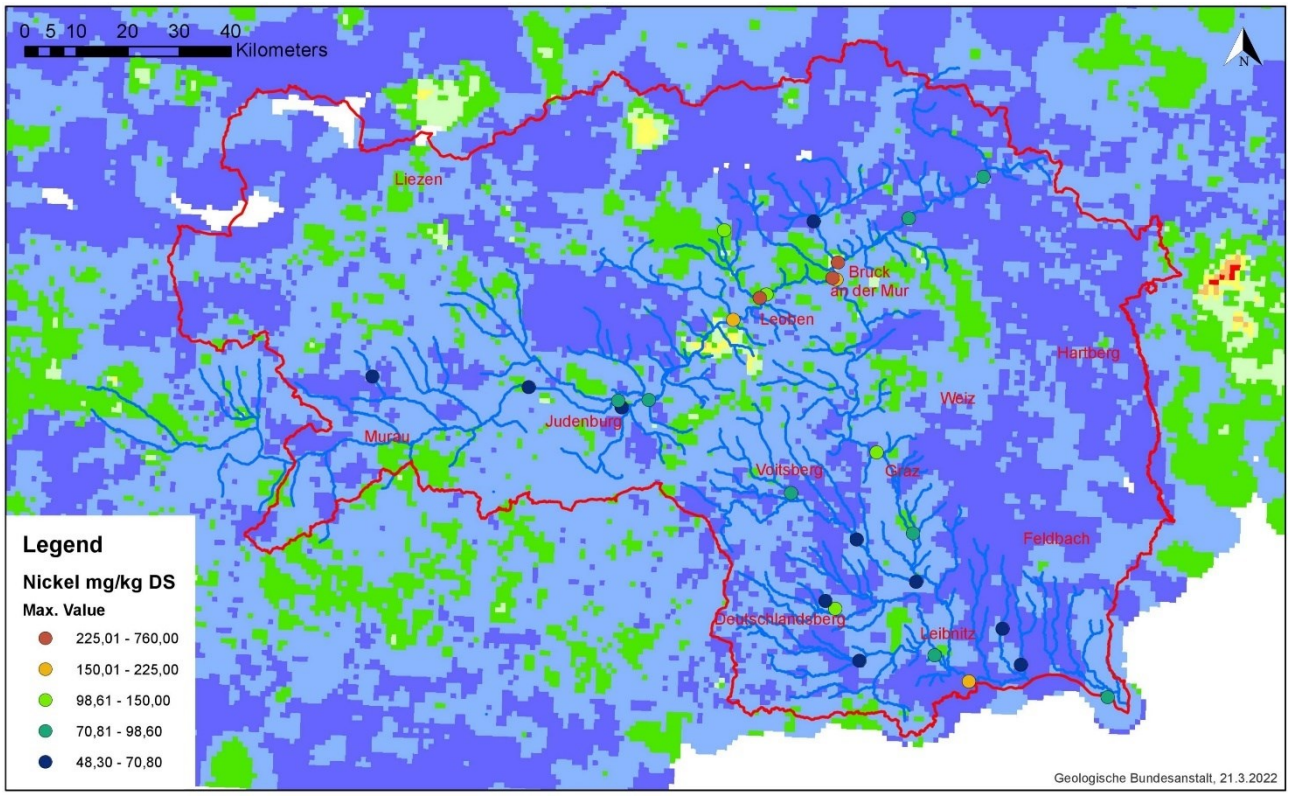


*Figure 134: Comparison of Geochemical Atlas and H2O database - Ni S-Parameter Maximum Values; (Geologische Bundesanstalt, 2018)*

### 1.22.5 Lead

For lead, there are geogenically two main sources in stream sediments, as trace and minor constituent in the lattice of feldspars and in polysulphide and specific *Pb-Zn* mineralisations such as in the Graz Palaeozoic. Anthropogenic contaminations have been detected, for example, in the Vienna Basin (Pirkl et al., 2015).

In addition to the anomaly in the Graz Palaeozoic, other elevated areas are found in the west on the border to Carinthia around the Hochgolling. In this area, the polymetallic ore district Schladming-Seckau nappe system (Duisitz-Eschach-Roßblei) is found. Another anomaly is found near to the lead-zinc mineralisation in the Thajagraben south of Teufenbach (Geologische Bundesanstalt, 2018).

When comparing the two databases, the problem of missing sampling points around Leoben in the Geochemical Atlas is again apparent with regard to monitoring site FW61400187. The situation is different when comparing the measured values around Bruck an der Mur. Here there are elevated values both in the maximum values of the F-parameters and in the S-parameters, which are not shown in the Geochemical Atlas, although there are sufficient sampling points. The elevated measured values in the H2O database are not mapped in the Geochemical Atlas. The same applies to monitoring site FW61400247 - the elevated values in the H2O database are not visible in the stream sediment layer. Furthermore, it is noticeable that the sediment values of some other measuring points in the H2O database indicate significantly higher values than the Geochemical Atlas would suggest. Worth mentioning is measuring point FW61400127 south of Graz. Here, too, there is an anomaly in the F maximum values and S parameters. This is also not shown in the Geochemical Atlas.

Also for *Pb* there is no clear correlation between the lead content in sediment and water. In principle, the two parameters are again in a similar range at low measured values, but anomalies usually only occur in one of the two parameters. In the case of the F-parameters, only monitoring site FW61400187 in the Vordernbergerbach shows a clear outlier upwards (0.00115 mg/l), all other monitoring sites are within the Styrian median (0.0 mg/l). In the case of the maximum values, monitoring site FW61400247 shows a very similar deflection to FW61400187. In the sediment sample data, however, no anomalies are detected at this monitoring site.

Figure 135 - 140

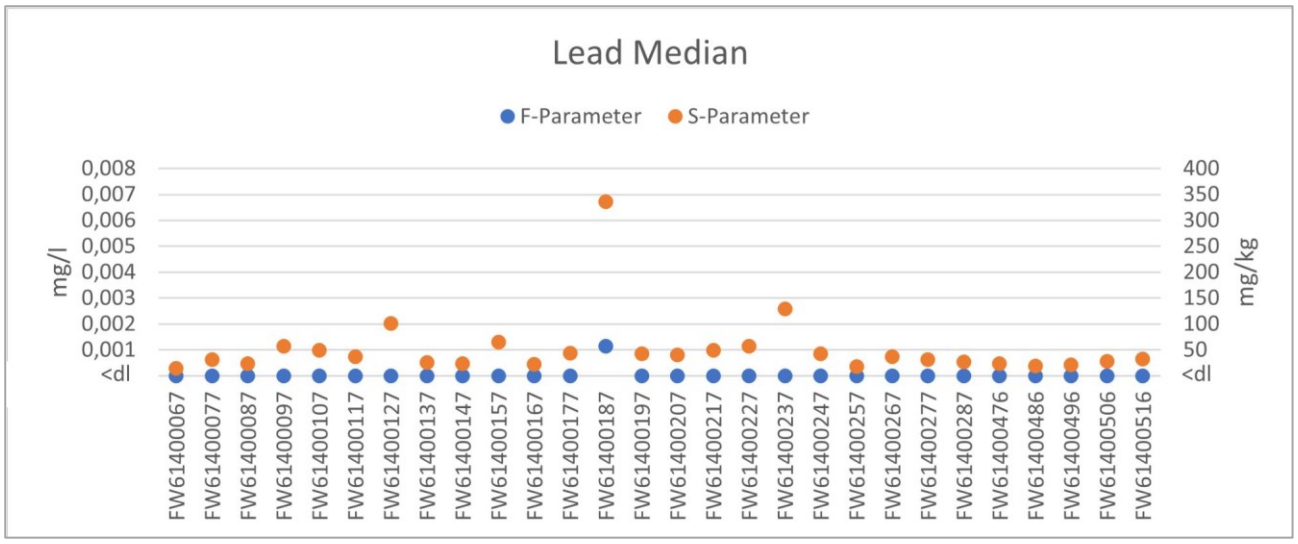


*Figure 135: Lead - Comparison F-Parameters and S-Parameters - Median*

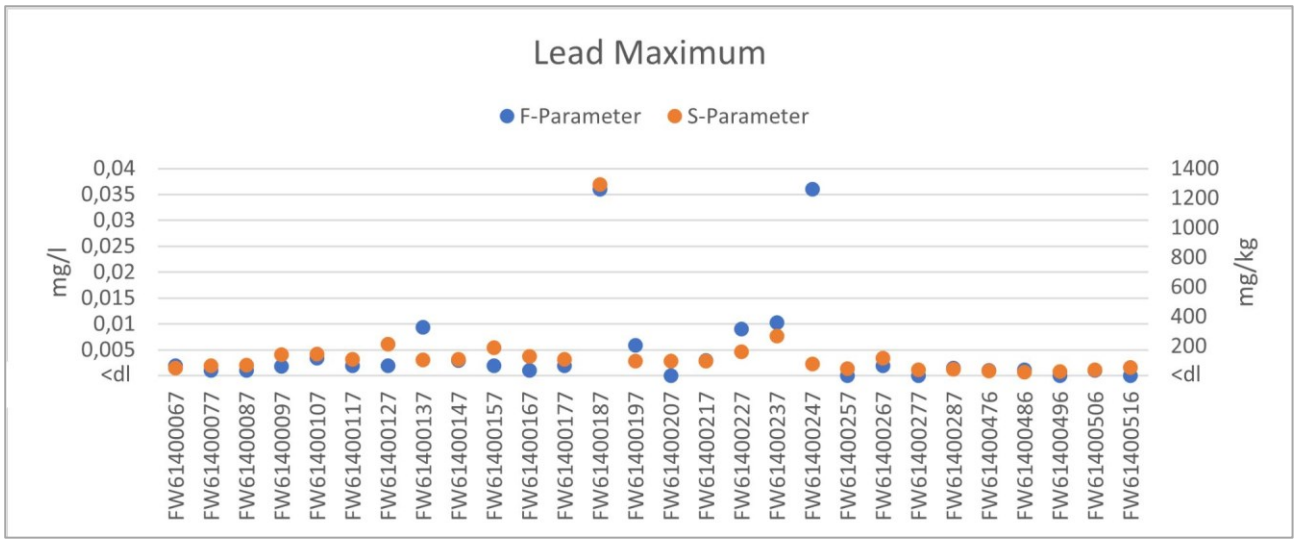


*Figure 136: Lead - Comparison F-Parameters and S-Parameters – Maximum*

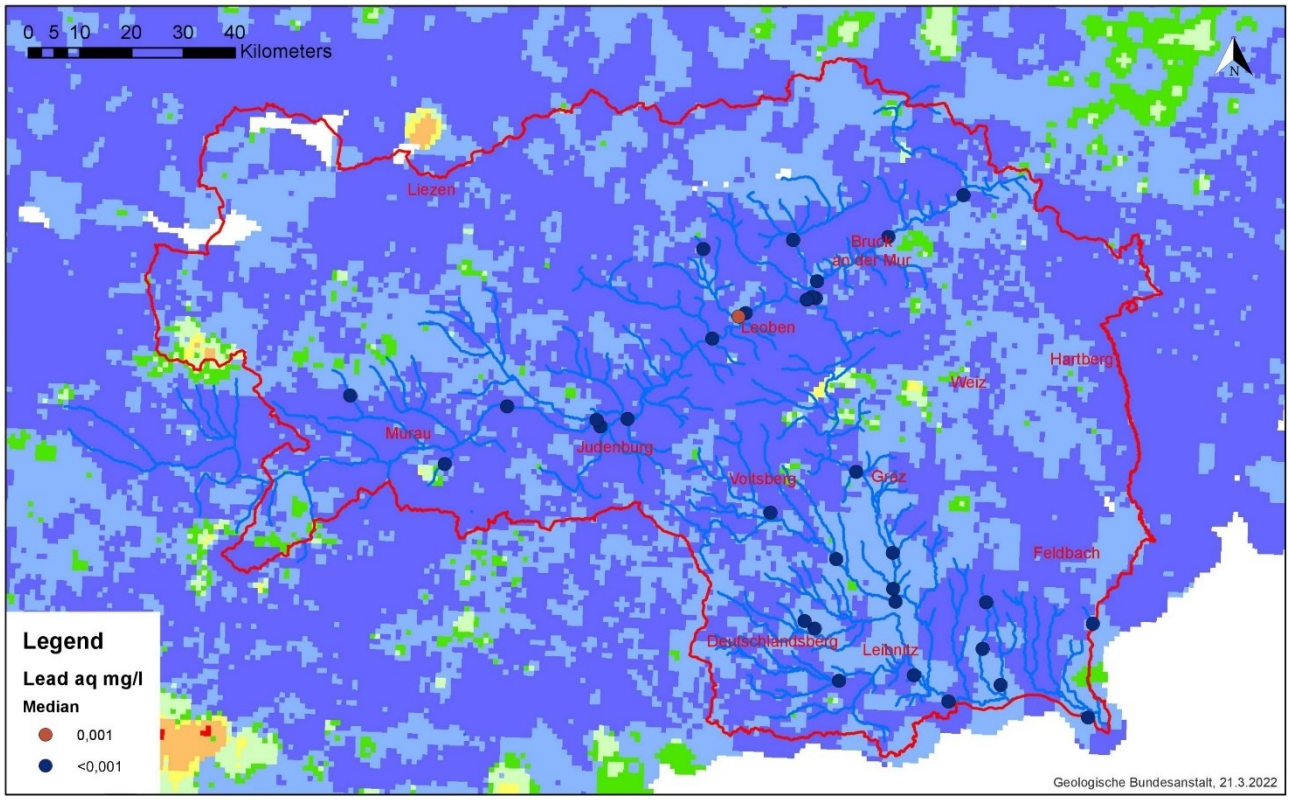


*Figure 137: Comparison of Geochemical Atlas and H2O database - Pb F-Parameter Median Values; (Geologische Bundesanstalt, 2018)*

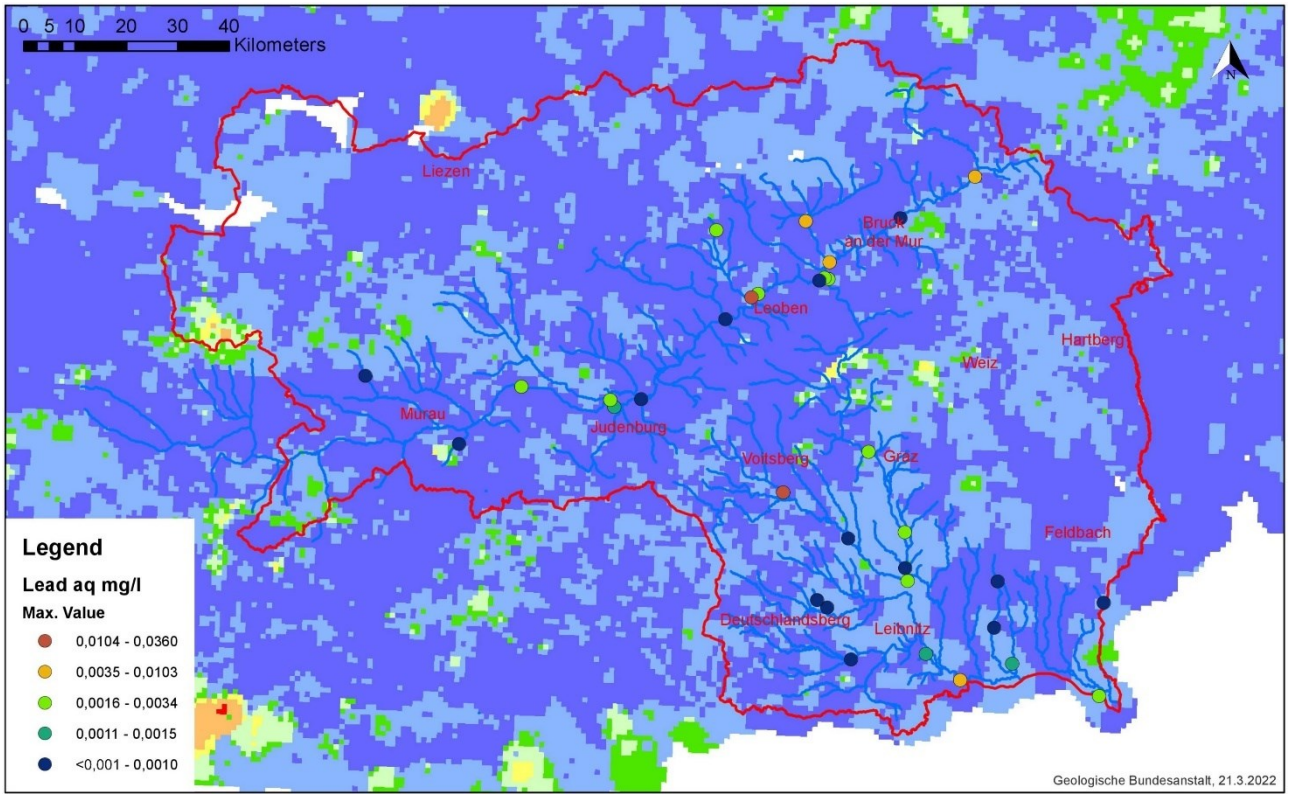


*Figure 138: Comparison of Geochemical Atlas and H2O database - Pb F-Parameter Maximum Values; (Geologische Bundesanstalt, 2018)*

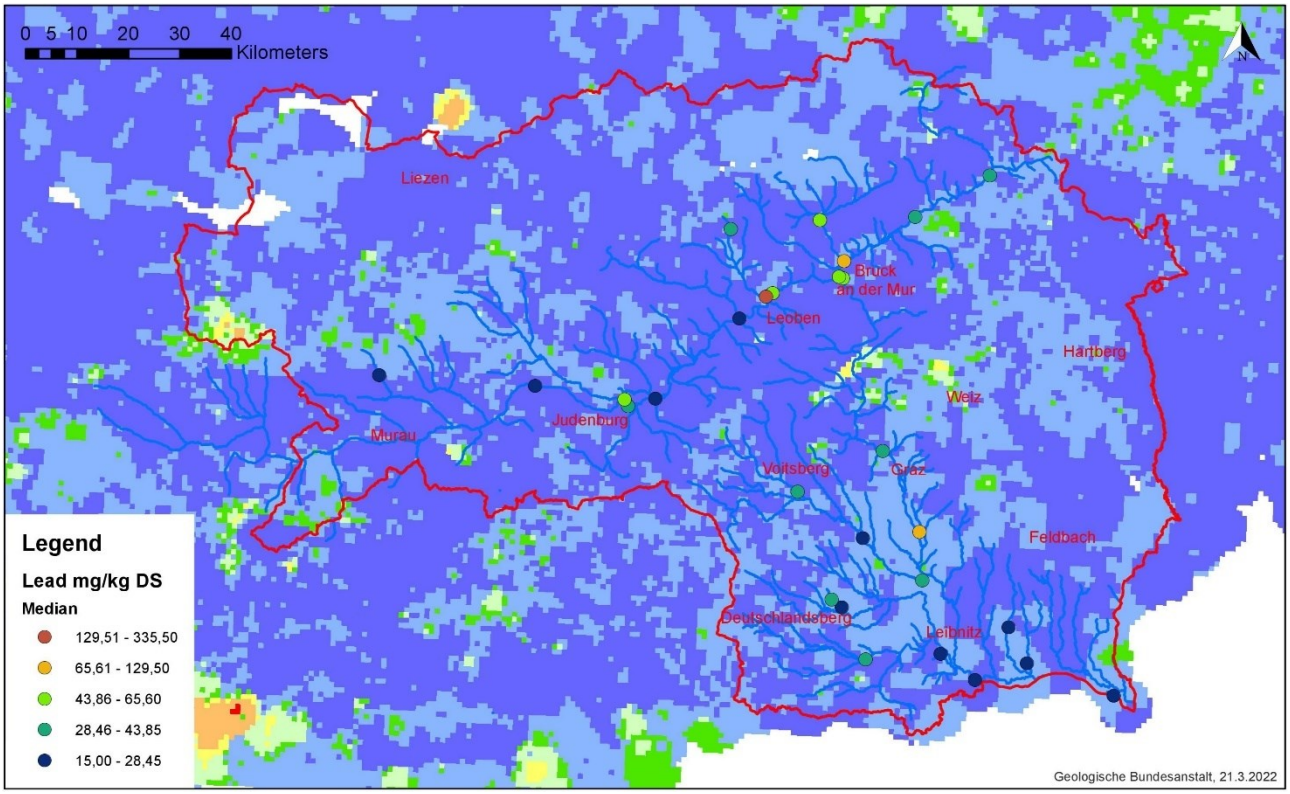


*Figure 139: Comparison of Geochemical Atlas and H2O database - Pb S-Parameter Median Values; (Geologische Bundesanstalt, 2018)*

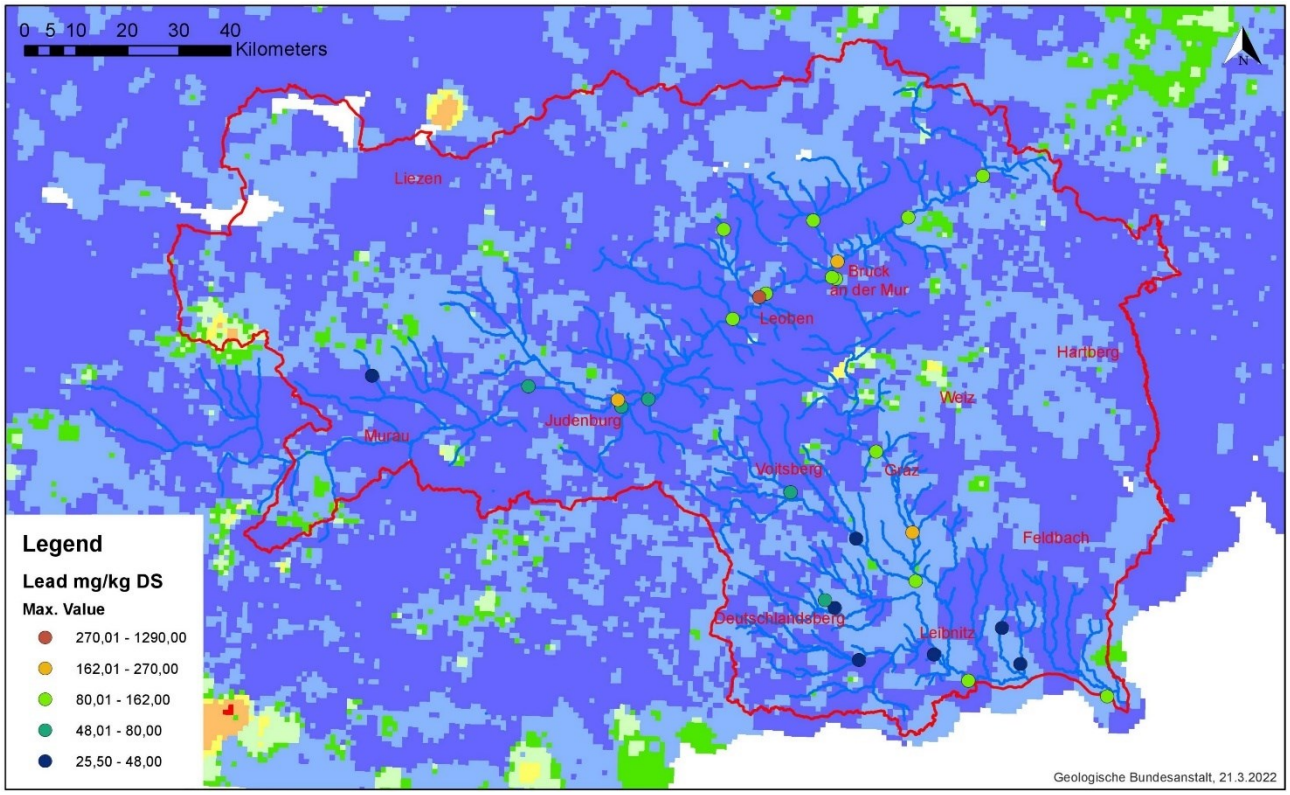


*Figure 140: Comparison of Geochemical Atlas and H2O database - Pb S-Parameter Maximum Values; (Geologische Bundesanstalt, 2018)*

### 1.22.6 Zinc

Very high geogenic zinc concentrations are found in the vicinity of *Pb-Zn* mineralisations, such as in the Graz Palaeozoic as the only clear anomaly in Styria. However, anthropogenic high concentrations are also found in rivers, which are interpreted as "residual" pollution. These originate from immissions in conurbations (e.g. Marchfeld) or from the impact of smelting and metal processing (Pirkl et al., 2015; Geologische Bundesanstalt, 2018).

Again, no clear agreement can be found in the comparison of the two databases. Low concentrations in the Geochemical Atlas do not necessarily result in low concentrations in the H2O data. The areas around Leoben and Bruck an der Mur are once more conspicuous.

For a better comparison of the data, the measuring point FW61400187 and the maximum value of the measuring point FW614237 were excluded, as the values are exorbitantly high compared to the other measuring points. As with the previously considered elements, there is no clear correlation between the sediment samples and the water samples, especially when considering the anomalies. The F-median value of the measuring point FW61400097 shows a slight anomaly in contrast to the S-median value, the same applies to FW61400227. In the case of the maximum values, it is noticeable that the S-parameters have a significantly larger fluctuation range than the F-parameters. In addition, the maximum value of the F-parameter of measuring point FW61400117 shows a clear upward outlier, which is not shown in the S-parameter.

Figure 141 - 146

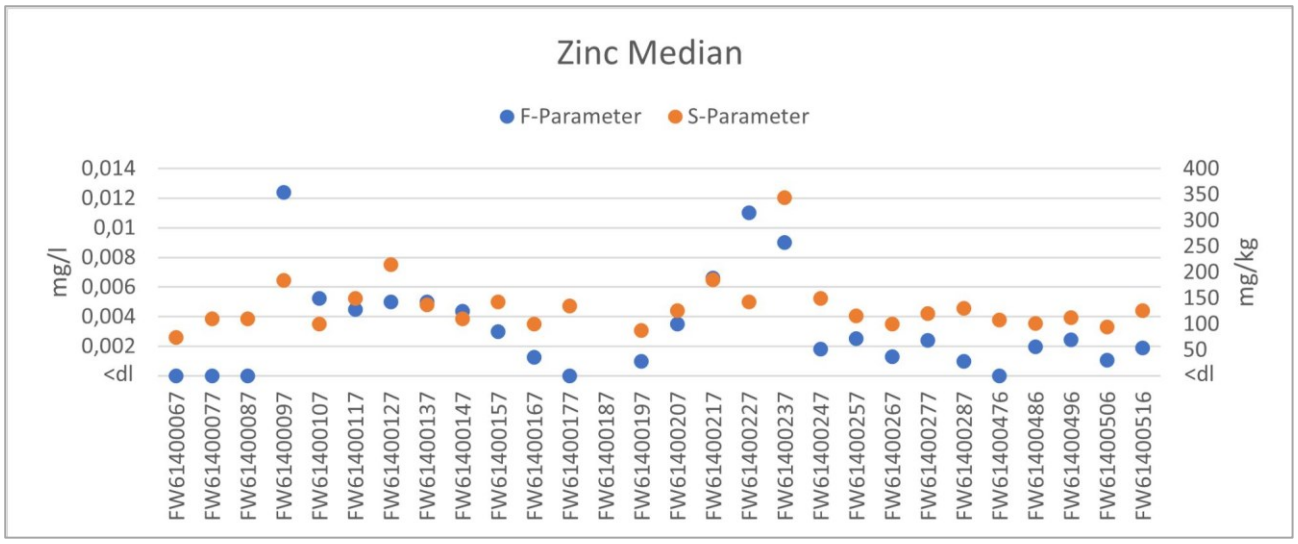


*Figure 141: Zinc - Comparison F-Parameters and S-Parameters – Median*

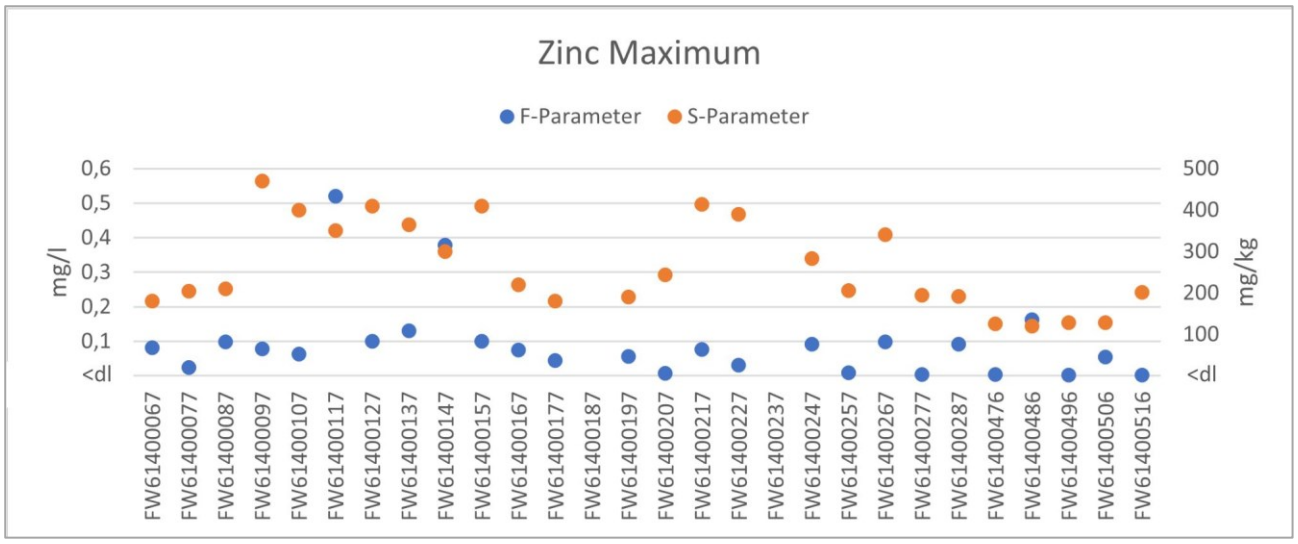


*Figure 142: - Comparison F-Parameters and S-Parameters – Maximum*

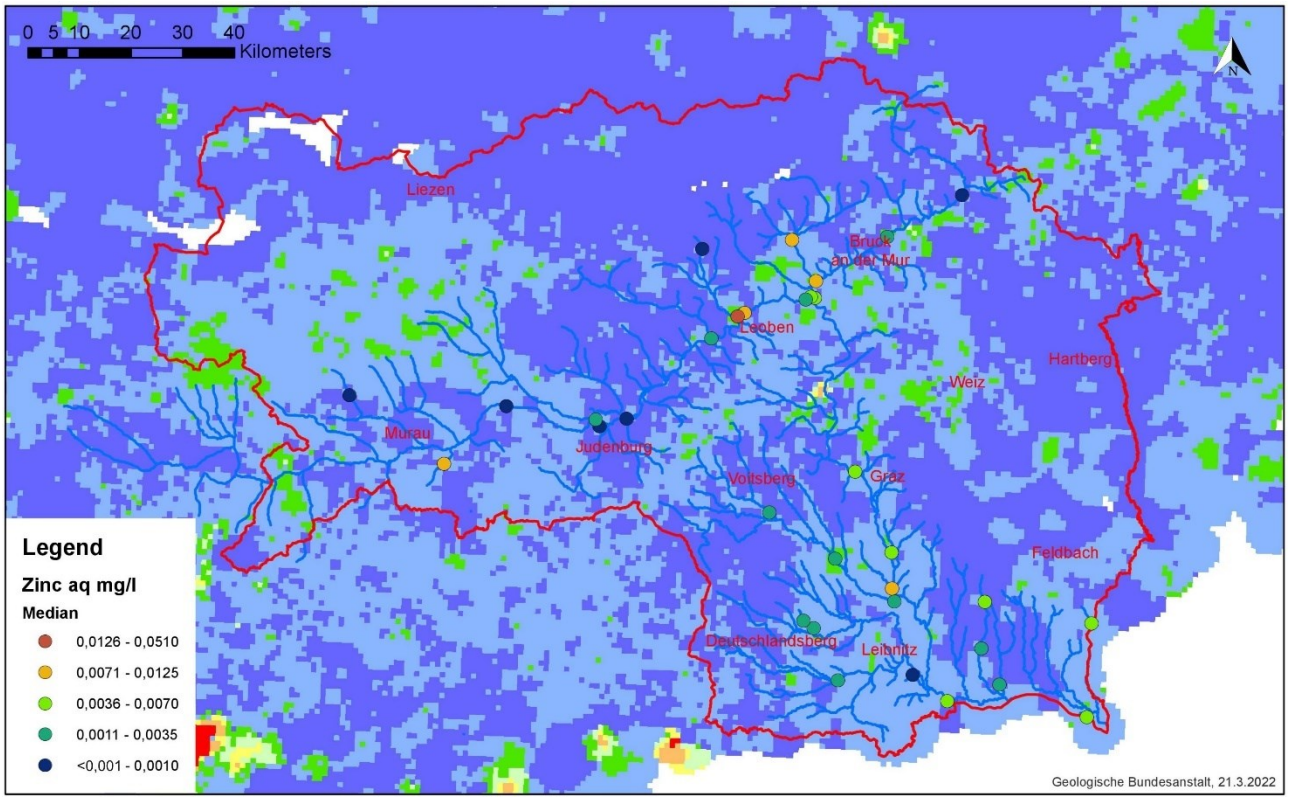


*Figure 143: Comparison of Geochemical Atlas and H2O database - Zn F-Parameter Median Values; (Geologische Bundesanstalt, 2018)*

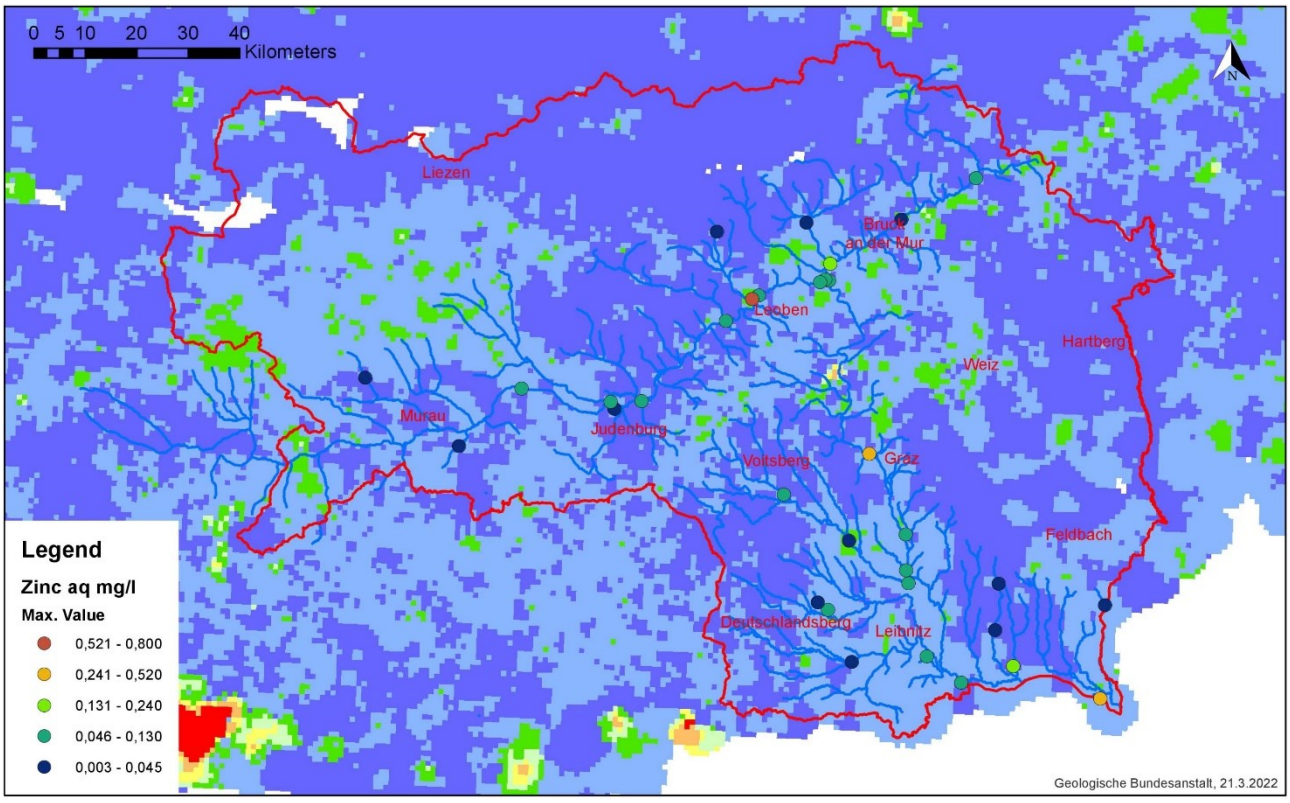


*Figure 144: Comparison of Geochemical Atlas and H2O database - Zn F-Parameter Maximum Values; (Geologische Bundesanstalt, 2018)*

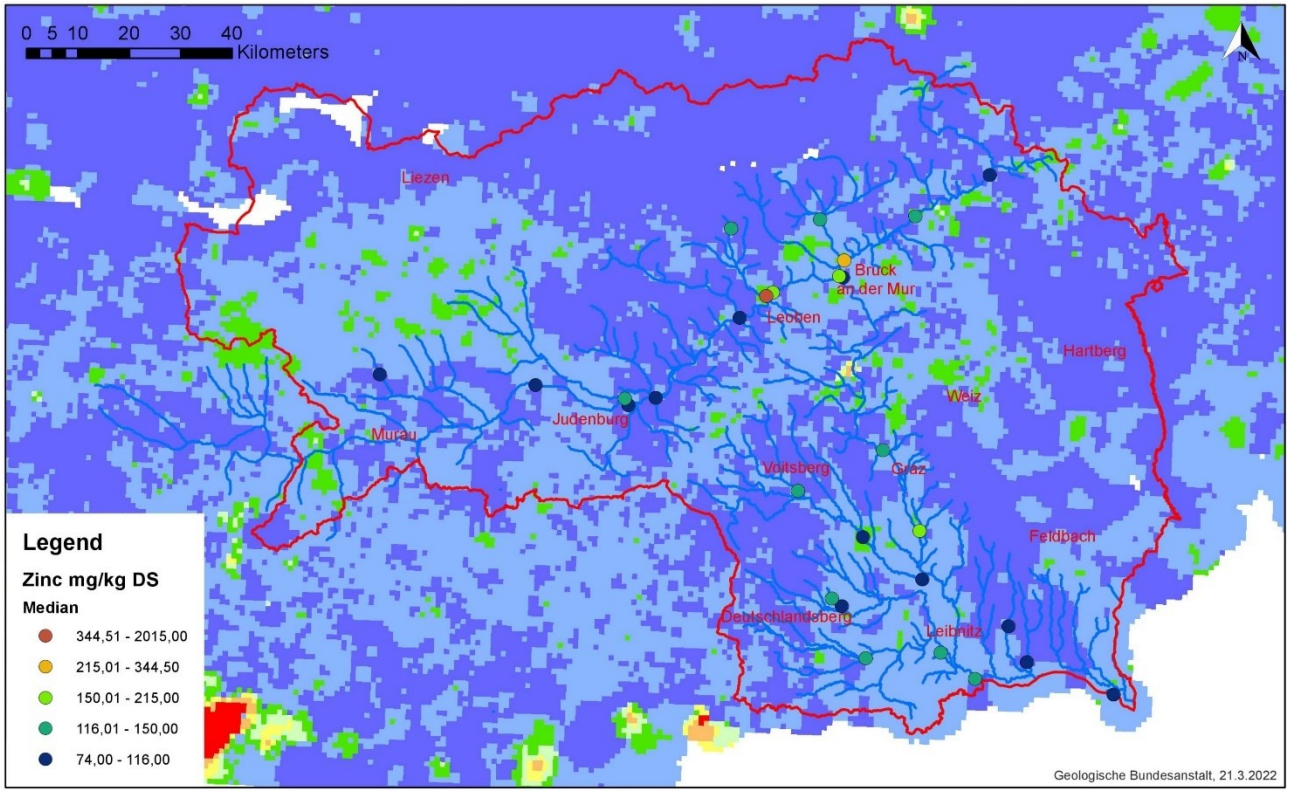


*Figure 145: Comparison of Geochemical Atlas and H2O database - Zn S-Parameter Median Values; (Geologische Bundesanstalt, 2018)*

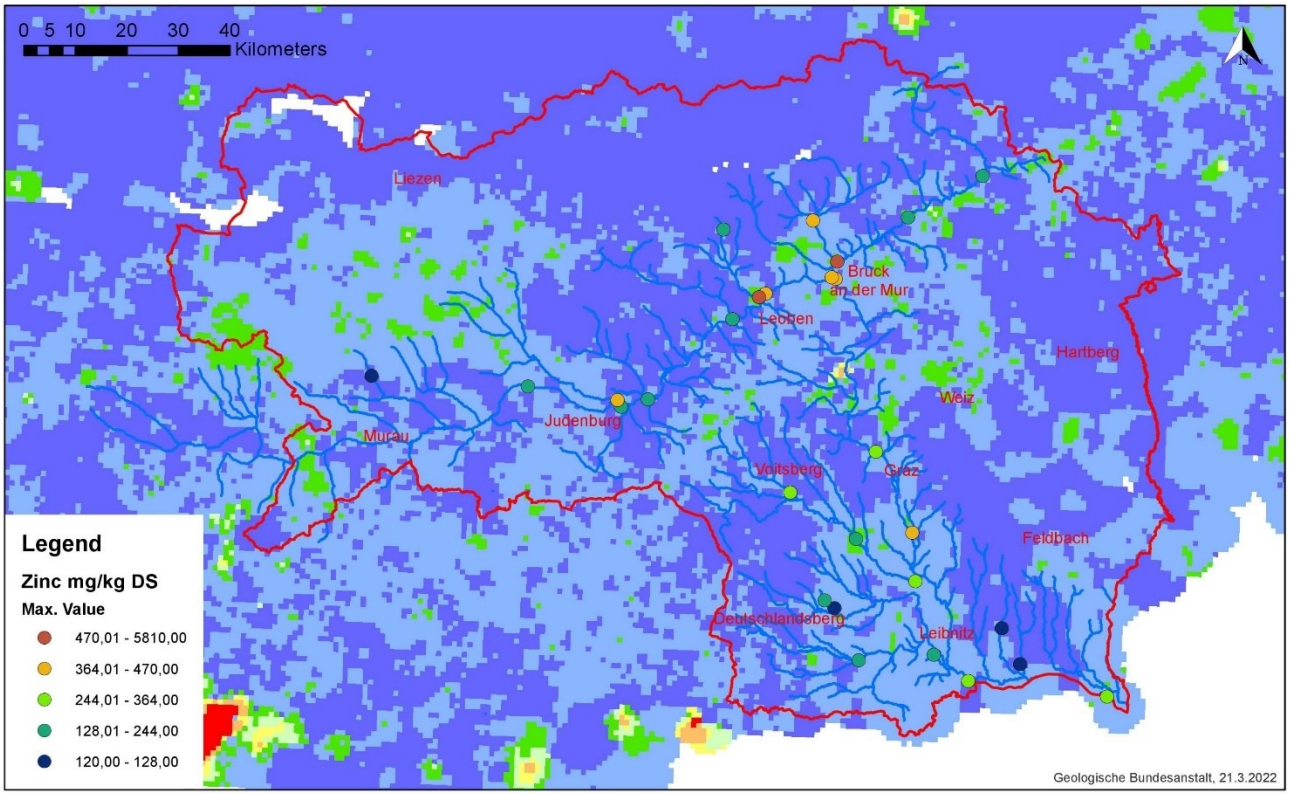


*Figure 146: Comparison of Geochemical Atlas and H2O database - Zn S-Parameter Maximum Values; (Geologische Bundesanstalt, 2018)*

### 1.22.7 General observations

If the data of the H2O database and those of the Geochemical Atlas are compared, it is obvious that the stream sediment layer represents the geogenic background and the S-parameters of the H2O database provide snapshots, since the measurements at these sampling sites are far apart and were not carried out very often. If there is no anomaly in the Geochemical Atlas but there is an anomaly in the H2O database, this could assign an anthropogenic contamination. This is probably most clearly visible at measurement point FW61400187 (Leoben), which shows an anomaly for many elements in the H2O database, which is not recognisable in the Geochemical Atlas. Furthermore, no reliable correlation between the F and S parameters is identified. It is stated that significantly elevated S and F parameters at one monitoring site point probably to anthropogenic influences (e.g. monitoring site FW61400187).

## 1.23 Comparison with the Leoben survey

In the following, the results of the sampling points are compared with those of the database. For this purpose, the measuring points FW61400187, which is near to sample point Mur2 and FW61400097, which corresponds to sample point Mur5, are considered.

### 1.23.1 FW61400187 / Mur2

As already shown in Chapter 5.14, the measuring point Mur2 shows elevated values for almost no element in the single measurement based on the sampling on 27 October 2021. Only the *LOI, CaO, Ni* and *Zn* values show abnormalities. In the database, measuring point FW61400187 also shows increased median values for the *Ni* and *Zn* F-parameters. Looking at the S-parameters, the measuring point FW61400187 has deviations in the median and maximum values for both nickel and zinc.

In Schedl et al. (2010), the *Ni* value is slightly elevated to increased in the entire Vordernbergerbach and around Leoben; in the case of the Zn values, only the measuring point at the end of the Vordernbergerbach (position about Mur2) is raised in this observation area. The measurements of Neinavaie & Prikl (1996), which were carried out in the Vordernbergerbach, showed dust particles of the Donawitz plant, but also remnants of older smelters in Trofaiach and Vordernberg. Furthermore, geogenic nickel and chrome carriers were found in the rolled chippings of the Kraubath serpentine. Although the Mur2 monitoring site indicates elevated values in some elements, these are not present to such an extent (number of elevated elements) compared to the values from the H2O database (FW61400187).

### 1.23.2 FW61400097 / Mur5

In contrast to measuring point FW61400187, the situation is reversed here. In the sampling carried out on 27 October 2021, clearly elevated values were found for several elements at measuring point Mur5. This could not be perceived in the data of the H2O database. An example of this is the element *Pb*. A value of 1185 ppm lead was measured at sample point Mur5. When comparing with the measuring point FW61400097 of the database, neither the median value nor the maximum value show deviations from the Styrian values (F-parameter and S-parameter). Also, in Schedl et al. (2010) no increased Pb values around Leoben is found. No correlation between elevated S and F parameters has been identified at this monitoring site either. With a significantly increased *Al*-value in the F-parameters (91 measured values; minimum value 0.02 mg/l; maximum value 2.88 mg/l; median 0.1 mg/l), the data of the sampling point Mur5 show a value of 14.52% Al2O3. Likewise, no increased correlation between the flow rate and the F-parameters is observed.

# Chapter 7 – Conclusions

With the help of Geochemical Atlas and H2O-Database and own sampling, a chemical analysis of the Mur and its catchment area was carried out. The aim of this work was to identify the anomalies with regard to their geogenic or anthropogenic background, as well as to verify the correlation between water and sediment data. The data from the databases were summarised, processed and presented in graphs and maps. The measurements of the samples taken around Leoben were analysed with XRF. Two sampling sites match those of the H2O database (FW61400187/Mur2 and FW61400097/Mur5) in order to establish comparability. In addition to a general evaluation, a time-dependent comparison of flow and heavy metal concentration in water was carried out at these two sampling points.

Elevated readings in a sediment sample at a monitoring site are generally not related to elevated readings in the water sample. Furthermore, increased measured values in the stream sediment layer of the Geochemical Atlas are not always reflected in the data of the H2O database and vice versa. If no anomaly is detected in the Geochemical Atlas, but detected in the H2O database, an anthropogenic contamination is likely. This is striking at monitoring site FW61400187 (Leoben), where elevated values were detected in both the water and sediment samples, but not in the Geochemical Atlas. This therefore suggests an anthropogenic influence (industry). In the Mur2 measurement, however, the above-average measurement results of this measuring point could only be reproduced to a limited extent.

Furthermore, no correlation between an increased flow rate and an increased or lower heavy metal concentration in the water sample is seen.

# List of Figures

## List of Tables

# References


Berka, R. (2015). *Zur Geologie der großen Beckengebiete des Ostalpenraumes*. *Abhandlungen der Geologischen Bundesanstalt in Wien*(64), 71–141.

Berner, E. K., & Berner, R. A. (2012). *Global environment: Water, air, and geochemical cycles* (2nd ed). Princeton University Press.

Blöschl, G., Kiss, A., Viglione, A., Barriendos, M., Böhm, O., Brázdil, R., Coeur, D., Demarée, G., Llasat, M. C., Macdonald, N., Retsö, D., Roald, L., Schmocker-Fackel, P., Amorim, I., Bělínová, M., Benito, G., Bertolin, C., Camuffo, D., Cornel, D., … Wetter, O. (2020). Current European flood-rich period exceptional compared with past 500 years. *Nature*, *583*(7817), 560–566. https://doi.org/10.1038/s41586-020-2478-3

BMLRT, B. L., Regionen und Tourismus. (2021). *H2O Fachdatenbank* (6.2.11) [Computer software]. https://wasser.umweltbundesamt.at/h2odb/index.xhtml

BMLRT, B. L., Regionen und Tourismus. (2022). *INFO-Seiten des BMLRT*. https://info.bmlrt.gv.at/themen/wasser/wisa/datenverbund/xmlschnittstelle/qualitaet/H2O-Tools.html; https://info.bmlrt.gv.at/themen/wasser/wisa/daten-karten.html

Flügel, H. W., & Hubmann, B. (Hrsg.). (2000). *Das Paläozoikum von Graz: Stratigraphie und Bibliographie*. Verl. der Österr. Akad. der Wiss.

Flügel, H. W., & Neubauer, F. (1984). *Steiermark: Erläuterungen zur geologischen Karte der Steiermark, 1:200.000*. Geologische Bundesanstalt.

Förstner, U. (1983). *Assessment of metal pollution in rivers and estuaries* (S. 395–423).

Friebe, G. (1990). *Lithostratigraphische Neugliederung und Sedimentologie der Ablagerungen des Badeniens (Miozän) um die Mittelsteirische Schwelle (Steirisches Becken, Österreich)*. *Jahrbuch der Geologischen Bundesanstalt*(133(2)), 223–257.

Frisch, W., & Gawlick, H.-J. (2003). The nappe structure of the central Northern Calcareous Alps and its disintegration during Miocene tectonic extrusion?a contribution to understanding the orogenic evolution of the Eastern Alps. *International Journal of Earth Sciences*, *1*(1), 1–1. https://doi.org/10.1007/s00531-003-0357-4

Fritz, I. (1996). *Notes on the Plio-/Pleistocene volcanism of the Styrian Basin*. *Mitteilungen der Gesellschaft der Geologie-und Bergbaustudenten in Österreich*(41), 87–100.

Gasser, D., Gusteruhuber, J., Krische, O., Puhr, B., Scheucher, L., Wagner, T., & Stüwe, K. (2009). *Geology of Styria: An overview*. *Mitteilungen des naturwissenschaftlichen Vereins für Steiermark*(139), 5–36.

Gasser, D., Stüwe, K., & Fritz, H. (2010). Internal structural geometry of the Paleozoic of Graz. *International Journal of Earth Sciences*, *99*(5), 1067–1081. https://doi.org/10.1007/s00531-009-0446-0

Geologische Bundesanstalt. (2018). *IRIS - Interaktives Rohstoffinformationssystem*. https://www.geologie.ac.at/services/webapplikationen/iris-interaktives-rohstoffinformationssystem/

Getzner, M., Jungmeier, M., Köstl, T., & Weiglhofer, S. (2011). *Fließstrecken der Mur – Ermittlung der Ökosystemleistungen – Endbericht* (S. 86) [Studie im Auftrag von: Landesumweltanwaltschaft Steiermark]. E.C.O. Institut für Ökologie. https://www.verwaltung.steiermark.at/cms/dokumente/11304363_74837139/76feac38/esmu10_endbericht_v11_110531_final_gesamt.pdf

Gross, M. (1998). *Aoren- und Faziesentwicklung im Unterpannonium (Obermiozän) des Oststeirischen Neogenbeckens (Österreich)*. *Geologisch-Paläontologische Mitteilungen Innsbruck*(23), 1–35.

Gross, M. (2000). *Das Pannonium im Oststeirischen Becken*. *Berichte des Institutes für Geologie und Paläontologie der Karl-Franzens-Universität Graz*(2), 47–86.

Hanesch, M., Rantitsch, G., Hemetsberger, S., & Scholger, R. (2007). Lithological and pedological influences on the magnetic susceptibility of soil: Their consideration in magnetic pollution mapping. *The Science of the total environment*, *382*, 351–363. https://doi.org/10.1016/j.scitotenv.2007.04.007

Hanesch, M., Scholger, R., & Rey, D. (2003). Mapping dust distribution around an industrial site by measuring magnetic parameters of tree leaves. *Atmospheric Environment*, *37*(36), 5125–5133. https://doi.org/10.1016/j.atmosenv.2003.07.013

Hermann, S. (1992). *Die Steirische Grauwackenzone am Kaintaleck: Geologie, Petrographie, Struktur, Geochemie und Rb-Sr-Datierungen* [Diplomarbeit].
Kammerlander, J., Achleitner, S., Schöber, J., & Hofer, B. (2017). Geschiebehaushalt in kleinen Hochgebirgsbächen der Nordtiroler Zentralalpen. *Österreichische Wasser- und Abfallwirtschaft*, *69*(3–4), 114–124. https://doi.org/10.1007/s00506-017-0378-z
Kollmann, K. (1964). *Jungtertiär im Steirischen Becken*. *Austrian Journal of Earth Sciences*(57), 479–632.
Krystyn, L., Lein, R., & Richoz, S. (2008). *Der Gamsstein: Werden und Vergehen einer Wettersteinkalk-Plattform*. *Journal of Alpine Geology*(49), 157–172.
Levinson, A. A. (1980). *Introduction to exploration geochemistry* (2.). Applied Publishing. https://go.exlibris.link/0PwXyR8k
Lipiarski, P., Weber, L., Schedl, A., Heger, H., & Reischer, J. (2019). *IRIS Online – Interaktives Rohstoffinformationssystem für Österreich*. *Arbeitstagung 2019 der Geologischen Bundesanstalt*(2019), 179–189.
Mandl, G. W. (2000). The Alpine sector of the Tethyan shelf—Examples of Triassic to Jurassic sedimentation and deformation from the Northern Calcareous Alps. *Mitteilungen Der Österreichischen Geologischen Gesellschaft*, *92*, 61–77.
Manser, P., Plass, N., & Scholger, R. (1989). *Umweltgeologische Untersuchungen an rezenten Sedimenten der Mur (Steiermark, Österreich)*. *Geologisch-Paläontologische Mitteilungen Innsbruck*(016), 77–78.
Muhar, S., Kainz, M., Kaufmann, M., & Schwarz, M. (1998). Erhebung und Bilanzierung flusstypspezifisch erhaltener Fliessgewässerabschnitte in Österreich. *Österreichische Wasser- und Abfallwirtschaft*, *50*(5–6).
Neinavaie, H., & Prikl, H. (1996). *Bewertung von Schwermetallverteilungen in Böden und Flußsedimenten mit Hilfe angewandt mineralogischer und geostatistischer Werkzeuge*. *Berichte der Geologischen Bundesanstalt*(34), 1–67.
Neubauer, F., Handler, R., Hermann, S., & Paulus, G. (1994). Revised lithostratigraphy and structure of the Eastern Graywacke Zone (Eastern Alps). *Mitt Österr Geol Ges*, *86*, 61–74.
Neubauer, F., & Pistotnik, J. (1984). Das Altpaläozoikum und Unterkarbon des Gurktaler Deckensystems (Ostalpen) und ihre paläogeographischen Beziehungen. *Geologische Rundschau*, *73*(1), 149–174. https://doi.org/10.1007/BF01820365
Neubauer, F., & Vozarova, A. (1990). *The Noetsch-Veitsch-North Gemeric Zone of Alps and Carpathians; correlation, paleogeography and significance for Variscan Orogeny*. *Thirty years of geological cooperation between Austria and Czechoslovakia*, 167–171.
Pirkl, H., Schedl, A., Pfleiderer, S., & Geologische Bundesanstalt (Austria : 1945- ). (2015). *Geochemischer Atlas von Österreich: Bundesweite Bach- und Flusssedimentgeochemie (1978-2010)*.
Pöschl, I. (1991). A Model for the Depositional Evolution of the Volcanoclastic Succession of a Pliocene Maar Volcano in the Styrian Basin (Austria). *Jahrbuch der Geologischen Bundesanstalt*, *134*(4), 809–843.
Rantitsch, G. (2001). The fractal properties of geochemical landscapes as an indicator of weathering and transport processes within the Eastern Alps. *Journal of Geochemical Exploration*, *73*(1), 27–42. https://doi.org/10.1016/S0375-6742(01)00168-6
Ratschbacher, L. (1987). *Stratigraphy, tectonics and paleogeography of the Veitsch Nappe (Greywacke Zone, Eastern Alps: A rearrangement. Pre-Variscan and Variscan events in the Alpine-Mediterranean mountain belts*, 407–414.
Sachsenhofer, R., Sperl, H., & Wagini, A. (1996). Structure, development and hydrocarbon potential of the Styrian Basin (Pannonian Basin system, Austria). *Wessely, G. & Liebl, W. (Eds.): Oil and Gas in Alpidic Thrustbelts and Basins of Central and Eastern Europe*, *EAGE Special Publication*(No. 5), 393–414.
Salomons, W., & Förstner, U. (1984). *Metals in the Hydrocycle*. Springer Berlin Heidelberg. https://doi.org/10.1007/978-3-642-69325-0
Schedl, A., Prikl, H., Neinavaie, H., Pfleiderer, S., Lipiarski, P., Hobiger, G., Benold, C., Haslinger, E., Massimo, D., Atzenhofer, B., & Mauracher, J. (2010). *Umweltgeochemische Untersuchung der Bach- und Flusssedimente Steiermarks auf Haupt- und Spurenelemente zur Erfassung und Beurteilung geogener und anthropogener Schadstoffbelastungen („Umweltgeochemie Steiermark"): Endbericht 2010* (Endbericht Projekt St-C-076; S. 53).

Schmid, S. M., Fügenschuh, B., Kissling, E., & Schuster, R. (2004). Tectonic map and overall architecture of the Alpine orogen. *Eclogae Geologicae Helvetiae*, *97*(1), 93–117. https://doi.org/10.1007/s00015-004-1113-x

Schönlaub, H. P. (1980). Die Grauwackenzone. In Geologische Bundesanstalt (Hrsg.), *Der Geologische Aufbau Österreichs* (S. 265–289). Springer Vienna. https://doi.org/10.1007/978-3-7091-3744-4_16

Schuster, K., Berka, R., Draganits, E., Frank, W., & Schuster, R. (2001). Lithologien, Metamorphosegeschichte und tektonischer Bau der kristallinen Einheiten am Alpenostrand. *Arbeitstagung der Geologischen Bundesanstalt Blatt 104 Mürzzuschlag, Neuberg a.d. Mürz 3.-7. September 2001*, 29–56.

Schuster, R. (2004). *The austroalpine crystalline units in the Eastern Alps. Berichte des Institutes für Geologie und Paläontologie der Karl-Franzens-Universität Graz*(9), 30–36.

Schuster, R. (2015). *Zur Geologie der Ostalpen*. *Abhandlungen der Geologischen Bundesanstalt in Wien*(64), 143–165.

Tollmann, A. (1985). *Geologie von Österreich. 2: Ausserzentralalpiner Anteil*. Deuticke.

# Annex

## Table of Content

# 1 H2O database: Tables resulting from the data cleaning

## 1.1 Aluminum

### 1.1.1 F-Parameters

| GZÜV ID | Parameter ID | Parameter Name | Median | Standard deviation | Number of Measurements | Minimum value | Maximum Value |
|---|---|---|---|---|---|---|---|
| FW61302327 | F160 | Al mg/l | <0,01 | 0,0000 | 1 | <0,01 | <0,01 |
| FW61400067 | F160 | Al mg/l | <0,01 | 0,0146 | 91 | <0,01 | 0,08 |
| FW61400077 | F160 | Al mg/l | <0,01 | 0,0243 | 57 | <0,01 | 0,14 |
| FW61400087 | F160 | Al mg/l | 0,016 | 0,0143 | 91 | <0,01 | 0,07 |
| FW61400097 | F160 | Al mg/l | 0,1 | 0,3753 | 91 | 0,02 | 2,88 |
| FW61400107 | F160 | Al mg/l | 0,01 | 0,0253 | 92 | <0,01 | 0,216 |
| FW61400117 | F160 | Al mg/l | 0,06 | 0,5118 | 58 | 0,01 | 3,9 |
| FW61400127 | F160 | Al mg/l | 0,015 | 0,0246 | 115 | <0,01 | 0,1793 |
| FW61400137 | F160 | Al mg/l | 0,02 | 0,0557 | 248 | <0,01 | 0,7 |
| FW61400147 | F160 | Al mg/l | 0,015 | 0,0374 | 126 | <0,01 | 0,25 |
| FW61400157 | F160 | Al mg/l | 0,0345 | 0,0197 | 92 | 0,018 | 0,15 |
| FW61400167 | F160 | Al mg/l | <0,01 | 0,0120 | 77 | <0,01 | 0,06 |
| FW61400177 | F160 | Al mg/l | <0,01 | 0,0184 | 59 | <0,01 | 0,12 |
| FW61400187 | F160 | Al mg/l | 0,02 | 0,0453 | 71 | <0,01 | 0,37 |
| FW61400197 | F160 | Al mg/l | <0,01 | 0,0162 | 93 | <0,01 | 0,1 |
| FW61400207 | F160 | Al mg/l | 0,005 | 0,0076 | 6 | <0,01 | 0,02 |
| FW61400217 | F160 | Al mg/l | 0,01 | 0,0129 | 128 | <0,01 | 0,07 |
| FW61400227 | F160 | Al mg/l | <0,01 | 0,0000 | 5 | <0,01 | <0,01 |
| FW61400237 | F160 | Al mg/l | 0,013 | 0,0351 | 60 | <0,01 | 0,14 |
| FW61400247 | F160 | Al mg/l | 0,02 | 0,0249 | 59 | <0,01 | 0,15 |
| FW61400257 | F160 | Al mg/l | 0,015 | 0,0256 | 6 | <0,01 | 0,075 |
| FW61400267 | F160 | Al mg/l | 0,01115 | 0,0259 | 129 | <0,01 | 0,1899 |
| FW61400277 | F160 | Al mg/l | 0,016 | 0,0187 | 6 | 0,01 | 0,06 |
| FW61400287 | F160 | Al mg/l | 0,013 | 0,0469 | 125 | <0,01 | 0,3 |
| FW61400476 | F160 | Al mg/l | <0,01 | 0,0618 | 44 | <0,01 | 0,416 |
| FW61400486 | F160 | Al mg/l | <0,01 | 0,0468 | 44 | <0,01 | 0,236 |
| FW61400496 | F160 | Al mg/l | <0,01 | 0,0000 | 2 | <0,01 | <0,01 |
| FW61400506 | F160 | Al mg/l | 0,01 | 0,0237 | 44 | <0,01 | 0,106 |
| FW61400516 | F160 | Al mg/l | 0,011 | 0,0010 | 2 | 0,01 | 0,012 |
| FW61400597 | F160 | Al mg/l | 0,0124 | 0,0397 | 35 | <0,01 | 0,2193 |
| FW61404547 | F160 | Al mg/l | 0,0158 | 0,0293 | 12 | <0,01 | 0,0935 |
| FW61404607 | F160 | Al mg/l | <0,01 | 0,0000 | 2 | <0,01 | <0,01 |
| FW61404617 | F160 | Al mg/l | 0,0244 | 0,0000 | 1 | 0,0244 | 0,0244 |

## 1.2 Iron

### 1.2.1 F-Parameters

| GZÜV ID | Parameter ID | Parameter Name | Median | Standard deviation | Number of Measurements | Minimum value | Maximum Value |
|---|---|---|---|---|---|---|---|
| FW61302327 | F148 | Fe mg/l | 0,0263 | 0 | 1 | 0,0263 | 0,0263 |
| FW61400067 | F148 | Fe mg/l | 0,01444 | 0,018911 | 97 | <0,01 | 0,082 |
| FW61400077 | F148 | Fe mg/l | 0,017 | 0,020233 | 63 | <0,01 | 0,0979 |
| FW61400087 | F148 | Fe mg/l | 0,017 | 0,01992 | 97 | <0,01 | 0,11 |
| FW61400097 | F148 | Fe mg/l | 0,0139 | 0,02238 | 97 | <0,01 | 0,166 |
| FW61400107 | F148 | Fe mg/l | 0,01486 | 0,037356 | 98 | <0,01 | 0,36 |
| FW61400117 | F148 | Fe mg/l | 0,032 | 0,018771 | 64 | <0,01 | 0,1 |
| FW61400127 | F148 | Fe mg/l | 0,025 | 0,037994 | 121 | <0,01 | 0,3569 |
| FW61400137 | F148 | Fe mg/l | 0,041055 | 0,100684 | 252 | <0,01 | 1,2 |
| FW61400147 | F148 | Fe mg/l | 0,038 | 0,056376 | 132 | <0,01 | 0,45 |
| FW61400157 | F148 | Fe mg/l | 0,0222 | 0,016982 | 98 | <0,01 | 0,11 |
| FW61400167 | F148 | Fe mg/l | <0,01 | 0,012337 | 110 | <0,01 | 0,089 |
| FW61400177 | F148 | Fe mg/l | <0,01 | 0,012137 | 65 | <0,01 | 0,061 |
| FW61400187 | F148 | Fe mg/l | 0,014 | 0,110736 | 77 | <0,01 | 0,885 |
| FW61400197 | F148 | Fe mg/l | <0,01 | 0,02062 | 99 | <0,01 | 0,182 |
| FW61400207 | F148 | Fe mg/l | <0,01 | 0,016405 | 6 | <0,01 | 0,044 |
| FW61400217 | F148 | Fe mg/l | 0,012 | 0,018384 | 134 | <0,01 | 0,1444 |
| FW61400227 | F148 | Fe mg/l | 0,0254 | 0,023864 | 5 | 0,017 | 0,08258 |
| FW61400237 | F148 | Fe mg/l | 0,016 | 0,039982 | 66 | <0,01 | 0,29 |
| FW61400247 | F148 | Fe mg/l | 0,022 | 0,029326 | 65 | <0,01 | 0,19 |
| FW61400257 | F148 | Fe mg/l | 0,03445 | 0,039133 | 6 | <0,01 | 0,12 |
| FW61400267 | F148 | Fe mg/l | 0,0469 | 0,062643 | 135 | <0,01 | 0,5047 |
| FW61400277 | F148 | Fe mg/l | 0,08285 | 0,026042 | 6 | 0,044 | 0,12 |
| FW61400287 | F148 | Fe mg/l | 0,104 | 0,070607 | 131 | <0,01 | 0,5834 |
| FW61400476 | F148 | Fe mg/l | 0,01215 | 0,017506 | 44 | <0,01 | 0,106 |
| FW61400486 | F148 | Fe mg/l | 0,0417 | 0,094696 | 44 | 0,0112 | 0,53 |
| FW61400496 | F148 | Fe mg/l | 0,0203 | 0,0038 | 2 | 0,0165 | 0,0241 |
| FW61400506 | F148 | Fe mg/l | 0,06155 | 0,064163 | 44 | 0,0207 | 0,36693 |
| FW61400516 | F148 | Fe mg/l | 0,585065 | 0,454935 | 2 | 0,13013 | 1,04 |
| FW61400597 | F148 | Fe mg/l | 0,017 | 0,088875 | 35 | <0,01 | 0,4832 |
| FW61404547 | F148 | Fe mg/l | 0,02395 | 0,040099 | 12 | 0,011 | 0,133 |
| FW61404607 | F148 | Fe mg/l | 0,00925 | 0,00925 | 2 | <0,01 | 0,0185 |
| FW61404617 | F148 | Fe mg/l | 0,106 | 0 | 1 | 0,106 | 0,106 |

## 1.3 Manganese

### 1.3.1 F-Parameters

| GZÜV ID | Parameter ID | Parameter Name | Median | Standard deviation | Number of Measurements | Minimum value | Maximum Value |
|---|---|---|---|---|---|---|---|
| FW61302327 | F150 | Mn mg/l | 0,0175 | 0 | 1 | 0,0175 | 0,0175 |
| FW61400067 | F150 | Mn mg/l | <0,01 | 0,001974 | 97 | <0,01 | 0,013 |
| FW61400077 | F150 | Mn mg/l | <0,01 | 0,00429 | 63 | <0,01 | 0,033 |
| FW61400087 | F150 | Mn mg/l | <0,01 | 0,007769 | 97 | <0,01 | 0,056 |
| FW61400097 | F150 | Mn mg/l | <0,01 | 0,008018 | 97 | <0,01 | 0,058 |
| FW61400107 | F150 | Mn mg/l | <0,01 | 0,008313 | 98 | <0,01 | 0,034 |
| FW61400117 | F150 | Mn mg/l | 0,025 | 0,011738 | 64 | <0,01 | 0,07 |
| FW61400127 | F150 | Mn mg/l | 0,014 | 0,012459 | 121 | <0,01 | 0,058 |
| FW61400137 | F150 | Mn mg/l | 0,02161 | 0,016583 | 254 | <0,01 | 0,11 |
| FW61400147 | F150 | Mn mg/l | 0,013 | 0,015445 | 134 | <0,01 | 0,087 |
| FW61400157 | F150 | Mn mg/l | 0,01325 | 0,018894 | 98 | <0,01 | 0,073 |
| FW61400167 | F150 | Mn mg/l | 0,0125 | 0,005692 | 5 | 0,01 | 0,025 |
| FW61400177 | F150 | Mn mg/l | <0,01 | 0,004532 | 65 | <0,01 | 0,035 |
| FW61400187 | F150 | Mn mg/l | 0,034 | 0,197474 | 77 | <0,01 | 1,7 |
| FW61400197 | F150 | Mn mg/l | <0,01 | 0,00795 | 99 | <0,01 | 0,0547 |
| FW61400207 | F150 | Mn mg/l | <0,01 | 0,005238 | 6 | <0,01 | 0,012 |
| FW61400217 | F150 | Mn mg/l | 0,01 | 0,019285 | 134 | <0,01 | 0,2 |
| FW61400227 | F150 | Mn mg/l | <0,01 | 0 | 5 | <0,01 | <0,01 |
| FW61400237 | F150 | Mn mg/l | <0,01 | 0,023555 | 66 | <0,01 | 0,15 |
| FW61400247 | F150 | Mn mg/l | 0,022 | 0,013662 | 65 | <0,01 | 0,078 |
| FW61400257 | F150 | Mn mg/l | 0,0123 | 0,005295 | 6 | <0,01 | 0,017 |
| FW61400267 | F150 | Mn mg/l | 0,0214 | 0,018178 | 135 | <0,01 | 0,14 |
| FW61400277 | F150 | Mn mg/l | 0,012 | 0,006644 | 6 | <0,01 | 0,016 |
| FW61400287 | F150 | Mn mg/l | 0,0321 | 0,015529 | 131 | <0,01 | 0,1 |
| FW61400476 | F150 | Mn mg/l | <0,01 | 0 | 44 | <0,01 | <0,01 |
| FW61400486 | F150 | Mn mg/l | 0,0923 | 0,130449 | 44 | <0,01 | 0,608 |
| FW61400496 | F150 | Mn mg/l | 0,139125 | 0,115525 | 2 | 0,0236 | 0,25465 |
| FW61400506 | F150 | Mn mg/l | 0,0399 | 0,294582 | 44 | <0,01 | 1,44 |
| FW61400516 | F150 | Mn mg/l | 0,21742 | 0,14722 | 2 | 0,0702 | 0,36464 |
| FW61400597 | F150 | Mn mg/l | 0,0187 | 0,022217 | 35 | <0,01 | 0,143 |
| FW61404547 | F150 | Mn mg/l | 0,01655 | 0,007339 | 12 | 0,01 | 0,0339 |
| FW61404607 | F150 | Mn mg/l | <0,01 | 0 | 2 | <0,01 | <0,01 |
| FW61404617 | F150 | Mn mg/l | 0,042 | 0 | 1 | 0,042 | 0,042 |

## 1.4 Arsenic

### 1.4.1 F-Parameters

| GZÜV ID | Parameter ID | Parameter Name | Median | Standard deviation | Number of Measurements | Minimum value | Maximum Value |
|---|---|---|---|---|---|---|---|
| FW61302327 | F168 | As mg/l | <0,0007 | 0 | 1 | <0,0007 | <0,0007 |
| FW61400067 | F168 | As mg/l | <0,0007 | 0,000629 | 107 | <0,0007 | 0,0026 |
| FW61400077 | F168 | As mg/l | 0,00045 | 0,000924 | 74 | <0,0007 | 0,0032 |
| FW61400087 | F168 | As mg/l | <0,0007 | 0,000757 | 108 | <0,0007 | 0,004 |
| FW61400097 | F168 | As mg/l | <0,0007 | 0,000684 | 108 | <0,0007 | 0,003 |
| FW61400107 | F168 | As mg/l | <0,0007 | 0,000771 | 109 | <0,0007 | 0,0032 |
| FW61400117 | F168 | As mg/l | <0,0007 | 0,000744 | 75 | <0,0007 | 0,0027 |
| FW61400127 | F168 | As mg/l | <0,0007 | 0,000783 | 132 | <0,0007 | 0,0031 |
| FW61400137 | F168 | As mg/l | <0,0007 | 0,000727 | 264 | <0,0007 | 0,0051 |
| FW61400147 | F168 | As mg/l | <0,0007 | 0,000744 | 144 | <0,0007 | 0,003 |
| FW61400157 | F168 | As mg/l | <0,0007 | 0,00031 | 109 | <0,0007 | 0,002 |
| FW61400167 | F168 | As mg/l | 0,0011 | 0,000804 | 121 | <0,0007 | 0,0025 |
| FW61400177 | F168 | As mg/l | <0,0007 | 0,00032 | 76 | <0,0007 | 0,002 |
| FW61400187 | F168 | As mg/l | <0,0007 | 0,000776 | 88 | <0,0007 | 0,0026 |
| FW61400197 | F168 | As mg/l | <0,0007 | 0,000753 | 109 | <0,0007 | 0,0034 |
| FW61400207 | F168 | As mg/l | 0,00159 | 0,000733 | 6 | <0,0007 | 0,0024 |
| FW61400217 | F168 | As mg/l | 0,001 | 0,000745 | 144 | <0,0007 | 0,0036 |
| FW61400227 | F168 | As mg/l | <0,0007 | 0 | 5 | <0,0007 | <0,0007 |
| FW61400237 | F168 | As mg/l | <0,0007 | 0,000509 | 77 | <0,0007 | 0,0025 |
| FW61400247 | F168 | As mg/l | <0,0007 | 0,000838 | 76 | <0,0007 | 0,004 |
| FW61400257 | F168 | As mg/l | <0,0007 | 0 | 6 | <0,0007 | <0,0007 |
| FW61400267 | F168 | As mg/l | <0,0007 | 0,000296 | 146 | <0,0007 | 0,0015 |
| FW61400277 | F168 | As mg/l | <0,0007 | 0 | 6 | <0,0007 | <0,0007 |
| FW61400287 | F168 | As mg/l | <0,0007 | 0,000277 | 142 | <0,0007 | 0,002 |
| FW61400476 | F168 | As mg/l | <0,0007 | 0,000433 | 43 | <0,0007 | 0,00167 |
| FW61400486 | F168 | As mg/l | <0,0007 | 0,000781 | 44 | <0,0007 | 0,0025 |
| FW61400496 | F168 | As mg/l | 0,003655 | 0,001725 | 2 | 0,00193 | 0,00538 |
| FW61400506 | F168 | As mg/l | <0,0007 | 0,000298 | 44 | <0,0007 | 0,00126 |
| FW61400516 | F168 | As mg/l | <0,0007 | 0 | 2 | <0,0007 | <0,0007 |
| FW61400597 | F168 | As mg/l | <0,0007 | 0,000512 | 35 | <0,0007 | 0,0013 |
| FW61404547 | F168 | As mg/l | 0,00125 | 0,000531 | 12 | <0,0007 | 0,0017 |
| FW61404607 | F168 | As mg/l | 0,0105 | 0,007049 | 12 | <0,0007 | 0,023 |
| FW61404617 | F168 | As mg/l | 0,0013 | 0 | 1 | 0,0013 | 0,0013 |

### 1.4.2 S-Parameters

| GZÜV ID | Parameter ID | Parameter Name | Median | Standard deviation | Number of Measurements | Minimum value | Maximum Value |
|---|---|---|---|---|---|---|---|
| FW61400067 | S103 | As mg/kg DS < 40 µm | 14 | 8,627172 | 10 | 10,9 | 40 |
| FW61400077 | S103 | As mg/kg DS < 40 µm | 18 | 13,371372 | 9 | 11 | 56,1 |
| FW61400087 | S103 | As mg/kg DS < 40 µm | 9,28 | 7,700267 | 11 | 5 | 31,4 |
| FW61400097 | S103 | As mg/kg DS < 40 µm | 16 | 7,365162 | 10 | 6 | 25 |
| FW61400107 | S103 | As mg/kg DS < 40 µm | 11 | 8,396207 | 11 | 7 | 32,1 |
| FW61400117 | S103 | As mg/kg DS < 40 µm | 16 | 7,301026 | 9 | 7,9 | 27,5 |
| FW61400127 | S103 | As mg/kg DS < 40 µm | 18,5 | 11,862792 | 8 | 7,69 | 48 |
| FW61400137 | S103 | As mg/kg DS < 40 µm | 11,1 | 5,177654 | 10 | 6 | 19,3 |
| FW61400147 | S103 | As mg/kg DS < 40 µm | 12 | 5,846677 | 11 | 4,72 | 22 |
| FW61400157 | S103 | As mg/kg DS < 40 µm | 13 | 4,496246 | 10 | 3,64 | 18 |
| FW61400167 | S103 | As mg/kg DS < 40 µm | 16 | 6,258495 | 11 | 9,6 | 32,4 |
| FW61400177 | S103 | As mg/kg DS < 40 µm | 19,9 | 3,472391 | 8 | 15 | 25 |
| FW61400187 | S103 | As mg/kg DS < 40 µm | 26,45 | 14,985446 | 8 | 18 | 69 |
| FW61400197 | S103 | As mg/kg DS < 40 µm | 46 | 19,995839 | 9 | 16,8 | 88 |
| FW61400207 | S103 | As mg/kg DS < 40 µm | 22 | 8,933286 | 10 | 14 | 42 |
| FW61400217 | S103 | As mg/kg DS < 40 µm | 19,5 | 9,472254 | 10 | 11 | 44,4 |
| FW61400227 | S103 | As mg/kg DS < 40 µm | 9,65 | 2,74565 | 8 | 5 | 14 |
| FW61400237 | S103 | As mg/kg DS < 40 µm | 14,65 | 4,448999 | 8 | 8,6 | 22 |
| FW61400247 | S103 | As mg/kg DS < 40 µm | 9 | 2,230277 | 9 | 7 | 14 |
| FW61400257 | S103 | As mg/kg DS < 40 µm | 6,055 | 2,02627 | 10 | 5 | 10,5 |
| FW61400267 | S103 | As mg/kg DS < 40 µm | 6,65 | 2,68279 | 8 | 1,56 | 10,5 |
| FW61400277 | S103 | As mg/kg DS < 40 µm | 5,4 | 3,355104 | 10 | 2,3 | 12,8 |
| FW61400287 | S103 | As mg/kg DS < 40 µm | 7,7 | 9,209126 | 10 | 4 | 37,7 |
| FW61400476 | S103 | As mg/kg DS < 40 µm | 57,2 | 22,2 | 2 | 35 | 79,4 |
| FW61400486 | S103 | As mg/kg DS < 40 µm | 16,7 | 2,7 | 2 | 14 | 19,4 |
| FW61400496 | S103 | As mg/kg DS < 40 µm | 19 | 2 | 2 | 17 | 21 |
| FW61400506 | S103 | As mg/kg DS < 40 µm | 12,65 | 3,15 | 2 | 9,5 | 15,8 |
| FW61400516 | S103 | As mg/kg DS < 40 µm | 11,8 | 7 | 2 | 4,8 | 18,8 |

## 1.5 Cadmium

### 1.5.1 F-Parameters

| GZÜV ID | Parameter ID | Parameter Name | Median | Standard deviation | Number of Measurements | Minimum value | Maximum Value |
|---|---|---|---|---|---|---|---|
| FW61302327 | F152 | Cd mg/l | <0,0001 | 0 | 1 | <0,0001 | <0,0001 |
| FW61400067 | F152 | Cd mg/l | <0,0001 | 0,000047 | 107 | <0,0001 | 0,0003 |
| FW61400077 | F152 | Cd mg/l | <0,0001 | 0,000069 | 73 | <0,0001 | 0,0003 |
| FW61400087 | F152 | Cd mg/l | <0,0001 | 0,000051 | 107 | <0,0001 | 0,0003 |
| FW61400097 | F152 | Cd mg/l | <0,0001 | 0,000053 | 107 | <0,0001 | 0,00037 |
| FW61400107 | F152 | Cd mg/l | <0,0001 | 0,000058 | 108 | <0,0001 | 0,0004 |
| FW61400117 | F152 | Cd mg/l | <0,0001 | 0,00029 | 74 | <0,0001 | 0,0023 |
| FW61400127 | F152 | Cd mg/l | <0,0001 | 0,000091 | 131 | <0,0001 | 0,001 |
| FW61400137 | F152 | Cd mg/l | <0,0001 | 0,000073 | 264 | <0,0001 | 0,001 |
| FW61400147 | F152 | Cd mg/l | <0,0001 | 0,000032 | 144 | <0,0001 | 0,00022 |
| FW61400157 | F152 | Cd mg/l | <0,0001 | 0,000074 | 108 | <0,0001 | 0,00041 |
| FW61400167 | F152 | Cd mg/l | <0,0001 | 0,000031 | 120 | <0,0001 | 0,0002 |
| FW61400177 | F152 | Cd mg/l | <0,0001 | 0,000057 | 75 | <0,0001 | 0,0003 |
| FW61400187 | F152 | Cd mg/l | <0,0001 | 0,000357 | 87 | <0,0001 | 0,0031 |
| FW61400197 | F152 | Cd mg/l | <0,0001 | 0,000046 | 109 | <0,0001 | 0,0003 |
| FW61400207 | F152 | Cd mg/l | <0,0001 | 0 | 6 | <0,0001 | <0,0001 |
| FW61400217 | F152 | Cd mg/l | <0,0001 | 0,000186 | 137 | <0,0001 | 0,00192 |
| FW61400227 | F152 | Cd mg/l | <0,0001 | 0 | 5 | <0,0001 | <0,0001 |
| FW61400237 | F152 | Cd mg/l | <0,0001 | 0,000068 | 76 | <0,0001 | 0,0005 |
| FW61400247 | F152 | Cd mg/l | <0,0001 | 0,000145 | 75 | <0,0001 | 0,0012 |
| FW61400257 | F152 | Cd mg/l | <0,0001 | 0 | 6 | <0,0001 | <0,0001 |
| FW61400267 | F152 | Cd mg/l | <0,0001 | 0,000092 | 145 | <0,0001 | 0,0011 |
| FW61400277 | F152 | Cd mg/l | <0,0001 | 0 | 6 | <0,0001 | <0,0001 |
| FW61400287 | F152 | Cd mg/l | <0,0001 | 0,000116 | 141 | <0,0001 | 0,0012 |
| FW61400476 | F152 | Cd mg/l | <0,0001 | 0,000042 | 44 | <0,0001 | 0,00028 |
| FW61400486 | F152 | Cd mg/l | <0,0001 | 0,000033 | 44 | <0,0001 | 0,00022 |
| FW61400496 | F152 | Cd mg/l | <0,0001 | 0 | 2 | <0,0001 | <0,0001 |
| FW61400506 | F152 | Cd mg/l | <0,0001 | 0,000039 | 44 | <0,0001 | 0,00026 |
| FW61400516 | F152 | Cd mg/l | <0,0001 | 0 | 2 | <0,0001 | <0,0001 |
| FW61400597 | F152 | Cd mg/l | <0,0001 | 0 | 35 | <0,0001 | <0,0001 |
| FW61404547 | F152 | Cd mg/l | <0,0001 | 0 | 12 | <0,0001 | <0,0001 |
| FW61404607 | F152 | Cd mg/l | <0,0001 | 0 | 2 | <0,0001 | <0,0001 |
| FW61404617 | F152 | Cd mg/l | <0,0001 | 0 | 1 | <0,0001 | <0,0001 |

### 1.5.2 S-Parameters

| GZÜV ID | Parameter ID | Parameter Name | Median | Standard deviation | Number of Measurements | Minimum value | Maximum Value |
|---|---|---|---|---|---|---|---|
| FW61400067 | S105 | Cd mg/kg dS < 40 µm | 0,2 | 0,847991 | 10 | <0,05 | 3 |
| FW61400077 | S105 | Cd mg/kg dS < 40 µm | 0,2 | 0,776555 | 9 | <0,05 | 2,6 |
| FW61400087 | S105 | Cd mg/kg dS < 40 µm | 0,2 | 0,8305 | 11 | <0,05 | 2,9 |
| FW61400097 | S105 | Cd mg/kg dS < 40 µm | 0,6125 | 1,104032 | 10 | <0,05 | 2,9 |
| FW61400107 | S105 | Cd mg/kg dS < 40 µm | 0,2 | 1,210278 | 11 | <0,05 | 3,9 |
| FW61400117 | S105 | Cd mg/kg dS < 40 µm | 0,784 | 1,151052 | 9 | 0,24 | 4,2 |
| FW61400127 | S105 | Cd mg/kg dS < 40 µm | 0,8315 | 1,00537 | 8 | <0,05 | 3,4 |
| FW61400137 | S105 | Cd mg/kg dS < 40 µm | 0,275 | 0,728853 | 10 | <0,05 | 2,6 |
| FW61400147 | S105 | Cd mg/kg dS < 40 µm | 0,3 | 0,71828 | 11 | <0,05 | 2,4 |
| FW61400157 | S105 | Cd mg/kg dS < 40 µm | 0,3315 | 0,971514 | 10 | <0,05 | 2,9 |
| FW61400167 | S105 | Cd mg/kg dS < 40 µm | 0,2 | 0,529532 | 11 | <0,05 | 1,9 |
| FW61400177 | S105 | Cd mg/kg dS < 40 µm | 0,485 | 0,873465 | 8 | 0,145 | 2,9 |
| FW61400187 | S105 | Cd mg/kg dS < 40 µm | 10,04 | 23,763387 | 8 | 0,5 | 75,1 |
| FW61400197 | S105 | Cd mg/kg dS < 40 µm | 0,4 | 0,95354 | 9 | <0,05 | 3,3 |
| FW61400207 | S105 | Cd mg/kg dS < 40 µm | 0,366 | 0,934011 | 10 | <0,05 | 3,2 |
| FW61400217 | S105 | Cd mg/kg dS < 40 µm | 0,433 | 1,09186 | 10 | <0,05 | 3,8 |
| FW61400227 | S105 | Cd mg/kg dS < 40 µm | 0,5675 | 1,209641 | 8 | 0,3 | 4,2 |
| FW61400237 | S105 | Cd mg/kg dS < 40 µm | 0,555 | 1,464031 | 8 | <0,05 | 4,6 |
| FW61400247 | S105 | Cd mg/kg dS < 40 µm | 0,5 | 1,203311 | 9 | 0,15 | 4,2 |
| FW61400257 | S105 | Cd mg/kg dS < 40 µm | 0,3135 | 0,634225 | 10 | <0,05 | 2 |
| FW61400267 | S105 | Cd mg/kg dS < 40 µm | 0,25 | 0,1622 | 8 | <0,05 | 0,5 |
| FW61400277 | S105 | Cd mg/kg dS < 40 µm | 0,343 | 0,547786 | 10 | <0,05 | 1,9 |
| FW61400287 | S105 | Cd mg/kg dS < 40 µm | 0,339 | 0,489862 | 10 | <0,05 | 1,7 |
| FW61400476 | S105 | Cd mg/kg dS < 40 µm | <0,05 | <0,05 | 2 | <0,05 | <0,05 |
| FW61400486 | S105 | Cd mg/kg dS < 40 µm | 0,092 | 0,092 | 2 | <0,05 | 0,184 |
| FW61400496 | S105 | Cd mg/kg dS < 40 µm | 0,0445 | 0,0445 | 2 | <0,05 | 0,089 |
| FW61400506 | S105 | Cd mg/kg dS < 40 µm | 0,0735 | 0,0735 | 2 | <0,05 | 0,147 |
| FW61400516 | S105 | Cd mg/kg dS < 40 µm | 0,138 | 0,138 | 2 | <0,05 | 0,276 |

## 1.6 Chrome

### 1.6.1 F-Parameters

| GZÜV ID | Parameter ID | Parameter Name | Median | Standard deviation | Number of Measurements | Minimum value | Maximum Value |
|---|---|---|---|---|---|---|---|
| FW61302327 | F164 | Cr mg/l | <0,001 | 0 | 1 | <0,001 | <0,001 |
| FW61400067 | F164 | Cr mg/l | <0,001 | 0 | 99 | <0,001 | <0,001 |
| FW61400077 | F164 | Cr mg/l | <0,001 | 0,000332 | 65 | <0,001 | 0,0027 |
| FW61400087 | F164 | Cr mg/l | <0,001 | 0,00049 | 99 | <0,001 | 0,0049 |
| FW61400097 | F164 | Cr mg/l | <0,001 | 0,00025 | 99 | <0,001 | 0,0022 |
| FW61400107 | F164 | Cr mg/l | <0,001 | 0,000371 | 100 | <0,001 | 0,0027 |
| FW61400117 | F164 | Cr mg/l | <0,001 | 0,000581 | 66 | <0,001 | 0,0043 |
| FW61400127 | F164 | Cr mg/l | <0,001 | 0,000437 | 123 | <0,001 | 0,0033 |
| FW61400137 | F164 | Cr mg/l | <0,001 | 0,000584 | 256 | <0,001 | 0,0068 |
| FW61400147 | F164 | Cr mg/l | <0,001 | 0,000379 | 136 | <0,001 | 0,0029 |
| FW61400157 | F164 | Cr mg/l | <0,001 | 0,000629 | 100 | <0,001 | 0,0058 |
| FW61400167 | F164 | Cr mg/l | <0,001 | 0,000232 | 112 | <0,001 | 0,0018 |
| FW61400177 | F164 | Cr mg/l | <0,001 | 0,000243 | 67 | <0,001 | 0,002 |
| FW61400187 | F164 | Cr mg/l | <0,001 | 0,000525 | 79 | <0,001 | 0,0036 |
| FW61400197 | F164 | Cr mg/l | <0,001 | 0,000386 | 101 | <0,001 | 0,003 |
| FW61400207 | F164 | Cr mg/l | <0,001 | 0,003651 | 6 | <0,001 | 0,01 |
| FW61400217 | F164 | Cr mg/l | <0,001 | 0,000365 | 136 | <0,001 | 0,0022 |
| FW61400227 | F164 | Cr mg/l | <0,001 | 0 | 5 | <0,001 | <0,001 |
| FW61400237 | F164 | Cr mg/l | <0,001 | 0,00058 | 68 | <0,001 | 0,003 |
| FW61400247 | F164 | Cr mg/l | <0,001 | 0,000401 | 67 | <0,001 | 0,0028 |
| FW61400257 | F164 | Cr mg/l | <0,001 | 0 | 6 | <0,001 | <0,001 |
| FW61400267 | F164 | Cr mg/l | <0,001 | 0,000323 | 137 | <0,001 | 0,0034 |
| FW61400277 | F164 | Cr mg/l | <0,001 | 0 | 6 | <0,001 | <0,001 |
| FW61400287 | F164 | Cr mg/l | <0,001 | 0,000215 | 133 | <0,001 | 0,0019 |
| FW61400476 | F164 | Cr mg/l | <0,001 | 0 | 44 | <0,001 | <0,001 |
| FW61400486 | F164 | Cr mg/l | <0,001 | 0 | 44 | <0,001 | <0,001 |
| FW61400496 | F164 | Cr mg/l | <0,001 | 0 | 2 | <0,001 | <0,001 |
| FW61400506 | F164 | Cr mg/l | <0,001 | 0 | 44 | <0,001 | <0,001 |
| FW61400516 | F164 | Cr mg/l | <0,001 | 0 | 2 | <0,001 | <0,001 |
| FW61400597 | F164 | Cr mg/l | <0,001 | 0 | 35 | <0,001 | <0,001 |
| FW61404547 | F164 | Cr mg/l | <0,001 | 0,000304 | 12 | <0,001 | 0,0011 |
| FW61404607 | F164 | Cr mg/l | <0,001 | 0 | 2 | <0,001 | <0,001 |
| FW61404617 | F164 | Cr mg/l | <0,001 | 0 | 1 | <0,001 | <0,001 |

### 1.6.2 S-Parameters

| GZÜV ID | Parameter ID | Parameter Name | Median | Standard deviation | Number of Measurements | Minimum value | Maximum Value |
|---|---|---|---|---|---|---|---|
| FW61400067 | S106 | Cr mg/kg DS < 40 µm | 40,5 | 17,350896 | 10 | 26 | 80,9 |
| FW61400077 | S106 | Cr mg/kg DS < 40 µm | 50,8 | 17,353158 | 9 | 27 | 75,7 |
| FW61400087 | S106 | Cr mg/kg DS < 40 µm | 47 | 21,201205 | 11 | 24 | 91,3 |
| FW61400097 | S106 | Cr mg/kg DS < 40 µm | 58,5 | 30,824213 | 10 | 33 | 121 |
| FW61400107 | S106 | Cr mg/kg DS < 40 µm | 58,3 | 45,95482 | 11 | 30 | 153 |
| FW61400117 | S106 | Cr mg/kg DS < 40 µm | 57 | 33,444348 | 9 | 41 | 139 |
| FW61400127 | S106 | Cr mg/kg DS < 40 µm | 60,5 | 25,44984 | 8 | 37 | 120 |
| FW61400137 | S106 | Cr mg/kg DS < 40 µm | 44,5 | 46,415704 | 10 | 30 | 187 |
| FW61400147 | S106 | Cr mg/kg DS < 40 µm | 45 | 26,515534 | 11 | 29 | 122 |
| FW61400157 | S106 | Cr mg/kg DS < 40 µm | 51,5 | 24,995762 | 10 | 31 | 101 |
| FW61400167 | S106 | Cr mg/kg DS < 40 µm | 26 | 19,523662 | 11 | 20 | 82,3 |
| FW61400177 | S106 | Cr mg/kg DS < 40 µm | 34 | 11,289818 | 8 | 24 | 54 |
| FW61400187 | S106 | Cr mg/kg DS < 40 µm | 73 | 55,420974 | 8 | 30 | 194 |
| FW61400197 | S106 | Cr mg/kg DS < 40 µm | 60 | 36,45088 | 9 | 20 | 124 |
| FW61400207 | S106 | Cr mg/kg DS < 40 µm | 63 | 33,875472 | 10 | 28 | 130 |
| FW61400217 | S106 | Cr mg/kg DS < 40 µm | 160 | 91,958088 | 10 | 57 | 381 |
| FW61400227 | S106 | Cr mg/kg DS < 40 µm | 29,5 | 17,317075 | 8 | 5 | 55,8 |
| FW61400237 | S106 | Cr mg/kg DS < 40 µm | 1650 | 1448,87223 | 8 | 270 | 4400 |
| FW61400247 | S106 | Cr mg/kg DS < 40 µm | 41 | 15,290698 | 9 | 28 | 72 |
| FW61400257 | S106 | Cr mg/kg DS < 40 µm | 32,5 | 14,676515 | 10 | 26 | 71,2 |
| FW61400267 | S106 | Cr mg/kg DS < 40 µm | 34,55 | 18,565724 | 8 | 25 | 76,3 |
| FW61400277 | S106 | Cr mg/kg DS < 40 µm | 44,95 | 19,009022 | 10 | 20 | 82,3 |
| FW61400287 | S106 | Cr mg/kg DS < 40 µm | 49 | 24,266324 | 10 | 29 | 119 |
| FW61400476 | S106 | Cr mg/kg DS < 40 µm | 45,55 | 18,55 | 2 | 27 | 64,1 |
| FW61400486 | S106 | Cr mg/kg DS < 40 µm | 50,3 | 13,3 | 2 | 37 | 63,6 |
| FW61400496 | S106 | Cr mg/kg DS < 40 µm | 56,35 | 13,35 | 2 | 43 | 69,7 |
| FW61400506 | S106 | Cr mg/kg DS < 40 µm | 81,5 | 43,5 | 2 | 38 | 125 |
| FW61400516 | S106 | Cr mg/kg DS < 40 µm | 56,2 | 30,2 | 2 | 26 | 86,4 |

## 1.7 Copper

### 1.7.1 F-Parameters

| GZÜV ID | Parameter ID | Parameter Name | Median | Standard deviation | Number of Measurements | Minimum value | Maximum Value |
|---|---|---|---|---|---|---|---|
| FW61302327 | F158 | Cu mg/l | <0,001 | 0 | 1 | <0,001 | <0,001 |
| FW61400067 | F158 | Cu mg/l | <0,001 | 0,000855 | 99 | <0,001 | 0,005 |
| FW61400077 | F158 | Cu mg/l | <0,001 | 0,001873 | 65 | <0,001 | 0,013 |
| FW61400087 | F158 | Cu mg/l | <0,001 | 0,001691 | 99 | <0,001 | 0,013 |
| FW61400097 | F158 | Cu mg/l | <0,001 | 0,003889 | 99 | <0,001 | 0,031 |
| FW61400107 | F158 | Cu mg/l | <0,001 | 0,002923 | 100 | <0,001 | 0,024 |
| FW61400117 | F158 | Cu mg/l | 0,001 | 0,001965 | 66 | <0,001 | 0,014 |
| FW61400127 | F158 | Cu mg/l | 0,001 | 0,001236 | 123 | <0,001 | 0,0067 |
| FW61400137 | F158 | Cu mg/l | 0,001 | 0,002153 | 256 | <0,001 | 0,028 |
| FW61400147 | F158 | Cu mg/l | 0,001 | 0,001759 | 136 | <0,001 | 0,015 |
| FW61400157 | F158 | Cu mg/l | <0,001 | 0,001809 | 100 | <0,001 | 0,016 |
| FW61400167 | F158 | Cu mg/l | <0,001 | 0,001658 | 112 | <0,001 | 0,014 |
| FW61400177 | F158 | Cu mg/l | <0,001 | 0,002444 | 67 | <0,001 | 0,0139 |
| FW61400187 | F158 | Cu mg/l | 0,00195 | 0,003073 | 79 | <0,001 | 0,02 |
| FW61400197 | F158 | Cu mg/l | <0,001 | 0,001781 | 101 | <0,001 | 0,014 |
| FW61400207 | F158 | Cu mg/l | 0,00215 | 0,001449 | 6 | <0,001 | 0,004 |
| FW61400217 | F158 | Cu mg/l | 0,001 | 0,002125 | 136 | <0,001 | 0,017 |
| FW61400227 | F158 | Cu mg/l | 0,001 | 0,00259 | 5 | <0,001 | 0,006 |
| FW61400237 | F158 | Cu mg/l | 0,002 | 0,002599 | 68 | <0,001 | 0,016 |
| FW61400247 | F158 | Cu mg/l | 0,003 | 0,003769 | 67 | <0,001 | 0,023 |
| FW61400257 | F158 | Cu mg/l | <0,001 | 0,001118 | 6 | <0,001 | 0,003 |
| FW61400267 | F158 | Cu mg/l | <0,001 | 0,001113 | 137 | <0,001 | 0,006 |
| FW61400277 | F158 | Cu mg/l | <0,001 | 0,002192 | 6 | <0,001 | 0,006 |
| FW61400287 | F158 | Cu mg/l | <0,001 | 0,001159 | 133 | <0,001 | 0,0054 |
| FW61400476 | F158 | Cu mg/l | <0,001 | 0,000149 | 44 | <0,001 | 0,001 |
| FW61400486 | F158 | Cu mg/l | 0,001 | 0,001083 | 44 | <0,001 | 0,0034 |
| FW61400496 | F158 | Cu mg/l | 0,0011 | 0,0001 | 2 | 0,001 | 0,0012 |
| FW61400506 | F158 | Cu mg/l | 0,001 | 0,001115 | 44 | <0,001 | 0,006 |
| FW61400516 | F158 | Cu mg/l | 0,00155 | 0,00045 | 2 | 0,0011 | 0,002 |
| FW61400597 | F158 | Cu mg/l | <0,001 | 0,000942 | 35 | <0,001 | 0,004 |
| FW61403646 | F158 | Cu mg/l | <0,001 | 0,00066 | 3 | <0,001 | 0,0014 |
| FW61403656 | F158 | Cu mg/l | <0,001 | 0 | 3 | <0,001 | <0,001 |
| FW61403666 | F158 | Cu mg/l | <0,001 | 0 | 3 | <0,001 | <0,001 |
| FW61403676 | F158 | Cu mg/l | <0,001 | 0,000519 | 3 | <0,001 | 0,0011 |
| FW61403686 | F158 | Cu mg/l | <0,001 | 0,013576 | 3 | <0,001 | 0,0288 |
| FW61403696 | F158 | Cu mg/l | <0,001 | 0,003488 | 3 | <0,001 | 0,0074 |
| FW61404547 | F158 | Cu mg/l | <0,001 | 0,000614 | 12 | <0,001 | 0,0016 |
| FW61404607 | F158 | Cu mg/l | <0,001 | 0 | 2 | <0,001 | <0,001 |
| FW61404617 | F158 | Cu mg/l | 0,0012 | 0 | 1 | 0,0012 | 0,0012 |

### 1.7.2 S-Parameters

| GZÜV ID | Parameter ID | Parameter Name | Median | Standard deviation | Number of Measurements | Minimum value | Maximum Value |
|---|---|---|---|---|---|---|---|
| FW61400067 | S107 | Cu mg/kg DS < 40 µm | 23,5 | 23,864428 | 10 | 17 | 79,5 |
| FW61400077 | S107 | Cu mg/kg DS < 40 µm | 42 | 25,720022 | 9 | 16 | 85,4 |
| FW61400087 | S107 | Cu mg/kg DS < 40 µm | 36,8 | 23,654262 | 11 | 15 | 85,3 |
| FW61400097 | S107 | Cu mg/kg DS < 40 µm | 42 | 31,646839 | 10 | 14 | 91,4 |
| FW61400107 | S107 | Cu mg/kg DS < 40 µm | 36 | 37,261349 | 11 | 19 | 119 |
| FW61400117 | S107 | Cu mg/kg DS < 40 µm | 42 | 24,531723 | 9 | 25,6 | 98 |
| FW61400127 | S107 | Cu mg/kg DS < 40 µm | 53 | 33,637479 | 8 | 27 | 137 |
| FW61400137 | S107 | Cu mg/kg DS < 40 µm | 23,75 | 23,80212 | 10 | 17 | 85,8 |
| FW61400147 | S107 | Cu mg/kg DS < 40 µm | 27 | 20,796944 | 11 | 13 | 72,3 |
| FW61400157 | S107 | Cu mg/kg DS < 40 µm | 44,75 | 29,806174 | 10 | 22 | 100 |
| FW61400167 | S107 | Cu mg/kg DS < 40 µm | 48 | 30,282791 | 11 | 27 | 109 |
| FW61400177 | S107 | Cu mg/kg DS < 40 µm | 46,4 | 13,816453 | 8 | 25 | 68,2 |
| FW61400187 | S107 | Cu mg/kg DS < 40 µm | 70,8 | 92,936749 | 8 | 32 | 328 |
| FW61400197 | S107 | Cu mg/kg DS < 40 µm | 38,8 | 10,717379 | 9 | 20 | 54 |
| FW61400207 | S107 | Cu mg/kg DS < 40 µm | 39,7 | 15,043833 | 10 | 13 | 56 |
| FW61400217 | S107 | Cu mg/kg DS < 40 µm | 58,7 | 23,648951 | 10 | 20 | 91 |
| FW61400227 | S107 | Cu mg/kg DS < 40 µm | 37,95 | 25,549413 | 8 | 7 | 80 |
| FW61400237 | S107 | Cu mg/kg DS < 40 µm | 250 | 227,31586 | 8 | 74 | 760 |
| FW61400247 | S107 | Cu mg/kg DS < 40 µm | 48 | 42,699183 | 9 | 25 | 140 |
| FW61400257 | S107 | Cu mg/kg DS < 40 µm | 31,5 | 22,985537 | 10 | 17 | 92,3 |
| FW61400267 | S107 | Cu mg/kg DS < 40 µm | 29 | 31,042149 | 8 | 17,2 | 92,3 |
| FW61400277 | S107 | Cu mg/kg DS < 40 µm | 35 | 17,073784 | 10 | 12 | 76,3 |
| FW61400287 | S107 | Cu mg/kg DS < 40 µm | 40 | 15,264275 | 10 | 15 | 69,5 |
| FW61400476 | S107 | Cu mg/kg DS < 40 µm | 43,25 | 14,25 | 2 | 29 | 57,5 |
| FW61400486 | S107 | Cu mg/kg DS < 40 µm | 30,45 | 4,45 | 2 | 26 | 34,9 |
| FW61400496 | S107 | Cu mg/kg DS < 40 µm | 34,6 | 1,6 | 2 | 33 | 36,2 |
| FW61400506 | S107 | Cu mg/kg DS < 40 µm | 28,35 | 10,35 | 2 | 18 | 38,7 |
| FW61400516 | S107 | Cu mg/kg DS < 40 µm | 43 | 27 | 2 | 16 | 70 |

## 1.8 Mercury

### 1.8.1 F-Parameters

| GZÜV ID | Parameter ID | Parameter Name | Median | Standard deviation | Number of Measurements | Minimum value | Maximum Value |
|---|---|---|---|---|---|---|---|
| FW61302327 | F154 | Hg mg/l | <0,0001 | 0 | 1 | <0,0001 | <0,0001 |
| FW61400067 | F154 | Hg mg/l | <0,0001 | 0 | 99 | <0,0001 | <0,0001 |
| FW61400077 | F154 | Hg mg/l | <0,0001 | 0 | 65 | <0,0001 | <0,0001 |
| FW61400087 | F154 | Hg mg/l | <0,0001 | 0 | 99 | <0,0001 | <0,0001 |
| FW61400097 | F154 | Hg mg/l | <0,0001 | 0,000024 | 108 | <0,0001 | 0,00025 |
| FW61400107 | F154 | Hg mg/l | <0,0001 | 0 | 100 | <0,0001 | <0,0001 |
| FW61400117 | F154 | Hg mg/l | <0,0001 | 0 | 66 | <0,0001 | <0,0001 |
| FW61400127 | F154 | Hg mg/l | <0,0001 | 0 | 123 | <0,0001 | <0,0001 |
| FW61400137 | F154 | Hg mg/l | <0,0001 | 0,000012 | 256 | <0,0001 | 0,0002 |
| FW61400147 | F154 | Hg mg/l | <0,0001 | 0,000017 | 136 | <0,0001 | 0,0002 |
| FW61400157 | F154 | Hg mg/l | <0,0001 | 0 | 100 | <0,0001 | <0,0001 |
| FW61400167 | F154 | Hg mg/l | <0,0001 | 0 | 112 | <0,0001 | <0,0001 |
| FW61400177 | F154 | Hg mg/l | <0,0001 | 0 | 67 | <0,0001 | <0,0001 |
| FW61400187 | F154 | Hg mg/l | <0,0001 | 0,000034 | 79 | <0,0001 | 0,00028 |
| FW61400197 | F154 | Hg mg/l | <0,0001 | 0 | 101 | <0,0001 | <0,0001 |
| FW61400207 | F154 | Hg mg/l | <0,0001 | 0 | 6 | <0,0001 | <0,0001 |
| FW61400217 | F154 | Hg mg/l | <0,0001 | 0 | 136 | <0,0001 | <0,0001 |
| FW61400227 | F154 | Hg mg/l | <0,0001 | 0 | 5 | <0,0001 | <0,0001 |
| FW61400237 | F154 | Hg mg/l | <0,0001 | 0 | 67 | <0,0001 | <0,0001 |
| FW61400247 | F154 | Hg mg/l | <0,0001 | 0 | 67 | <0,0001 | <0,0001 |
| FW61400257 | F154 | Hg mg/l | <0,0001 | 0 | 6 | <0,0001 | <0,0001 |
| FW61400267 | F154 | Hg mg/l | <0,0001 | 0 | 137 | <0,0001 | <0,0001 |
| FW61400277 | F154 | Hg mg/l | <0,0001 | 0 | 6 | <0,0001 | <0,0001 |
| FW61400287 | F154 | Hg mg/l | <0,0001 | 0,000071 | 133 | <0,0001 | 0,0004 |
| FW61400476 | F154 | Hg mg/l | <0,0001 | 0 | 44 | <0,0001 | <0,0001 |
| FW61400486 | F154 | Hg mg/l | <0,0001 | 0 | 44 | <0,0001 | <0,0001 |
| FW61400496 | F154 | Hg mg/l | <0,0001 | 0 | 2 | <0,0001 | <0,0001 |
| FW61400506 | F154 | Hg mg/l | <0,0001 | 0 | 44 | <0,0001 | <0,0001 |
| FW61400516 | F154 | Hg mg/l | <0,0001 | 0 | 2 | <0,0001 | <0,0001 |
| FW61400597 | F154 | Hg mg/l | <0,0001 | 0 | 35 | <0,0001 | <0,0001 |
| FW61404547 | F154 | Hg mg/l | <0,0001 | 0 | 12 | <0,0001 | <0,0001 |
| FW61404607 | F154 | Hg mg/l | <0,0001 | 0 | 2 | <0,0001 | <0,0001 |
| FW61404617 | F154 | Hg mg/l | <0,0001 | 0 | 1 | <0,0001 | <0,0001 |

### 1.8.2 S-Parameters

| GZÜV ID | Parameter ID | Parameter Name | Median | Standard deviation | Number of Measurements | Minimum value | Maximum Value |
|---|---|---|---|---|---|---|---|
| FW61400067 | S109 | Hg mg/kg DS <40µm | 0,077 | 0,12638 | 10 | 0 | 0,422 |
| FW61400077 | S109 | Hg mg/kg DS <40µm | 0,14 | 0,083044 | 9 | 0,025 | 0,301 |
| FW61400087 | S109 | Hg mg/kg DS <40µm | 0,09 | 0,104284 | 11 | 0 | 0,339 |
| FW61400097 | S109 | Hg mg/kg DS <40µm | 0,2655 | 0,296133 | 10 | 0 | 0,84 |
| FW61400107 | S109 | Hg mg/kg DS <40µm | 0,37 | 0,312455 | 11 | 0,067 | 1,1 |
| FW61400117 | S109 | Hg mg/kg DS <40µm | 0,35 | 0,16001 | 9 | 0,13 | 0,68 |
| FW61400127 | S109 | Hg mg/kg DS <40µm | 0,36 | 0,339165 | 8 | 0,139 | 1,09 |
| FW61400137 | S109 | Hg mg/kg DS <40µm | 0,219 | 0,155474 | 10 | 0,05 | 0,597 |
| FW61400147 | S109 | Hg mg/kg DS <40µm | 0,15 | 0,493626 | 11 | 0 | 1,8 |
| FW61400157 | S109 | Hg mg/kg DS <40µm | 0,261 | 0,15533 | 10 | 0 | 0,457 |
| FW61400167 | S109 | Hg mg/kg DS <40µm | 0,17 | 0,158124 | 11 | 0 | 0,497 |
| FW61400177 | S109 | Hg mg/kg DS <40µm | 0,552 | 0,208774 | 8 | 0,18 | 0,738 |
| FW61400187 | S109 | Hg mg/kg DS <40µm | 1,97 | 3,900929 | 8 | 0,85 | 10,8 |
| FW61400197 | S109 | Hg mg/kg DS <40µm | 0,13 | 0,097747 | 9 | 0,06 | 0,39 |
| FW61400207 | S109 | Hg mg/kg DS <40µm | 0,1835 | 0,10622 | 10 | 0 | 0,29 |
| FW61400217 | S109 | Hg mg/kg DS <40µm | 0,18 | 0,122635 | 10 | 0,076 | 0,489 |
| FW61400227 | S109 | Hg mg/kg DS <40µm | 0,555 | 0,413945 | 8 | 0,092 | 1,5 |
| FW61400237 | S109 | Hg mg/kg DS <40µm | 0,367 | 0,204279 | 8 | 0 | 0,69 |
| FW61400247 | S109 | Hg mg/kg DS <40µm | 0,21 | 0,257308 | 9 | 0,14 | 0,99 |
| FW61400257 | S109 | Hg mg/kg DS <40µm | 0,168 | 0,126782 | 10 | 0 | 0,461 |
| FW61400267 | S109 | Hg mg/kg DS <40µm | 0,123 | 0,190926 | 8 | 0 | 0,63 |
| FW61400277 | S109 | Hg mg/kg DS <40µm | 0,134 | 0,112979 | 10 | 0 | 0,431 |
| FW61400287 | S109 | Hg mg/kg DS <40µm | 0,13 | 0,039347 | 10 | 0,042 | 0,18 |
| FW61400476 | S109 | Hg mg/kg DS <40µm | 0,078 | 0,078 | 2 | 0 | 0,156 |
| FW61400486 | S109 | Hg mg/kg DS <40µm | 0,066 | 0,066 | 2 | 0 | 0,132 |
| FW61400496 | S109 | Hg mg/kg DS <40µm | 0,0575 | 0,0575 | 2 | 0 | 0,115 |
| FW61400506 | S109 | Hg mg/kg DS <40µm | 0,056 | 0,056 | 2 | 0 | 0,112 |
| FW61400516 | S109 | Hg mg/kg DS <40µm | 0,1105 | 0,1105 | 2 | 0 | 0,221 |

## 1.9 Nickel

### 1.9.1 F-Parameters

| GZÜV ID | Parameter ID | Parameter Name | Median | Standard deviation | Number of Measurements | Minimum value | Maximum Value |
|---|---|---|---|---|---|---|---|
| FW61302327 | F166 | Ni mg/l | <0,001 | 0 | 1 | <0,001 | <0,001 |
| FW61400067 | F166 | Ni mg/l | <0,001 | 0,000419 | 99 | <0,001 | 0,0022 |
| FW61400077 | F166 | Ni mg/l | <0,001 | 0,000225 | 65 | <0,001 | 0,0012 |
| FW61400087 | F166 | Ni mg/l | <0,001 | 0,000219 | 99 | <0,001 | 0,001 |
| FW61400097 | F166 | Ni mg/l | <0,001 | 0,000487 | 99 | <0,001 | 0,003 |
| FW61400107 | F166 | Ni mg/l | <0,001 | 0,000714 | 100 | <0,001 | 0,0034 |
| FW61400117 | F166 | Ni mg/l | <0,001 | 0,000758 | 66 | <0,001 | 0,0036 |
| FW61400127 | F166 | Ni mg/l | <0,001 | 0,000876 | 123 | <0,001 | 0,0037 |
| FW61400137 | F166 | Ni mg/l | <0,001 | 0,000865 | 256 | <0,001 | 0,0078 |
| FW61400147 | F166 | Ni mg/l | 0,001 | 0,000825 | 136 | <0,001 | 0,003 |
| FW61400157 | F166 | Ni mg/l | <0,001 | 0,000605 | 100 | <0,001 | 0,0035 |
| FW61400167 | F166 | Ni mg/l | <0,001 | 0,000213 | 112 | <0,001 | 0,0015 |
| FW61400177 | F166 | Ni mg/l | <0,001 | 0 | 67 | <0,001 | <0,001 |
| FW61400187 | F166 | Ni mg/l | 0,002 | 0,001434 | 79 | <0,001 | 0,008 |
| FW61400197 | F166 | Ni mg/l | <0,001 | 0,000819 | 101 | <0,001 | 0,0052 |
| FW61400207 | F166 | Ni mg/l | <0,001 | 0,012378 | 6 | <0,001 | 0,033 |
| FW61400217 | F166 | Ni mg/l | 0,001 | 0,001961 | 136 | <0,001 | 0,016 |
| FW61400227 | F166 | Ni mg/l | <0,001 | 0 | 5 | <0,001 | <0,001 |
| FW61400237 | F166 | Ni mg/l | 0,001 | 0,000948 | 68 | <0,001 | 0,0041 |
| FW61400247 | F166 | Ni mg/l | <0,001 | 0,000369 | 67 | <0,001 | 0,0013 |
| FW61400257 | F166 | Ni mg/l | <0,001 | 0,000789 | 6 | <0,001 | 0,002 |
| FW61400267 | F166 | Ni mg/l | <0,001 | 0,000329 | 137 | <0,001 | 0,0015 |
| FW61400277 | F166 | Ni mg/l | <0,001 | 0,00041 | 6 | <0,001 | 0,0011 |
| FW61400287 | F166 | Ni mg/l | <0,001 | <0,00155 | 133 | <0,001 | 0,0025 |
| FW61400476 | F166 | Ni mg/l | <0,001 | 0,000492 | 44 | <0,001 | 0,0033 |
| FW61400486 | F166 | Ni mg/l | <0,001 | 0,000748 | 44 | <0,001 | 0,0025 |
| FW61400496 | F166 | Ni mg/l | 0,0012 | 0,0002 | 2 | 0,001 | 0,0014 |
| FW61400506 | F166 | Ni mg/l | 0,0018 | 0,000686 | 44 | 0,001 | 0,004 |
| FW61400516 | F166 | Ni mg/l | 0,0017 | 0,0003 | 2 | 0,0014 | 0,002 |
| FW61400597 | F166 | Ni mg/l | <0,001 | 0,000292 | 35 | <0,001 | 0,0014 |
| FW61404547 | F166 | Ni mg/l | <0,001 | 0 | 12 | <0,001 | <0,001 |
| FW61404607 | F166 | Ni mg/l | <0,001 | 0 | 2 | <0,001 | <0,001 |
| FW61404617 | F166 | Ni mg/l | <0,001 | 0 | 1 | <0,001 | <0,001 |

### 1.9.2 S-Parameters

| GZÜV ID | Parameter ID | Parameter Name | Median | Standard deviation | Number of Measurements | Minimum value | Maximum Value |
|---|---|---|---|---|---|---|---|
| FW61400067 | S108 | Ni mg/kg DS < 40 µm | 28,5 | 19,817066 | 10 | 21 | 70,8 |
| FW61400077 | S108 | Ni mg/kg DS < 40 µm | 48 | 16,67938 | 9 | 21 | 63,9 |
| FW61400087 | S108 | Ni mg/kg DS < 40 µm | 36,8 | 23,654262 | 11 | 15 | 85,3 |
| FW61400097 | S108 | Ni mg/kg DS < 40 µm | 59 | 38,926804 | 10 | 30,7 | 138 |
| FW61400107 | S108 | Ni mg/kg DS < 40 µm | 52 | 57,660484 | 11 | 34 | 225 |
| FW61400117 | S108 | Ni mg/kg DS < 40 µm | 50 | 26,626766 | 9 | 35,9 | 114 |
| FW61400127 | S108 | Ni mg/kg DS < 40 µm | 53,5 | 20,772454 | 8 | 37 | 98,6 |
| FW61400137 | S108 | Ni mg/kg DS < 40 µm | 33,5 | 43,688242 | 10 | 24 | 171 |
| FW61400147 | S108 | Ni mg/kg DS < 40 µm | 41 | 20,464264 | 11 | 19 | 85,7 |
| FW61400157 | S108 | Ni mg/kg DS < 40 µm | 47,5 | 23,250482 | 10 | 26 | 84,6 |
| FW61400167 | S108 | Ni mg/kg DS < 40 µm | 44,4 | 56,757043 | 11 | 24 | 208 |
| FW61400177 | S108 | Ni mg/kg DS < 40 µm | 84,85 | 28,721679 | 8 | 56 | 150 |
| FW61400187 | S108 | Ni mg/kg DS < 40 µm | 82 | 146,699044 | 8 | 60 | 520 |
| FW61400197 | S108 | Ni mg/kg DS < 40 µm | 43 | 21,470497 | 9 | 17 | 96 |
| FW61400207 | S108 | Ni mg/kg DS < 40 µm | 39,6 | 18,175547 | 10 | 21 | 81 |
| FW61400217 | S108 | Ni mg/kg DS < 40 µm | 108,5 | 129,593557 | 10 | 34 | 454 |
| FW61400227 | S108 | Ni mg/kg DS < 40 µm | 36 | 20,126351 | 8 | 5 | 60 |
| FW61400237 | S108 | Ni mg/kg DS < 40 µm | 250 | 227,31586 | 8 | 74 | 760 |
| FW61400247 | S108 | Ni mg/kg DS < 40 µm | 59 | 17,877947 | 9 | 36,8 | 89 |
| FW61400257 | S108 | Ni mg/kg DS < 40 µm | 33,5 | 17,131168 | 10 | 23 | 69,4 |
| FW61400267 | S108 | Ni mg/kg DS < 40 µm | 28 | 18,859808 | 8 | 20,6 | 68 |
| FW61400277 | S108 | Ni mg/kg DS < 40 µm | 36,5 | 16,431996 | 10 | 16 | 67 |
| FW61400287 | S108 | Ni mg/kg DS < 40 µm | 50 | 17,379655 | 10 | 22 | 81,3 |
| FW61400476 | S108 | Ni mg/kg DS < 40 µm | 43 | 12 | 2 | 31 | 55 |
| FW61400486 | S108 | Ni mg/kg DS < 40 µm | 40,65 | 7,65 | 2 | 33 | 48,3 |
| FW61400496 | S108 | Ni mg/kg DS < 40 µm | 48 | 9 | 2 | 39 | 57 |
| FW61400506 | S108 | Ni mg/kg DS < 40 µm | 78 | 37 | 2 | 41 | 115 |
| FW61400516 | S108 | Ni mg/kg DS < 40 µm | 46,35 | 23,35 | 2 | 23 | 69,7 |

## 1.10 Lead

### 1.10.1 F-Parameters

| GZÜV ID | Parameter ID | Parameter Name | Median | Standard deviation | Number of Measurements | Minimum value | Maximum Value |
|---|---|---|---|---|---|---|---|
| FW61302327 | F162 | Pb mg/l | <0,001 | 0 | 1 | <0,001 | <0,001 |
| FW61400067 | F162 | Pb mg/l | <0,001 | 0,000226 | 100 | <0,001 | 0,002 |
| FW61400077 | F162 | Pb mg/l | <0,001 | 0,00018 | 66 | <0,001 | 0,0011 |
| FW61400087 | F162 | Pb mg/l | <0,001 | 0,00016 | 100 | <0,001 | 0,001 |
| FW61400097 | F162 | Pb mg/l | <0,001 | 0,000391 | 100 | <0,001 | 0,0018 |
| FW61400107 | F162 | Pb mg/l | <0,001 | 0,000512 | 101 | <0,001 | 0,0034 |
| FW61400117 | F162 | Pb mg/l | <0,001 | 0,000482 | 67 | <0,001 | 0,002 |
| FW61400127 | F162 | Pb mg/l | <0,001 | 0,000353 | 124 | <0,001 | 0,002 |
| FW61400137 | F162 | Pb mg/l | <0,001 | 0,000711 | 255 | <0,001 | 0,0094 |
| FW61400147 | F162 | Pb mg/l | <0,001 | 0,000497 | 137 | <0,001 | 0,003 |
| FW61400157 | F162 | Pb mg/l | <0,001 | 0,000406 | 101 | <0,001 | 0,002 |
| FW61400167 | F162 | Pb mg/l | <0,001 | 0,000132 | 113 | <0,001 | 0,001 |
| FW61400177 | F162 | Pb mg/l | <0,001 | 0,000291 | 68 | <0,001 | 0,002 |
| FW61400187 | F162 | Pb mg/l | 0,00115 | 0,005912 | 80 | <0,001 | 0,036 |
| FW61400197 | F162 | Pb mg/l | <0,001 | 0,000634 | 101 | <0,001 | 0,0059 |
| FW61400207 | F162 | Pb mg/l | <0,001 | 0 | 6 | <0,001 | <0,001 |
| FW61400217 | F162 | Pb mg/l | <0,001 | 0,00051 | 136 | <0,001 | 0,003 |
| FW61400227 | F162 | Pb mg/l | <0,001 | 0,003487 | 5 | <0,001 | 0,009 |
| FW61400237 | F162 | Pb mg/l | <0,001 | 0,001629 | 69 | <0,001 | 0,0103 |
| FW61400247 | F162 | Pb mg/l | <0,001 | 0,004335 | 68 | <0,001 | 0,036 |
| FW61400257 | F162 | Pb mg/l | <0,001 | 0 | 6 | <0,001 | <0,001 |
| FW61400267 | F162 | Pb mg/l | <0,001 | 0,000312 | 138 | <0,001 | 0,002 |
| FW61400277 | F162 | Pb mg/l | <0,001 | 0 | 6 | <0,001 | <0,001 |
| FW61400287 | F162 | Pb mg/l | <0,001 | 0,000305 | 134 | <0,001 | 0,0015 |
| FW61400476 | F162 | Pb mg/l | <0,001 | 0,000149 | 44 | <0,001 | 0,001 |
| FW61400486 | F162 | Pb mg/l | <0,001 | 0,00031 | 44 | <0,001 | 0,0012 |
| FW61400496 | F162 | Pb mg/l | <0,001 | 0 | 2 | <0,001 | <0,001 |
| FW61400506 | F162 | Pb mg/l | <0,001 | 0,000152 | 44 | <0,001 | 0,001 |
| FW61400516 | F162 | Pb mg/l | <0,001 | 0 | 2 | <0,001 | <0,001 |
| FW61400597 | F162 | Pb mg/l | <0,001 | 0,000167 | 35 | <0,001 | 0,001 |
| FW61404547 | F162 | Pb mg/l | <0,001 | 0 | 12 | <0,001 | <0,001 |
| FW61404607 | F162 | Pb mg/l | <0,001 | 0 | 2 | <0,001 | <0,001 |
| FW61404617 | F162 | Pb mg/l | <0,001 | 0 | 1 | <0,001 | <0,001 |

### 1.10.2 S-Parameters

| GZÜV ID | Parameter ID | Parameter Name | Median | Standard deviation | Number of Measurements | Minimum value | Maximum Value |
|---|---|---|---|---|---|---|---|
| FW61400067 | S104 | Pb mg/kg DS < 40 µm | 15 | 17,973404 | 10 | 8 | 52,4 |
| FW61400077 | S104 | Pb mg/kg DS < 40 µm | 31,6 | 20,60894 | 9 | 7 | 67,3 |
| FW61400087 | S104 | Pb mg/kg DS < 40 µm | 24 | 23,044477 | 11 | 11,2 | 70,2 |
| FW61400097 | S104 | Pb mg/kg DS < 40 µm | 57 | 41,925612 | 10 | 11 | 141 |
| FW61400107 | S104 | Pb mg/kg DS < 40 µm | 49 | 51,489668 | 11 | 12 | 145 |
| FW61400117 | S104 | Pb mg/kg DS < 40 µm | 37 | 34,522642 | 9 | 16,3 | 112 |
| FW61400127 | S104 | Pb mg/kg DS < 40 µm | 101 | 64,093208 | 8 | 25,6 | 215 |
| FW61400137 | S104 | Pb mg/kg DS < 40 µm | 26 | 29,099718 | 10 | 14 | 108 |
| FW61400147 | S104 | Pb mg/kg DS < 40 µm | 24 | 30,342061 | 11 | 13 | 110 |
| FW61400157 | S104 | Pb mg/kg DS < 40 µm | 65,6 | 55,913255 | 10 | 26,5 | 190 |
| FW61400167 | S104 | Pb mg/kg DS < 40 µm | 22 | 34,296527 | 11 | 7,9 | 133 |
| FW61400177 | S104 | Pb mg/kg DS < 40 µm | 43,85 | 29,339668 | 8 | 20 | 110 |
| FW61400187 | S104 | Pb mg/kg DS < 40 µm | 335,5 | 500,018187 | 8 | 34 | 1290 |
| FW61400197 | S104 | Pb mg/kg DS < 40 µm | 43 | 24,103363 | 9 | 24 | 99,1 |
| FW61400207 | S104 | Pb mg/kg DS < 40 µm | 40,1 | 26,616874 | 10 | 18 | 98,8 |
| FW61400217 | S104 | Pb mg/kg DS < 40 µm | 49 | 24,337151 | 10 | 20 | 100 |
| FW61400227 | S104 | Pb mg/kg DS < 40 µm | 57,05 | 52,49126 | 8 | 18 | 162 |
| FW61400237 | S104 | Pb mg/kg DS < 40 µm | 129,5 | 84,524312 | 8 | 27 | 270 |
| FW61400247 | S104 | Pb mg/kg DS < 40 µm | 42,5 | 24,352083 | 9 | 12,1 | 80 |
| FW61400257 | S104 | Pb mg/kg DS < 40 µm | 17,5 | 14,384561 | 10 | 13 | 48 |
| FW61400267 | S104 | Pb mg/kg DS < 40 µm | 37,5 | 35,566904 | 8 | 9,54 | 119 |
| FW61400277 | S104 | Pb mg/kg DS < 40 µm | 31,7 | 10,197063 | 10 | 11 | 39 |
| FW61400287 | S104 | Pb mg/kg DS < 40 µm | 26,35 | 11,349718 | 10 | 8,8 | 43,2 |
| FW61400476 | S104 | Pb mg/kg DS < 40 µm | 23,3 | 11,3 | 2 | 12 | 34,6 |
| FW61400486 | S104 | Pb mg/kg DS < 40 µm | 19,25 | 6,25 | 2 | 13 | 25,5 |
| FW61400496 | S104 | Pb mg/kg DS < 40 µm | 21,1 | 6,1 | 2 | 15 | 27,2 |
| FW61400506 | S104 | Pb mg/kg DS < 40 µm | 28,45 | 11,45 | 2 | 17 | 39,9 |
| FW61400516 | S104 | Pb mg/kg DS < 40 µm | 32,95 | 22,95 | 2 | 10 | 55,9 |

## 1.11 Zinc

### 1.11.1 F-Parameters

| GZÜV ID | Parameter ID | Parameter Name | Median | Standard deviation | Number of Measurements | Minimum value | Maximum Value |
|---|---|---|---|---|---|---|---|
| FW61302327 | F156 | Zn mg/l | 0,005 | 0 | 1 | 0,005 | 0,005 |
| FW61400067 | F156 | Zn mg/l | <0,001 | 0,008778 | 99 | <0,001 | 0,081 |
| FW61400077 | F156 | Zn mg/l | <0,001 | 0,003688 | 65 | <0,001 | 0,024 |
| FW61400087 | F156 | Zn mg/l | <0,001 | 0,010425 | 99 | <0,001 | 0,098 |
| FW61400097 | F156 | Zn mg/l | 0,0124 | 0,015023 | 108 | <0,001 | 0,078 |
| FW61400107 | F156 | Zn mg/l | 0,00525 | 0,009572 | 100 | <0,001 | 0,063 |
| FW61400117 | F156 | Zn mg/l | 0,0045 | 0,065215 | 66 | <0,001 | 0,52 |
| FW61400127 | F156 | Zn mg/l | 0,005 | 0,010813 | 123 | <0,001 | 0,1 |
| FW61400137 | F156 | Zn mg/l | 0,005 | 0,014813 | 256 | <0,001 | 0,13 |
| FW61400147 | F156 | Zn mg/l | 0,00435 | 0,033605 | 136 | <0,001 | 0,378 |
| FW61400157 | F156 | Zn mg/l | 0,003 | 0,011115 | 100 | <0,001 | 0,1 |
| FW61400167 | F156 | Zn mg/l | 0,00125 | 0,014027 | 112 | <0,001 | 0,0756 |
| FW61400177 | F156 | Zn mg/l | <0,001 | 0,008845 | 67 | <0,001 | 0,045 |
| FW61400187 | F156 | Zn mg/l | 0,051 | 0,159841 | 79 | 0,0015 | 0,8 |
| FW61400197 | F156 | Zn mg/l | 0,001 | 0,008426 | 101 | <0,001 | 0,0564 |
| FW61400207 | F156 | Zn mg/l | 0,0035 | 0,002159 | 6 | 0,002 | 0,008 |
| FW61400217 | F156 | Zn mg/l | 0,0066 | 0,012096 | 136 | <0,001 | 0,0758 |
| FW61400227 | F156 | Zn mg/l | 0,011 | 0,009931 | 5 | 0,0024 | 0,031 |
| FW61400237 | F156 | Zn mg/l | 0,009 | 0,029625 | 68 | <0,001 | 0,24 |
| FW61400247 | F156 | Zn mg/l | 0,0018 | 0,018195 | 67 | <0,001 | 0,092 |
| FW61400257 | F156 | Zn mg/l | 0,0025 | 0,003236 | 6 | <0,001 | 0,009 |
| FW61400267 | F156 | Zn mg/l | 0,0013 | 0,015797 | 137 | <0,001 | 0,0992 |
| FW61400277 | F156 | Zn mg/l | 0,0024 | 0,001699 | 6 | <0,001 | 0,0041 |
| FW61400287 | F156 | Zn mg/l | 0,001 | 0,013028 | 133 | <0,001 | 0,091 |
| FW61400476 | F156 | Zn mg/l | <0,001 | 0,001056 | 44 | <0,001 | 0,0044 |
| FW61400486 | F156 | Zn mg/l | 0,00195 | 0,024392 | 44 | <0,001 | 0,163 |
| FW61400496 | F156 | Zn mg/l | 0,00245 | 0,00045 | 2 | 0,002 | 0,0029 |
| FW61400506 | F156 | Zn mg/l | 0,00105 | 0,008342 | 44 | <0,001 | 0,055 |
| FW61400516 | F156 | Zn mg/l | 0,0019 | 0,0009 | 2 | 0,001 | 0,0028 |
| FW61400597 | F156 | Zn mg/l | 0,0012 | 0,018728 | 35 | <0,001 | 0,0844 |
| FW61404547 | F156 | Zn mg/l | 0,01075 | 0,030193 | 12 | 0,0016 | 0,0911 |
| FW61404607 | F156 | Zn mg/l | 0,01065 | 0,00935 | 2 | 0,0013 | 0,02 |
| FW61404617 | F156 | Zn mg/l | 0,0067 | 0 | 1 | 0,0067 | 0,0067 |

### 1.11.2 S-Parameters

| GZÜV ID | Parameter ID | Parameter Name | Median | Standard deviation | Number of Measurements | Minimum value | Maximum Value |
|---|---|---|---|---|---|---|---|
| FW61400067 | S110 | Zn mg/kg DS < 40 µm | 74 | 47,56638 | 10 | 47 | 180 |
| FW61400077 | S110 | Zn mg/kg DS < 40 µm | 110 | 50,506325 | 9 | 48 | 204 |
| FW61400087 | S110 | Zn mg/kg DS < 40 µm | 110 | 64,84578 | 11 | 41 | 210 |
| FW61400097 | S110 | Zn mg/kg DS < 40 µm | 184,5 | 167,963039 | 10 | 46 | 470 |
| FW61400107 | S110 | Zn mg/kg DS < 40 µm | 100 | 149,022079 | 11 | 58 | 400 |
| FW61400117 | S110 | Zn mg/kg DS < 40 µm | 150 | 95,036321 | 9 | 92 | 351 |
| FW61400127 | S110 | Zn mg/kg DS < 40 µm | 215 | 111,852582 | 8 | 103 | 410 |
| FW61400137 | S110 | Zn mg/kg DS < 40 µm | 137 | 106,627593 | 10 | 65 | 364 |
| FW61400147 | S110 | Zn mg/kg DS < 40 µm | 110 | 87,336719 | 11 | 48 | 300 |
| FW61400157 | S110 | Zn mg/kg DS < 40 µm | 143,25 | 123,671349 | 10 | 63 | 410 |
| FW61400167 | S110 | Zn mg/kg DS < 40 µm | 100 | 48,570644 | 11 | 56 | 220 |
| FW61400177 | S110 | Zn mg/kg DS < 40 µm | 134,5 | 50,43173 | 8 | 56 | 180 |
| FW61400187 | S110 | Zn mg/kg DS < 40 µm | 2015 | 2259,61772 | 8 | 137 | 5810 |
| FW61400197 | S110 | Zn mg/kg DS < 40 µm | 87,2 | 44,501397 | 9 | 63 | 190 |
| FW61400207 | S110 | Zn mg/kg DS < 40 µm | 125,5 | 64,432057 | 10 | 52 | 244 |
| FW61400217 | S110 | Zn mg/kg DS < 40 µm | 185 | 93,231111 | 10 | 74 | 414 |
| FW61400227 | S110 | Zn mg/kg DS < 40 µm | 142,5 | 131,443369 | 8 | 45 | 390 |
| FW61400237 | S110 | Zn mg/kg DS < 40 µm | 344,5 | 1218,81354 | 8 | 103 | 4000 |
| FW61400247 | S110 | Zn mg/kg DS < 40 µm | 150 | 69,732122 | 9 | 66 | 283 |
| FW61400257 | S110 | Zn mg/kg DS < 40 µm | 116 | 48,27836 | 10 | 59 | 206 |
| FW61400267 | S110 | Zn mg/kg DS < 40 µm | 100 | 94,415726 | 8 | 59,8 | 340 |
| FW61400277 | S110 | Zn mg/kg DS < 40 µm | 120 | 41,427044 | 10 | 55 | 195 |
| FW61400287 | S110 | Zn mg/kg DS < 40 µm | 130 | 38,770402 | 10 | 55 | 191 |
| FW61400476 | S110 | Zn mg/kg DS < 40 µm | 108 | 17 | 2 | 91 | 125 |
| FW61400486 | S110 | Zn mg/kg DS < 40 µm | 101,5 | 18,5 | 2 | 83 | 120 |
| FW61400496 | S110 | Zn mg/kg DS < 40 µm | 112,5 | 15,5 | 2 | 97 | 128 |
| FW61400506 | S110 | Zn mg/kg DS < 40 µm | 94,5 | 33,5 | 2 | 61 | 128 |
| FW61400516 | S110 | Zn mg/kg DS < 40 µm | 126 | 75 | 2 | 51 | 201 |

# 2 Time dependent comparison: data basis

## 2.1 FW61400097

| GZÜV-ID | Parameter ID | Parameter Name | Jul 1996 | Aug 1996 | Sep 1996 | Okt 1996 | Nov 1996 | Dez 1996 |
|---|---|---|---|---|---|---|---|---|
| FW61400097 | F107 | Flow ratio $m^3/s$ | 97,4 | 60,9 | 131,0 | 181,0 | 116,0 | 67,5 |
| FW61400097 | F167 | As [mg/l] | <0,0007 | 0,0007 | <0,0007 | 0,0011 | <0,0007 | <0,0007 |
| FW61400097 | F152 | Cd [mg/l] | <0,0001 | <0,0001 | <0,0001 | <0,0001 | <0,0001 | <0,0001 |
| FW61400097 | F163 | Cr [mg/l] | <0,001 | <0,001 | <0,001 | <0,001 | <0,001 | <0,001 |
| FW61400097 | F157 | Cu [mg/l] | 0,016 | 0,0093 | 0,0035 | 0,006 | 0,018 | 0,007 |
| FW61400097 | F153 | Hg [mg/l] | <0,0001 | <0,0001 | <0,0001 | <0,0001 | <0,0001 | 0,00025 |
| FW61400097 | F165 | Ni [mg/l] | <0,001 | <0,001 | <0,001 | <0,001 | <0,001 | <0,001 |
| FW61400097 | F161 | Pb [mg/l] | <0,001 | <0,001 | <0,001 | <0,001 | <0,001 | 0,001 |
| FW61400097 | F155 | Zn [mg/l] | 0,006 | 0,007 | 0,0131 | 0,052 | 0,078 | 0,036 |

| GZÜV-ID | Parameter ID | Parameter Name | Jan 1997 | Feb 1997 | Mär 1997 | Apr 1997 | Mai 1997 | Jul 1997 (1) | Jul 1997 (2) |
|---|---|---|---|---|---|---|---|---|---|
| FW61400097 | F107 | Flow ratio $m^3/s$ | 36,1 | 29,9 | 37,8 | 46,2 | 149,0 | 129,0 | 120,0 |
| FW61400097 | F167 | As [mg/l] | <0,0007 | 0,001 | 0,0011 | 0,0009 | 0,00177 | 0,0012 | 0,00164 |
| FW61400097 | F152 | Cd [mg/l] | <0,0001 | <0,0001 | 0,00037 | <0,0001 | | | |
| FW61400097 | F163 | Cr [mg/l] | <0,001 | <0,001 | 0,0012 | 0,0022 | <0,001 | <0,001 | 0,0016 |
| FW61400097 | F157 | Cu [mg/l] | 0,0114 | 0,0037 | 0,0044 | 0,0051 | 0,00274 | 0,0022 | 0,00297 |
| FW61400097 | F153 | Hg [mg/l] | <0,0001 | <0,0001 | <0,0001 | <0,0001 | <0,0001 | <0,0001 | <0,0001 |
| FW61400097 | F165 | Ni [mg/l] | <0,001 | <0,001 | 0,0023 | 0,0012 | 0,0018 | 0,0011 | 0,0017 |
| FW61400097 | F161 | Pb [mg/l] | <0,001 | <0,001 | 0,0015 | 0,0013 | 0,00382 | 0,00101 | 0,00137 |
| FW61400097 | F155 | Zn [mg/l] | 0,065 | 0,014 | 0,046 | 0,014 | 0,0119 | 0,0121 | 0,0166 |

## 2.2 FW61400187

| GZÜV-ID | Parameter ID | Parameter Name | Jul 1996 | Aug 1996 | Sep 1996 | Okt 1996 | Nov 1996 | Dez 1996 |
|---|---|---|---|---|---|---|---|---|
| FW61400187 | F107 | Flow ratio m³/s | 6,02 | 4,16 | 9,61 | 15,6 | 4,69 | 3,61 |
| FW61400187 | F167 | As [mg/l] | <0,0007 | <0,0007 | <0,0007 | <0,0007 | <0,0007 | <0,0007 |
| FW61400187 | F161 | Pb [mg/l] | <0,001 | <0,001 | <0,001 | <0,001 | 0,002 | <0,001 |
| FW61400187 | F152 | Cd [mg/l] | <0,0001 | <0,0001 | <0,0001 | <0,0001 | <0,0001 | <0,0001 |
| FW61400187 | F163 | Cr [mg/l] | <0,001 | <0,001 | <0,001 | <0,001 | <0,001 | <0,001 |
| FW61400187 | F157 | Cu [mg/l] | 0,003 | 0,003 | <0,001 | 0,001 | 0,02 | 0,017 |
| FW61400187 | F165 | Ni [mg/l] | <0,001 | 0,001 | 0,0039 | <0,001 | <0,001 | 0,002 |
| FW61400187 | F153 | Hg [mg/l] | <0,0001 | <0,0001 | <0,0001 | <0,0001 | <0,0001 | <0,0001 |
| FW61400187 | F155 | Zn [mg/l] | 0,026 | 0,013 | 0,019 | 0,016 | 0,086 | 0,042 |

| GZÜV-ID | Parameter ID | Parameter Name | Jan 1997 | Feb 1997 | Mär 1997 | Apr 1997 | Mai 1997 | Jul 1997 (1) | Jul 1997 (2) |
|---|---|---|---|---|---|---|---|---|---|
| FW61400187 | F107 | Flow ratio m³/s | 1,81 | 1,63 | 1,87 | 5,44 | 10,1 | 5,5 | 9,69 |
| FW61400187 | F167 | As [mg/l] | <0,0007 | <0,0007 | 0,0009 | <0,0007 | 0,00113 | <0,0007 | <0,0007 |
| FW61400187 | F161 | Pb [mg/l] | 0,0012 | <0,001 | 0,002 | 0,0017 | 0,08105 | 0,01184 | 0,00231 |
| FW61400187 | F152 | Cd [mg/l] | <0,0001 | <0,0001 | <0,0001 | <0,0001 | 0,00239 | 0,00027 | <0,0001 |
| FW61400187 | F163 | Cr [mg/l] | <0,001 | 0,0015 | <0,001 | 0,0017 | 0,0013 | <0,001 | <0,001 |
| FW61400187 | F157 | Cu [mg/l] | 0,0061 | 0,0068 | 0,0043 | 0,0139 | 0,00583 | 0,00356 | 0,00228 |
| FW61400187 | F165 | Ni [mg/l] | 0,002 | 0,005 | 0,0024 | 0,0032 | 0,0041 | 0,0022 | <0,001 |
| FW61400187 | F153 | Hg [mg/l] | <0,0001 | 0,0003 | <0,0001 | <0,0001 | <0,0001 | <0,0001 | <0,0001 |
| FW61400187 | F155 | Zn [mg/l] | 0,108 | 0,034 | 0,048 | 0,012 | 0,1303 | 0,1566 | 0,0451 |